

Optimization Under Uncertainty in Building Energy Management

Zur Erlangung des akademischen Grades eines
Doktors der Ingenieurwissenschaften

(Dr.-Ing.)

von der KIT-Fakultät für Wirtschaftswissenschaften
des Karlsruher Instituts für Technologie (KIT)

genehmigte

DISSERTATION

von

Dipl.-Phys. Jan Müller

Tag der mündlichen Prüfung: 30. Juli 2019

Referent: Prof. Dr. Hartmut Schmeck

Korreferent: Prof. Dr. Wolf Fichtner

Abstract

The introduction of decentralized energy resources as well as energy storage systems to the energy system calls for new control and coordination mechanisms and systems. This is also true for buildings, which make up a significant share of the final energy consumption. In the course of this energy transition from fossil energy carriers and centralized power plants towards renewable energy sources and distributed generation more and more decentralized energy resources, such as photovoltaic systems and battery energy storage systems, are introduced to building energy systems. An optimized operation of buildings comprising decentralized generation and energy storage systems can be achieved by a building energy management system. They control and coordinate the operation of individual devices in a building's energy system to achieve given goals, such as the increase of energy efficiency, the decrease of carbon emissions, the minimization of operating costs or the provision of demand response measures. In recent years in particular, building energy management systems that use predictions of the future energy generation and consumption in the building have been investigated. These systems have proven to work particularly well in the presence of time-dependent electricity consumption and feed-in tariffs.

This thesis picks up on this idea and extends the ongoing research by presenting an approach to the optimized operation of building energy systems that includes the uncertainties in the predictions of the future energy generation and consumption into the control scheme of a building energy management system. To do so, this thesis identified the use of a scenario-based consideration of the uncertainties to be best suited. Thus, the presented approach uses a rolling horizon optimization approach with a stochastic two-stage optimization problem, which considers several forecast scenarios in the optimization. It targets the minimization of the average of the operating costs of the building's energy system that occur to in forecast scenarios. This thesis, only considers uncertainties in the forecasts of the electricity generation of the photovoltaic system, and neglects the uncertainties in the forecasts of the energy consumption. To do so, a suitable forecast mechanism has to be developed, which generates several forecast scenarios based on historical data. In this thesis, a probabilistic forecast that provides different forecast scenarios based on a quantile regression is proposed. Its derived quantiles are used as forecast scenarios to approximate the range possible electricity generation profiles of the photovoltaic system.

The presented approach is evaluated in nine evaluation scenarios using a specific building configuration assuming the presence of time-dependent electricity consumption and feed-in

tariffs. In each evaluation scenario the feed-in tariff and the season are varied. The investigated building configuration comprises a controllable washing machine, a controllable battery energy storage systems and a controllable micro combined heat and power plant as well as additional electricity and heat consumption from non-controllable sources. In the evaluation, the presented approach is compared to a reference control scheme, using a perfect forecast of the electricity generation from the photovoltaic system, to a state-of-the-art rolling horizon optimization that uses a single-point forecast and to a rule-based control scheme.

The evaluation results show that in seven scenarios, the approach presented in this thesis performs similar to the state-of-the-art approach, whereas in two scenarios it outperforms the state-of-the-art approach. Both of these two scenarios are scenarios which have high electricity generation from the photovoltaic system and a low heat consumption. They are the scenarios with the highest load shifting potential as well as the tariffs that reward load shifting the most. However, the presented approach leads to higher optimization times than the state-of-the-art approach.

In conclusion, the presented approach yields a performance increase with respect to the state-of-the-art approach in some scenarios but increases the computational effort. It is in particular suitable in scenarios with a high electricity generation from a photovoltaic system, which are scenarios that either have a large photovoltaic system or have a high solar irradiation. Furthermore, it is suitable in scenarios with time dependent electricity consumption and feed-in tariffs. Because only in these cases, the full load shifting potential of a battery energy storage system can be utilized. Therefore, an application in a commercial building energy system has to be well-considered. In addition, this thesis provides a justification of the choice of single-point forecasts in building energy management systems in scenarios with limited photovoltaic generation. Furthermore, the observed computational efforts motivate the use of heuristics.

Acknowledgments

First of all, I would like to thank my supervisor Prof. Hartmut Schmeck, for giving me the opportunity to do my doctorate as well as his constant support and the freedom to pursue this work.

Additionally, I would like to express my thanks to Prof. Wolf Fichtner for his valuable advice and comments as well as to Prof. Andreas Oberweis and Prof. Marliese Uhrig-Homburg for serving on my thesis committee.

Furthermore, I would like to thank all my colleagues at the Karlsruhe Institute of Technology and FZI Research Center for Information Technology for their feedback, cooperation, the lively discussions and for all the fun we have had.

In particular, I would like to thank Ingo Mauser, Sebastian Kochannek, Mischa Ahrens and Kaibin Bao for supporting my research, proofreading and discussing my thesis as well as their constructive feedback and ideas.

Moreover, I would like to thank Christian Gitte, Fabian Rigoll, Christian Hirsch, Fredy Rios, Lukas König and Marlon Braun for all the things they taught me.

Finally, I would like to thank my family for supporting me at all times and especially Malin, for enabling me to get the best out of me.

Contents

List of Figures	XI
List of Tables	XV
List of Abbreviations	XIX
1 Introduction	1
1.1 Scope	2
1.2 Major Contributions	3
1.3 Related Publications by the Author	5
1.4 Structure	6
2 Background on Energy Systems	7
2.1 Energy Policy	7
2.2 Generation, Transmission, Distribution and Consumption of Energy	7
2.3 Energy Transition	8
2.4 Energy Storage	10
2.4.1 Electrical Energy Storage Systems	10
2.4.2 Thermal Energy Storage Systems	11
2.5 Electricity Grid	12
2.6 Microgrids	14
2.7 Smart Grid	14
2.8 Building Energy Systems	15
2.9 Coordination and Management	16
2.9.1 Electricity Trading	16
2.9.2 Electricity Tariffs	17
2.9.3 Balancing Groups and Power Plant Scheduling	18
2.9.4 Operating Reserve	19
2.9.5 Demand Side Management and Demand Response	20
2.10 Flexibility in Energy Systems	21
2.11 Optimization in Building Energy Systems	21
2.12 Economic and Technical Design of the Building Energy Systems	22
2.13 Optimized Operation of Building Energy Systems	24

2.14	Building Energy Management Systems	24
2.15	Coordination and Building Energy Management in Distribution Grids . . .	27
3	Theoretical Concepts of Modeling and Optimization	31
3.1	Model Building	31
3.2	Optimization	31
3.3	Off-line and On-line Optimization	32
3.4	Optimization of Discrete Time Systems	33
3.5	Rolling Horizon Optimization	34
3.6	Time-Dependent Parameters and Stage Costs	37
3.7	Approximation and Numerical Solution	39
3.8	Decision Making Under Uncertainty	40
3.8.1	Modeling of Uncertainty	40
3.8.2	Decision Criteria	41
3.9	Optimization Under Uncertainty	44
3.10	Robust Optimization	44
3.11	Stochastic Programming	45
3.11.1	Two-stage Problem	46
3.11.2	Multi-stage Problem	47
3.11.3	Sampling Methods	49
3.12	Mixed-integer Linear Programming	49
3.13	Modeling of Energy Systems in Buildings	50
4	Related Work	53
4.1	Related Work on Modeling in Building Energy Management	53
4.1.1	Electricity Consumption, User Behavior, and Electricity Consumption Forecast	53
4.1.2	Battery Energy Storage Systems	54
4.1.3	Micro Combined Heat and Power Plants	57
4.1.4	PV System	57
4.1.5	PV Generation Forecast	58
4.1.6	Deferrable Loads and Appliances	63
4.1.7	HVAC System	64
4.1.8	Tariffs	66
4.2	Related Work on Building Energy Management Systems	66
4.2.1	Objectives in Building Energy Management	67
4.2.2	Commonly Controlled Devices in Building Energy Management . .	68
4.3	Related Work on the Optimization of the Operation of Energy Systems in Buildings	70
4.3.1	Controllers and Rule-based Approaches	70
4.3.2	Day-ahead Scheduling Approaches	71
4.3.3	Rolling Horizon Optimization in Buildings	71
4.3.4	Optimization Under Uncertainty	73

4.3.5	Comparison	76
5	Model and Optimization Approach	79
5.1	Notation and Introductory Remarks	79
5.2	Choice of Scenario	80
5.2.1	Smart Building Configuration	81
5.2.2	Assumptions	82
5.2.3	Forecast Uncertainties	82
5.3	Overall Goal	82
5.4	Building Simulation	84
5.5	Rolling Horizon Optimization Approach	88
5.6	Model of the Energy System	90
5.6.1	Batteries Energy Storage System	90
5.6.2	Micro Combined Heat and Power Plant	96
5.6.3	PV System	101
5.6.4	Appliances	104
5.6.5	Electric Base Load	109
5.6.6	Space Heating	111
5.6.7	Domestic Hot Water Consumption	112
5.6.8	Hot Water Tank	113
5.6.9	Tariffs	115
5.6.10	Device Interaction Model and Grid Interaction Model	118
5.7	Formulation of the State-of-the-art One-stage Rolling Horizon Optimization Problem	120
5.7.1	Objective Function	122
5.7.2	Constraints	123
5.7.3	Summary of the Optimization Problem	125
5.8	Formulation of the Stochastic Two-stage Rolling Horizon Optimization Problem	126
5.8.1	Objective Function	128
5.8.2	Constraints	129
5.8.3	Summary of the Optimization Problem	134
5.9	Implementation	134
5.10	Adaptivity of the Approach	135
6	Evaluation	137
6.1	Smart Building Configuration	137
6.2	Smart Building Simulation	137
6.3	Overview of the Evaluation Scenarios	140
6.4	Simulation Process	142
6.5	Parameter Tuning	145
6.6	Evaluation Results	146
6.6.1	Reference Control Scheme	146
6.6.2	Choice of Tuning Parameters	153

6.6.3	State-of-the-art and Stochastic Control Scheme	155
6.6.4	Rule-based Micro-CHP Control Scheme	163
6.6.5	Rule-based Control Scheme	170
6.6.6	Scenario Comparison	173
6.7	Discussion of the Results	181
6.7.1	Limitations	183
6.7.2	Future Opportunities	183
7	Conclusion	185
7.1	Summary and Conclusion	185
7.2	Outlook	187
	Bibliography	189
	A Formulation of the Optimization Problem	211
	B Additional Results	221
B.1	Reference Control Scheme	221
B.2	State-of-the-art and Stochastic Control Scheme	240
B.3	Rule-based Micro-CHP Scenario	248
	C Related Publications by the Author	257

List of Figures

2.1	Residual load duration curves in Germany	9
2.2	Classification and applications of energy storage system	10
2.3	General layout of the electricity network	13
2.4	Exemplary smart building	15
2.5	Definition of flexibility	22
2.6	Economic and technical design of the technical setup	23
2.7	Layers for the control of building energy systems	25
2.8	Scheme of a building energy management system	27
2.9	Coordination patterns	28
3.1	Process of model building and problem definition	32
3.2	Visualization of the rolling horizon optimization approach	35
3.3	Visualization of time-dependent parameters	38
3.4	Visualization of the two-stage problem in this thesis	47
3.5	Visualization of a multi-stage problem	48
4.1	Constant-current constant-voltage charging	55
4.2	Power converter efficiency	56
4.3	Effect of cloudiness of the PV generation	59
4.4	Example of PV generation scenario sampling	60
4.5	PV generation forecast methods	62
4.6	Interval forecast of the PV generation	63
4.7	Shiftable loads and appliances	64
4.8	Visualization of averaging effects	69
5.1	Overview of the smart building scenario	80
5.2	Overview of the PV system and the BESS.	91
5.3	Battery energy storage system controller	93
5.4	Micro-CHP electricity generation model and measurement	99
5.5	PDFs of the number of starts of the appliances	105
5.6	PDFs of the times of usage the appliances	105
5.7	Load profiles of the appliances	106
5.8	Visualization of the appliance scheduling	107

5.9	Visualization of the washing machine model	108
5.10	Electricity consumption profiles	110
5.11	Heating system heat load profiles	111
5.12	DHW heat load profile	112
5.13	Electricity consumption and feed-in tariffs.	116
6.1	Visualization of an optimization window that exceeds the simulation period	142
6.2	Visualization of the electrical loads and ESS states in the building energy system using the reference control scheme	147
6.3	Dependence of the total costs on the optimization window in the reference control scheme with FT-1	150
6.4	Dependence of the total costs on the optimization window for reference control schemes with FT-2	151
6.5	Dependence of the total costs on the optimization window in the reference control scheme with FT-3	152
6.6	Optimization times in dependence on the tuning parameters in the reference control scheme in the summer scenario with FT-2	154
6.7	Exemplary results for the state-of-the-art control scheme	156
6.8	Exemplary probabilistic PV generation forecasts and resulting electrical loads for $M = 9$ on an exemplary day	157
6.9	Dependence of the total costs on the optimization window and the number of forecast scenarios in the state-of-the-art and stochastic control schemes in the scenarios with FT-1	159
6.10	Dependence of the total costs on the optimization window and the number of forecast scenarios in the state-of-the-art and stochastic control schemes in the scenarios with FT-2	160
6.11	Dependence of the total costs on the optimization window and the number of forecast scenarios in the state-of-the-art and stochastic control schemes in the scenarios with FT-3	161
6.12	Optimization times in the state-of-the-art and stochastic control schemes in the summer scenario in dependence on the tuning parameters	162
6.13	Visualization of the rule-based micro-CHP control scheme evaluation	164
6.14	Dependence of the total costs on the optimization window in the rule-based micro-CHP control scheme in the scenarios with FT-1	166
6.15	Dependence of the total costs on the optimization window in the rule-based micro-CHP control scheme in the scenarios with FT-2	167
6.16	Dependence of the total costs on the optimization window in the rule-based micro-CHP control scheme in the scenarios with FT-3	168
6.17	Optimization times in the rule-based micro-CHP control scheme in the summer scenarios in dependence on the tuning parameters	169
6.18	Visualization of the rule-based control scheme evaluation	171
6.19	Results of the rule-based operation	172

6.20 Comparison of the evaluation results for the different control schemes in the different scenarios	174
6.21 Comparison of the evaluation results for the different control schemes in the different scenarios	175
6.22 Visualization of the grid exchange powers in the spring scenarios for FT-1 .	178
6.23 Visualization of the grid exchange powers in the summer scenarios for FT-1	180
B.1 Visualization of the electrical loads and ESS states in the building energy system using the reference control scheme	230
B.2 Optimization times in dependence on the tuning parameters in the reference control scheme in the summer scenario with FT-1	231
B.3 Optimization times in dependence on the tuning parameters in the reference control scheme in the summer scenario with FT-2	232
B.4 Optimization times in dependence on the tuning parameters in the reference control scheme in the summer scenario with FT-3	233
B.5 Optimization times in dependence on the tuning parameters in the reference control scheme in the winter scenario with FT-1	234
B.6 Optimization times in dependence on the tuning parameters in the reference control scheme in the winter scenario with FT-2	235
B.7 Optimization times in dependence on the tuning parameters in the reference control scheme in the winter scenario with FT-3	236
B.8 Optimization times in dependence on the tuning parameters in the reference control scheme in the spring scenario with FT-1	237
B.9 Optimization times in dependence on the tuning parameters in the reference control scheme in the spring scenario with FT-2	238
B.10 Optimization times in dependence on the tuning parameters in the reference control scheme in the spring scenario with FT-3	239
B.11 Optimization times in the state-of-the-art and stochastic control scheme in the summer scenario in dependence on the tuning parameters	245
B.12 Optimization times in the state-of-the-art and stochastic control scheme in the winter scenario in dependence on the tuning parameters	246
B.13 Optimization times in the state-of-the-art and stochastic control scheme in the spring scenario in dependence on the tuning parameters	247
B.14 Optimization times in the rule-based micro-CHP control scheme spring in the summer scenario in dependence on the tuning parameters	253
B.15 Optimization times in the rule-based micro-CHP control scheme in the winter scenario in dependence on the tuning parameters	254
B.16 Optimization times in the rule-based micro-CHP control scheme in the spring scenario in dependence on the tuning parameters	255

List of Tables

2.1	Electricity Grids	12
4.1	List of objectives in building energy management	67
4.2	List of devices in energy management systems	68
4.3	Comparison of related work	77
5.1	Smart building configuration	82
5.2	Overview of the predictions of generation and consumption.	83
5.3	Energy generation and consumption, and energy storage system states in the building simulation	86
5.4	Control inputs in the building simulation	86
5.5	Parameters of the BESS model.	91
5.6	Parameters of the micro-CHP model.	97
5.7	Parameters of the deferrable appliances.	105
5.8	Parameters of the hot water tank model.	113
5.9	List of decision variables in the state-of-the-art one-stage rolling horizon optimization problem	121
5.10	List of decision variables in the stochastic two-stage rolling horizon optimization problem	127
6.1	Overview of the evaluation scenario	138
6.2	Parameters of the Simulation	139
6.3	Overview of the load profile resolutions	139
6.4	Overview of the electricity tariffs	141
6.5	Overview of the starting times of the simulations	141
6.6	Overview of the different device control schemes in the evaluation	142
6.7	Parameters of the Optimization (Part 1)	143
6.8	Parameters of the optimization (Part 2)	144
6.9	Simulation results of the reference control scheme in the summer scenario and with FT-2	148
6.10	Simulation results of the state-of-the-art and stochastic control schemes in the summer scenarios with FT-2	158

6.11	Simulation results of the rule-based micro-CHP control scheme in the summer scenario with FT-2	165
6.12	Results of the rule-based operation	171
6.13	Best tuning parameter combinations in the evaluation scenarios	176
6.14	Self-consumption and self-sufficiency rates for different control schemes in the spring scenario with FT-1	179
6.15	Self-consumption and self-sufficiency rates for different control schemes in the summer scenario with FT-1	179
B.1	Simulation results of the reference control scheme in the summer and with FT-1	221
B.2	Simulation results of the reference control scheme in the summer scenario with FT-2	222
B.3	Simulation results of the reference control scheme in the summer scenario with FT-3	223
B.4	Simulation results of the reference control scheme in the spring scenario and with FT-1	224
B.5	Simulation results of the reference control scheme in the spring scenario with FT-2	225
B.6	Simulation results of the reference control scheme in the spring scenario with FT-3	226
B.7	Simulation results of the reference control scheme in the winter scenario with FT-1	227
B.8	Simulation results of the reference control scheme in the winter scenario with FT-2	228
B.9	Simulation results of the reference control scheme in the winter scenario with FT-3	229
B.10	Simulation results of the state-of-the-art and stochastic control scheme in the summer scenario and with FT-1	240
B.11	Simulation results of the state-of-the-art and stochastic control scheme in the summer scenario with FT-2	240
B.12	Simulation results of the state-of-the-art and stochastic control scheme in the summer scenario and with FT-3	241
B.13	Simulation results of the state-of-the-art and stochastic control scheme in the winter with FT-1	241
B.14	Simulation results of the state-of-the-art and stochastic control scheme in the winter scenario with FT-2	242
B.15	Simulation results of the rule-based state-of-the-art and stochastic control scheme in the winter scenario with FT-3	242
B.16	Simulation results of the state-of-the-art and stochastic control scheme in the spring scenario with FT-1	243
B.17	Simulation results of the state-of-the-art and stochastic control scheme in the spring scenario with FT-2	243

B.18 Simulation results of the state-of-the-art and stochastic control scheme in the spring scenario with FT-3	244
B.19 Simulation results of the rule-based micro-CHP control scheme in the summer scenario with FT-1	248
B.20 Simulation results of the rule-based micro-CHP control scheme in the summer scenario with FT-2	248
B.21 Simulation results of the rule-based micro-CHP control scheme in the summer scenario with FT-3	249
B.22 Simulation results of the rule-based micro-CHP control scheme in the winter scenario with FT-1	249
B.23 Simulation results of the rule-based micro-CHP control scheme in the winter scenario with FT-2	250
B.24 Simulation results of the rule-based micro-CHP control scheme in the winter scenario with FT-3	250
B.25 Simulation results of the rule-based micro-CHP control scheme in the spring scenario with FT-1	251
B.26 Simulation results of the rule-based micro-CHP control scheme in the spring scenario with FT-2	251
B.27 Simulation results of the rule-based micro-CHP control scheme spring in the spring scenario with FT-3	252
C.1 Related Publications by the author	257

List of Abbreviations

(k)-NN	k-nearest neighbor
A/C	Air-Conditioning
AC	Alternating Current
ANN	Artificial Neural Network
BEMS	Building Energy Management System
BESS	Battery Energy Storage System
BMS	Battery Management System
CCCV	Constant-Current Constant-Voltage
CDF	Cumulative Distribution Function
CHP	Combined Heat and Power Plant
COP	Coefficient of Performance
CPP	Critical Peak Pricing
DC	Direct Current
DEP	Deterministic Equivalent Program
DER	Distributed Energy Resource
DG	Distributed (Electricity) Generation
DHW	Domestic Hot Water
DR	Demand Response
DSM	Demand Side Management
EA	Evolutionary Algorithm
EE	Energy Efficiency
EEX	European Energy Exchange

List of Abbreviations

EMP	Energy Management Panel
EMPC	Economic Model Predictive Control
EMS	Energy Management System
ESHL	Energy Smart Home Lab
ESS	Energy Storage System
ET	Electricity Tariff
EU	European Union
EV	Electric Vehicle
FT-1	Constant Feed-in Tariff
FT-2	Time-dependent Feed-in Tariff 1
FT-3	Time-dependent Feed-in Tariff 2
FZI	FZI Research Center for Information Technology
GA	Genetic Algorithm
GUI	Graphical User Interface
HoLL	House of Living Labs
HS	Heating System
HVAC	Heating, Ventilation, and Air-Conditioning
HWT	Hot Water Tank
ICT	Information and Communication Technology
KIT	Karlsruhe Institute of Technology
LP	Linear Programming
MAPE	Mean Absolute Percent Error
micro-CHP	Micro Combined Heat and Power Plant
MILP	Mixed Integer Linear Programming
MINP	Mixed Integer Non-linear Programming
MPC	Model Predictive Control
OBC	Optimization-based Control
OSH	Organic Smart Home
PCM	Phase-Change Material
PDF	Probability Density Function
PV	Photovoltaic
RBC	Rule-based Control
RES	Renewable Energy Source

RMSE	Root Mean Square Error
RTP	Real-time Pricing
SoC	State of Charge
TOU	Time-of-use
UPS	Uninterruptible Power Supply
VPP	Virtual Power Plant

1. Introduction

The fight against the climate change is currently one of the most important challenges for society, politics and science [248]. Its main task is the reduction of greenhouse gas emissions, which is supposed to be achieved by two means: the transition from carbon based energy generation towards generation that harnesses Renewable Energy Sources (RESs), as well as increasing the efficiency of energy usage [211].

An increased usage of RESs leads to a higher volatility in the electricity generation caused by the intermittent availability of wind and solar radiation. This can lead to a situation in which the electricity generation does no longer follow the consumption. Instead, the conventional central paradigm of electricity distribution changes from “supply follows demand” to “demand follows supply” [145, 195]. Here, Demand Side Management (DSM) enables the demand side to respond to intermittent and decentralized energy feed-in from RESs to balance the generation and consumption in a specific part of the electricity grid. The resulting behavior is expected to increase the efficiency of the energy system, reduce the electricity costs and support the operation of the electricity grids [98, 195]. Concrete measures to adapt the generation and consumption are called Demand Response (DR) measures. The application of DSM and DR measures is a recent field of research and multiple different approaches are under investigation.

In order to provide DR measures, participants in a DR program have to adapt their electricity consumption and generation based on external signals, e. g., direct control signals for specific devices, power limit signals or time-dependent tariffs. The participants can be all electric energy consumers and generators on the former demand side. However, the types of DR measures a participant can provide depend on the flexibility of the participant’s energy system. The flexibility of an energy system refers to an amount of possible ways it can be operated to provide all mandatory energy services [162]. Based on the high contribution to the whole energy consumption, building energy systems are promising participants in DR programs [151]. In 2015, the share of the global final energy consumption of buildings has

been 30 % [123]. To make the flexibility of building energy systems accessible, Building Energy Management Systems (BEMSs) can be used [20]. BEMSs control all devices in a building's energy system to achieve given goals like the increase of energy efficiency [49], the decrease of carbon emissions, the minimization of operating costs or the provision of DR measures. Typically, energy systems in buildings include different devices and energy carriers, such as electricity, hot water or natural gas [20]. The flexibility of a building's energy system can be harnessed most effectively when all devices and energy carriers are included into a BEMS [163]. To do so, a multi-modal energy management is necessary [163].

To enable communication between demand side managers, participants and grid operators, a suitable Information and Communication Technology (ICT) infrastructure is needed [76]. This is one of the reasons for the development of a smart grid, as the combination of the ICT infrastructure and the energy system in combination with novel control schemes is often called [52].

1.1 Scope

BEMSs enable an optimized operation of building energy systems with respect to given goals. Three objectives are commonly targeted in the optimal operation of a building energy system. However, in the literature, the reduction of operating costs has been identified to be the most discussed goal for building energy management. Costs can be seen as the most compelling goal for the owner or the operator of a building, since costs are easy to understand and consequences are evident. In addition, other goals, e. g., the reduction of carbon dioxide emissions, can be modeled as costs by means of considering artificial or actual costs. Therefore, this thesis defines an optimal system operation to be an operation that leads to minimal operation costs in a given time interval.

Furthermore, optimized operation of a building's energy system with respect to time-dependent tariffs enables a potential participation in a DR program that uses these tariffs as a measure of coordination. However, the explicit design of such a DR program is not investigated in this thesis. An example of such a DR program is presented in [96].

In the literature, the rolling horizon optimization method is most often stated to provide the best performance. The method uses generation and consumption forecasts in combination with a model of the building energy system to determine the control inputs for the devices that lead to minimal operating costs within a given time interval. The determination of the control inputs is achieved by formulating an optimization problem that is then solved. This problem is repetitively formulated and solved, typically in a distinct time interval. In general, the forecasts are subject to a certain degree of uncertainty. This means that the forecasts only provide an estimate of the future energy generation or consumption, whereas the actual generation or consumption values become only known at the time of generation or consumption. The state-of-art methods in building energy management use single point forecasts [20, 163]. Thus, the optimization determines the schedule that is optimal with

respect to a specific single forecast value. It is important to note that those schedules are not necessarily optimal when the realizations of the uncertain parameters change from the forecast. Therefore, the incorporation of additional knowledge of the uncertainties in the forecasts and into the optimization in building energy management are expected to increase the performance of a BEMS. This leads to the first research question addressed in this thesis:

Research Question 1: How can uncertainties be included in the optimization in building energy management?

An optimization-based operation of building energy systems uses forecasts of the energy consumption and generation in the building. Here, it is important to choose suitable forecast methods since the forecast quality and method is expected to influence the performance of the control scheme. This also holds true when the uncertainties in the forecasts are incorporated into the optimization. The uncertainties in the forecast have to be suitably described and the chosen description has to be integrated with the approach to the optimization. Consequently, the following research question has to be addressed in this thesis:

Research Question 2: How can a suitable forecast for BEMSs be achieved?

The combination of the energy forecasts and the approach to the optimization of a building's energy system defines the presented approach to the optimization in building energy management. To investigate the application of optimization under uncertainty in building energy management, an evaluation scenario has to be defined. The evaluation scenario includes a building configuration, i. e., a list of installed devices, present tariff schemes, electricity and heat consumption profiles and Photovoltaic (PV) generation profiles. This thesis targets on evaluating the presented approach in dependence on the tariff schemes as well as the consumption and generation profiles for electricity and heat. Hence, this thesis works on the following research question:

Research Question 3: What is the performance of the proposed approach?

Every control scheme that targets on minimizing the operating costs has to perform in various conditions. Therefore, the performance of the presented approach is tested for different conditions and scenarios.

1.2 Major Contributions

This thesis contributes to the field of energy informatics and in particular to the research on BEMSs by investigating the application of optimization under uncertainty in building energy management.

An optimized operation of Distributed Energy Resources (DERs) under presence of time-dependent prices is one approach to DSM and one step towards smart grids. This thesis

focuses on smart buildings as a form of DER or as a conglomerate of DERs that is operated by an automated BEMS. The major contribution of this thesis is an optimization-based control scheme that incorporates the uncertainties in the forecasts of the energy consumption and generation to reduce the operating costs of a building energy system.

To this end, this thesis provides a literature review that gives insights into the current state of the energy system and in particular building energy systems, their coordination and their control schemes. In addition, appropriate models and modeling techniques are investigated. Based on this, this thesis identified the use of a scenario-based consideration of the uncertainties to be best suited. Thus, the presented approach uses a rolling horizon optimization approach with a stochastic two-stage optimization problem, which considers several forecast scenarios in the optimization. It targets the minimization of the average operating costs of the building's energy system that occur in forecast scenarios. The presented approach uses a Mixed Integer Linear Programming (MILP) model of the building energy system and a probabilistic PV generation forecast. The developed stochastic two-stage rolling horizon optimization approach optimizes the joint operation of all devices and energy systems in the building concurrently and exploits the flexibility of the building's devices and energy systems while considering the constraints of devices and energy flows in a building. The first stage relates to the first time step in the optimization and uses a single point forecast, whereas the second stage relates to all other time steps. The goal of the optimization is then to minimize the operating costs in the first stage and the average operating costs that occur in the forecast scenarios in the second stage. In general, a large number of forecast scenarios lead to a good estimation of the range of possible PV generations but leads to high computation times [226][227, p. 8]. Consequently, probabilistic forecasts that provide low number of scenarios are needed. In the literature, this problem is not yet solved in building energy management.

With regard to the second research question, this thesis presents a probabilistic forecast, which generates several forecast scenarios based on historical data. This forecast provides different forecast scenarios based on a quantile regression. Its derived quantiles are used as forecast scenarios to approximate the range of possible electricity generation profiles of the photovoltaic system.

To investigate the application of optimization under uncertainty in building energy management, an exemplary building energy system has been defined. It provides the basis of the evaluation of the approach to the optimization under uncertainty presented as the main contribution of this thesis. Based on an analysis of the most commonly addressed devices in the literature, the considered building is defined with several controllable and non-controllable devices, namely a PV system, a controllable washing machine, a controllable Battery Energy Storage System (BESS), a controllable Micro Combined Heat and Power Plant (micro-CHP) and other non controllable appliances. In addition, electricity and heat consumption profiles are defined that mimic the consumption in a residential building. The building energy system has been modeled, providing individual models for the devices, a model for the interaction of the devices and the energy grid, and models for the

energy consumption and generation. The energy generation models include a probabilistic forecast of the electricity generation of a PV system, whereas the forecast of the energy consumption is defined to be perfect. The model of the building energy system is then used in the approach to the optimization under uncertainty. A similar model is used in a simulation of the building energy system, which is used to evaluate the optimization approach.

The developed stochastic two-stage rolling horizon optimization approach has been evaluated and compared to state-of-the-art as well as an artificial benchmark control scheme in building energy management in nine evaluation scenarios using a specific smart building configuration. In each evaluation scenario the feed-in tariff and the season are varied. Furthermore, an analysis of the tuning parameters of the presented approach is performed, analyzing the impact of the duration of the optimization window, the time step duration in the optimization and the number of forecast scenarios on the performance of the approach.

The results show that the presented approach yields an advantage over a state-of-the-art approach in some scenarios while in other scenarios simpler control schemes are superior. It is in particular suitable in scenarios with a high electricity generation from a photovoltaic system, because only in these cases the full load shifting potential of a battery energy storage system can be utilized. These scenarios either have a large photovoltaic system or have a high solar irradiation. Therefore, an application in a commercial building energy system has to be well-considered. In addition, this thesis provides a justification of the choice of single-point forecasts in building energy management systems in scenarios with limited photovoltaic generation. Furthermore, an investigation of the optimization times shows that the application of heuristics in combination with an associated modeling approach is justified and could improve the performance. Additionally, this work proposes a suitable approach to a PV generation forecast and motivates future investigations on the dependence of the forecast scenario generation on the performance of the control scheme.

This thesis extends the literature on BEMS by the investigation of optimization approaches that incorporate uncertainties in the forecast of energy generation and consumption and by proposing a specific approach. Furthermore, it supports future work with making the decisions on the approaches to the optimized operation of building energy systems and BEMSs by presenting an analysis and comparison of several control schemes in nine evaluation scenarios. The achieved lower operating costs support the realization of affordable energy supply. Furthermore, the load profiles that are the result of the optimized operation with respect to time-dependent tariffs are expected to contribute to the goals of DSM, for example the balancing of energy generation and supply or the support of the technical operation of the energy grids.

1.3 Related Publications by the Author

A list of related publications by the author of this thesis and their relation to this thesis is presented in Table C.1.

1.4 Structure

This thesis is structured as follows: In Chapter 2, background information on the topics addressed in this thesis is given. In particular, the relevant context of the energy system in Germany and Europe and building energy systems is presented. This includes an introduction to their coordination and management and in particular building energy management and the respective BEMSs. Chapter 3 gives an introduction to the theoretical concepts and formulations related to the modeling of discrete time systems and their optimized operation by a rolling horizon optimization. In Chapter 4, the related work in the field of building energy management is presented and discussed. This includes related work on the modeling of building energy systems and their devices as well as related work on the optimization of the operation of building energy systems. Chapter 5 presents the rolling horizon optimization approach to the optimization of the operation of a building energy system that uses a stochastic two-stage optimization. This includes the description of the scenario, the building simulation, the model of the devices in the building and their interaction and in particular the stochastic two-stage optimization. In Chapter 6, an evaluation of the performance of the stochastic two-stage rolling horizon optimization is presented. The stochastic two-stage rolling horizon optimization is compared to a rolling horizon optimization that uses perfect predictions as well as approaches that use controllers for the BESS and the micro-CHP. Finally, Chapter 7 summarizes and concludes this thesis and gives an outlook to potential further research.

2. Background on Energy Systems

This chapter provides the relevant context on energy systems and in particular electric energy systems in Europe and Germany.

2.1 Energy Policy

The European Union (EU) energy policy pursues the following three objectives [55, Section II 28]:

1. Secure supply of energy.
2. Affordable energy.
3. Environmental sustainability.

These targets are also pursued by the energy policies of individual countries, e. g., Germany (§ 1 EEG [2]).

The energy system is built to achieve these three objectives. When working in the field of energy systems, e. g., by introducing new generation and consumption technologies, or control policies, the three objectives of the energy system listed above have to be respected. As a consequence, the participation in energy systems in the EU and Germany is regulated by law. Usually, this influences the application of new business models and technologies. The security of supply is secured while respecting the requirements on affordability and environmental sustainability [209].

2.2 Generation, Transmission, Distribution and Consumption of Energy

The main task of the energy system is to provide a secure supply of energy. In this context, energy typically means secondary energy that can be used by end users, i. e., the consumers.

The first step to provide secondary energy includes the conversion from primary energy to secondary energy. Primary energy is energy which has not been subjected to any conversion process. It includes, for example, energy from fuels, e. g., oil, coal, natural gas, or RESs, e. g., wind power, hydro power or solar radiation. Secondary energy is energy which has been subjected to conversion process in order to provide forms of energy that are easier to transport or use. It includes, for example, electricity, heat, cold or gasoline. This step is often called generation of energy or in the case of electric energy the step is called electricity generation [221, p. 53].

In a second step, the secondary energy has to be distributed to the consumers. To achieve this, often specialized transmission systems are used. Two prominent examples are the electricity and the gas grid.

In the final step, the energy is used to provide energy services [103] to the end user. Energy services include all services that are provided by the use of energy. They include heating, lighting, transportation and the operation of machines. The provision of these energy services is often called consumption¹ and the users of the services are called consumers [221, p. 53]. [52]

Because of the physical principle of conservation of energy, the amounts of energy generation and consumption in an energy system, e. g., in the German electricity grid, have to be equal at each point in time. Imbalances lead to a change in the frequency and to voltage deviations in the electricity grid. In particular, frequency deviations can damage devices in the energy system, for example by applying torsional moments to the axle in generators, and hence cause blackouts [221, p. 918]. Thus, the balance of generation and consumption is one of the main tasks of energy systems and various mechanisms are implemented to achieve this balance (see Section 2.9).

2.3 Energy Transition

As described in Chapter 1 and Section 2.1, the EU decided to target environmental sustainability and to change the energy generation towards RESs. This affects the energy system in two ways: Firstly, the generation changes from large power plants using fossil resources towards power plants using RESs like wind and solar power. However, wind and solar power are intermittent energy sources, calling for some sort of energy storage. The energy that is generated at times with a surplus of generation from intermittent RESs, has to be shifted in time to be released at times with a deficit of generation from RESs [42].

This can be motivated by investigating the residual load, i. e., the difference between the total electrical load and the electricity generation by renewables. If the residual energy is lower or equal to zero at all times, the energy system does not need conventional generation.

¹It has to be noted that because of the physical principle of conservation of energy, energy cannot be generated, consumed or lost. However, these terms are used in the field of energy systems, emphasizing the processes targeted by the energy system while omitting unwanted processes.

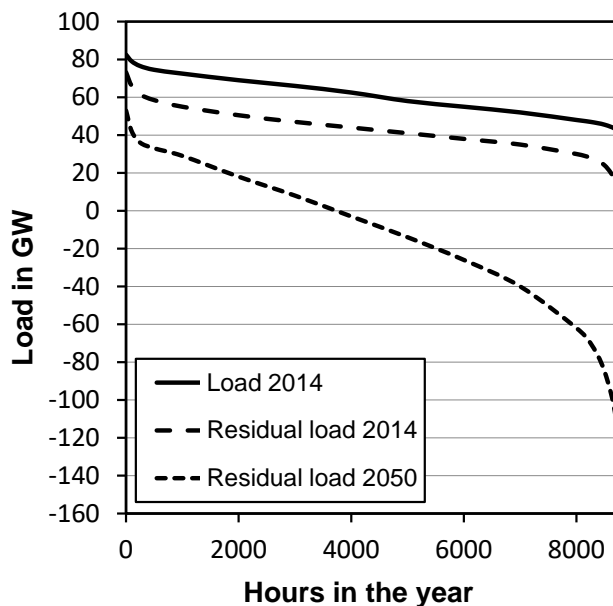


Figure 2.1: Measured total load per hour in the year 2014, measured residual load per hour in the year 2014 and predicted residual load per hour in 2050 in Germany. The hours are ordered from the hour with the highest load to the hour with the lowest load. The visualization is based on [218], the data of 2014 are taken from [40], the data of 2050 are taken from [112].

It has a surplus of generation by renewables. Typically, this is considered as the ideal case that is targeted by the energy policies as defined in Section 2.1. If the residual load is larger or equal to zero at all times, the energy system utilizes all renewable generation, but conventional generation is needed whenever the residual load is larger than zero. This is the case in Germany in the year 2014 [40].

Several studies state that the residual load in Germany is expected to become negative in some hours in a year while a similar number of hours with a positive residual load remain (see Figure 2.1). This indicates a need of storage in the German energy system to shift the energy surplus from hours with negative residual energy to times with positive residual energy [40, 112, 217].

Secondly, the average generation per power plants becomes smaller. This is a consequence of the increasing number of wind and solar power plants that are typically smaller than conventional plants like coal or nuclear power plants. This leads to a high number of devices that generate energy, often called DERs [125]. In contrast to the conventional power plants, most of the renewable generation is not located at the extra high or high voltage levels of the grid anymore, but at the medium and low voltage levels [92]. With rising numbers and share of installed capacity, this Distributed (Electricity) Generation (DG) [4] causes problems to the electricity grids, e. g., a reversal of power flows (see Figure 2.3) or an impact in the local voltage level [200].

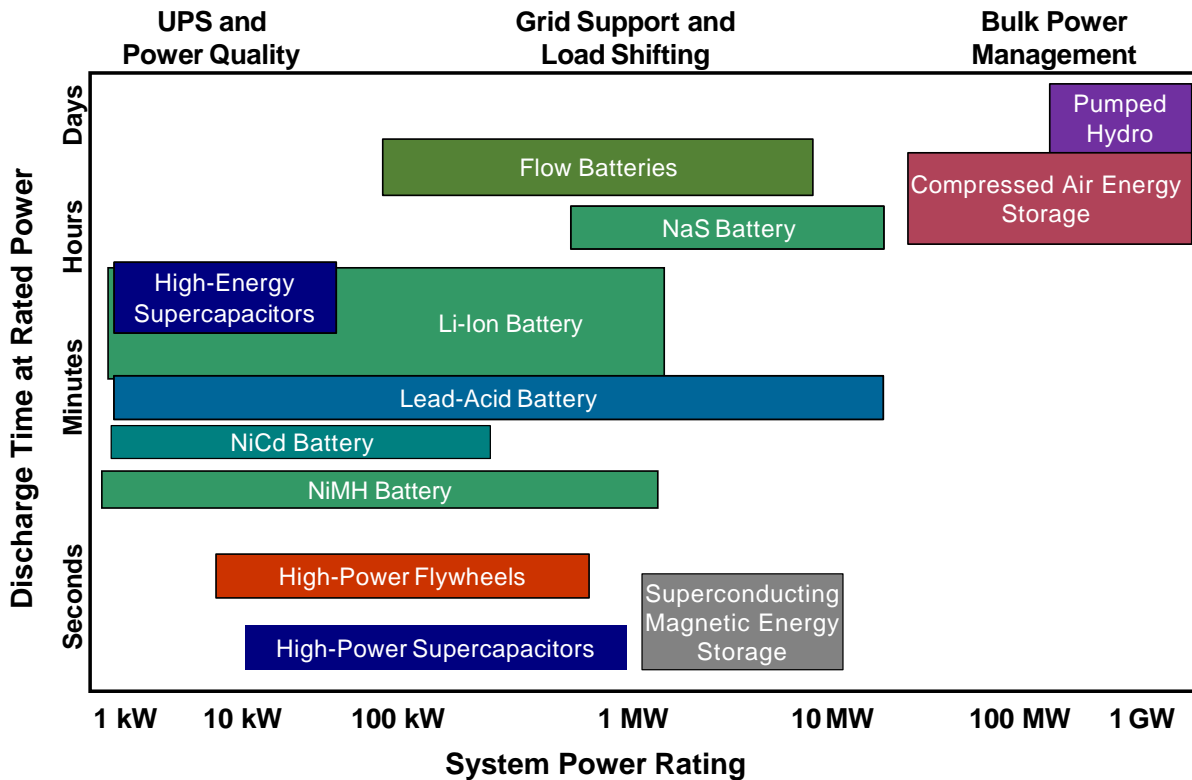


Figure 2.2: Visualization of the classification and applications of energy storage systems. The classification is based on the power rating and the discharge time at the rated power (based on [122] and [8, p. 29]).

2.4 Energy Storage

As described above, a high penetration of RESs requires Energy Storage Systems (ESSs) [46]. Various technologies have been developed to store energy from RESs [42, 46, 122, 249], each focusing on a different application. ESSs differ in the energy they are supposed to store, e.g., electric energy, chemical energy, thermal energy, potential energy, kinetic energy or chemical energy. Often energy storage involves conversion processes, converting electric energy to forms of energy that are easier to store. This leads to conversion losses and thus to a reduced efficiency.

2.4.1 Electrical Energy Storage Systems

Electrical energy storage systems are ESSs designed to store electricity. Often, these systems do not store the electricity itself, as it is done by a capacitor, but use conversion processes to store types of energy that are easier to store. Examples are BESSs that store chemical energy and pumped hydroelectric energy storage systems, which use potential energy.

In general, electrical energy storage systems can be categorized by power rating, i.e., the maximal charge and discharge values, and storage capacity [46, 122, 249]. Poten-

tial applications range from the large scale, or sometimes called bulk, generation and transmission-related systems to systems installed in residential buildings [46]. Vazquez et al. [249] and Chen et al. [46] summarize various applications of ESSs, including:

Load Leveling Load leveling refers to the use of electricity stored during times of low demand to supply peak electricity demand, which reduces the need to draw on electricity from peaking power plants or increase the grid infrastructure [249].

Energy Arbitrage Energy arbitrage refers to earning a profit by charging electrical energy storage systems with cheap electricity when the demand is low and selling the stored energy at a higher price when the demand is high [249].

Primary Frequency Regulation This application refers to the utilization of energy storage systems to provide grid frequency stability support [249].

Voltage Regulation Several techniques are used to mitigate several undesired grid voltage effects at the end-user level [46, 249].

Power Reliability Storage provides emergency power and thus enables an uninterruptible power supply in cases of blackouts [46].

Forecast Hedge Storage mitigates shortfalls in wind or solar energy generation predictions prior to required delivery, thus reducing volatility of spot prices and mitigating risk exposure of consumers to this volatility.

Even though, the definition and naming of application cases is not always consistent in the literature (cf. [46, 249]) and the application cases sometimes overlap, the coverage of the application cases is similar. In Figure 2.2, various storage technologies are arranged depending on their power rating as well as their discharge time. Based on this inconsistency, they have been further categorized into three application cases [8, p. 29][122]: Uninterruptible Power Supply (UPS) and power quality, grid support and load shaping, and bulk power management. In this figure, building energy management, as targeted in this thesis, is located between UPS and power quality, and grid support, load shaping, ranging from a power rating of 1 to 100 kW and a discharge time of minutes. In the meantime, lithium-ion batteries are more and more popular than Lead-acid batteries.

2.4.2 Thermal Energy Storage Systems

In buildings, thermal energy storage systems are commonly used. In contrast to electrical energy storage systems, technical solutions for thermal energy storage systems do not use conversion processes but store the thermal energy directly [62]. In the simplest case the thermal energy, i. e., the heat, is stored by raising the temperature of a specific material. Dependent on the temperature and the application case, several materials are common. The most common material is water. There are direct methods, where water is heated directly, and there are indirect methods where storage material is heated up and the needed hot water is heated up by flowing through that hot material, e. g., stones or salt. More

Table 2.1: List of common classes of electricity grids and assigned levels and tasks. Common values in the German electricity grid [221, p. 39].

Class	Levels	Voltage	Task
Transmission grid	Extra high voltage	380 kV, 220 kV	Transmission
	High voltage	110 kV	Subtransmission
Distribution grid	Medium voltage	10 kV, 20 kV	Distribution
	Low voltage	6 kV	Very large consumers
		0.6 kV	Large consumers
		0.4 kV	Small consumers

advanced approaches use the change in phase that occurs as a consequence of the deployed heat [228], e. g., Phase-Change Materials (PCMs).

Similar to electrical energy storage systems, thermal energy storage systems are used to decouple the generation and consumption of thermal energy. Hence, allowing for application cases similar to ones of electrical energy storage systems. These application cases become increasingly interesting when the heat and electricity systems are coupled, e. g., by the application of electric heaters or Combined Heat and Power Plants (CHPs). These systems are called multi-modal energy systems [163] or multi-energy systems [159].

2.5 Electricity Grid

The electricity grid connects electricity generators with consumers and takes care of transmission, distribution and voltage transformation. Typically, the electricity grids can be separated into two classes: the transmission grids and distribution grids. Each class can be divided into two levels, resulting in four levels: the extra high, the high, the medium and the low voltage level. The levels differ in voltage, power and task (see Tables 2.1 and Figure 2.3). Even though, this classification holds in the EU, the specific technical implementation of the electricity grid differs between countries. [221, p. 37]

Except for specific lines, the European electricity grid is an interconnected Alternating Current (AC) grid using a synchronized frequency of 50 Hz. This has the advantage of connecting numerous generators and power reserves improving reliability as well as allowing for an economy of scale. [221]

The transport of the electricity via the electricity grid is restricted. Firstly, the lines have limited transmission capacities. This introduces the need of taking the topology of the grid as well as the spatial allocation of generators and consumers into account. Secondly, line impedances are larger than zero. Consequently, energy flows lead to energy losses and voltage deviations. [221]

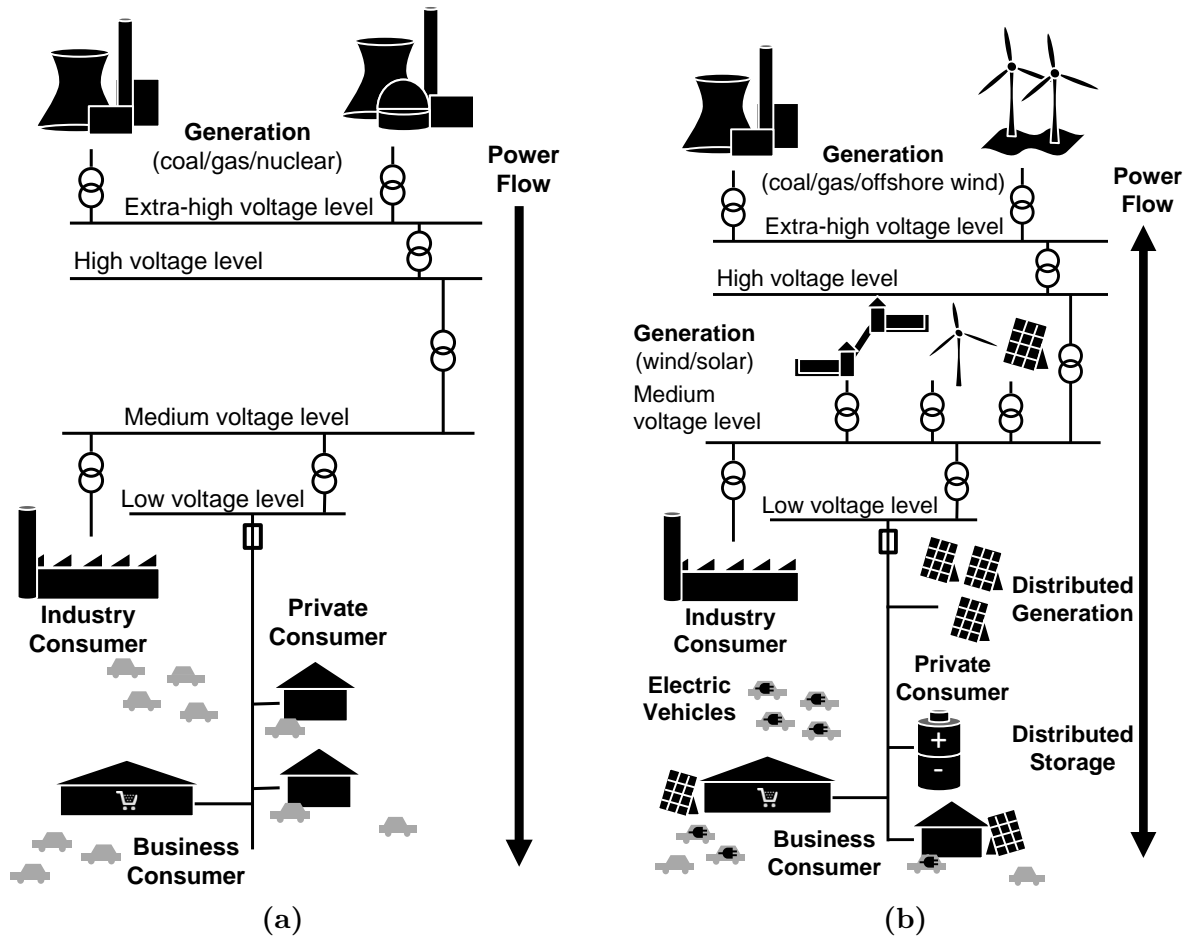


Figure 2.3: Visualization of the general layout of electricity network as well as the types and their respective location of electricity generation and consumption before (a) and after the energy transition (b).

2.6 Microgrids

Microgrids are a special kind of electricity grid that become more and more interesting in the context of DERs. However, the term *microgrid* is defined in various ways. The two most common definitions are given by the U.S. Department of Energy Microgrid Exchange Group and the CIGRÉ C6.22 Working Group. The former defines a microgrid as follows:

“A microgrid is a group of interconnected loads and distributed energy resources within clearly defined electrical boundaries that acts as a single controllable entity with respect to the grid. A microgrid can connect and disconnect from the grid to enable it to operate in both grid-connected or island-mode.” [64]

The definition of the CIGRÉ C6.22 Working Group reads as follows:

“Microgrids are electricity distribution systems containing loads and distributed energy resources, (such as distributed generators, storage devices, or controllable loads) that can be operated in a controlled, coordinated way either while connected to the main power network or while islanded.” [50]

Both definitions highlight the clearly defined boundaries of the electrical grid and some sort of balancing mechanism of local generation and consumption, leading to some sort of islanding capability. The grid is limited to a small spatial area and only a few distinct coupling points to a higher-level electricity grid are assumed.

Because of these special properties, Katiraei et al.[131] state that “Depending on the type and depth of penetration of distributed energy resource (DER) units, load characteristics and power quality constraints, and market participation strategies, the required control and operational strategies of a microgrid can be significantly, and even conceptually different from those of the conventional power systems”. The reasons they list for their statement can be summarized as:

- Significant degree of imbalance due to the presence of single-phase loads and/or DER units.
- Noticeable amount of “noncontrollable” energy sources, e. g., wind-based units.
- Presence of short- and long-term energy storage units.

Building energy systems that are the focus of this thesis are also referred to as a specific kind of microgrid [131]. Because of that, the approaches to the operation and management of building energy systems and other microgrids are often related and comparisons can be valuable.

2.7 Smart Grid

In addition to the energy transition, the digitization enables new approaches to tackle the challenges in the energy systems and energy grids. The most famous approach is

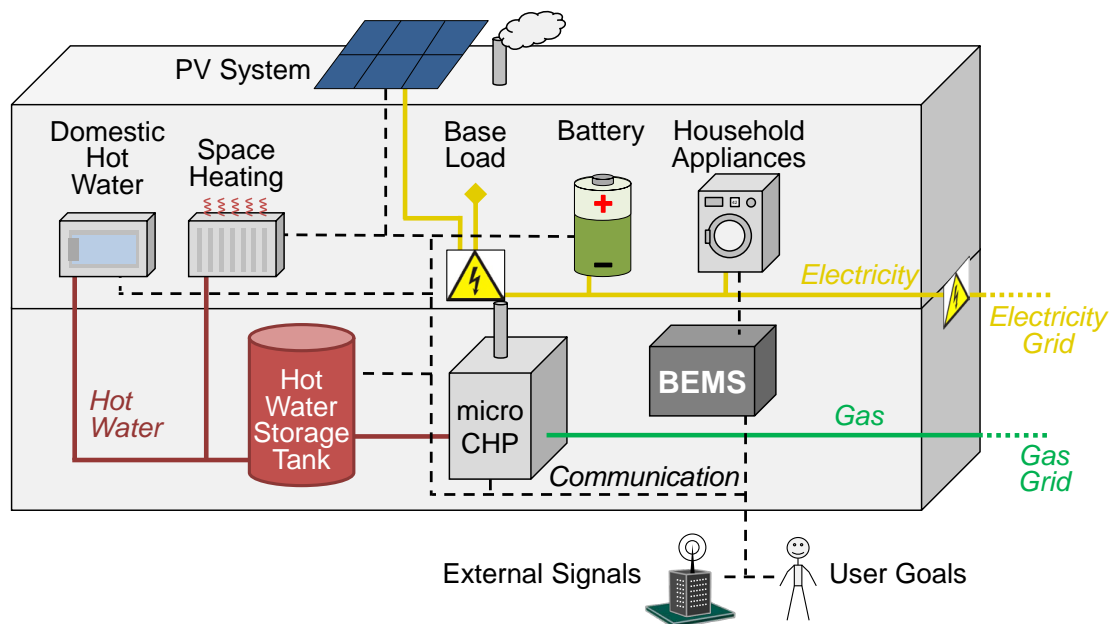


Figure 2.4: Scheme of an exemplary smart building equipped with an Energy Management System (EMS) (based on [165]).

the provision of communication networks to the energy grids to provide data for decision making. This combination of an energy grid and a two-way communication network between the utility and the consumer is commonly called smart grid [52]. The existence of communication networks allows for various applications, e. g., advanced management and control services, advanced grid reliability analysis, failure protection, and security and privacy protection services [75].

2.8 Building Energy Systems

In 2017, residential and commercial buildings caused about 40% of the final energy consumption² in the EU [63, p. 174]. This share motivates the close investigation of building energy systems. While residential and commercial buildings differ in the temporal distribution and amount of energy consumption, they share the need for heat, cold and electricity. This allows for similar modeling and operating strategies. Hence, in the following, the term *building energy system* is used for residential and commercial buildings (see Figure 2.4).

Traditionally, building energy systems consist of local energy grids and consumers, commonly in the domains of natural gas, hot and chilled water, and electricity. The corresponding devices are designed to provide the energy services desired by the residents, e. g., heating, cooling, lighting, cooking or entertainment. While the generation of heat and cold is a

²Sum of the residential and the service sector.

traditional task of building energy systems, electricity generation systems have only become popular in recent years. This results from the availability of economic PV systems as well as the increasing cost-effectiveness of CHPs, in particular micro-CHPs, which are CHPs with a maximum electricity generation of 50 kW [1]. In addition to the introduction of local generation, the presence of other new technologies changes building energy systems, notably Electric Vehicles (EVs), BESSs, smart electric heaters, micro-CHPs and heat pumps. Except for buildings in remote locations [86], buildings are typically connected to electricity grids, i. e., in the low or voltage level, as well as heat or natural gas grids.

While the design of building energy systems, i. e., the dimensioning and choice of devices, is a field of research on its own, this thesis focuses on the operation of building energy systems. In this context, four goals are targeted in recent research: energy efficiency, cost reduction, the integration of renewables and potential provision of ancillary services [20, 195][163, p. 76].

In addition to the operating costs, the self-consumption rate [154, 258] and the self-sufficiency rate [163, p. 13] are performance indicators commonly used in the literature. The self-consumption rate is defined as [163, p. 13]:

$$\text{self-consumption rate} = \frac{\text{total generated energy} - \text{fed-in energy}}{\text{total generated energy}}. \quad (2.1)$$

The self-sufficiency rate is defined as [163, p. 13]:

$$\text{self-sufficiency rate} = \frac{\text{total generated energy} - \text{fed-in energy}}{\text{total consumed energy}}. \quad (2.2)$$

This thesis targets the cost reduction by an optimized operation of the building's energy system. The increase of energy efficiency, the integration of renewables and ancillary services are considered based on their potential contribution to the cost reduction. The self-consumption rate and the self-sufficiency rate will be used to indicate consequences of the approach presented in Chapter 5.

2.9 Coordination and Management

Various coordination mechanisms and management systems are used to match generation and consumption of electricity. The mechanisms described in this section refer to the German energy system.

2.9.1 Electricity Trading

To cover their electricity demand, consumers have to buy electricity from power plant operators or electricity retailers. Depending on the amount of electricity and the maximum power that is needed, there are several alternatives to buy electricity [221, p. 962].

Over the Counter Trading

Consumers can buy the electricity directly from the power plant operator. This process is called over the counter trading, a trade between two parties without any supervision of a market place. Typically, this mechanism is used by large consumers or retailers to buy a basic supply of electricity. Contracts are made for a long time period with fixed consumption schedules [270, p. 283].

Electricity Market

Electricity markets provide platforms to trade electricity. This is done by trading specified products. The definition of the electricity markets and the specified products depends on the corresponding countries and energy systems. The largest energy market in Europe is the European Energy Exchange (EEX), where deals reaching up to six years in the future can be closed. Electricity for the near future can be traded at the EPEX SPOT exchange, most commonly at the day-ahead and the intraday markets.

Typically, the access to electricity markets is heavily regulated, limiting the trading to large electricity consumers, power plant operators and electricity retailers [270, p. 269].

End User Supply

End-users like households or small and medium-sized enterprises typically buy the electricity from electricity retailers. Since the consumers do not have to provide a prediction of their consumption, the electricity retailer has to predict the consumption on its own in order to buy the needed amount of energy beforehand [221, pp. 962].

2.9.2 Electricity Tariffs

The simplest electricity tariff has an energy price that does not depend on the time of use. This means that the electricity consumption of an end-user is charged based on the annual energy consumption. In addition to this simple electricity tariff, other tariffs have been used by the electricity retailers, in particular, time-dependent energy prices. Time-dependent energy prices can be divided into three categories [150, p. 273]: Time-of-use (TOU) prices, Real-time Pricing (RTP), Critical Peak Pricing (CPP).

Time-of-use Pricing TOU tariffs define different time periods, each having a different energy price. The resulting price profile is typically defined for a rather long time period, e. g., one year. The number of time periods is often limited to a few periods, e. g., peak, partial-peak, and off-peak. The daily price profiles can vary between seasons and weekdays. TOU tariffs are used to incentivize load shaping and do not necessarily reflect the market prices [53, p. 203].

Real-time Pricing RTP also uses price profiles. However, RTP uses more time periods than TOU pricing and the price profiles are defined for shorter time periods, e. g., one day, and are regularly communicated at shorter notice, e. g., one day ahead. RTP tariffs reflect the current market prices. [53, p. 204]

Critical Peak Pricing CPP extends TOU and RTP tariffs by adding event based price changes. The price changes are introduced based on specific trigger conditions and are communicated at a short notice, e. g., minutes or hours ahead. CPP may reflect the current state of the electricity grid as well as the current market prices [150, p. 273].

In addition to energy prices, capacity prices exist. Capacity prices depend on the power drawn from the grid. Two types of capacity prices are common: Firstly, a fee that depends on the maximum power drawn from the grid during a specific time period. Secondly, a power price that varies the energy price based on the power drawn from the grid. For example, Allerdig [9] notes energy prices that are dependent on the power drawn from the grid. More precisely, the energy price increases when the power drawn from the grid is higher than a specific power value. The specific power value is called power limit.

Especially the increasing popularity of small PV systems (see Section 2.8) increases the number of end users that do not only consume but also generate and feed-in electricity. The electricity that is fed into the grid is sold to energy retailers. To support the generation of electricity from RESs, this sale is subsidized in some countries. Similar to TOU electricity tariffs, time-dependent feed-in compensations are a viable method to value distributed generation [72, 179]. Even though time-dependent feed-in compensations are not yet popular in Europe or Germany, they are used in other areas like Victoria, Australia [72].

This thesis picks up on both of these approaches, TOU tariffs and time-dependent feed-in compensations. A more detailed description and motivation of the tariffs that are used in this thesis are presented in Chapter 5.

2.9.3 Balancing Groups and Power Plant Scheduling

As described in Section 2.2, the generation and consumption have to be equal at any time. Since the prediction of the electricity consumption of stochastic consumers is uncertain, imbalances will occur inevitably. Therefore, the electricity providers group consumers to improve the predictions. These improvements are based on the superposition of the stochastic behavior of the consumers, creating consumption profiles that are easy to predict. In a next step, electricity is bought from the power plant operators to match the expected consumption. Based on the expected consumption profiles, the power plant operators schedule their power plants to provide the requested electricity cost-effectively. The sum of the involved consumers and generators is called balancing group. Here, it is important to note that a balancing group is a virtual aggregation that aims at easing the billing process. [221, p. 800]

To incorporate the topology of the grid, the balancing group managers have to send the expected load and generation profiles for the next 24 hours to the grid operators, which then estimate possible violations of the constraints of the electricity grids, e. g., overload of lines based on limited transmission capacities. If necessary, the grid operators request a redispatch of the scheduled power plants to solve the expected problems. Even though the

redispatch solves the expected problems, the new schedules can lead to higher electricity costs [221, pp. 792].

The manager of the balancing group, e. g., the electricity retailer, is responsible to ensure the balance of generation and consumption in the balancing group. The equality is monitored by the grid operators. If necessary, they have to initiate measures to balance the generation and consumption. [221, p. 800]

2.9.4 Operating Reserve

In case of deviations of generation and consumption, the operating reserve provides short-term control power to balance generation and consumption. It is important to note that there is positive and negative control power. Provision of positive control power describes the additional feed-in of electricity (or, equivalently, a reduction of consumption) while provision of negative control power describes a reduction of the feed-in of energy (or, equivalently, an increase of consumption). Dependent on the time between request and provision, three classes of operating reserve can be distinguished [221, p. 800]: primary, secondary and tertiary reserve.

Primary Reserve

Primary reserve provides control power independently and automatically dependent on the current power frequency. The control power has to be provided within 30s and a provision of up to 15 min has to be guaranteed. In the case of electrical machines, the provision of primary control power is done by adapting the rotational speed of the generators. The primary reserve is provided for the entire European grid system [221, p. 738]. Primary reserve is also called Frequency Containment Reserve.

Secondary Reserve

Similar to primary reserve, the secondary reserve generates control power independently and automatically dependent on the current power frequency and the balance of the control area. In case of need, the full control power has to be provided after 5 min. In contrast to the primary reserve, the secondary reserve is organized by the grid operators individually. In the German power system this task is done by the managers of the four control areas [221, p. 738]. Secondary reserve is also called Frequency Restoration Reserve.

Tertiary Reserve or Minutes Reserve

Tertiary reserve has to be provided after 15 min. In contrast to the primary and secondary reserve, the tertiary reserve is retrieved individually when needed. The retrieval is performed by the grid operator, using a specific signal, e. g., via telephone [221, p. 738].

2.9.5 Demand Side Management and Demand Response

In addition to the control of power plants, the demand side can also be controlled to achieve the balance of generation and consumption. Traditionally, utilities influence customers in ways that will produce desired changes in load shapes. The planning and implementation of these activities is called DSM [90, 91]. In this context, Gellings [91] defines six load-shape objectives: peak clipping, valley filling, load shifting, strategic conservation, strategic load growth and flexible load shape.

In the context of energy transition and the predicted decrease of large-scale power plants and increase of DERs (see Section 2.3), Palensky et al. define DSM differently [195]. They propose: “While DSM was ‘utility driven’ in the past, it might move a bit towards a ‘customer driven’ activity in the near future.” [195]. They define four categories of DSM [195]: Energy Efficiency (EE), Time of Use (TOU), DR and Distributed Spinning Reserve. This idea has been continued and enhanced in the literature, e. g., by [9, 163, 215, 240]. The four categories are shortly described in the following paragraphs.

Energy Efficiency Energy efficiency measures on the demand side focus on improving the energy efficiency of buildings, i. e., reducing the quantity of energy used per unit service provided [52]. Energy efficiency measures are also defined in ISO 50001 [61], which also defines Energy Management Systems (EMSs) to implement concrete measures.

Time of Use Time of use refers to the use of TOU and RTP tariffs. The use of time-dependent tariffs targets on penalizing the electricity import from the grid in certain periods in time, e. g., in the evening, while rewarding the electricity import from the grid in other periods, e. g., periods of high renewable generation, by lower prices [195]. The use of TOU and RTP tariffs is supposed to introduce a change in energy consumption by the customer, especially in combination with automated EMSs.

Demand Response Demand Response (DR) refers to various measures that incentivize the demand side to adapt their consumption in order to support the electricity system or reflect market conditions [52, 195]. Even though the term *demand response* suggests the limitation to demand and energy consumption, often DR measures also include the adoption of the local generation or the sum of the local generation and consumption [163]. The measures of load adaption can be categorized using the load-shape objectives defined by Gellings [91]. Typically, they include the scheduling of shiftable loads, i. e., devices of which the operation can be shifted in time, e. g., intelligent appliances, CHPs [9, 163], heat pumps [146] or EVs [181], or the usage of energy storage systems, e. g., batteries [179] or thermal energy storage systems, e. g., Hot Water Tanks (HWTs) [9, 163].

Distributed Spinning Reserve Distributed spinning reserve aims at supporting the providers of ancillary services by imitating their behavior. On the demand side, this means that load can be reduced or increased in dependence on the grid frequency [195].

2.10 Flexibility in Energy Systems

The balancing of the generation and consumption in an energy system typically uses the flexibility of energy systems [18]. Thus, DSM and DR are often linked to the flexibility of the energy system. The term *flexibility* is defined in various ways, depending on the domain of the one who defines the term as well as the concrete application cases that are investigated.

The definition of the CEN-CENELEC-ETSI Smart Grid Coordination Group [45] reads as follows:

“The flexibility in demand and supply in the context of Smart Grids [...] covers the changes in consumption/injection of electrical power from/to the power system from their current/normal patterns in response to certain signals, either voluntarily or mandatory.” [45, p. 12]

Here, the flexibility is defined as deviations from the usual behavior of demand and supply. Roossien (2010) [212] and Neugebauer et al.(2015) [184] give the following similar definition:

“The possibility to influence the operation mode of energy producers or consumers by shifting production or consumption under given constraints is called flexibility[.]” [184, p. 1]

This definition emphasizes the ability to shift the operation of a producer or consumer.

In the context of this thesis, an additional definition [162] has been developed that is inspired by the energy flexibility corridor [100], flexibility space [32] and the control space [245], i. e., the set containing all feasible schedules for a source of flexibility (see Figure 2.5). The definition reads as follows:

“The flexibility of an energy system is the collection of valid combinations of system inputs and their state dependent outputs in terms of all energy carriers, i. e., all combinations that provide all mandatory energy services in a manner ensuring system stability.” [162]

To enable a comparison of the flexibilities of different energy systems, a quantitative description of the flexibility is needed in addition.

2.11 Optimization in Building Energy Systems

Typically, optimization in building energy systems focuses on the following topics:

1. Technical design of the energy system
2. Economic design of the energy system
3. Optimized operation of the energy system

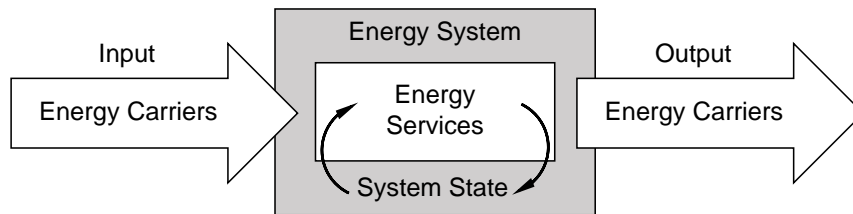


Figure 2.5: Visualization of an energy system that provides internal energy services based on its current state as well as the in- and outputs of energy carriers. The system’s flexibility is defined as the set of possible in- and output combinations that allow to provide the required energy services [162].

This work focuses on the third topic. However, all three topics often use similar modeling techniques, energy system models and optimization algorithms. Thus, an analysis is worthwhile.

The economic and technical design of a building energy system is the process of finding the best combination of technical devices and subsystems for the defined task of the building. Here, the best combination can be defined in several ways, targeting several goals, e. g., the provision of sufficient heat in cold winters or the provision of enough electric power. The most important goal for a building energy system is to provide the necessary energy services. The necessary energy services include all services that has to be provided by the building and its energy system. Depending on the purpose of the building, they may include lighting, heating, cooling, or the provision of electricity for plug loads. The goal of the economic design of building energy systems is to find a combination of technical devices that yield minimal costs while providing all necessary energy services.

In contrast, the optimization of the operation of the energy system targets the determination of optimal operation strategies or control schemes for all devices in the energy system. The three topics are described in the next sections.

2.12 Economic and Technical Design of the Building Energy Systems

To ensure the provision of necessary energy services, the technical setup has to be designed appropriately. Therefore, the expected usage, e. g., electricity consumption profiles, the environment of the building, e. g., ambient temperature profiles or solar radiation profiles, and the services, e. g., desired indoor temperatures, have to be defined. After this, the energy system has to be designed and its performance in the given scenario has to be evaluated (see Figure 2.6). This is done by solving an optimization problem in which the environment, the usage profiles, and the building model are fixed while the technical setup and the respective operation strategies are varied. The technical setup can include the parameters of the devices in the building energy system, e. g., the size of a BESS, the nominal power of a micro-CHP or the size of an HWT.

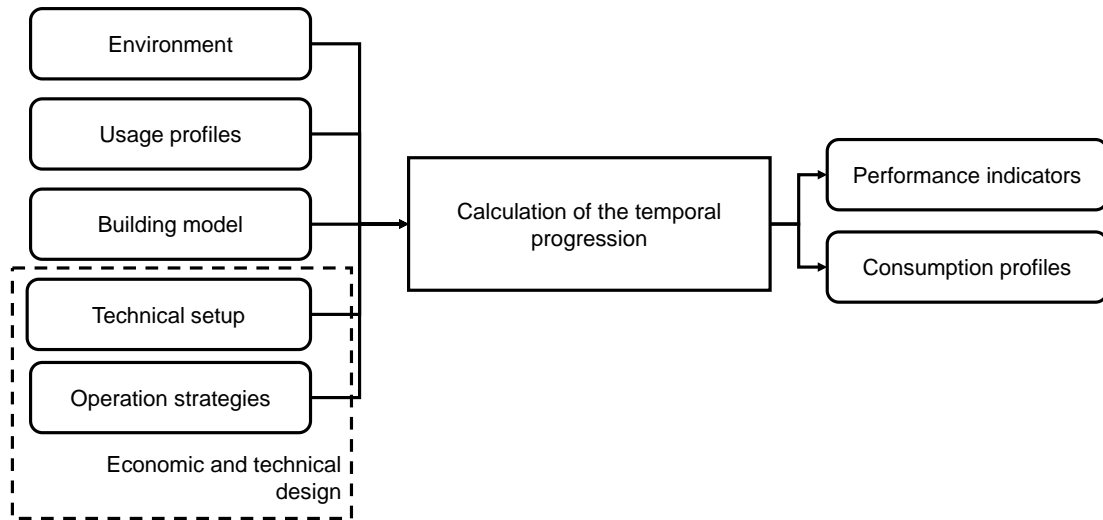


Figure 2.6: Economic and technical design of the technical setup using a simulation model. Typically, the environment, the usage profiles, and the building model are assumed to be fixed while the technical setup and the respective operation strategies are varied.

In the context of simulation-based models, various simulation programs for building energy systems have been developed [56], e. g., EnergyPlus [57], the Transient System Simulation Tool (TRNSYS) or ESP-r, that allow to evaluate the performance of a given energy system in a given scenario [152, 158].

In the technical design, an optimization is performed to find suitable technical setups for the building energy systems. This is important for buildings with specific needs, e. g., buildings in remote locations [86]. The technical design is often done in combination with an economic design. This means that the composition of an energy system is chosen to minimize the operating costs as well as the investment cost.

This can be done by formulating a two-stage decision problem [130, 222] (see Section 3.11.1). In the first stage an investment problem is formulated. In the second stage the optimization problem targeting the operation of the energy system is modeled. The second stage is similar to the optimization problem targeted in this thesis. The economic design is an off-line optimization problem that targets an optimal operation of an energy system over a relatively long temporal period. Typically, one year or more is modeled with a low temporal resolution of one hour or more. The optimization is performed to get an estimate of the expected energy costs over the lifetime of the energy system. The resulting schedules for the devices are not meant to be used for an actual control of the devices, because no uncertainties are taken into account. Even though the approach presented in this thesis is also utilizing a two-stage approach, it differs in the assignment of the stages. A more detailed description of optimization approaches that target a predictive operation of a building energy system is given in Section 2.13

Sometimes also multi-objective optimization approaches are used during the design phase of an energy system, taking technical, economic, environmental and additional goals into account [79, 204].

2.13 Optimized Operation of Building Energy Systems

The optimized operation of building energy systems is an on-line optimization approach that determines the optimal operation strategies or control schemes for all the devices in the building energy system. As shown in Figure 2.7, the operation strategies can be split into different tasks and the respective time-scales. In the context of this thesis, the optimized operation of the building energy system is restricted to the planning of the scheduling of the devices and their joint operation. When looking at Figure 2.7, this corresponds to the “Real-time Optimization” and the “Advanced Control” layers. This focus typically results in taking a time-scale of hours or minutes into account [20]. Hence, this thesis assumes that the control algorithms in the devices are fixed and cannot be changed by the optimization. The task of optimizing the operation of a building energy system is called building energy management. A system that enables energy management in buildings is called BEMS.

2.14 Building Energy Management Systems

To enable local DSM and provide DR measures in buildings, the local energy system has to be monitored and controlled. Systems that perform this task are called BEMSs. BEMSs monitor and control associated energy systems to achieve a given goal. In general, the goals are similar to the ones of DSM (see Section 2.9.5), often extended by goals addressing user comfort [20, 66]. Here it is important to note that such a system should not be confused with an EMS as defined by the ISO 50001 [61]. The ISO 50001 defines an EMS as follows:

“Set of interrelated or interacting elements of an organization to establish energy policy and objectives and to achieve those objectives.” [61]

BEMSs as considered in this thesis are more related to the VDI Guideline 4602 [251] that defines an EMS as a system that controls a corresponding energy system in order to achieve given goals.

“The energy management system is a control loop in which, starting with set targets, an energy task is performed and the results checked and evaluated. [...] The term ‘energy management system’ covers not only the organisational and information structures required for implementing the energy management system but also the technical resources needed for this (software and hardware, for example).” [251, p. 8]

In recent years, the design, development and evaluation of BEMSs have been active fields of research [20, 66]. In addition to BEMSs developed by researchers, commercial BEMSs occurred in recent time, e. g., the QIVICON Home Base by Deutsche Telekom, SMA Smart

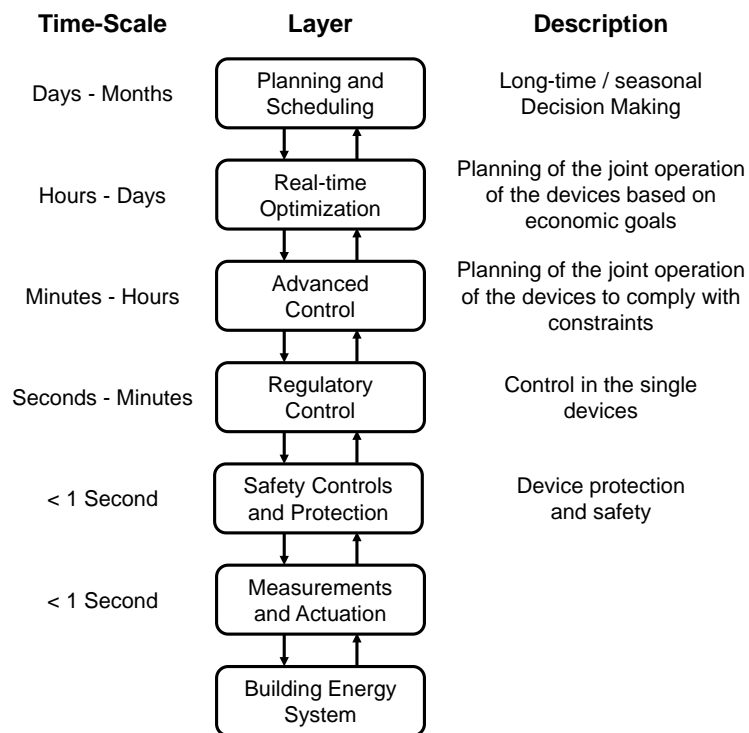


Figure 2.7: Layers for planning, scheduling, optimization, and control of building energy systems (based on [71, 224]).

Home, Innogy SmartHome or RWE easyOptimize. However, the commercial systems often focus on energy efficiency and user comfort goals and lack other features like load shaping to enable DR measures. The lack of sophisticated BEMSs deployed in the field, indicates that this field of research is still relevant.

BEMSs differ in the chosen software architectures as well as in their optimization and control [20, 66]. Some use rule-based approaches [65, 132], some use rolling horizon optimization [269] or model predictive control approaches [191], others use metaheuristics [9, 163, 165, 174, 179, 233]. Typically, BEMSs are used to plan the joint operation of devices in a building's energy system to minimize the operating costs while complying with constraints, e. g., minimal and maximal room temperatures. In addition to the central BEMS, other controllers may be present in energy systems in buildings. Examples are hysteresis controllers in water boilers or battery management systems that coordinate the cells in a BESS. The BEMS typically is limited to the joint operation of devices (see Figure 2.7).

This thesis presents a rolling horizon optimization that considers the uncertainty in the local generation and consumption by using a stochastic programming approach. The optimization targets the minimization of operating costs that are based on TOU tariffs as well as the maximization³ of the feed-in compensation from local generation of a micro-CHP and a PV system that is compensated based on a time-dependent feed-in rate. The optimization is used to determine the optimal schedule of the devices that can be controlled by the BEMS, i. e., a BESS, a micro-CHP and shiftable loads, e. g., shiftable appliances.

A more detailed description and motivation of the optimization approach for energy systems in buildings will be presented in Chapter 5. The next chapter introduces the theoretical concepts and formulations that are used in the optimization of the BEMS developed in this thesis.

Application of Building Energy Management and Operating Systems

To enable the application in real buildings, the actual devices have to be connected to the optimization algorithm. This means, the states of the devices have to be communicated to the optimizer and the determined schedules and control inputs have to be communicated back to the devices (see Figure 2.8). However, the communication with devices in building energy systems is not standardized. Therefore, the connected devices have to be abstracted to ensure compatibility with the optimization model.

The standardization of communication and modeling of devices in building energy systems is currently developing suitable approaches, e. g., the EEBus by the EEBus Initiative, but no solution has established itself as a gold standard.

A data interface enables to incorporate signals and data from external entities (see Figure 2.8), e. g., TOU tariffs or forecasts of the local generation and consumption as

³In this thesis, earnings from electricity that is fed into the grid are modeled as negative costs. Thus, the resulting optimization problem is a single-objective minimization problem.

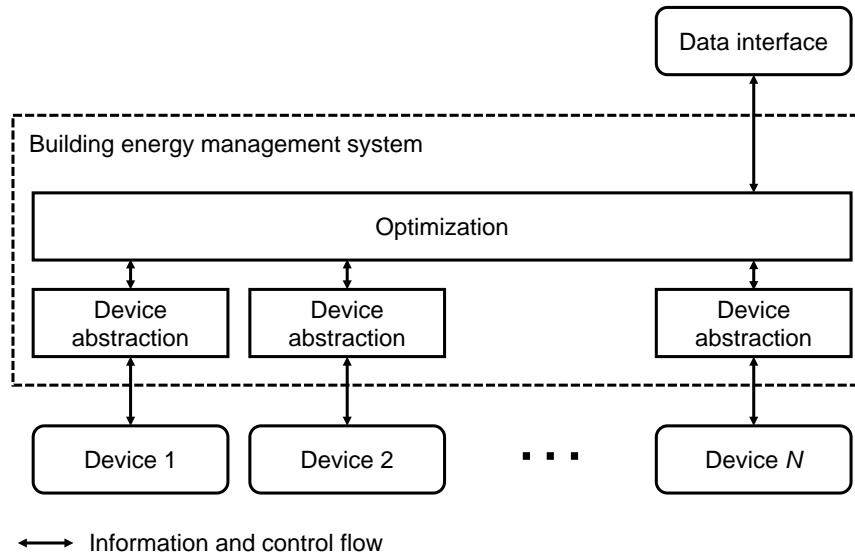


Figure 2.8: Visualization of the information and control flows in a BEMS that controls several devices. The communication between the optimization part and the devices has to be abstracted to enable a standardized and integrated optimization.

well as user preferences. In addition, the goals, i. e., the objective function, can be entered by the user. This can be done for example by specific interfaces, e. g., the Energy Management Panel (EMP) presented in [21].

BEMSs may be a part of a building operating system. These operating systems address ICT related services other than energy management. Examples are assistance, comfort, entertainment, health, information, safety, and security functionality [163, p. 86].

This thesis does not consider abstraction of devices and communication of data. Instead, this thesis focuses on evaluation using simulations. In addition, the configuration of the system, e. g., the adaption of the model to the real energy system and the specific devices and the parameterization of the model, is not addressed in this thesis. As part of this doctoral project, an approach that enables an efficient configuration of DERs and BEMSs has been developed and is presented in [175].

2.15 Coordination and Building Energy Management in Distribution Grids

BEMSs are a popular tool to enable customer driven DSM (see Section 2.9.5). They are widely seen as a component to realize and support smart grids. BEMSs are typically used to optimize the operating costs. They perform very well in the combination with TOU tariffs and other more complicated tariff structures like power prices (see Sections 2.9.2 and 4.2.1). However, the shaping of energy profiles has been identified to support the operation

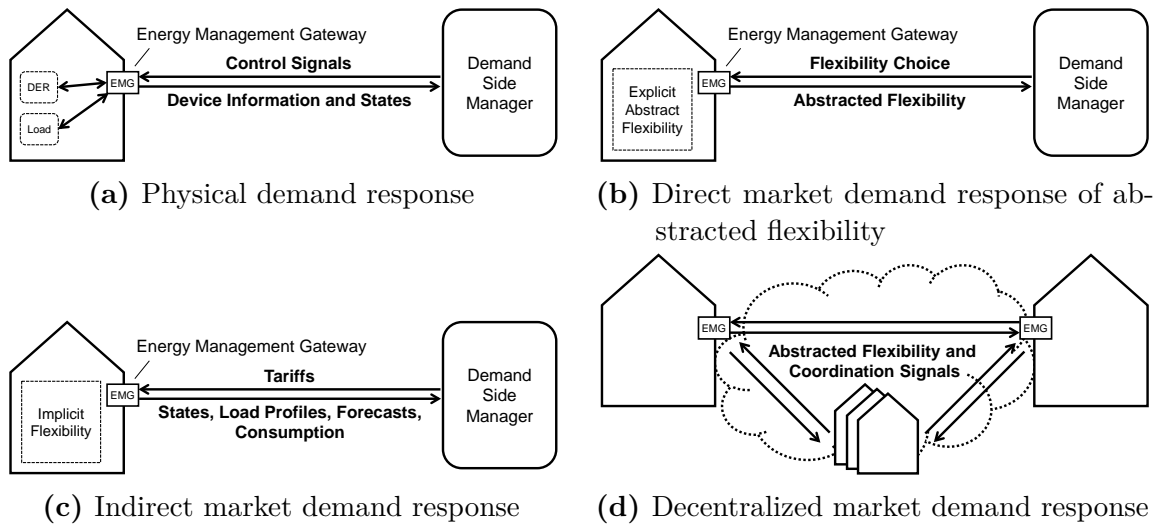


Figure 2.9: Visualization of four coordination patterns for the exploitation of flexibility that is provided to a demand side manager (based on [162]).

of distribution grids and to possibly provide ancillary services, in particular for electricity generation and consumption profiles.

To achieve these goals, a suitable coordination method for buildings equipped with a BEMS has to be introduced to the distribution grid. Here, different coordination methods have been proposed in the literature. As part of this doctoral project, one approach has been developed and is presented in [162]. It distinguishes between four categories (see Figure 2.9): physical demand response, direct market demand response, indirect market demand response and decentralized market demand response (see Figure 2.9).

Even though the coordination mechanisms do not cover the optimization in buildings directly, the investigation of possible future mechanisms can be worthwhile, in particular with regard to the design of BEMSs. Furthermore, BEMSs and an optimized operation of building energy systems can be seen as enabler of DR [229].

Physical Demand Response

Physical demand response refers to an approach in which the DERs, e. g., the devices in buildings, are controlled directly by a demand side manager, i. e., an entity that supervises the DR efforts (see Figure 2.9a).

An exemplary approach that presents a direct load control model for virtual power plant management has been published in [185]. Another approach to physical demand response has been presented in [120], targeting direct load control and interruptible load management to provide instantaneous reserves.

Direct Market Demand Response

Direct market demand response refers to approaches in which participants communicate their flexibility in combination with some sort of realization costs in some predefined abstracted way to a central demand side manager. In this process, the flexibility can, for example, be modeled as a list of possible load profiles. A load profile is a time series of energy consumption values, e. g., heat or electricity consumption values. Sometime load profiles are also called load traces [133].

This central entity then determines the optimal load profiles for all participants and sends them back, so that the participants can operate their energy systems in a way to realize the proposed load profiles (see Figure 2.9d).

Hirsch [113] presents such a schedule-based coordination mechanism to coordinate buildings in order to support the operation of a distribution grid, in particular to support voltage maintenance. This is achieved by obtaining an optimal schedule for the distribution grid using a multi-objective Evolutionary Algorithm (EA) to determine the optimal sum of the individual schedules. Hirsch presents an integrated approach that utilizes concepts of *Organic Computing* [180]. It includes ideas of the communication of data and implementation of the software.

Indirect Market Demand Response

In indirect market demand response approaches a TOU tariff is used to incentivize participants, e. g., buildings equipped with a BEMS, to perform load shaping. The demand side manager determines and distributes the TOU tariffs. However, the reaction of the participants is not known exactly. Therefore, models have to be derived that can predict the stochastic behavior (see Figure 2.9c), e. g., data-driven models.

Gottwald et al. evaluate household behavior under variable prices using simulations [96, 97, 98]. They utilize power-based surcharges and group prices to avoid herding effects. The results are compared to a physical demand response approach that solves an optimization problem which covers all participating devices at once.

Rios [210] presents a method that targets the tracking of a predefined target profile by giving households a RTP tariff-based incentive to shift their load profiles. However, the method uses some sort of iterative approach that is stated to be a closed-loop approach [210, p. 97].

Jargstorf et al. [124] investigate the user reaction on tariffs. The users are assumed to have PV generation and BESSs. They investigate the influence of different tariff schemes on the user reaction and possible consequences for the grid. In addition, tariff components related to the grid upgrade costs are investigated.

Decentralized Market Demand Response

In contrast to the approaches above, decentralized market demand response does not include a centralized entity that is responsible for the DR measures, e. g., a demand side manager

(see Figure 2.9d). Related approaches are based on distributed optimization approaches, like the one presented in [35], distributed auctions or peer-to-peer trading.

A peer-to-peer DR approach is presented by Mengelkamp et al. [168]. It presents a design of energy markets that uses blockchain-based local energy trading. The design is evaluated using a case study, the Brooklyn Microgrid.

Molina-García et al. [177] present a decentralized market demand response approach to enable a decentralized demand-side contribution to primary frequency control.

3. Theoretical Concepts of Modeling and Optimization

In this chapter, theoretical concepts and formulations related to the modeling of discrete time systems and their optimized operation by a rolling horizon optimization are introduced. In addition, an introduction to decision-making under uncertainty and the respective mathematical concepts is given. This is followed by the introduction of MILP and approaches to the solving of such problems. The chapter ends with a discussion of the approaches to the modeling of energy systems in buildings.

3.1 Model Building

The general approach to solving an optimization problem has several steps (see Figure 3.1). Firstly, an initial problem definition using a verbal description or technical specification has to be formalized. This step is often performed using mathematical relationships such as equations, inequalities and logical dependencies [260, p. 3]. The collection of all mathematical relationships is called *model*. Secondly, a suitable optimization algorithm has to be found to solve the problem. Depending on the problem, analytical or computer-based, numerical approaches can be used. If the problem cannot be solved in a given time, it sometimes has to be transformed to obtain a problem more suitable to be solved. [196, p. 5] However, it is important that the mathematical model describes the modeled system adequately. Where adequately should always be defined with respect to the research questions or the optimization objectives. Both goals, the ease of solving as well as the model quality are often opposing. This leads to a trade-off in the choice of the model.

3.2 Optimization

Typically, the task of finding optimal solutions is synonymous with finding the minimum or maximum of a given mathematical equation. The task of maximization can easily be

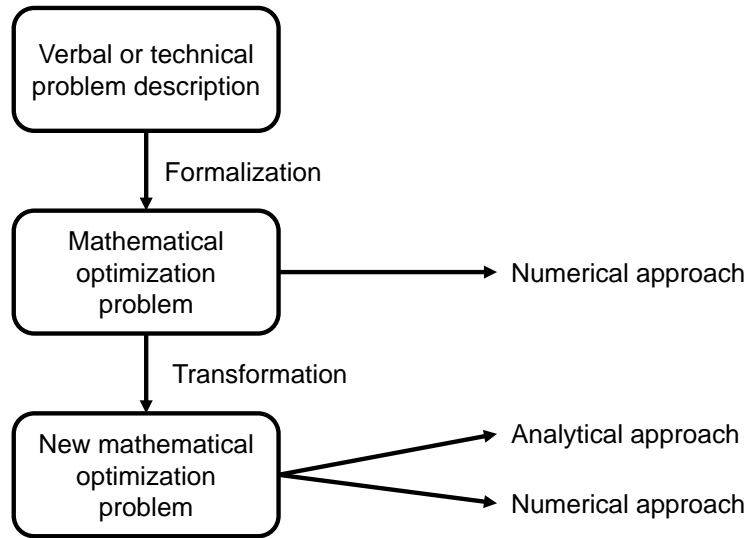


Figure 3.1: Process of model building and problem definition based on [196, p. 5].

transformed into the task of minimization. In this thesis, the term *optimization* is defined to be equal to the minimization of an optimization function.

An example of a generic optimization problem is given by [196, p. 11]:

$$\min_{\mathbf{x}} g(\mathbf{x}), \quad \mathbf{x} \in \mathbb{R}^n \quad (3.1)$$

subject to:

$$\mathbf{e}(\mathbf{x}) = \mathbf{0} \quad (3.2a)$$

$$\mathbf{i}(\mathbf{x}) \leq \mathbf{0} \quad (3.2b)$$

where g is the objective function that has to be minimized, \mathbf{x} is a vector of decision variables. Equations 3.2a and 3.2b are the equality and inequality constraints, respectively.

3.3 Off-line and On-line Optimization

When considering optimization problems, a distinction is made between off-line and on-line optimization. In the case of building energy systems, off-line optimization refers to problems that have to be solved during the design of the building energy system (see Section 2.12). In contrast, on-line optimization problems have to be solved during the run-time of the energy system to find the optimal operation schedule.

Off-line and on-line calculations impose specific requirements on the choice of the system model and the optimization algorithm. Often, off-line calculations are only performed once. Therefore, long calculation times can be tolerated. In contrast, on-line calculations are

typically performed regularly, and sometimes real-time requirements have to be considered. [196, p. 6]

According to this categorization, investment and operating problems as defined in Section 2.11 can be characterized as follows: The technical and the economic design of the energy system are off-line optimization approaches, while the optimized operation of the energy system that is targeted by this thesis is an on-line optimization approach.

3.4 Optimization of Discrete Time Systems

In the domain of BEMSs as defined in Section 2.14, energy systems are often modeled as discrete time systems. In the literature, this decision is not always motivated. However, discrete time models are well suited because of the time-discrete behavior of several devices, e. g., appliances, and because of the common time-discrete measurements of the local energy states and power flows.

The goal of BEMSs is to find optimal control inputs for the corresponding building energy system. Here, the optimality condition has to be defined by the designer of the BEMS. In general, the optimality condition can be defined as the minimum of an objective function J . In this thesis, the building energy system is described by a discrete time model. In general, the temporal progression of a discrete time model is described by the state equation [196, p. 343][102, p. 13][10, 12]:

$$\mathbf{x}_{t+1} = \mathbf{f}(\mathbf{x}_t, \mathbf{u}_t), \quad \forall t \in \{0, \dots, T-1\}, \quad (3.3)$$

with the state of the energy system $\mathbf{x} \in \mathcal{X} \subset \mathbb{R}^n$, the control input $\mathbf{u} \in \mathcal{U} \subset \mathbb{R}^m$ and the state transition map $f : \mathcal{X} \times \mathcal{U} \rightarrow \mathcal{X}$ that connects the time step t with the next time step $t + 1$ [12]. Here, T is the number of time steps that is of interest in the model and each time step has a duration of Δ_t . The time period considered in the optimization is called optimization window. In energy management, $\Delta_t \cdot T$ actually is the lifetime of the building energy system or a shorter time that allows making inferences about the performance in the lifetime of the building energy system. Here, often one year is chosen to include all seasons.

The following matrices can be defined to ease the reading [196, p. 344]:

$$\mathbf{X} = (\mathbf{x}_0, \dots, \mathbf{x}_T) \in \mathcal{X}^{T+1}, \quad (3.4a)$$

$$\mathbf{U} = (\mathbf{u}_0, \dots, \mathbf{u}_{T-1}) \in \mathcal{U}^T. \quad (3.4b)$$

Additionally, the temporal progression of the system (see Equation 3.3) can be subject to constraints involving both system states and control inputs:

$$(\mathbf{x}_t, \mathbf{u}_t) \in \mathcal{Y}, \quad \forall t \in \{0, \dots, T-1\}, \quad (3.5)$$

for some compact set $\mathcal{Y} \subset \mathcal{X} \times \mathcal{U}$ [12].

The task of the BEMS is to find the control inputs \mathbf{U}^* that minimize the objective function, $J : \mathcal{X} \times \mathcal{U} \rightarrow \mathbb{R}$ while fulfilling the constraints presented in Equations 3.3 and 3.5. The objective function has to be chosen by the designer of the BEMS. Common objectives in building energy management are the reduction of operating costs, carbon dioxide emission or energy consumption. A detailed list of common objectives in building energy management is presented in Section 4.2.1 and Table 4.1. Often, the objective function J is defined as a sum of stage costs $l(\mathbf{x}_t, \mathbf{u}_t) : \mathcal{X} \times \mathcal{U} \rightarrow \mathbb{R}$, i. e., the costs in each time step t (cf. [12]):

$$J(\mathbf{X}, \mathbf{U}) = \sum_{t \in \{0, \dots, T-1\}} l(\mathbf{x}_t, \mathbf{u}_t). \quad (3.6)$$

This leads to the optimization problem [10]:

$$J^* = \min_{\mathbf{u} \in \mathcal{U}^T} \sum_{t \in \{0, \dots, T-1\}} l(\mathbf{x}_t, \mathbf{u}_t), \quad (3.7)$$

subject to:

$$(\mathbf{x}_t, \mathbf{u}_t) \in \mathcal{Y}, \quad \forall t \in \{0, \dots, T-1\}, \quad (3.8a)$$

$$\mathbf{x}_{t+1} = \mathbf{f}(\mathbf{x}_t, \mathbf{u}_t), \quad \forall t \in \{0, \dots, T-1\}. \quad (3.8b)$$

In order to find the optimal control inputs, Equation 3.7 has to be solved. To do so, firstly, the building energy system has to be modeled as a discrete time system to satisfy Equation 3.8b and, secondly, additional constraints have to be formulated to obtain Equation 3.8a. Here, the optimization is performed only once dealing with a time period of $\Delta_t \cdot T$ that represents the lifetime of the building energy system. This approach of finding the optimal control inputs for a dynamic system based on a single off-line optimization is often called *optimal control* [196, p. 343].

3.5 Rolling Horizon Optimization

The approach outlined in Section 3.4 enables the calculation of control inputs that are optimal with respect to a given objective function. However, Equation 3.7 describes a rather long time period that may lead to a computationally challenging optimization problem. In addition, the approach presented in Section 3.4 is not able to react on possible deviations from the predicted temporal evolution of the system to the real system.

The rolling horizon optimization approach addresses both points. To make the problem computationally more tractable, the optimization window is reduced from T to N time steps $k \in \{0, \dots, N-1\}$ [10] with $N \ll T$ (see Figure 3.2). In so doing, the optimization window considers a time period that begins at $t_0 \cdot \Delta_t$ and ends at $t_0 \cdot \Delta_t + k \cdot \Delta_k$. Here, $t_0 \cdot \Delta_t$ is called start time of the optimization and the end time of the optimization window $\Delta_k \cdot N$ is called optimization horizon.

To differentiate between the variables in the rolling horizon optimization approach and the variables in the actual system, the symbols z and v are chosen instead of x and u to

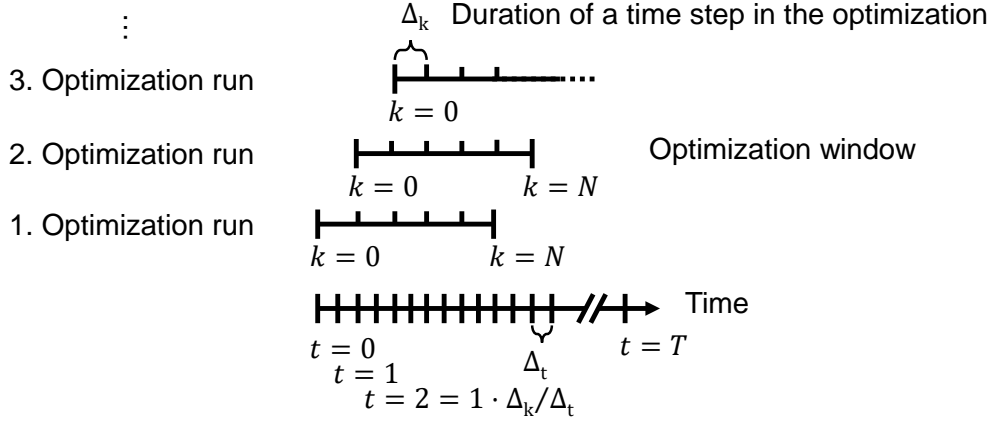


Figure 3.2: Visualization of the rolling horizon optimization approach. (based on [174])

denote the system states $\mathbf{z} \in \mathcal{X} \subset \mathbb{R}^n$ and the control inputs $\mathbf{v} \in \mathcal{U} \subset \mathbb{R}^m$ in the rolling horizon optimization approach¹. To ease the reading, the following matrices are defined [196, p. 344]:

$$\mathbf{Z} = (\mathbf{z}_0, \dots, \mathbf{z}_N) \in \mathcal{X}^{N+1}, \quad (3.9a)$$

$$\mathbf{V} = (\mathbf{v}_0, \dots, \mathbf{v}_{N-1}) \in \mathcal{U}^N. \quad (3.9b)$$

Here, \bullet_k defines the value of the respective variable at the time $t_0 \cdot \Delta_t + N \cdot \Delta_k$. Where, $t_0 \cdot \Delta_t$ is the starting time of the optimization window, Δ_k is the length of a time step in the optimization window, N is the number of time steps in the optimization and $\Delta_k \cdot N$ is the optimization horizon.

The resulting objective function is defined as:

$$J_N(\mathbf{Z}, \mathbf{V}) = \sum_{k=0}^{N-1} l(\mathbf{z}_k, \mathbf{v}_k) + C(\mathbf{z}_N), \quad (3.10)$$

with the terminal costs $C : \mathcal{X} \rightarrow \mathbb{R}$.

The initial system state in the optimization window \mathbf{z}_0 is initialized with the value of the current state \mathbf{x}_{t_0} :

$$\mathbf{z}_0 = \mathbf{x}_{t_0}. \quad (3.11)$$

This leads to the optimization problem [10]:

$$\min_{\mathbf{v} \in \mathcal{U}^N} J_N(\mathbf{Z}, \mathbf{V}), \quad (3.12)$$

subject to:

$$(\mathbf{z}_k, \mathbf{v}_k \in \mathcal{Y}, \quad \forall k \in \{0, \dots, N-1\}, \quad (3.13a)$$

$$\mathbf{z}_{k+1} = \mathbf{f}(\mathbf{z}_k, \mathbf{v}_k), \quad \forall k \in \{0, \dots, N-1\}, \quad (3.13b)$$

$$\mathbf{z}_0 = \mathbf{x}_{t_0}, \quad \mathbf{z}_N \in \mathcal{X}_N. \quad (3.13c)$$

¹In the actual definition of the optimization approach for energy systems in buildings that is presented in Chapter 5 this is done by marking the variables in the actual energy system with a tilde ($\tilde{\cdot}$).

with the terminal state \mathbf{z}_N being constrained to some set $\mathcal{X}_N \subset \mathcal{X}$. Based on Equation 3.11, the optimal system states \mathbf{Z}^* and the control inputs \mathbf{V}^* are dependent on \mathbf{x}_{t_0} [10].

When \mathbf{V}^* are found, the first control input is applied to the real system by setting

$$\hat{\mathbf{u}}_t := \mathbf{v}_0^*, \quad \forall t \in \{t_0, \dots, \lfloor t_0 + \frac{\Delta_k}{\Delta_t} \rfloor - 1\}. \quad (3.14)$$

In time step $\lfloor t_0 + \frac{\Delta_k}{\Delta_t} \rfloor$, the process is repeated and Equation 3.12 is solved with $\mathbf{z}(0) = \mathbf{x}_{\lfloor t_0 + \frac{\Delta_k}{\Delta_t} \rfloor}$ ². This allows the rolling horizon optimization approach to react on the current states of the real system. In addition, the optimization horizon is moved to a later point in time. This behavior of moving the optimization horizon further in time leads to the name *Rolling Horizon Optimization*.

In so doing, the problem defined in Section 3.4 can be approximated by finding the control inputs \mathbf{u}_t for all time steps $t \in \{0, \dots, T-1\}$.

The costs that result by applying the rolling horizon optimization \hat{J} are given by:

$$\hat{J}(\mathbf{X}, \mathbf{U}) = \sum_{t \in \{0, \dots, T-1\}} l(\hat{\mathbf{x}}_t, \hat{\mathbf{u}}_t), \quad (3.15)$$

with:

$$\hat{\mathbf{x}}_{t+1} = \mathbf{f}(\hat{\mathbf{x}}_t, \hat{\mathbf{u}}_t), \quad \hat{\mathbf{x}}_0 = \mathbf{x}_0, \quad \forall t \in \{0, \dots, T-1\}, \quad (3.16)$$

Here, the hat ‘ $\hat{\cdot}$ ’ indicates that \hat{J} is an estimation for J^* given in Equation 3.7 that uses the rolling horizon approach to determine the control inputs instead of solving the optimization problem for T time steps. The control inputs that are given by the rolling horizon optimization are used to simulate the temporal progression of the energy system based on the state equation given in Equation 3.3.

In Figure 3.2, a visualization of the process is presented. Depending on the scientific domain, this approach is called rolling horizon optimization, receding horizon optimization, on-line scheduling or Model Predictive Control (MPC) [20]. Following the terminology defined in Section 3.3, the approach presented in this section is categorized as on-line optimization.

As stated before, the approach presented in this section has various names. In the domain of control engineering it is called MPC. Here, it is important to note that the approach that is typically called MPC is *tracking* MPC. It differs from the approach pursued in this thesis.

This thesis presents an approach to the optimization of the operation of an energy system in buildings that is similar to Economic Model Predictive Control (EMPC).

Ellis et al. formulate the difference between *tracking* MPC and EMPC as follows [71, p. 5]:

²Here, $\lfloor \cdot \rfloor = \text{floor}(\cdot)$ denotes the floor function in the square bracket notation introduced by Gauss.

“The main difference between tracking MPC and economic MPC is that the tracking MPC problem is formulated with a tracking cost functional, while the economic MPC problem is formulated with an economic cost functional. The tracking cost functional usually uses a quadratic stage cost that penalizes the deviation of state and inputs from their corresponding steady-state, target, or reference values. However, the EMPC cost functional may potentially use any general stage cost that reflects the process/system economics. Since the idea of EMPC is to compute control actions that directly account for the economic performance, economic-oriented constraints may also be added.”

In other words, EMPC does not have the assumption that [11, 207]:

$$l(\mathbf{z}_k^*, \mathbf{v}_k^*) \leq l(\mathbf{z}_k, \mathbf{v}_k) \text{ for all admissible } (\mathbf{z}_k, \mathbf{v}_k), \forall k \in \{0, \dots, N-1\}. \quad (3.17)$$

where \mathbf{z}_k^* are the state vectors and \mathbf{v}_k^* are the control inputs that are optimal with respect to Equation 3.12.

Here, it is important to note that the choice of N and Δ_k has to be done by the designer of the rolling horizon optimization approach. However, the choice affects the performance of the rolling horizon optimization and the optimal choice is not obvious [88]. These parameters are called *tuning parameters* and the process of estimating the tuning parameters is called *parameter tuning* [88]. Typically, the tuning parameters are estimated in some sort of off-line optimization, i. e., before the operation of the system starts [88]. In [261], it is suggested that the optimization window should be chosen so large that further increment has no significant effect on the performance of the rolling horizon approach. Although, the optimization horizon and time resolution have to be chosen in a way that the computational effort to solve the optimization problem stays manageable [88]. In addition to off-line tuning method, self-tuning methods exist that update the tuning parameters during the run-time of the system in an on-line optimization [88].

3.6 Time-Dependent Parameters and Stage Costs

In practical application, the stage costs in the rolling horizon optimization (see Equation 3.10) can be dependent on time-dependent parameters. In building energy management, examples for time-dependent parameters are the electricity tariffs and the forecast of the local energy generation and consumption (see Figure 3.3). The time-dependent parameters described by the vector $\boldsymbol{\theta} \in \mathcal{B} \subset \mathbb{R}^p$:

$$l(\boldsymbol{\theta}_k, \mathbf{z}_k, \mathbf{v}_k) : \mathcal{B} \times \mathcal{X} \times \mathcal{U} \rightarrow \mathbb{R}. \quad (3.18)$$

The temporal evolution of the parameter vector $\boldsymbol{\theta}$, i. e., its value in every time step k in the optimization window, can also be dependent on the time of optimization t_0 , i. e., the point in time in which the optimization is performed.

$$\Theta = (\boldsymbol{\theta}_k, \dots, \boldsymbol{\theta}_{N-1}) \in \mathcal{B}^N. \quad (3.19)$$

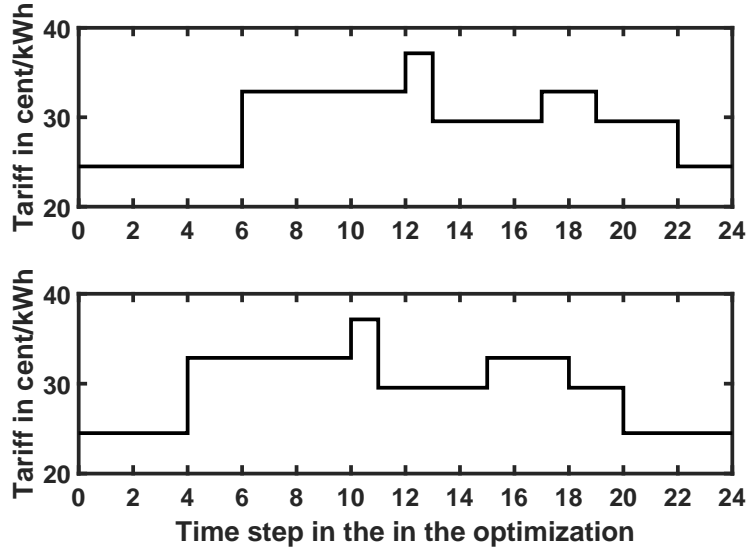


Figure 3.3: Visualization of time-dependent parameters. The two graphs show the temporal evolution of the electricity tariff in two different optimization runs. The electricity tariff is an example of a time-dependent parameter. The upper figure shows the electricity tariff in an optimization started at midnight and the lower figure shows the electricity tariff in an optimization run that is started two hours later.

In this case, the objective function (see Equation 3.10) can be formulated as follows:

$$J_N(\Theta, \mathbf{Z}, \mathbf{V}) = \sum_{k=0}^{N-1} l(\theta_k, \mathbf{z}_k, \mathbf{v}_k) + C(\mathbf{z}_N). \quad (3.20)$$

In the domain of building energy management systems, the constraints on the system states and the control inputs (see Equation 3.8a) can also be dependent on the time-dependent parameter vector θ :

$$(\theta_k, \mathbf{z}_k, \mathbf{v}_k) \in \mathcal{Y}_\theta, \quad \forall k \in \{0, \dots, N-1\}, \quad (3.21)$$

for some compact set $\mathcal{Y}_\theta \subset \mathcal{B} \times \mathcal{X} \times \mathcal{U}$.

This leads to the following rolling horizon optimization problem:

$$\min_{\mathbf{V} \in \mathcal{U}^N} J_N(\Theta, \mathbf{Z}, \mathbf{V}), \quad (3.22)$$

subject to:

$$(\theta_k, \mathbf{z}_k, \mathbf{v}_k) \in \mathcal{Y}_\theta, \quad \forall k \in \{0, \dots, N-1\}, \quad (3.23a)$$

$$\mathbf{z}_{k+1} = \mathbf{f}(\theta_k, \mathbf{z}_k, \mathbf{v}_k), \quad \forall k \in \{0, \dots, N-1\}, \quad (3.23b)$$

$$\mathbf{z}_0 = \mathbf{x}_{t_0}, \quad \mathbf{z}_N \in \mathcal{X}_N. \quad (3.23c)$$

It is important to highlight that this means that the optimization problem varies over time. Thus, the optimization problem is dependent on the time of optimization t_0 .

In the domain of BEMs, time-dependent electricity tariffs or time-dependent electricity generation or electricity and heat consumption are examples for the time-dependent parameter vector θ .

3.7 Approximation and Numerical Solution

It is important to highlight that the costs that result by applying the rolling horizon approach described in Section 3.5 (see Equation 3.15) are in general higher than the costs defined by Equation 3.7. However, as described in Section 3.5, the application of the rolling horizon approach is necessary in practical applications.

Often, it is not possible to find an analytic solution for the optimization problem in the rolling horizon approach (see Equations 3.15 and 3.22) [196, p. 24]. Hence, numerical methods have to be used to solve the optimization problem. It is often assumed that at least one solution for the problem exists even if this is not explicitly proven. In the domain of BEMs, MILP models are common [20]. The literature states that these models describe the building energy systems reasonably well and the time to solve the resulting optimization problems is often appropriate for the applications [20]. In addition, solvers exist that are easy to handle and work well out of the box, e.g., CPLEX or Gurobi. Typically, they use the *branch and bound* and *branch and cut* methods. These methods also are able to guarantee that the determined solution to an optimization problem is the global optimal solution. Methods that can give this guarantee are called exact optimization methods [213, p. 45].

To reduce the run-time of these methods, the optimization algorithm can be stopped before it has found the optimal solution. For example, this can be done after a given optimality gap³ [128, p. 95], i.e., the difference between the best-known solution to the optimization problem and the best solution to the relaxed linear problem found so far, or when a given time limit has been reached.

In addition to these exact optimization methods, heuristics can be used [230][213, p. 85]. Heuristics are optimization methods that use problem-specific knowledge to find a solution to an optimization problem. Heuristics cannot give a guarantee that they find the optimal solution. However, in practical applications approximate solutions often suffice. In addition to these problem specific heuristics, metaheuristics exist, can be applied to a wider range of problems [213, p. 92]. Examples for metaheuristics are genetic algorithms and particle swarm optimization. Both optimization methods have been used in building energy management, for example in [165, 198].

³The optimality gap is sometimes called duality gap, integrality gap or MILP gap (cf. [104, p. 557]).

3.8 Decision Making Under Uncertainty

In general, all physical systems are subject to uncertainty. Hence, when modeling a physical system like the energy system in a building, uncertainties have to be considered [253]. Depending on the influence of uncertainty on the system, the uncertainty can be included in the model directly or may be omitted. A variety of theories and methodologies to cope with these problems have been developed across various domains of research [214].

In a first step, the decision maker has to define the decision criteria and the environment the decision has to be made in. The environment defines the sources and knowledge of the uncertainty as well as the structure of the decision process, e. g., if the decision maker is exclusively responsible for making the decision. According to Willett [259] as well as Knight and Jones [134], a distinction can be made between measurable uncertainty, i. e., risk, and situations with non-quantitative knowledge. Willett as well as Knight and Jones propose that the term uncertainty should be limited to the latter case and measurable uncertainty should be called risk. However, in the literature the term uncertainty is often used for both situations. Risk is typically limited to situations in which the probability distributions are known to the decision maker.

Examples of processes in building energy systems that are subject to uncertainty are the electricity generation from solar irradiation or the electricity consumption caused by the actions of the inhabitants. When considering the task to find optimal schedules for the devices in a building energy system, the future generated power can be predicted but the amount of power that is actually generated is unknown before the time of generation. In this situation, the decision on the schedule has to be made before the realization of the random variables. Aside from building energy systems, a large variety of problems requires that decisions are made under the presence of uncertainty, e. g., portfolio selection or production scheduling.

3.8.1 Modeling of Uncertainty

The uncertainty in an energy system, e. g., the uncertainty in the prediction of the electricity consumption, can be modeled by handling the respective parameters of the system model as random variables. This approach can also be used to model other processes that are subject to uncertainty [227, p.2].

When \mathbf{w} is a continuous random variable distributed according to the Probability Density Function (PDF) $p(\mathbf{w})$, the expected value $\mathbb{E}(\mathbf{w})$ is defined by [254]:

$$\mathbb{E}(\mathbf{w}) = \int_{-\infty}^{\infty} \mathbf{w}p(\mathbf{w})d\mathbf{w}. \quad (3.24)$$

In case of a discrete random variable $\mathbf{w} \in \mathcal{W} = \{\mathbf{w}_1, \dots, \mathbf{w}_M\}$ with the uncertainty set \mathcal{W} (cf. [29]), the expected value is defined by:

$$\mathbb{E}(\mathbf{w}) = \sum_{m=1}^M \mathbf{w}_m p(\mathbf{w}_m), \quad (3.25)$$

where M is the number of possible outcomes of the random number \mathbf{w} .

In the following, random variables $\mathbf{w}_k \in \mathcal{W}$ with the uncertainty set \mathcal{W} and

$$\mathbf{W} = (\mathbf{w}_0, \dots, \mathbf{w}_{N-1})^\top \in \mathcal{W}^N, \quad (3.26)$$

are introduced⁴ to the system model. They can be seen as a disturbance of the known time-dependent model parameters Θ as defined in Section 3.6. In this case, the state equation is given by:

$$\mathbf{z}_{k+1} = \mathbf{f}(\boldsymbol{\theta}_k, \mathbf{w}_k, \mathbf{z}_k, \mathbf{v}_k), \quad \forall k \in \{0, \dots, N-1\}. \quad (3.27)$$

In addition to the state equation, other constraints can be influenced by the disturbance:

$$(\boldsymbol{\theta}_k, \mathbf{w}_k, \mathbf{z}_k, \mathbf{v}_k) \in \mathcal{Y}_\theta, \quad \forall \mathbf{w}_k \in \mathcal{W}, \forall k \in \{0, \dots, N-1\}, \quad (3.28)$$

The disturbance vector can also influence the stage costs:

$$l(\boldsymbol{\theta}_k, \mathbf{w}_k, \mathbf{z}_k, \mathbf{v}_k) : \mathcal{W} \times \mathcal{B} \times \mathcal{X} \times \mathcal{U} \rightarrow \mathbb{R}. \quad (3.29)$$

In the following, parameters that are subject to uncertainty are modeled as random variables. When considering the rolling horizon approach described in Sections 3.5 and 3.6, the random variables are introduced by replacing Equation 3.23b with Equation 3.27, Equation 3.23a with Equation 3.28 and Equation 3.18 with Equation 3.29. This results in the following optimization Problem:

$$\min_{\mathbf{V} \in \mathcal{U}^N} \sum_{k=0}^{N-1} l(\boldsymbol{\theta}_k, \mathbf{w}_k, \mathbf{z}_k, \mathbf{v}_k) + C(\mathbf{z}_N), \quad (3.30)$$

subject to:

$$(\boldsymbol{\theta}_k, \mathbf{w}_k, \mathbf{z}_k, \mathbf{v}_k) \in \mathcal{Y}_\theta, \quad \forall \mathbf{w}_k \in \mathcal{W}, \forall k \in \{0, \dots, N-1\}, \quad (3.31a)$$

$$\mathbf{z}_{k+1} = \mathbf{f}(\boldsymbol{\theta}_k, \mathbf{w}_k, \mathbf{z}_k, \mathbf{v}_k), \quad \forall \mathbf{w}_k \in \mathcal{W}, \forall k \in \{0, \dots, N-1\}, \quad (3.31b)$$

$$\mathbf{z}_0 = \mathbf{x}t_0, \quad \mathbf{z}_N \in \mathcal{X}_N. \quad (3.31c)$$

As defined in Equations 3.31a and 3.31b, the constraints have to hold for all possible outcomes of the random variables \mathbf{W} . This can be modeled by introducing additional constraints. More precisely, the number of constraints increases linearly with the number of the possible outcomes of the random variables \mathbf{W} .

3.8.2 Decision Criteria

When facing uncertainty, the preferences of the decision maker as well as the appropriate decision criteria have to be defined. The decision criteria define which choice is considered optimal. The choice of the decision criteria depends on the decision problem and the preferences of the decision maker. Common choices of decision criteria [140, p. 84] are described in this section. To be in line with the definition in Section 3.2, minimal objective values will be regarded as optimal objective values in the following. Each decision criterion can easily be adapted to maximization problems.

⁴In contrast to conventions in probability theory, random variables are not described by capital letters.

Minimax Criterion

The minimax or Wald criterion [256] assesses the maximal objective value of the objective function $g(x, w)$, i. e., the worst possible outcome, that can occur based on the random variable w with respect to a fixed decision variable x :

$$\max_w g(x, w). \quad (3.32)$$

The decision variable x is then chosen in a way that Equation 3.32 becomes minimal [140, p. 84]:

$$\min_x \max_w g(x, w). \quad (3.33)$$

This decision criterion is only focused on the worst possible outcome of an uncertain parameter and therefore suiting pessimistic decision makers. In the case of a maximization problem, the minimax criterion translates into a maximin criterion.

Among other applications, the minimax decision criterion is sometimes used for robust MPC that targets the minimization of the distance between a controlled variable and reference value [149]. In the presence of uncertainty, minimax approaches to robust MPC target at minimizing the worst-case performance of the system under control while complying with all constraints. In the domain of energy systems, minimax or worst-case MPC is applied in environments that are similar to the one discussed in this thesis while the application cases differ [108, 183]. In algorithm engineering the minimax criterion relates to the worst case [54, p. 27].

Minimin Criterion

In contrast to the pessimistic minimax criterion, the minimin criterion values only the possible best-case performance. Hence, the decision variable x is chosen in a way that the best-case outcome:

$$\min_w g(x, w), \quad (3.34)$$

becomes minimal [140, p. 84]:

$$\min_x \min_w g(x, w). \quad (3.35)$$

The minimin criterion suites an optimistic decision maker that targets the maximization of the best possible outcome. In the case of a maximization problem, the minimin criterion translates into a maximax criterion. In algorithm engineering The minimin criterion relates to the best case [54, p. 27].

Bayes and Laplace Criteria

The downside of the minimax and minimin criteria is that they consider only one possible outcome, the worst and the best, respectively. The Bayes criterion considers all possible outcomes and their probability of occurrence by evaluating the expected outcome. Thus,

the best decision variable x is defined to be the one that minimizes the expected objective value $g(x, w)$:

$$\min_x \mathbb{E}(g(x, w_m)) = \min_x \sum_{m=1}^M p(w_m) \cdot g(x, w_m), \quad (3.36)$$

where w is a discrete random variable, $\{w_1, \dots, w_M\}$ are its possible outcomes and $p(w_m)$ the respective probability of occurrence.

The Laplace criterion is a special case of the Bayes criterion that can be used if the probability of occurrence for the possible outcomes is not known. It assumes that the probability of occurrence for every possible outcome is equal. This leads to a probability of occurrence of:

$$p(w_m) = \frac{1}{M}, \quad \forall m \in \{1, \dots, M\}. \quad (3.37)$$

Equation 3.36 then turns into:

$$\min_x \mathbb{E}(g(x, w_m)) = \min_x \frac{1}{M} \sum_{m=1}^M g(x, w_m). \quad (3.38)$$

The Bayes and the Laplace criterion are suited for decision makers that target an average performance of a decision. These criteria are widely used in economic decision-making, especially in stochastic programming, which is used in this thesis to find optimal schedules for the devices in a building energy system. Stochastic programming is described in detail in Section 3.11. In algorithm engineering the Laplace criterion relates to the average case [54, p. 28].

Other Criteria

In addition to the criteria listed above, more decision criteria have been developed that target variations of worst-case, best-case and average performance [140, p. 84]. One example is the Hurwicz criterion, which uses a weighted sum of the best-case and the worst-case outcome of a decision. Whereby, the weights can be chosen to represent the preferences of the decision maker [121]. The Niehans-Savage criterion targets the minimization of a regret value instead of the performance of a decision [187, 216].

Jin and Branke [126] present a decision criterion that targets on finding a solution that “should still work satisfactorily when the design variables change slightly”. It can be seen as a special case of the Laplace criterion that only considers additive uncertain perturbations on the decision variables. The authors of [126] call the solutions that are optimal with respect to their decision criteria *robust solutions*. Here, it is important to note that this naming is inconsistent to the usage of the term *robust* as defined in Section 3.10 since it refers to solutions that are optimal with respect to the specific decision criterion in contrast to solutions that are viable in all possible scenarios.

This thesis uses the Laplace decision criterion as a specific case of the Bayes criterion. In contrast to the minimin, the maximin and the Hurwicz decision criteria, it accounts

for all possible scenarios. It is also more general than the criterion defined in [126]. In addition, it is assumed that the minimization of possible losses, i. e., regret, is less important in building energy management than the minimization of the expected operating costs. Also, the Bayes decision criterion does not need additional parameters from the decision maker. This eases the handling of a BEMS that uses the approach presented in this thesis. However, the investigation of other decision criteria can be useful in related scenarios. The choice of the Bayes decision criterion also fits the assumption of a user that acts as a *homo economicus* [202].

3.9 Optimization Under Uncertainty

The decision criterion, as described in Section 3.8.2, defines optimal decisions. This section describes how the optimal decision is found. In the context of this thesis, the decision problem is to find an optimal schedule that minimizes the expected operating costs and maximizes the expected revenues from the compensation for the fed-in electricity when considering the uncertainty in the predictions of the local consumption and generation.

There are various methods to find optimal decisions involving uncertainty targeting different aspects of solving an optimization problem with uncertainty. Bertsimas et al. [30] distinguish robust and stochastic optimization: In robust optimization “the decision-maker constructs a solution that is feasible for any realization of the uncertainty in a given set” while stochastic programming “is seeking to immunize the solution in some probabilistic sense to stochastic uncertainty”. This definition is similar to the definition of proposed by Jin and Branke [126], although they use the term robust. When looking at this definition of robust optimization, the feasibility of a solution, i. e., decision, for any realization of the uncertainty is not taken into account by the decision criteria defined in Section 3.8.2. However, the feasibility of a solution is often an important issue in optimization under uncertainty. Another important question is whether decisions have to be made here and now, i. e., have to persist, or if decisions can be changed in the future. While robust optimization targets decisions that have to be made here and now [27, p. xi], stochastic programming often handles decisions that have multiple stages of decision-making [214].

3.10 Robust Optimization

Ben-Tal et al. define robust optimization on the basis of three assumptions on the underlying decision environment [27, p. xii]:

Firstly, “all entries in the decision vector x represent ‘here and now’ decisions: they should get specific numerical values as a result of solving the problem before the actual data ‘reveals itself’”.

Secondly, “the decision maker is fully responsible for consequences of the decisions to be made when, and only when, the actual data is within the prespecified uncertainty set”.

Finally, “the constraints [...] in question are ‘hard’ – the decision maker cannot tolerate violations of constraints when the data is in \mathcal{U} ”.

Thus, robust optimization targets decisions that have to be made here and now. In addition, the decisions, i. e., solutions of the optimization problem, have to be made in such a way that no constraints are violated for any expected outcome of the uncertainty. Hence, robust optimization targets on giving a guarantee that a solution is viable.

In contrast to the definition by Ben-Tal et al., some approaches loosen the condition that the constraints are not allowed to be violated for any expected outcome [227]. This is done by allowing the violation of constraints in some cases. Thus, the decision maker can choose the trade-off between robustness and performance and the corresponding level of protection according to his preferences [30]. This is done by introducing *chance constraints* which are also called *probability constraints* [227, p. 5]. In the case of an inequality constraint $g(x, w) \leq 0$, the corresponding chance constraint is [227, p. 5]:

$$p(g(x, w) \leq 0) \leq \alpha. \quad (3.39)$$

Here, x is the decision variable, w is a random variable and α is the significance level defined by the decision maker. Probabilistic constraints give probabilistic guarantees.

Robust optimization is closely related to robust control [30], which is often used in the optimization of energy systems and building energy systems [14, 108, 183]. However, these applications typically do not focus on economic optimization. Examples include the determination of optimal control parameters that enable an operation at predefined operating points.

3.11 Stochastic Programming

*Stochastic programming*⁵ as defined in this thesis targets problems that have multiple stages. In each stage, the respective decisions have to be made before the realization of the respective uncertainty. This means that at a given time, only the variables that belong to the next stage have to be decided on, while the variables that belong to all later stages can be changed later on. Thereby, stochastic programming provides an approach to consider the uncertainty in the later stages and the consequences of possible future decisions [31, 214, 227].

Stochastic programming is based on Bellman’s principle of optimality [26, p. 83]:

“Principle of Optimality: An optimal policy has the property that whatever the initial state and initial decision are, the remaining decisions must constitute an optimal policy with regard to the state resulting from the first decision.”

⁵In the context of this thesis, the word *programming* refers to *planning* [25] and can be used as a synonym for *optimization*. It should not be confused with computer programming.

A more detailed description can be found in [196, p. 358]. It is important to note that the terms *stochastic programming*, *dynamic programming* and *stochastic dynamic programming* are not used consistently and often intended to mean the same while highlighting different aspects (cf. [196, p. 357], [196, p. 433] and [p. 64][227]). Papageorgiou et al. [196] call optimization approaches that are based on Bellman's principle of optimality dynamic programming while these approaches are called stochastic dynamic programming if random variables are present. Following this convention, the approach presented in this thesis is categorized as stochastic dynamic programming. However, the idea has been initially presented by Bellman in 1952 [24]. Bellman used the term *dynamic programming* for the optimization of dynamic stochastic processes and it was only later recognized that the approach can also be used for deterministic problems [25].

3.11.1 Two-stage Problem

The simplest problem in stochastic programming is a two-stage problem [19, 58]. The idea is that the variables that belong to the first stage have to be decided on immediately, here and now, while the variables that belong to the second stage can be changed later on.

However, the first-stage decision variables are chosen by taking their future effects into account. Typically, the first stage is assumed to have no uncertainty, while the second stage is assumed to include uncertainty. The uncertainty is included via random variables with known possible outcomes but unknown realizations. A standard formulation of a two-stage problem is [31, 214, 227]:

$$\min_{x \in X} g_1(x) + \mathbb{E}(Q(x, w)), \quad (3.40)$$

with $Q(x, w)$ being the optimal value of the second-stage problem:

$$Q(x, w) = \min_{y \in Y} g_2(y, w), \quad (3.41)$$

subject to:

$$T(w) \cdot x + D(w) \cdot y \leq h(w). \quad (3.42)$$

Here, w is a random variable and x and y are the decision variables in the first-stage problem and the second-stage problem, respectively. The respective objective functions are $g_1(x)$ and $g_2(y, w)$. The constraints on the second-stage problem are given by the stochastic parameters $T(w)$, $D(w)$ and $h(w)$, where the term $D(w) \cdot y$ can be seen as a compensation for a possible inconsistency of the system $T(w) \cdot x \leq h(w)$ [31, p. 59].

The two-stage problem as defined in Equation 3.40 contains a deterministic term $f_1(x)$ and a term $\mathbb{E}(Q(x, w))$ that contains the expected value of $f_2(y, w)$ over all possible realizations of the random variable w . For each possible realization of the random variable w , the optimal value for y is a result of an optimization problem [31, p. 59].

For a given realization of w , $Q(x, w)$ is defined as:

$$Q(x, w) = \min_{y \in Y} \{g_2(y, w) \mid T(w) \cdot x + D(w) \cdot y \leq h(w)\}. \quad (3.43)$$

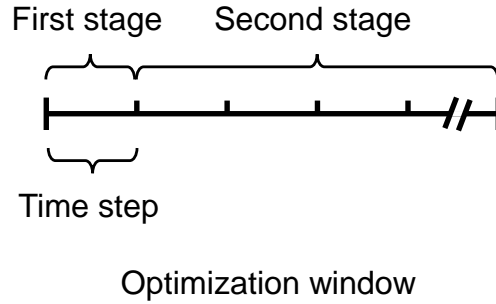


Figure 3.4: Visualization of the two-stage problem in this thesis. The first time step relates to the first stage, while all other time steps relate to the second-stage (cf. [31, p. 65]).

The corresponding second-stage value function $\mathcal{Q}(x)$ is then given by [31, p. 59]:

$$\mathcal{Q}(x) = \mathbb{E}(Q(x, w)). \quad (3.44)$$

Using this notation, the stochastic program in Equation 3.40 becomes:

$$\min_{x \in X} g_1(x) + \mathcal{Q}(x). \quad (3.45)$$

This formulation is called the Deterministic Equivalent Program (DEP) [31]. If the second-stage value function $\mathcal{Q}(x)$ is given, a stochastic program becomes a deterministic optimization problem [31, p. 59]. This is also emphasized by the notation $\mathcal{Q}(x)$ that does not show any dependence on random variables.

This thesis uses a two-stage approach in the rolling horizon optimization of energy systems in buildings. The first stage refers to the first time step in the rolling horizon optimization (see Figure 3.4). In Equation 3.10 the first time step is the one with $k = 0$. The first time step differs from the other steps in the way that the respective control inputs have to be applied to the energy system right after the end of the optimization. All other control inputs can still be changed after the next optimization run. Thus, all other time steps belong to the second stage. Typically, the first stage includes the first time step while the second stage includes all other steps in the optimization window. In the first stage no uncertainty is considered. However, this can be justified by the accurate forecasts for small look-ahead times (see Section 4.1.5).

A more detailed description of the actual optimization problem and the definition of the two stages is given in Chapter 5.

3.11.2 Multi-stage Problem

A two-stage problem is a special case of a multi-stage problem with an arbitrary number of stages. For a problem with T stages that are numbered from $t = 1$ to $t = T$, the

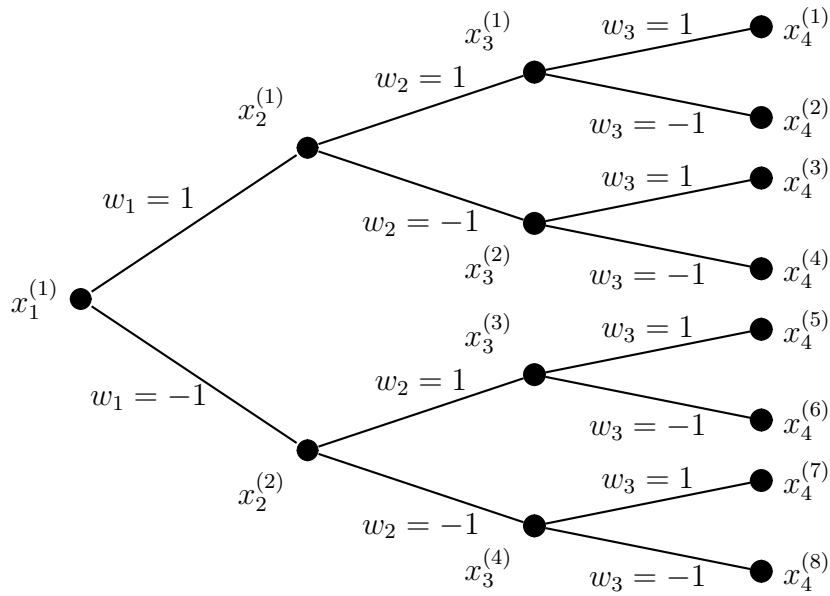


Figure 3.5: Visualization of the explosion in the number of realizations and corresponding decisions that have to be made to solve a multi-stage stochastic problem. The figure shows an exemplary three-stage problem with random variable w_t that has two possible outcomes in every stage $t \in \{1, 2, 3\}$. This problem leads to 8 possible decisions paths, i. e., the choice of the decision variables x_1 , x_2 , x_3 and x_4 . (inspired by [20, 148])

optimization problem can be formulated similarly to Equation 3.40 [227, p. 63]:

$$\min_{x_1 \in X_1} g_1(x_1) + \mathbb{E} \left(\min_{x_2 \in X_2(x_1, w_1)} g_2(x_2, w_2) + \mathbb{E} \left(\dots + \mathbb{E} \left(\min_{x_T \in X_T(x_{T-1}, w_{T-1})} g_T(x_T, w_T) \right) \right) \right). \tag{3.46}$$

A different formulation uses the corresponding dynamic programming equations initially developed by Bellman [24] (see [227, p. 64]).

Assuming that every random variable has a finite number of outcomes that are not correlated, the problem given in Equation 3.46 can be approximated by using the methods of deterministic programming. However, the optimization problem in each stage has to be solved for every possible outcomes of the previous stage’s random variable and choice of decision variables recursively going backwards in the series of stages. For a large number of variables, this approach becomes impractical (see Figure 3.5). This problem is called the “curse of dimensionality”. [227, p. 8] [226]

3.11.3 Sampling Methods

Using Equation 3.24 and the PDF $p(w)$, the expected value in the definition of the value function in Equation 3.44 is defined by:

$$\mathcal{Q}(x) = \int_{-\infty}^{\infty} Q(x, w)p(w)dw. \quad (3.47)$$

To solve the integral in Equation 3.47, often sampling approaches are used [31, p. 389]. One sampling approach to the two-stage stochastic program is to replace the value function $\mathcal{Q}(x)$ by a Monte Carlo estimate $\tilde{\mathcal{Q}}_W(x)$:

$$\tilde{\mathcal{Q}}_{\text{MC}}(x) = \sum_{m=1}^M Q(x, w_m)p(w_m), \quad (3.48)$$

When the sample of the random variable is assumed to be independent and identically distributed, the corresponding value function $\mathcal{Q}_{\text{MC}}(x)$ is given by [31, p. 390]:

$$\mathcal{Q}_{\text{MC}}(x) = \frac{1}{M} \sum_{m=1}^M Q(x, w_m), \quad (3.49)$$

3.12 Mixed-integer Linear Programming

In Section 3.5 the objective function (as defined in Equation 3.10) and the constraints (as defined in Equations 3.13a and 3.13b) are not defined in detail. These equations form the model of the building energy system. As described in Section 3.1, the model has to be chosen in a way that it describes the modeled system adequately. In addition, the optimization problem has to be formulated in a way that it can be solved in an appropriate time. In the domain of BEMS, often MILP models are used [20]. This thesis adopts this approach.

MILP models consist of one linear objective function and linear constraints. The decision variables are defined to be either continuous or integer variables. A linear objective function $g(\mathbf{x}, \mathbf{y})$ has the form [28]:

$$g(\mathbf{x}, \mathbf{y}) = \mathbf{c}^\top \mathbf{x} + \mathbf{d}^\top \mathbf{y}. \quad (3.50)$$

The constraints have the form:

$$\mathbf{A}\mathbf{x} + \mathbf{E}\mathbf{y} = \mathbf{b}, \quad (3.51)$$

$$\mathbf{0} \leq \mathbf{x} \quad (3.52)$$

and

$$\boldsymbol{\alpha} \leq \mathbf{y} \leq \boldsymbol{\beta}. \quad (3.53)$$

Here, $\mathbf{x} \in \mathbb{R}^m$ and $\mathbf{y} \in \mathbb{Z}^i$ are the decision variables and $\mathbf{c} \in \mathbb{R}^n$, $\mathbf{A} \in \mathbb{R}^{m \times n}$, $\mathbf{b} \in \mathbb{R}^m$, $\mathbf{E} \in \mathbb{R}^{i \times n}$, $\boldsymbol{\alpha} \in \mathbb{Z}^i$ and $\boldsymbol{\beta} \in \mathbb{Z}^i$ are the model parameters that are known before the optimization process.

The mixed-integer linear program is defined to be:

$$\min_{\mathbf{x}, \mathbf{y}} g(\mathbf{x}, \mathbf{y}) \quad (3.54)$$

such that

$$\mathbf{A}\mathbf{x} + \mathbf{E}\mathbf{y} = \mathbf{b}, \quad (3.55a)$$

$$\mathbf{0} \leq \mathbf{x}, \quad (3.55b)$$

$$\boldsymbol{\alpha} \leq \mathbf{y} \leq \boldsymbol{\beta}. \quad (3.55c)$$

To obtain a MILP model, the state equation (as defined in Equation 3.13b) of the building energy system has to be linear [196, p. 522]:

$$\mathbf{z}_{k+1} = \mathbf{A}_k \mathbf{z}_k + \mathbf{B}_k \mathbf{v}_{\text{Real},k} + \mathbf{C} \mathbf{v}_{\text{Integer},k}. \quad (3.56)$$

Where, $k \in \{0, \dots, N - 1\}$ is the time step, $\mathbf{z}_k \in \mathbb{R}^m$ are the states of the building energy system, $\mathbf{v}_{\text{Real},k} \in \mathbb{R}^m$ and $\mathbf{v}_{\text{Integer},k} \in \mathbb{Z}^m$ are the real valued and integer valued control inputs. $\mathbf{A}_k \in \mathbb{R}^{m \times n}$, $\mathbf{B}(k) \in \mathbb{R}^{m \times n}$ and $\mathbf{C}_k \in \mathbb{R}^{m \times n}$ are the model parameters. In the stochastic case as defined in Equation 3.27, the linear state equation is [196, p. 522]:

$$\mathbf{z}_{k+1} = \mathbf{A}_k \mathbf{z}_k + \mathbf{B}_k \mathbf{v}_{\text{Real},k} + \mathbf{C}_k \mathbf{v}_{\text{Integer},k} + \mathbf{D}(k) \mathbf{w}_k. \quad (3.57)$$

Here, \mathbf{w} is a vector of random variables.

3.13 Modeling of Energy Systems in Buildings

To evaluate the performance of the energy system, various approaches to the modeling of energy systems and in particular energy systems in buildings have been developed in recent years. In the context of this thesis, these models can be divided into two categories [153, 206], simulation-based models [163, 165] and mathematical programming models [18, 130, 222]. A more detailed description of the specific device models in building energy systems is given in Section 4.1.

Simulation-Based Models

Simulation based-models determine the temporal progression of the energy system, i. e., the energy consumption, electricity generation, storage states and operating times of the devices based on predefined operation strategies. The predefined operation strategies can include predefined schedules or rules. In general, simulation models can be formulated in various ways. Typical formulations use recurrence relation equations or program code. Simulation models also allow modeling stochastic processes using the Monte Carlo method [139]. Like EnergyPlus [57], the simulation models often are black box models. Here, black box models only provide an output based on a given input, but no internal variables and specific functions implied by the simulation's computer modules are known [85, p. 82].

Since the objective function cannot be computed exactly, the optimization can only be done with specific optimization algorithms [15, 85]. For simulation models that use the Monte Carlo method, the objective function cannot be computed exactly. They can only be estimated with some noise.

Such a problem using stochastic or Monte Carlo based simulation, is sometimes called “stochastic optimization” [85, p. 1]. It is important to note that this stochastic optimization is completely different from the stochastic programming described in Section 3.11.

Mathematical Programming Models

Mathematical programming models formulate the building energy system as an optimization problem using an objective function and constraints. The temporal progression is then obtained by solving the optimization problem. In contrast to the simulation model, this approach gives the temporal progression that is optimal with respect to the given problem. However, this approach is often limited in a way that only a simplified model of the building energy system can be used. Typically, MILP models are used in the field of building energy systems [18, 20]. Beaudin and Zareipour [20, Table 15] list 20 MILP models compared to twelve Linear Programming (LP) models, six quadratic programming models and only one Mixed Integer Non-linear Programming (MINP) model. This is supported by the availability of suitable solvers, e. g., CPLEX or Gurobi, that are easy to use and have a high out-of-the-box performance.

The optimization problem has to be solved to give any statement on the performance of the energy system. Since the time to solve the optimization problem can be very long, the temporal resolution and the considered time period are often limited. Common scheduling windows are about 24 h, typical resolutions range from 1 min to 1 h [20]. According to [20], the resulting number of time steps rarely exceeds 288.

In addition to optimization methods that provide exact solutions, meta-heuristics and heuristics are used. Even though heuristics are not guaranteed to be optimal, the meta-heuristics can often find good solutions with less computational effort than exact methods [20]. The review provided in [20, Table 15] lists 29 publications that utilize meta-heuristics and heuristics. However, it is important to note that these approaches sometimes use simulation-based models instead of mathematical programming models.

In addition to the approaches from research, commercial programs have been developed that enable the modeling and optimization of energy systems using mathematical programming models. Examples of these programs are BoFiT by ProCom, TOP Energy by gfai tech and BelVis by Kisters.

4. Related Work

This chapter presents an overview and discussion of the literature that is related to this thesis. The chapter starts with related work on modeling in the domain of energy management. In particular device models and the related literature are discussed in Section 4.1. This section includes comments on the fundamentals of the devices and the respective models. This topic is in particular important for the optimization approach presented in this thesis because it serves as a basis for the model presented in Chapter 5. In Section 4.2 remarks on BEMSs and concrete implementations of such are presented. After that, related work in the field of building energy management and approaches to the optimization of the operation of building energy systems are presented in Section 4.3. The presented models and approaches are compared and contrasted to the approach presented in this thesis.

4.1 Related Work on Modeling in Building Energy Management

This section presents models from the literature which have been developed to enable the optimization of the operation of energy systems. The models that are used in this thesis are presented in detail in Chapter 5.

4.1.1 Electricity Consumption, User Behavior, and Electricity Consumption Forecast

The electricity consumption of a building depends on the present loads. The loads that are present in a building depend on the purpose of the building, its size and the number of inhabitants and their needs [114]. Therefore, the electricity consumption of a commercial building differs from the one of residential buildings. This is, amongst other reasons, based on the different times of use. For example, a commercial building is mainly used during

office times while residential buildings are quite often not used during the day. Other reasons are different devices in the buildings. The devices can be divided into plug loads, i. e., a product powered by means of an ordinary AC plug [190], and other loads. These other loads include Heating, Ventilation, and Air-Conditioning (HVAC) systems, lighting and large appliances. The electricity consumption in buildings can be modeled using either top-down or bottom-up approaches [96, p. 33] [99, 242].

Top-down approaches consider the electricity as a whole. They do not distinguish between individual users and devices in the building. Typically, top-down models use an average of summed up historical electricity consumption as estimates for future energy consumption. In addition, the models use other parameters to further specify the model. These parameters include climatic conditions, estimates of appliance ownership and number of units [80]. The advantage of top-down models is that they only need aggregated data. However, the reliance on historical data and the lack of detail do not allow for the incorporation of future events such as advances in device technology. [242]

Bottom-up approaches model the electricity consumption profile as a sum of individual devices and their electricity consumption profiles [194]. The device usage is based on user behavior predictions [114] and statistical data [80, 238]. Thus, bottom-up models have the ability to model technological options and they can include user preferences and behavior to investigate possible improvements in the electricity usage. However, a much higher level of detail in the input data is required than in top-down models. [242]

In addition, combinations of top-down and bottom-up models exist. For example, in [9, 163, 165] the appliances are modeled individually by using individual load profiles and usage probabilities [238] while all other loads are modeled using a top-down approach based on German standard load profiles [250]. This thesis follows this approach. The following sections provide an introduction to the modeling of the individual devices that are considered in this thesis and present related work on the modeling of such devices.

4.1.2 Battery Energy Storage Systems

A BESS consists of a battery and a power converter. The power converter is used to convert between the AC of the grid and Direct Current (DC) of the battery. Hence, the power converter is a combination of a DC to AC and an AC to DC converter. In some cases, the battery is connected to a power source generating DC, e. g., a PV system. This type of wiring is not considered in this thesis. However, it can easily be included by adjusting the efficiency of the charging process accordingly. Thus, the model of a BESS includes the power converter as well as the battery.

Battery Models

This thesis focuses on lithium-ion batteries. However, the lithium-ion battery model that is used in the optimization can be adopted to other types like lead–acid batteries.

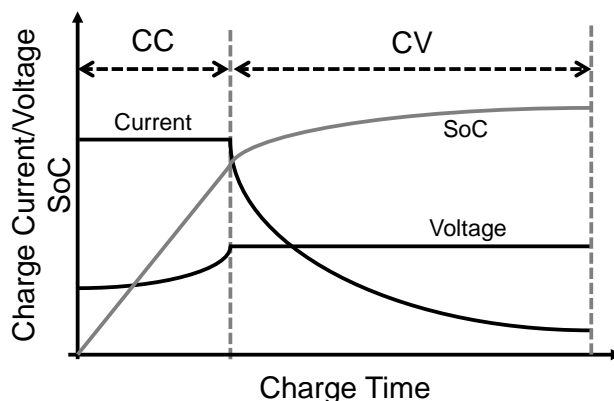


Figure 4.1: Exemplary visualization of the constant-current constant-voltage charging based on [208, p. 15.18]. The charging time is divided into a constant current (CC) and a constant voltage (CV) phase. In the case of lithium-ion batteries, an SoC of about 80 % is achieved after the CC phase.

In recent years, various types of models have been developed to simulate batteries of all kinds. The types of models differ based on the application area and the battery type. Common models are electrochemical models, electrical circuit models, kinetic battery models and buffer battery models. Electrochemical models are often used in battery design [67]. Electrical circuit models focus on the electrical properties of the battery and are often used in electrical engineering [47]. Analytical models describe the battery in a more abstracted way. One is the kinetic battery model [160], which specifically considers the apparent change in capacity as a function of (dis-)charge power.

However, in building energy management that relies on MILP models, often simplified models are preferred [3, 14, 59, 179]. Typically, a battery is modeled using only a few model parameters: the capacity, the charge and the discharge efficiencies, maximum and minimal charging and discharging powers and a maximal and minimal State of Charge (SoC). To prevent overcharging and to increase the lifetime, lithium-ion batteries are typically charged using the Constant-Current Constant-Voltage (CCCV) charging strategy (see Figure 4.1) [208, p. 15.18]. When applying CCCV charging, the maximum charging rate decreases exponentially when the SoC reaches about 80 %. This leads to an overall nonlinear behavior of the battery charging process. However, when using MILP models this behavior is often not addressed. This can be motivated by only using 80 % of the battery capacity. In addition, the modeling of individual cells and their internal voltages and currents are omitted in MILP models. This is the subject of Battery Management Systems (BMSs) which take care of the internal coordination of charging and discharging processes of the individual cells, including thermal management. This can be essential with respect to aging processes and lifetime considerations, but it is not in the scope of this thesis, which is abstracting from the BMS.

Sometimes the battery degradation is considered additionally [3, 69, 178]. The degradation

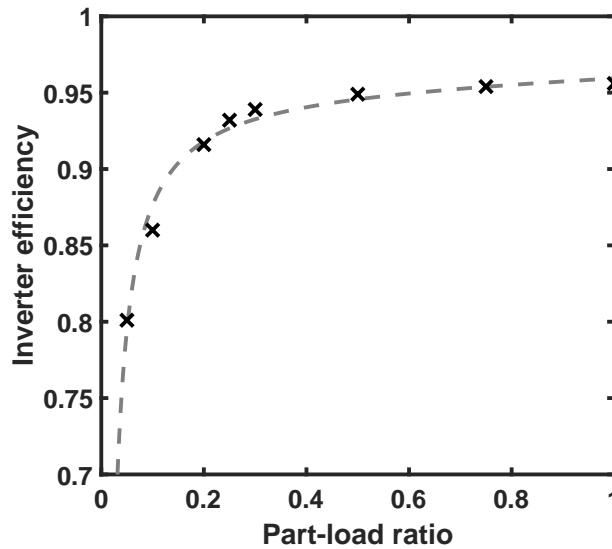


Figure 4.2: Visualization of the DC to AC power converter efficiency in dependence of the part-load ratio. Black Xs represent the values taken from a data sheet of a real power converter [84]). The dashed gray line represents a function that is based on the method presented in [219] fitted to the data points.

can be divided into a calendar and a cycle aging. While calendar aging is often omitted in building energy management, cycle aging is addressed in the literature [3]. Simplified approaches reduce the capacity of the BESS by a fixed amount of energy per (dis-)charge cycle [3]. Since, experimental research has shown that deep cycling causes the most significant degradation whereas smaller cycles are less significant [69], more complicated approaches have been developed that include the (dis-)charge power, the SoC and the degree of discharge [178].

This thesis uses a MILP model of the battery that does not consider aging. The exact model is described in detail in Section 5.6.1.

Power Converter Models

In building energy management, the power converter is typically modeled using (dis-)charge efficiency and possible maximal and minimal (dis-)charge values. According to Schmidt and Sauer [219], the power converter efficiency is dependent on the part-load ratio:

$$\text{part-load ratio} = \frac{\text{current load}}{\text{nominal load}}. \quad (4.1)$$

The authors of [219] also give a method to model the power converter efficiency based on the part-load ratio (see Figure 4.2)

However, typically the power converter losses are combined with the battery (dis-)charge efficiency [3, 14, 59]. The same approach is applied in this thesis.

4.1.3 Micro Combined Heat and Power Plants

To enable energy management in buildings with micro-CHPs, several models have been developed in the past. They range from detailed models considering the electrical and thermodynamic properties [118, 189] and more abstracted models that try to mimic the unique behavior of real micro-CHPs [9, 78, 163] to abstract MILP models [43, 68, 119, 172]. This thesis uses the latter.

MILP models presented in the literature, e. g., [43, 68, 119, 172], cover numerous properties of micro-CHPs including: ramping rates, required on and off times, predefined generation sequences and varying efficiencies.

This thesis uses a MILP model of the micro-CHP that is based on the Senertec Dachs micro-CHP located at the Energy Smart Home Lab (ESHL) in Karlsruhe, Germany. The model is based on the publications that are listed above and extended to mimic the Senertec Dachs G5.5. The exact model is described in detail in Section 5.6.2.

Heat-led and Power-led Micro-CHP Operation

Micro-CHPs that are sold today are typically operated by using a rule-based control algorithm (see for example [225]). However, an optimized operation in which the operating times of the micro-CHP are defined by a BEMS yield better results in specific scenarios [9, 20, 163, 165]. The rule-based control algorithm targets either the provision of heat or the provision of electricity while treating the generation of the other energy carrier as a byproduct. When heat is the target parameter, the operation is called *heat-led* or *heat-driven*. In the case of electricity being the target parameter, the operation is called *electricity-led* or *electricity-driven* [111].

In [111], Hawkes and Leach present and compare typical heat- and electricity-led rule-based control algorithms with an optimized operation. Based on a case study using typical UK residential energy demand profiles, they conclude that the optimal operation strategy is dependent on the tariff structure. However, they state that the optimized operation yields the best cost-reduction potential. The optimized operation is further described in [109]. It minimizes the cost of meeting the given electricity and heat demand while meeting the technical constraints of the system. The micro-CHP is used to charge and discharge a thermal energy storage on a cost-optimal basis, while electricity is imported and exported according to a combination of fuel prices, electricity import and export prices, and electrical and overall efficiency profiles.

4.1.4 PV System

This thesis considers buildings with a local electricity generation by a PV system. The generation profile of a PV system can be modeled based on the orientation of the solar panels in combination with a simulation of the solar irradiation. These models are typically called physical models. However, often a data-driven approach is used that models the

generation profiles of the PV system using measurements [9, 163, 165, 174, 179]. This thesis uses the latter approach (see Section 5.6.3).

In general, the electricity generation of a PV system can be reduced. However, this is only beneficial if the generated energy is not needed or the connected grid is congested [239]. In addition to a local control, a possibility of a remote control of the PV systems can be mandatory. For example, in Germany, all newly installed PV systems have to be equipped with a remote control [239]. However, PV systems with a peak power of less than 30 kW do not have to be equipped with a remote control if the active power feed-in to the grid is limited to 70% of the maximum capacity.

4.1.5 PV Generation Forecast

To be able to optimize building energy systems, the local generation and consumption have to be predicted. In the case of electricity generation from the PV system, this can be done by performing a forecast of the generation. The PV generation has to be modeled as a discrete stochastic process that is a set of random variables observed at discrete points in time. The prediction of the realizations of these random variables over time is called forecast.

The PV system generation depends on several physical processes:

1. The solar irradiation that depends on the position of the sun related to the position of the PV system [201].
2. The type and orientation of the PV system.
3. The size, motion and speed of clouds.
4. The ambient temperature of the PV system.

While the first two processes are mostly deterministic, the latter two processes are stochastic. Hence, the first two processes can be included in the PV generation forecast easily, while the latter are more challenging [70, 201]. In Figure 4.3 the effects of clouds on the PV generation profiles are shown. When no clouds are present the PV generation profile is only dependent on the solar irradiation and the type and orientation of the PV system. In this case, the day-ahead PV generation profiles can be predicted based on historical data. This condition is called clear sky [13]. In case of a low-level of cloudiness, the generation power and thus the amount of generated energy decreases. This effect occurs on a time scale down to days. Hence, the day-ahead PV generation profiles can be predicted based on historical data. A partial cloudiness induced by the movement of individual clouds leads to a high volatility of the PV generation profiles caused by short-time decreases of the PV generation power. It happens on a time scale of days and lower and thus, a day-ahead prediction based on historical data is not always possible. To predict these effects, further information, e.g., short term and very local weather forecast data, is needed. [13]

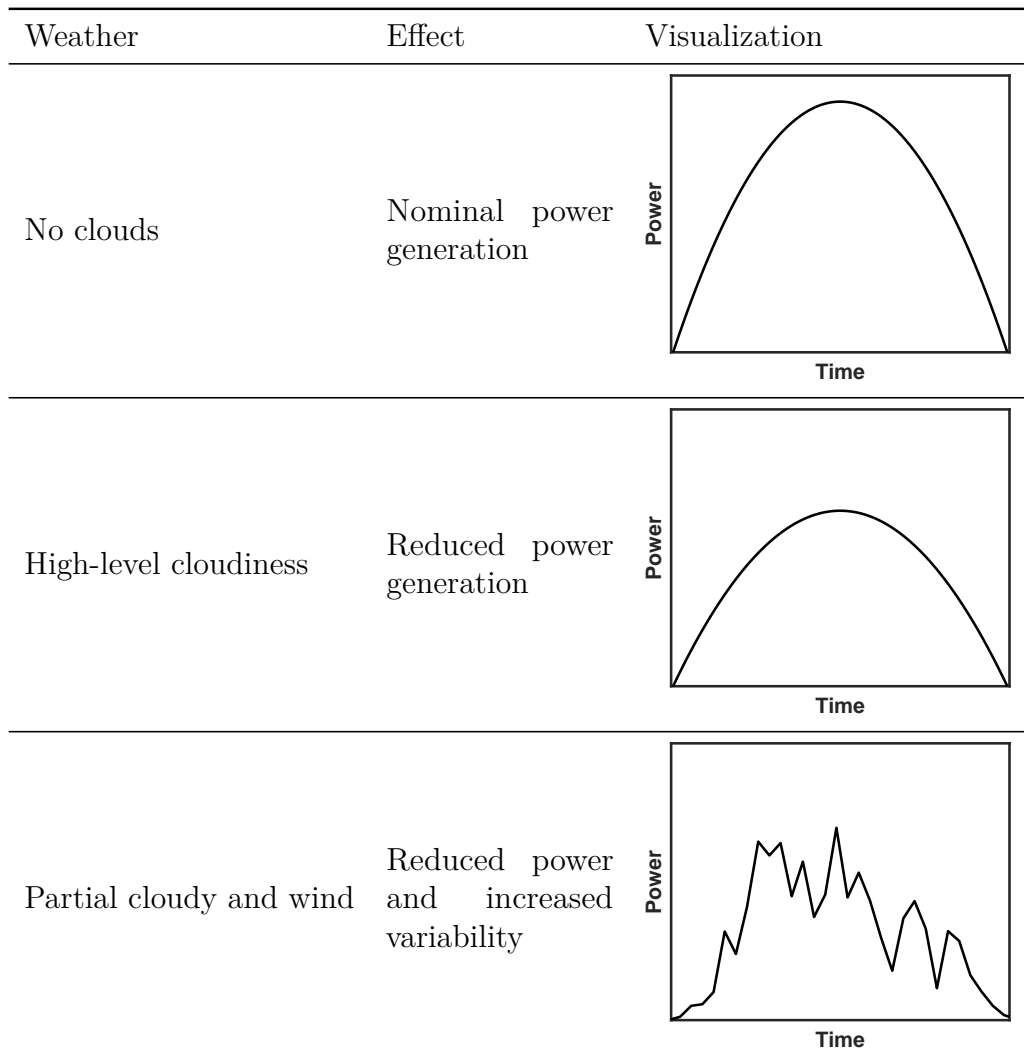


Figure 4.3: Effect of cloudiness on the PV system generation (based on [70])

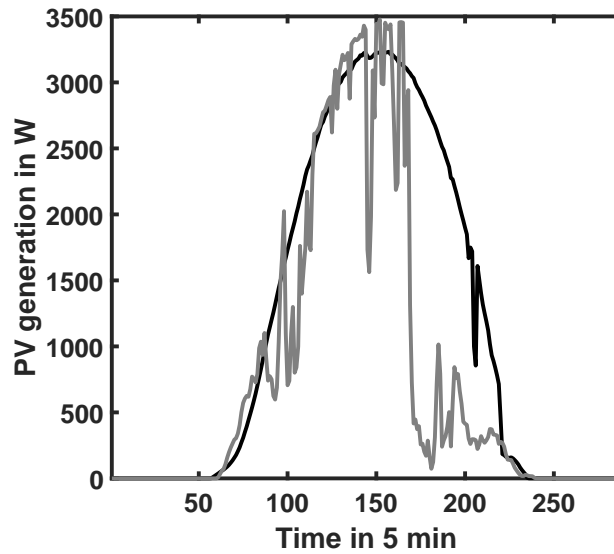


Figure 4.4: Example of scenario sampling based on Example of PV generation forecasts. Two scenarios of a PV generation profile forecast are shown. The black line represents a scenario with high solar irradiation during a whole day resulting in an almost perfect PV generation profile. The gray line represents a scenario with a predicted decrease in solar irradiation in the evening. Considering both scenarios in building energy management instead of only the one with higher probability can improve the performance of the BEMS.

Various forecasting methods have been developed in recent time. In general, the PV generation forecast comes down to a time series forecast [107, p. 72]. In this fashion the methodology is similar to wind power generation forecast or load forecast.

Forecasting methods can be divided into single point and probabilistic methods. Single point methods or single-valued methods [115] predict one value that is expected to be as close as possible to the realization of the considered random variable. In the case of PV generation forecasts, this results in one generation power value per time step. The single point prediction translates to the estimation of the most likely point of the PDF of the considered random variable. Probabilistic forecast methods predict the PDF of the considered random variable, in this case the PV generation in a time step. Hence, probabilistic forecast methods give more information about the stochastic process than single point methods. Hong and Fan [116] state that probabilistic forecasts can be used in most, if not all, places where single-valued load forecasts can be applied [115]. To enable optimization approaches like stochastic programming, often scenarios are sampled based on probabilistic forecasts [223] (see Sections 3.11.3 and Figure 4.4).

The use of probabilistic PV generation forecast is expected to increase the performance of building energy management. For example, in [70], El-Baz et al. state that a probabilistic forecast can lead to an increase in self-sufficiency and self-consumption by 24.2% and 17.7%, respectively. This is based on a case study with deferrable appliances in combination with

a local PV system.

Furthermore, forecasting methods can be divided into methods that use autoregressive models and in methods that do not (see Figure 4.5). Autoregressive models assume that in every time step, a random variable depends on the values of previous time steps and a stochastic term. Thus, the model is a stochastic difference equation. Examples are the autoregressive–moving-average (ARMA) model [257] and the autoregressive integrated moving average (ARIMA) model [34]. The ARMAX model extends both models, the ARMA and the ARIMA, by the use of exogenous parameters [142].

Forecast methods can further be divided into methods that use exogenous parameters, mostly weather forecasts [141, 167, 199] and methods that only use endogenous parameters. To determine the prediction models, various data mining techniques have been used [116]. Examples are Artificial Neural Networks (ANNs) [81, 167, 193] and k-nearest neighbor ((k)-NN) models [116, 268]. In addition, combinations of autoregressive models and non-autoregressive models also exist [138].

In the case of only using endogenous parameters, the prediction model that forecasts the PV generation for every time step $k \in \{1, \dots, H\}$ in a horizon H at time t_0 is defined by $f(\cdot)$ with [193]:

$$\hat{P}_{\text{PV},t_0+k} = f(P_{\text{PV},t_0+k-1}, \dots, P_{\text{PV},t_0+k-S}, \boldsymbol{\theta}) \quad \forall k \in \{1, \dots, H\}. \quad (4.2)$$

$\boldsymbol{\theta}$ are the parameters of the model and S is the number of past time periods the model uses in the prediction. The form of $f(\cdot)$ and the number of parameters $\boldsymbol{\theta}$ depend on the forecasting approach, In case of using exogenous parameters, the prediction model $f(\cdot)$ has additional time series data like weather forecasts [192].

The most simple approach is to use persistence models [193] that assume the expected PV generation power $\hat{P}_{\text{PV},t+H}$ in time step $t + H$ is given by the measured generation $P_{\text{PV},t}$, H time steps earlier, e. g., one time step or the number of time steps that are equal to a temporal shift of 24 hours, here indicated by an offset of H time steps:

$$\hat{P}_{\text{PV},t+H} = P_{\text{PV},t}. \quad (4.3)$$

Krishna et al. [138] compare several PV generation single point forecasts with different model types and input parameters. They state that persistence models perform very well against all other methods for small look-ahead times.

In the review of photovoltaic power forecasting [13], the investigated publications on day-ahead PV generation forecasts typically use a 1 h forecast resolution. Despite that, in the literature publications that use lower resolutions can be found, for example, [193] uses 15 min or [163] uses 1 min.

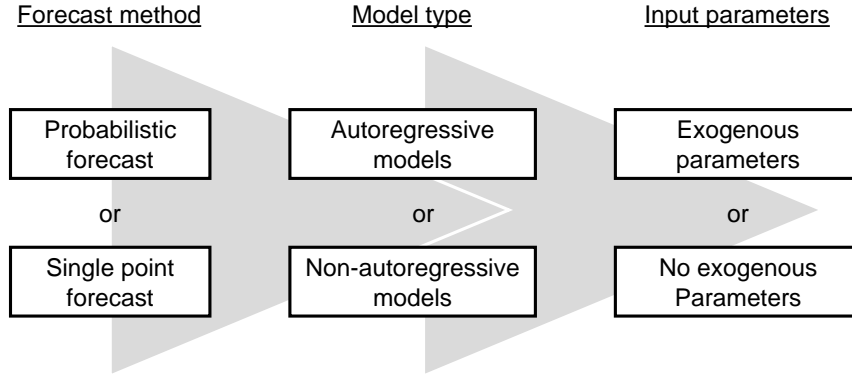


Figure 4.5: Visualization of a possible decision process on a PV generation forecast method.

Quantile Regression

One approach to generate probabilistic PV generation forecasts is quantile regression [137]. This approach has already been used successfully in wind power generation [38, 188] and PV generation forecasting [192]. A quantile regression is a point forecast that gives an approximation of a conditional quantile q instead of delivering the conditionally expected value. The prediction model is similarly to Equation 4.2 given by:

$$\hat{P}_{PV,q,t+H} = f_q(P_{PV,t}, \dots, P_{PV,t-H}, \boldsymbol{\theta}_q). \quad (4.4)$$

The difference to Equation 4.2 is the way of obtaining the parameters $\boldsymbol{\theta}_q$. Typically, they are obtained by minimizing the sum of the pinball-loss function [137, 192]. Since the pinball-loss is not differentiable, the minimization with standard algorithms and data mining techniques is a complicated task [192]. Hence, other approaches have been proposed in the literature. For example, in [192] a data-driven quantile regression based on (k)-NNs is presented. The data-driven quantile regression uses a training set of historical data containing an approximation of all possible PV generation values in every time step of the forecast horizon. Based on this training set, the Cumulative Distribution Functions (CDFs) of all possible PV generation values in every time step of the forecast horizon are calculated. They are then used to estimate the quantile $P_{PV,q}$ in the training set. The parameters $\boldsymbol{\theta}_q$ are then calculated by minimizing the distance of the prediction $\hat{P}_{PV,q}$ from the quantiles $P_{PV,q}$ in the training set with $q \in (0, 1)$.

Based on the quantile regressions, intervals with a given nominal coverage of $q_u - q_l$ can be calculated, where \hat{P}_{PV,q_u} and \hat{P}_{PV,q_l} are the upper interval bound and lower interval bound, respectively:

$$\hat{P}_{PV,(q_u-q_l)} = (\hat{P}_{PV,q_u}, \hat{P}_{PV,q_l})^\top. \quad (4.5)$$

If the stochastic model is correct, an interval with a nominal coverage of, for example, 50%, will contain 50% of all PV generation values [137].

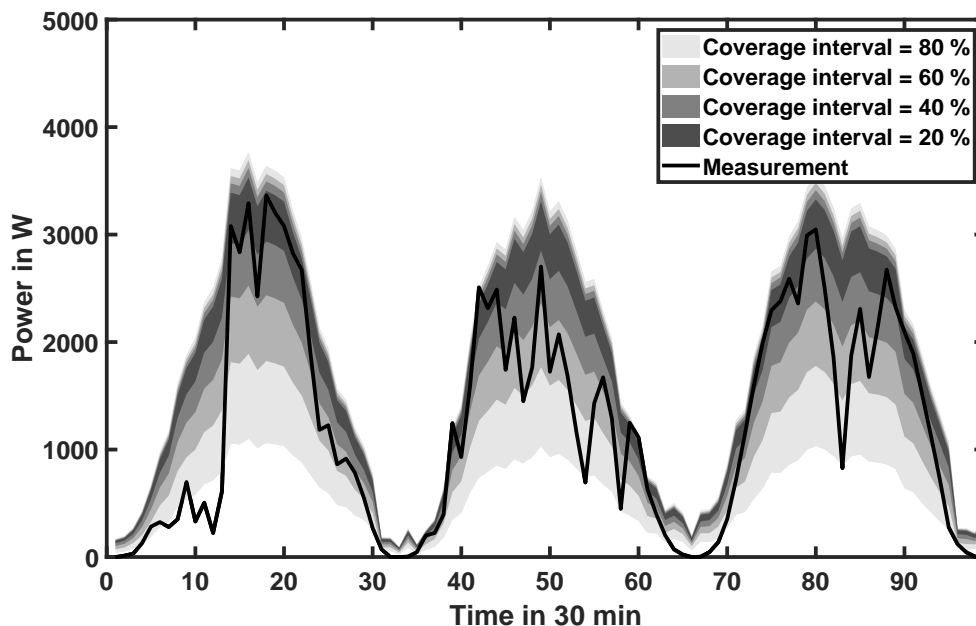


Figure 4.6: Interval forecast of the PV generation for three exemplary days. The solid line shows the realized PV generation. The four gray areas show four different predicted intervals with a coverage of 20 %, 40 %, 60 % and 80 %. The presented data has been measured in the FZI Research Center for Information Technology (FZI) House of Living Labs (HoLL) in Karlsruhe, Germany [22]. The figure only shows day-times, night values are erased to only use non-trivial values in the training of the model.

Exemplary results of the quantile regression used in this thesis are presented in Figure 4.6. The results of the quantile regression can then be used to create statistical scenarios [203] or can be used directly in robust optimization approaches [14]. In this thesis, quantile regressions are used to deduce statistical scenarios of the PV generation.

4.1.6 Deferrable Loads and Appliances

The use of deferrable loads is one of the earliest ideas of building energy management, especially the use of appliances like washing machines, dryers and dish washers. Their application has been evaluated in various publications [9, 98, 127, 163, 165, 236, 237].

Shiftable loads are loads with a defined load profile for a given energy service. The time of execution of the service is restrained to a given time interval. If the time interval is larger than the time of service, the performance of the service can be shifted in time (see Figure 4.7a). Loads which have the possibility of interrupting the energy service are additional devices that increase the flexibility in building energy management (see Figure 4.7b). In addition to the two types of appliances mentioned above, there are appliances that can change from one energy carrier to another, i. e., hybrid appliances, or

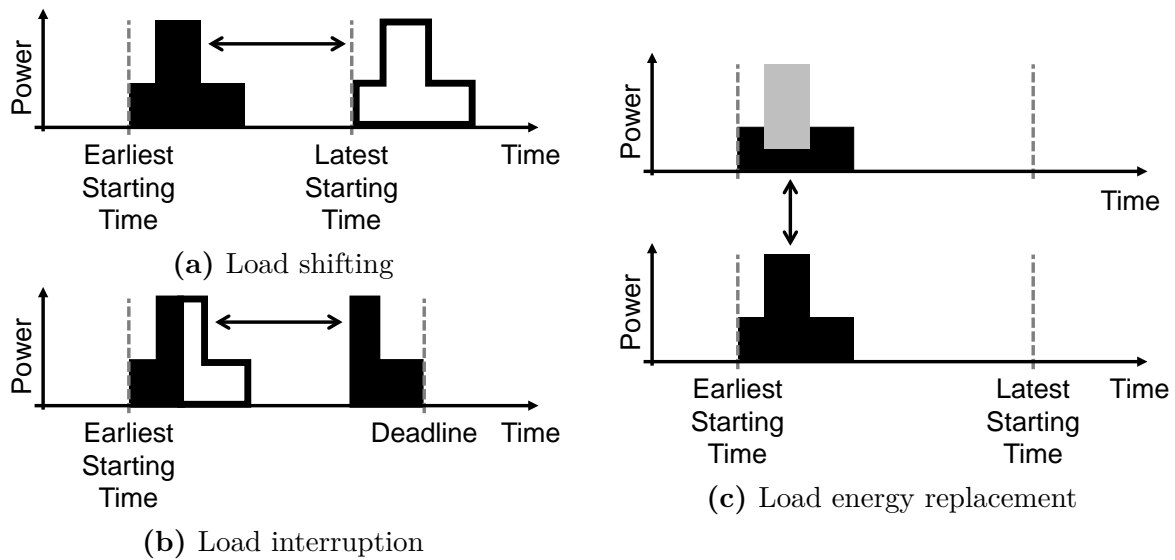


Figure 4.7: Visualization of the load profile shaping for (a) deferrable and (b) interruptible loads. The load profile shaping of hybrid appliances that are able to change from one energy carrier (yellow) to another (red) is visualized in (c). (based on [165])

that can adapt their load profile when necessary, e. g., use a longer heating phase with less power consumption (see Figure 4.7c).

Shiftable appliances have been investigated by Sou et al. [236, 237], Kaczmarczyk et al. [127] and Gottwald et al. [98] using MILP models. Tsui and Chen investigate the relaxation of MILP formulations for several types of appliances [246] and specific assumptions on the starting times. Allerdig [9] and Mauser et al. [163, 165] use non-linear models to describe a building energy system.

Typically, loads and in particular appliances are restricted to one energy carrier. Hybrid appliances are special appliances that are able to exchange the use of electricity by the use of heat [163, 166]. This increases the flexibility of the building energy system by means of utilizing different energy carriers. Mauser et al. state that hybrid home appliances that are managed by a BEMS reduce the energy costs by increasing the consumption of natural gas and decreasing the consumption of electricity. This may lead to a decrease of the self-consumption rate of locally generated electricity. In addition, the decrease of the total electricity consumption may lead to an increase in the self-sufficiency rate of electricity.

This thesis solely considers deferrable appliances, which are modeled using an integer programming approach. The model is defined in Section 5.6.4.

4.1.7 HVAC System

HVAC systems in buildings include combinations of the following devices: gas boilers, electric heating elements, heat pumps, micro-CHPs, radiators, surface heating systems, hot

and chilled water storages and Air-Conditionings (A/Cs). The devices are designed and their combination is chosen to provide the necessary heat, ventilation, hot water and chilled water in the building.

Heat Consumption

The heat consumption of a building can be categorized into space heating and Domestic Hot Water (DHW) consumption.

The traditional approach to model the heat consumption for space heating uses knowledge of the structure and physical and material properties of a building [206]. This knowledge is then used to construct a detailed building model based on physically interacting subsystems. Various simulation tools use this approach, for example, TRNSYS or EnergyPlus (see Section 3.13). However, these simulation-based models are often not suitable for predictive control purposes (see Section 3.13) [206]. In [206], various approaches that are more appropriate for control purposes are presented and categorized. One prominent approach is to use a resistance capacitance (RC) network analogously to electric circuitry to model the process dynamics [157, 206]. In addition, data-driven models are common, e. g., ARIMA models [206, 264]. A simple approach is to create a single-input single-output model that connects the outdoor temperature to the heat demand of the building [9, 163, 164, 165]

The heat consumption for DHW supply can be modeled similarly to the space heating demand. However, often top-down approaches are used. Some are directly based on own measurements [16, 33] while other models [163, 165] are based on guidelines and standards that utilize average or reference DHW consumption profiles, e. g., [252].

Thermal Energy Storage Systems

In addition to electrical energy storage systems, thermal energy storage systems are used in building energy systems. One of the most well-established techniques for thermal energy storage is the storage of hot and chilled water [17]. It is applied in domestic hot water cylinders, bulk HWTs associated with micro-CHPs and district heating schemes as well as in bulk storage of chilled water to reduce the peak loads of A/C systems. The design of storage tanks has to respect levels of stratification in the storage tanks and the trade-off between storage temperature and heat losses [17]. In addition to hot and chilled water storage tanks, systems based on the latent heat capacity of materials are used in building energy systems [17]. These systems include the use of various PCMs.

The heat losses of thermal energy storage systems are often modeled by introducing a standing loss. In general, the standing loss of a thermal energy storage, like the HWT considered in this thesis, is equal to the heat transfer Φ_{Transfer} to the surrounding of the thermal energy storage. It is dependent on the surface A of the thermal energy storage, the thermal transmittance U and the inside $\vartheta_{\text{Inside}}$ and outside $\vartheta_{\text{Outside}}$ temperatures of the thermal energy storage [23, p. 26]. When assuming a homogeneous inside temperature and homogeneous thermal transmittance, the heat transfer is given by:

$$\Phi_{\text{Transfer}} = U \cdot A \cdot (\vartheta_{\text{Inside}} - \vartheta_{\text{Outside}}). \quad (4.6)$$

Models based on this assumption are commonly used in optimization approaches [163, 222]. Stratification models do not make assumption of a homogeneous inside temperature of the thermal energy storage. They consider different levels, each with a homogeneous temperature [23, p. 35][220]. Other models treat the thermal energy storage system very similarly to an electric energy storage system [86, 267].

This thesis considers an HWT that uses a model based on Equation 4.6. The exact model as well as the parameterization are presented in Section 5.6.8.

4.1.8 Tariffs

Today, flat electricity tariffs are common in Germany and other countries in the EU. However, it is often expected that TOU tariffs will become more popular in future energy systems (see Section 2.9.2).

Even though it is hard to predict exact future tariff structures, several predicted TOU tariffs are used in the literature on building energy management. Typically, the tariffs are based on the prices at the electricity markets in combination with a constant base price including, amongst others, grid fees. For example, the publications [163, 174, 179] use the TOU tariffs presented in [143]. In addition, tariff design is often considered in the development of DSM coordination measures (see Section 2.15).

In addition to TOU tariffs, sometimes real-time pricing is assumed, e.g., in [48, 246]. Real-time pricing means that the electricity prices are only known for a short look-ahead time. The electricity prices after that short look-ahead time are subject to uncertainty.

Since TOU feed-in tariffs become more popular (see [72]), they are also more and more assumed in publications that investigate building energy management [174, 179].

4.2 Related Work on Building Energy Management Systems

A BEMS is an EMS that optimizes the operation of the energy system in a building. Sometimes BEMSs are also called Home Energy Management Systems (HEMSs) [20]. In the literature, the buildings equipped with a BEMS are mostly called smart buildings [7, 9] or intelligent buildings [186].

The optimized planning or scheduling of the devices is performed to achieve various goals. Beaudin and Zareipour [20] as well as Mauser [163, p. 103] state that the most common goal is the minimization of the operating costs of the energy system. A list of common goals that are targeted by BEMSs is presented in Table 4.1.

When considering DR as defined in Section 2.9.5, a BEMS is a tool to shape the energy consumption and generation profiles to, among other things, minimize the total costs. The

Table 4.1: List of common objectives of BEMSs based on [20] and [163, p. 104].

Objectives	Exemplary references
Cost	[3],[5],[6],[9],[36],[37],[48],[144],[145],[163],[165],[223],[244]
Carbon dioxide emission	[36],[37],[106]
Energy consumption	[36]
Grid stability	[176]
Load limitation, load shaping, and overloads	[9],[36],[163]
Self-consumption rate	[70]
Self-reliance and self-sufficiency rate	[70]
User comfort or discomfort	[5],[37],[106],[145]

load shaping is done by deferring loads, scheduling the use of energy storage and deferring and curtailing the local generation [20].

Numerous publications on EMSs have been released in the last years (see [20] and [163]). Section 4.3 gives an overview of the field. Especially approaches to the optimization of the operation of energy systems in buildings are presented.

In their review article [20], Beaudin and Zareipour state that the application of a BEMS could reduce the electricity cost by 23.1 % (calculated as the mean of 25 reviewed references) or reduce residential peak demand by 29.6 % (calculated as the mean of 18 reviewed references).

4.2.1 Objectives in Building Energy Management

Beaudin and Zareipour [20] as well as Mauser [163, p. 104] performed extensive analyses on the related work in the field of building energy management. Both publications identified the minimization of costs as the most common goal of energy management in buildings. In Table 4.1 a list of exemplary references is given for common objectives that have been investigated as part of this doctoral project. Even though each list has no claims for completeness, they indicate the importance of the specific goals. The choice of cost minimization as the objective fits the assumption of a user that acts as a *homo economicus*.

Sometimes more than one objective is addressed [20, Table 10]. In the literature, different techniques have been used to model these problems including the optimization of a weighted sum as well as the performance of multi-objective optimization and the determination of Pareto fronts, e. g., by Braun et al. [37].

However, this thesis focuses solely on the minimization of costs, assuming that all other important objectives are already included in the design of the energy tariffs, including the provision of services like the provision of ancillary services. This represents the most common objective in literature (see Table 4.1).

Table 4.2: List of commonly controlled devices in BEMSs based on [20] and [163, p. 103].

Devices	Exemplary references
Shiftable appliances	[5],[6],[9],[36],[37],[70],[98],[106],[127],[163],[165],[236],[237]
Micro-CHP	[9],[37],[48],[144],[163],[165],[176]
BESS	[3],[6],[36],[106],[144],[145],[176],[179],[174],[223],[244]
EV	[181],[244]
Smart electric heater	[163],[165],[223]
Thermal energy storage systems	[9],[36],[37],[106],[163],[165],[176],[223]
Gas heater	[37],[144],[145],[163]
Fuel cell	[244]
Adsorption chiller	[163],[164]

4.2.2 Commonly Controlled Devices in Building Energy Management

Table 4.2 lists commonly controlled devices in building energy management. Exemplary references are assigned to the devices to indicate the number of publications that deal with the specific device. The list has no claims for completeness. However, the extensive analyses on the related work in the field of building energy management performed by Beaudin and Zareipour [20] as well as Mauser [163, p. 104] show the same tendencies. In addition to these controllable devices, often non-controllable devices are considered. For example, almost all publications listed in Table 4.2 consider PV systems. The consideration of PV system control is rare in the domain of building energy management. PV systems can only reduce the generated power, which leads to a decrease of revenues in most cases.

Even though building energy management is a popular topic in the literature, the investigated scenarios and use cases often differ. In particular, the composition of the energy systems and the present devices varies over the literature and no standardized scenarios are present. However, several reference scenarios for electricity grids and the connected generation, energy storage systems and loads have been developed. They target the transmission level [60] as well as the distribution level [89].

However, this thesis focuses on the optimization of deferrable appliances, a micro-CHP, a BESS and a thermal energy storage system. The choice of the scenario is based on the configuration of the ESHL on the campus of the Karlsruhe Institute of Technology (KIT) in Karlsruhe, Germany (see Section 5.2). It comprises the devices that are most popular in literature. EVs, heat pumps, smart electric heaters and other devices are not covered, but can be added to the model.

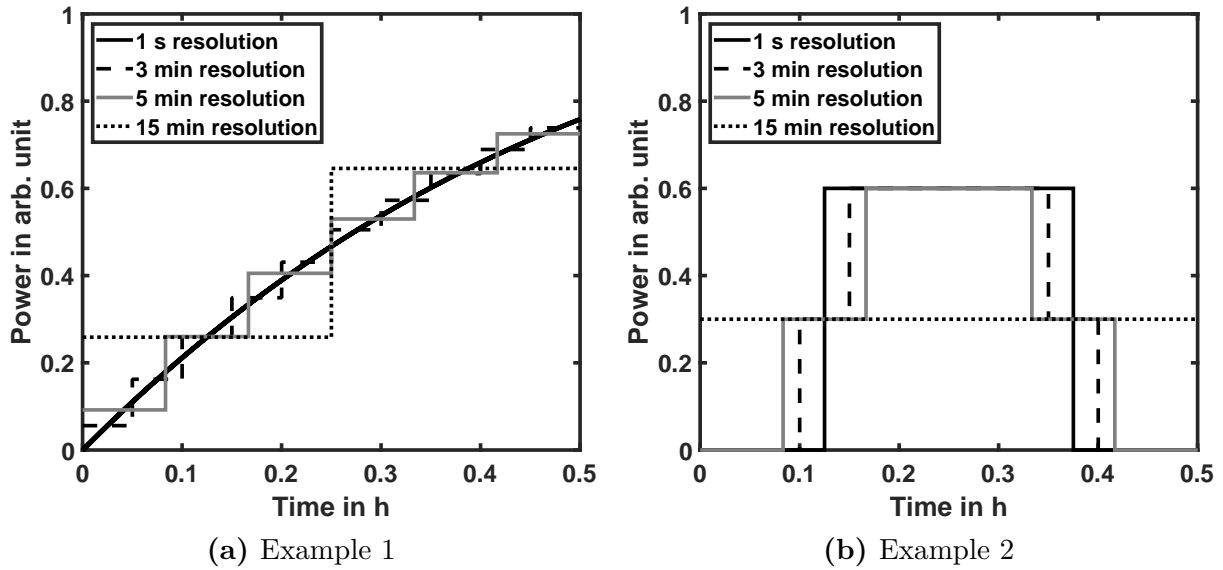


Figure 4.8: Visualization of averaging effects on two exemplary power consumption profiles. The graphs each show one consumption profiles with four different resolutions resembling the time step durations that are used in the evaluation: in the simulations, $\Delta_t = 1$ s, and the optimization, $\Delta_k = 3$ min, $\Delta_k = 5$ min and $\Delta_k = 15$ min.

Time Step Durations and Averaging Effects

In optimizations, building energy systems are typically modeled as a time discrete system. Within a time step, all values, e. g., the electricity generation and consumption, have a constant value. They represent the average value of the values in the actual energy system in each time step. This leads to averaging effects as depicted in Figure 4.8. Figure 4.8 shows visualizations of two exemplary power consumption profiles each in 4 different resolutions resembling the time step durations that are used in the evaluation: in the simulation $\Delta_t = 1$ s, and the optimization $\Delta_k = 3$ min, $\Delta_k = 5$ min and $\Delta_k = 15$ min.

These effects lead to an overestimation of the self-consumption and self-sufficiency rates, because fluctuations in the energy consumption and generation are equalized [110, 154]. Consequently, a large time step duration in the optimization leads to a deviation of the predicted behavior in the optimization window from the behavior of the actual building energy system. Thus, short time step durations in the optimization are beneficial to reduce averaging effects. However, various time step durations have been used in the literature on building energy management, ranging from 1 min to 1 h [20, Table 16]. In this thesis, the simulation and the optimization use different time step durations. The optimization uses 1 s, for the optimization time step durations of 3 min, 5 min and 15 min are investigated.

4.3 Related Work on the Optimization of the Operation of Energy Systems in Buildings

When considering the optimization of the operation of building energy systems with respect to the scheduling of device operation, various approaches have been developed utilizing different control methods. This section gives an introduction to these methods and several selected examples.

4.3.1 Controllers and Rule-based Approaches

In addition to the optimization approach presented in this work, controllers and rule-based approaches have been applied to building energy systems and related fields. As described in Figure 2.7, these regulatory control approaches are typically used to perform control tasks inside of the devices. However, several approaches have been developed to coordinate the interaction of devices to achieve a given goal and hold given constraints. Most common applications are rule-based control strategies for the operation of BESSs and HVAC systems.

Battery Energy Storage System Control

In the state-of-the-art operation of BESSs, they are commonly controlled by a fixed closed-loop controller targeting to minimize the net grid exchange power at the grid connection point.

For instance, in [44], a controller is used to maximize the self-consumption by minimizing the energy exchanges between the BESS and the grid. This is the conventional approach towards the operation of BESSs. The performance of such a closed-loop controller in combination with deferrable appliances and a scheduled micro-CHP is evaluated in [165].

In some cases, different closed-loop control strategies are compared with respect to costs and their effects on distribution grids. For instance, in [266], two different operating strategies are evaluated. Flerer and Stenzel [83] analyze the impact of different operation strategies to provide primary control reserve by performing a battery simulation that includes battery aging, focusing on large BESSs.

In other cases, the operation is defined by rules that consider a given time-dependent tariff. An evaluation of such a battery operating strategy using different tariffs is presented in [132]. The authors of [132] propose an operating strategy that does not rely on predictions and evaluate it by means of recorded data, showing that their strategy is able to realize a near-optimal performance in the evaluation scenario.

Finally, controllers are used to dimension BESSs and assess their economic benefits as well as impacts on grids. For instance, in [255], the sizing of PV systems with BESSs and their impact on grids in Germany and Australia is analyzed. In [247], a controller is used in the comparison of the economic benefit of different battery technologies. The authors of [243] developed a BESS control strategy that aims at supporting the dispatch of renewables. The BESS is used to smooth the electricity generation from RESs based on the predicted solar and wind conditions.

Heating Ventilation and Cooling System

In the domain of HVAC systems in buildings many publications have been issued. For example, Papantoniou et al. [197] present a BEMS that utilizes a set of control rules, including closed-loop feedback control, to control the HVAC system including all subsystems. Doukas et al. [65] present a similar model that also utilizes a set of control rules to, amongst others, control the HVAC system. The goal of the system is to preserve the comfort conditions of occupants while minimizing the energy consumption and costs.

4.3.2 Day-ahead Scheduling Approaches

Day-ahead scheduling approaches determine the optimal operation of a building energy system by identifying the optimal operation schedule of all the devices in the building with respect to a given optimization target, e. g., operating costs. In this context, day-ahead refers to a daily optimization, typically one optimization is performed at midnight with an optimization horizon of 24 h. The daily approach is similar to the rolling horizon approach (see Section 3.5 and 4.3.3) but differs in the frequency and in the kind of the optimization. The low number of optimizations reduces the possibility to change the schedule during the operation time of the energy system. This may be necessary when the state of the energy system differs from the expected states predicted by the building energy system model.

Typically, daily scheduling approaches are performed to optimize the energy costs at the day-ahead market (see Section 2.9.1) [87, 94, 161]. Often this is done for energy systems that are larger than building energy systems [161], e. g., hydro-generation plants [87], wind and solar generation plants [77, 263] or Virtual Power Plants (VPPs) [94], which potentially could comprise building energy systems. Some day-ahead scheduling approaches are designed to take the network constraints into account [95, 234]. Hence, supporting the operation of the grid and potentially providing ancillary services as DR.

4.3.3 Rolling Horizon Optimization in Buildings

Rolling horizon optimization (see Section 3.5) is one of the most common approaches to the optimization of the operation of building energy systems [20]. Rolling horizon optimization approaches enable the joint scheduling of the devices while considering the predicted generation and consumption.

These approaches can be restricted to subsystems of a building energy system or target the optimization of the whole building energy system (see Section 4.2.2). In this section, different examples of rolling horizon optimization approaches in buildings are presented. The examples are categorized by the main subsystems.

Heating Ventilation and Cooling System

Ma et al. [156] developed an economic model predictive control approach for the operation of building cooling systems that minimizes the electricity bill and maximizes the Coefficient

of Performance (COP) while satisfying the required cooling load. In addition, Široký et al. [231] present a similar approach to minimize the operating costs of a heating system. It has been tested in a two months experiment performed in a real building in Prague, Czech Republic. In addition, tracking MPC is often used for the optimization of the heating system. One example is presented by Oldenwurtel et al. [191]. They present a model predictive control that uses weather forecasts to reduce the total energy consumption of the HVAC system. Their approach targets the minimization of the energy consumption.

In [155], Ma et al. present an EMPC approach to reduce the energy consumption and costs for HVAC systems. They evaluate their approach with an EnergyPlus building simulation model. The EMPC approach leads to an energy savings of about 25 % and cost savings of about 28 %.

Battery Energy Storage System and Electric Vehicles

In building energy systems, BESSs are often operated by rule-based or closed-loop controllers. However, these controllers do not use a predictive optimization of the operation of BESSs and are not able to optimize the operation in combination with other devices. This can be achieved by utilizing a combination of scheduling and rule-based or closed-loop controllers [59, 174, 179] or by optimizing the battery directly [51, 169, 232]. Here, optimizing the battery directly means to determine the trace of charge and discharge power values for the optimization horizon.

In [232], charge and discharge power profiles of a BESS are determined by an EA. The authors of [169] compare a similar approach to optimization to three rule-based controllers. A model predictive control approach for the optimization of a BESS and a PV system is presented in [265]. Clastres et al. [51] present a MILP problem in which the objective is to maximize the profits of a combination of a PV, a BESS and deferrable appliances. Both approaches showed good results with slightly different focuses, models, temporal resolutions and application scenarios.

An increasing number of publications also targets optimized EV charging in the context of building energy systems and the incorporation of EVs in BEMSs. Some publications only consider the charging of EVs [96, 136], treating the EV as a deferrable load, while others also consider discharging, treating EVs similar to batteries [181, 223]. For example Mültin [181] extended an existing BEMS to optimize the charging of EVs to minimize the electricity costs. The optimization is done by using an EA in combination with a building simulation model. This work was applied to a real building and EV. Scott et al. [223] considers a building energy system with an EV that can be charged and discharged. The EV is modeled similar to a BESS, but with additional constraints considering the availability of the EV and a minimum energy that the EV battery should have in it at each time.

Complete Building Energy Systems

The Organic Smart Home (OSH) [9, 163, 165] is one example of a BEMS that is capable of optimizing the operation of a complete building energy system. It can be used in simulations

and in the operation of a real building while presenting an adaptive and flexible approach to the optimization. The software is built on the principles of organic computing presenting an open-source framework that can be expanded. Its optimization uses an EA that works on a simulation model as described in Section 3.13. The framework has been expanded to enable the optimization of various devices, e. g., EVs [181]. As part of this doctoral project BESSs have been included into the OSH [174, 179]. In [105], a similar approach is presented, it uses a multi-level control mechanism (see Figure 2.7).

Other approaches utilize MILP models. In [171], Missaoui et al. present a BEMS that targets minimizing a linear combination of the daily energy costs and the user discomfort. The controlled devices consist of a washing machine, a dish washer and the heating system. The optimization uses a non-linear building model.

This work presents an approach to the optimization of complete building energy systems. The exact scenario is presented in Section 5.2. However, this work incorporates the uncertainty in the forecast of the local generation and consumption by the use of a stochastic programming approach. The multiple levels of control (see Figure 2.7) are not taken into account directly.

4.3.4 Optimization Under Uncertainty

The approaches mentioned above do not incorporate the uncertainties in the predictions of the local energy generation and consumption directly. However, some approaches do it indirectly. For example, the BEMS presented in [9, 163, 165], i. e., the OSH, does have penalty costs that reward schedules leading to a behavior that is experienced to be robust to small errors in the predictions. Other approaches use closed-loop controllers that can react on the current states in the energy system reducing the reliance on predictions [59, 132, 174].

In contrast to these indirect measures, this work presents an approach that incorporates the uncertainty directly, using means of stochastic programming (see Section 3.11) to optimize the expected operating costs.

Soroudi and Amraee [235] present a state-of-the-art analysis of decision making under uncertainty in energy systems. They list various methods and examples. In the remainder of this section, related work in the two most common approaches, i. e., robust optimization and stochastic programming are presented (see Section 3.9). In addition, publications are discussed that use two-stage stochastic programming approaches that are closely related to the approach presented in this thesis.

Robust Optimization

As described in Section 3.10, robust optimization approaches target on not violating any constraints for all expected outcomes of the uncertainty.

Appino et al. [14] present an approach that uses a robust optimization formulation for generating reliable schedules. The approach consists of an off-line optimization that

determines dispatch schedules created in a way that an additional on-line optimization approach can ensure the on-line feasibility of the dispatch schedule with a given security level. The only controlled device is a BESS.

Liu and Fu [144] present an approach that considers uncertainty in the electric and thermal loads and solar power generation in the economic optimization of a building energy system. The considered building energy system comprises a BESS and a micro-CHP with a boiler unit. However, the approach includes the uncertainty only by the introduction of one additional constraint that considers the worst-case scenario. For the electric load balance, the authors define the worst case as a maximum increase in the electric load and the maximum decrease in solar power generation. For the thermal load balance, the worst case is defined as the maximum thermal load possible.

El-Baz [70] investigate the potential of incorporating a probabilistic PV generation forecast into building energy management and in particular day-ahead scheduling. They use an exhaustive enumeration method, i. e., they evaluate all possible solutions, to find an optimal schedule for household appliances in combination with PV generation. Here, an optimal schedule is defined by a maximum self-consumption and self-sufficiency. The algorithm considers a probabilistic PV generation forecast by using scenarios that represent the limits of given prediction intervals. Based on a case study, they state that the incorporation of a probabilistic PV generation forecast can lead to an increase in self-sufficiency and self-consumption by 24.2% and 17.7%, respectively.

Stochastic Optimization

Abdulla et al. [3] present an approach to optimize the operation of a BESS that uses dynamic stochastic programming in combination with a rolling horizon approach. The work incorporates degradation of the battery. Uncertain parameters are the PV generation and the electricity consumption. However, in the provided case study the number of possible future generation and consumption scenarios is set to one. This leads to a deterministic optimization not considering possible uncertainties directly as it is done in this thesis. In contrast to this work, only the BESS is optimized, and no other devices are controlled.

In [244], Tischer and Verbic present a stochastic dynamic programming approach to the optimization in BEMSs. The stochastic dynamic programming approach is then compared to a deterministic approach that reduces the computational complexity by approximating the random parameters by expected values. Based on a case study they state that the stochastic dynamic programming approach does lead to the same costs as the approach that only uses expected values.

A BEMS that uses a stochastic optimization, called *Energy Box*, is presented by Livengood and Larson [145]. It targets on minimizing the operating costs of a smart home while maximizing the user comfort. The BEMS uses an optimization horizon of 24 h and a time step length of 1 h. It considers the uncertainties with three possible future scenarios.

All three approaches state that the application of the stochastic optimization yields better results than the application of a deterministic optimization that for example only considers expected values of uncertain parameters. However, all state that a stochastic optimization leads to a high computational effort that can cause optimization times that are inappropriate for a BEMS.

Two-stage Stochastic Optimization

Some approaches, including this thesis, use a two-stage stochastic program as an approximation to a full multi-stage stochastic program [48, 223]. This can reduce the computational effort of solving the optimization problem significantly since multi-stage stochastic programs are computationally challenging [226] (see Section 3.11).

Chen et al. [48] compare two-stage stochastic programming and robust optimization techniques to the scheduling of residential loads. However, they only consider uncertainty in the RTP tariffs which are known exactly for the first time step of the optimization horizon and have to be predicted with uncertainty for all other steps. The first-stage relates to the first time step, the second-stage relates to all other time steps in the optimization horizon. Their objective is to minimize the expected operating costs as well as the number of possible scenarios whose operating costs exceed a given threshold. The results show that two-stage stochastic programming provides benefits over robust scheduling in this setting. Similar results are observed in this thesis.

Scott et al. [223] present an approach that is very similar to the one presented in this thesis. They developed a rolling horizon approach for building energy management that schedules an electrical HVAC system, hot water heating, a PV system, deferrable appliances, an EV and a BESS. It uses a two-stage stochastic program that uses sampled scenarios in the second-stage. In the paper, a reactive controller and an expected value based deterministic rolling horizon optimization are compared to the two-stage stochastic programming rolling horizon approach with probabilistic and perfect forecast. The rolling horizon approach uses an optimization horizon of 16 hours. The first time step, i. e., the first stage, has a duration of 15 min. All other steps have a duration of 30 min. They form the second stage. The results show that the two-stage approach performs close to the controller with perfect forecast. They achieve cost reductions over the two reactive controllers of 35 %. The authors expect the two-stage approach to be more conservative than the approach that uses the expected values and since it avoids having unmet demand of sampled upcoming peak demands. The approach presented in [223] differs from the one presented in this work by not considering a micro-CHP and TOU feed-in tariffs that lead to a need of smart battery (dis-)charge schedules that are expected to reward the use of a two-stage approach.

A two-stage robust approach that combines stochastic and robust optimization is presented in [241]. In the first stage, the decision maker observes demand and available wind power and determines a dispatch schedule with minimal costs for the first time step. The second-stage computes an optimal schedule that respects the worst-case dispatch cost for the remaining time steps in the optimization horizon.

4.3.5 Comparison

In Table 4.3, a selection of related work is listed. A comparison of the approaches shows that cost reduction is the most frequent objective. The most frequent uncertain parameters that are considered are the PV generation and the electric load. Most approaches target the control of a BESS while the other controllable devices differ. The considered optimization horizon is mostly 24 h. However, the number of time steps varies strongly. The number of time steps is often chosen to achieve a manageable complexity of the optimization problem and a suitable duration of the optimization process. The number of possible future scenarios, i. e., the number of Monte Carlo estimates for the random variables, varies between 1 and 60. However, the method to derive the scenarios varies. Some approaches use random scenarios with an equal probability of occurrence [48, 223], while others use scenarios that represent the limits of given prediction intervals [14, 70]. For example, El-Baz et al. [70] use PV generation scenarios that represent the limits of given prediction intervals of 70 %, 80 %, 90 %, 95 % and 99 %.

This thesis builds upon these approaches and extends them by presenting a two-stage stochastic optimization approach that uses a rolling horizon optimization with appropriate optimization horizon and resolution incorporating three classes of devices that can easily be extended (see Section 5.5). In addition, this thesis addresses the electricity and the heating system in a building.

Table 4.3: Comparison of a selection of related work (SP = stochastic programming, RO = robust optimization).

Reference	O+H4bjective	Approach	Uncertain parameter	Controlable devices	Number of time steps	Number of scenarios	Horizon in h
Mausser et al.[165], Mausser [163], Müller et al.[174, 179]	Cost reduction	Penalty costs	None	Micro-CHP, cooling, BESS, appliances,	Varies	1	Varies
El-Baz [70]	Self-sufficiency & self-con.	RO	PV generation	Appliances	Unknown	5	24
Liu and Fu [144]	Cost reduction	RO	PV generation, electricity load, heat load	Micro-CHP, gas boiler, BESS	24	2	24
Abdulla et al.[3]	Cost reduction	Multi-stage SP	PV generation, electricity load, EV behavior	BESS	48	1	24
Tischer and Verbic [244]	Cost reduction	Multi-stage SP	PV generation, electricity load	BESS,EV, fuel cell	96	Unknown	24
Livengood and Larson et al.[145]	Cost reduction plus comfort maximization	Multi-stage SP	wind turbine, heat load, real-time pricing	Heating, BESS	24	3	24
Chen et al.[48]	Cost reduction	Two-stage SP	Real-time pricing	Appliances	288	30	24
Scott et al.[223]	Cost reduction	Two-stage SP	Real-time pricing, electricity load, heat generation, PV generation	Heating, cooling, BESS,EV, appliances	32	60	16
This thesis	Cost reduction	Two-stage SP	PV generation	micro-CHP, BESS, appliances	288	1 - 10	24

5. Model and Optimization Approach

This chapter presents the main contribution of this thesis: A rolling horizon optimization approach to the optimization of the operation of a building energy system that uses a stochastic two-stage optimization. Firstly, the notation is introduced in Section 5.1. After that, a motivation of the scenario choice is presented Section 5.2. Then, the overall goal of the optimization of the operation of the building energy management and at particular the stochastic two-stage optimization is presented in Section 5.3. Section 5.4 presents the simulation of the building energy system. After that, an overview of the rolling horizon optimization approach and the simulation of the building energy system is presented in Section 5.5. Then the models of the devices as well as the device interactions are presented in detail in Section 5.6. Based on this, the optimization problem that has to be solved in the rolling horizon optimization approach is presented. For the sake of clarity, first the state-of-the-art one-stage optimization problem is presented in Section 5.7. In Section 5.8, the two-stage stochastic optimization problem is presented. The chapter finishes with remarks on the implementation of the approach and the used frameworks and tools, and remarks on the adaptivity of the approach in Sections 5.9 and 5.10, respectively.

5.1 Notation and Introductory Remarks

To ease the reading of this chapter, first comments on the notation that is used to present the simulation and the optimization models are presented. The definition of the rolling horizon approach described in Section 3.5 and visualized in Figure 3.2 shows the difference between the optimization and the simulation of the building energy system. The optimization is carried out repetitively to calculate the control inputs for the devices. The control inputs are then used to simulate the temporal progression of the building energy system. To differentiate between variables and parameters that are used in the simulation and optimization, variables and parameters that are used in the simulation are indicated by a tilde ($\tilde{\cdot}$). Predicted values are indicated by a hat ($\hat{\cdot}$). The simulation of the building energy

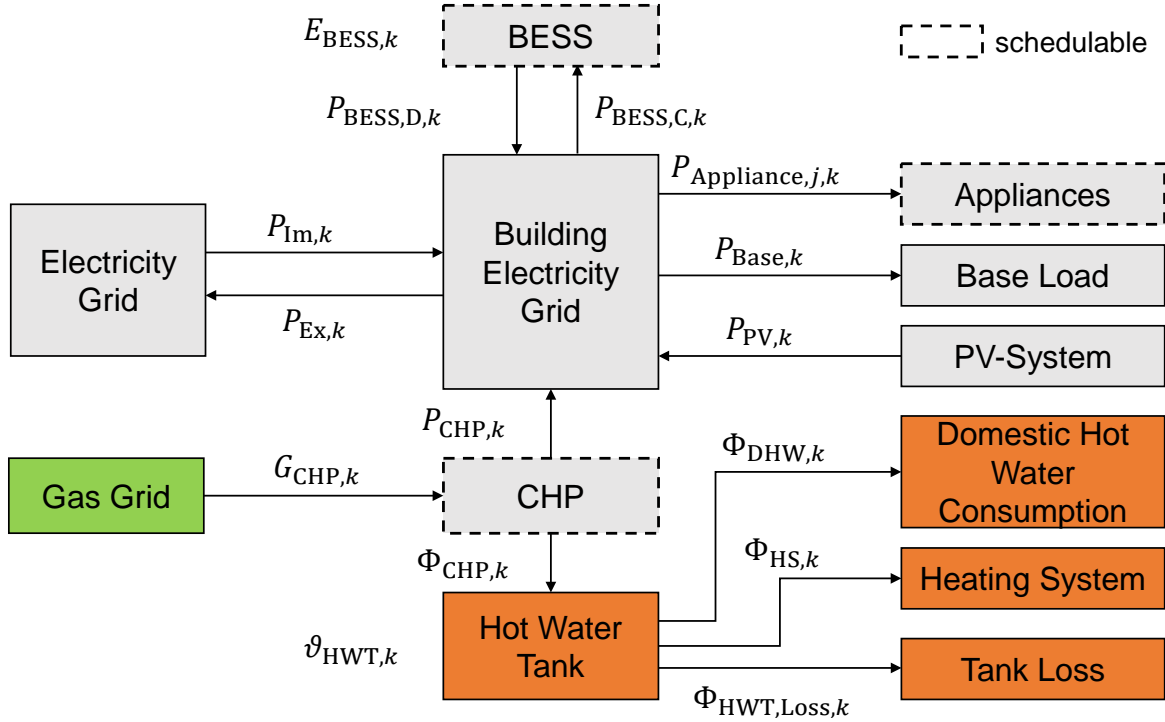


Figure 5.1: Overview of the smart building scenario. The arrows indicate the power flows while the labels show the corresponding symbols used in the definition of the model.

system is performed over T discrete time steps. Each time step is indicated by the variable $t \in \{1, \dots, T\}$. The duration of each time step is Δ_t . In contrast, the optimization consists of N discrete time steps. Each time step is indicated by the variable $k \in \{0, \dots, N\}$. The duration of each time step is Δ_k . Notably, the parameters Δ_t and Δ_k do not have to be equal.

In addition to the main contribution of this thesis, the stochastic two-stage rolling horizon optimization approach, a state-of-the-art one-stage approach as well as rule-based control algorithms are investigated. These are used as benchmark scenarios in the evaluation of the rolling horizon optimization approach that uses a stochastic two-stage optimization. The rule-based control algorithms are described in Section 5.6.

5.2 Choice of Scenario

This thesis investigates approaches to the optimal operation of building energy systems. It assumes a building that is equipped with an automated BEMS, forming a smart building. The automated BEMS allows for an automated control of the devices of the building energy system targeting the optimal operation of the building energy system. As described in Section 4.2.1, the optimal operation can be defined in many ways. However, the analysis in

Section 4.2.1 identifies the minimization of operating costs as the most common objective in the literature. This thesis picks up on the minimization of operating costs, since other objectives, e. g., the minimization of carbon dioxide emissions, can be included in the operating costs by the introduction of additional costs. The choice of cost minimization as the objective fits the assumption of a user that acts as a *homo economicus*. The provision of additional ancillary services is not investigated in this thesis. However, this can lead to further cost decreases.

As a main contribution, this thesis presents an approach to the optimization of the operation of a building energy system that includes the consideration of uncertainty in the predictions of generation and consumption. Here, the Laplace decision criterion is chosen to assess the uncertain prediction of the operating costs.

The design of an approach to the optimization of the operation of building energy system has to consider the targeted application scenarios, i. e., the building energy system and its environment. Hence, the targeted application scenarios can be restricted to contain one specific scenario, a specific range of scenarios or all possible scenarios. The approaches presented in literature often target the applicability in a specific range of scenarios, however they are often evaluated in a low number of evaluation scenarios or case studies. In particular, the optimization models are tailored to a specific set of devices. This allows for a clever choice of the optimization model leading to low optimization times. Generic models that allow for an application in various scenarios are hard to tune and commonly lead to longer optimization times. Thus, often heuristics are used when applicability is focused.

This thesis investigates the performance of an approach to the optimization of energy systems that considers uncertainty. Therefore, a specific application scenario has been chosen. Even though this choice does not allow making statements on the performance in various application scenarios or making statements on the general applicability, an in-depth investigation is eased. A scenario is chosen that comprises the devices that have been identified to be the most common in building energy management. Thus, it is assumed that the application scenario is relevant, and an application of the approach presented in this work is valuable. In addition, the scenario choice eases the comparison with other publications.

5.2.1 Smart Building Configuration

The chosen scenario consists of a smart building that is equipped with a BESS, a micro-CHP, an HWT, deferrable appliances and a PV system. In addition, other electric and thermal loads are present that are not defined in detail. The sum of the additional electric loads is called base load. The thermal loads are the heating system and a DHW consumption. Controllable devices, i. e., devices that can be controlled by the BEMS, are the BESS, the micro-CHP and the deferrable appliances. All other devices cannot be controlled by the BEMS. An overview of the smart building is visualized in Figure 5.1 a list of the devices is

Table 5.1: List of the devices in the investigated smart building configuration.

Device	Controllable	Description
Battery energy storage system	✓	Section 5.6.1
Micro combined heat and power plant	✓	Section 5.6.2
PV system	✗	Section 5.6.3
Controllable appliances: Washing machine	✓	Section 5.6.4
Non-controllable appliances: Dryer, dish washer, induction hob, oven	✗	Section 5.6.4
Electric base load	✗	Section 5.6.5
Space heating	✗	Section 5.6.6
Domestic Hot Water Consumption	✗	Section 5.6.7
Hot water tank	✗	Section 5.6.8

presented in Table 5.1. In Section 5.6 the models of the individual devices that are used in the simulation and the optimization of the building energy system are presented. The choice of the individual parameters is covered in Section 6.1.

5.2.2 Assumptions

In this thesis some assumption and considerations are made to define the model of the building energy system that is presented in Section 5.6. Firstly, the building is connected to the electricity and the gas grid at all times and the electricity and gas needs can be satisfied by the electricity and the gas grids at all times. Secondly, it is assumed that the micro-CHP generates enough heat in all cases (see Section 5.6.8). Furthermore, it is assumed that time-dependent electricity consumption tariffs and time-dependent electricity feed-in tariffs are present (see Section 5.6.9). Here, it is assumed that the electricity consumption price is always higher than the absolute value of the feed-in compensation (see Section 5.6.9). Moreover, no feed-in from the BESS into the grid is considered Section 5.6.1.

5.2.3 Forecast Uncertainties

In the building energy system, the PV system generation (see Section 5.6.3), the electricity consumption, the heat consumption and the tariffs have to be predicted. This thesis assumes a perfect prediction for all except the PV system generation (see Figure 5.2). For the PV system generation, a probabilistic forecast is used that is described in Section 5.6.3. An overview of the predictions of generation and consumption is given in Table 5.2.

5.3 Overall Goal

The goal pursued in this thesis is to present an approach to minimize the operating costs for the smart building configuration defined in Section 5.2. The operating costs are defined as

Table 5.2: Overview of the predictions of generation and consumption.

Predicted value	Method	Description
PV system generation	Probabilistic prediction	Section 5.6.3
Electricity consumption	Perfect prediction	Section 5.6.5
Heat consumption	Perfect prediction	Sections 5.6.6 and 5.6.7
Tariffs	Perfect prediction	Section 5.6.9

the sum of the cost of the electricity import from the grid, the earnings from the electricity export to the grid and the gas cost. The individual costs are calculated in every time step t of the time-discrete simulation of the building energy system (see Section 5.4). Hence, the total operating costs \tilde{C}_T for an operating time of $\Delta_t \cdot T$ are given by:

$$\tilde{C}_T = \sum_{t=1}^T \Delta_t \cdot [\tilde{\pi}_{\text{Ex},t} \cdot \tilde{P}_{\text{Ex},t} + \tilde{\pi}_{\text{Im},t} \cdot \tilde{P}_{\text{Im},t} + \tilde{\pi}_{\text{Gas},t} \cdot \tilde{G}_{\text{CHP},t}]. \quad (5.1)$$

$\tilde{\pi}_{\text{Ex},t}$ is the compensation for the electricity export to the grid in time step t in cent/kWh, $\tilde{\pi}_{\text{Im},t}$ is the price for the electricity import at time step t in cent/kWh and $\tilde{\pi}_{\text{Gas},t}$ is the price for gas in time step t in cent/kWh. The parameters $\tilde{P}_{\text{Ex},t}$, $\tilde{P}_{\text{Im},t}$ and $\tilde{G}_{\text{CHP},t}$ are the power that is fed into the grid in time step t in kW, the power that is drawn from the electricity grid in time step t in kW and the power that is drawn from the gas grid in time step t in kW, respectively. In Section 5.4, the simulation of the building energy system that is used to determine the parameters $\tilde{P}_{\text{Ex},t}$, $\tilde{P}_{\text{Im},t}$ and $\tilde{G}_{\text{CHP},t}$ is presented.

When minimizing the operating costs of a building energy system, it is important to define a timescale that is targeted. The most obvious approach is to minimize the operating costs over the lifetime of the energy system. However, this can lead to long computation times and thus typically shorter timescales are simulated (see Section 2.12). The simulation results are used to estimate the expected energy costs over the lifetime of the energy system. In Chapter 6, the timescales, i. e., the choices of T , that are used in the evaluation of the approach are listed.

Equation 5.1 does not consider the value of the energy stored in the energy storage systems in time step $T+1$, i. e., the energy stored in the BESS $\tilde{E}_{\text{BESS},T+1}$ and the energy stored in the HWT:

$$\tilde{E}_{\text{HWT},T+1} = (V_{\text{HWT}} \cdot \rho_{\text{Water}} \cdot c_{\text{Water}}) \cdot (\vartheta_{\text{HWT},T+1} - \vartheta_{\text{HWT}}). \quad (5.2)$$

ϑ_{HWT} is the minimum temperature of the HWT, ρ_{Water} is the volumetric mass density of water, the volume of the HWT V_{HWT} and c_{Water} is the specific heat capacity of water.

To enable an evaluation of approaches to the optimization of building energy systems, these final states have to be considered. This is based on the value of the energy that is stored in the energy storage systems. To do so, additional terms that are dependent on the final storage states have to be added to Equation 5.1. The value of the energy stored in the

BESS is approximated by applying the average electricity costs to the energy stored in the BESS times the efficiency η_{BESS} . Then the resulting values are treated as earnings. The value of the energy stored in the HWT is estimated by the cost that would occur when the HWT is heated up from its minimum temperature $\underline{\vartheta}_{\text{HWT}}$ to $\tilde{\vartheta}_{\text{HWT},T+1}$ while considering the efficiency of the micro-CHP. The resulting equation is given by:

$$\begin{aligned} \tilde{C}_T = & \sum_{t=1}^T \Delta_t \cdot [\tilde{\pi}_{\text{Ex},t} \cdot \tilde{P}_{\text{Ex},t} + \tilde{\pi}_{\text{Im},t} \cdot \tilde{P}_{\text{Im},t} + \tilde{\pi}_{\text{Gas},t} \cdot \tilde{G}_{\text{CHP},t}] \\ & - \sum_{i=1}^T \frac{\tilde{\pi}_{\text{Gas},i}}{T} \cdot \frac{G_{\text{CHP},\text{Nom}}}{\Phi_{\text{CHP},\text{Nom}}} \cdot (\tilde{E}_{\text{HWT},T+1} - \tilde{E}_{\text{HWT},\text{Initial}}) \\ & - \sum_{i=1}^T \frac{\tilde{\pi}_{\text{Im},i}}{T} \cdot \eta_{\text{BESS}} \cdot (\tilde{E}_{\text{BESS},T+1} - \tilde{E}_{\text{BESS},\text{Initial}}). \end{aligned} \quad (5.3)$$

For the evaluation scenario of the approach, the parameters of the building energy system as well as the tariff structure have to be chosen to represent a realistic scenario. However, drawing conclusions based on the specific value of the costs is not the main target of this thesis. It is rather about drawing conclusions on the performance of the approaches to the operation of the building based on the differences of the operating costs for different approaches. This means that the approach to the operation of the building that leads to the lowest operating costs in the simulation period $\Delta_T = \Delta_t \cdot T$, is assumed to perform best.

5.4 Building Simulation

A building energy system is simulated using a time-discrete simulation. The simulation is carried out for T time steps $t \in \{1, \dots, T\}$ with each time step having a duration of Δ_t seconds. The temporal progression of a discrete time model is described by the following state equation (see Section 3.4):

$$\tilde{\mathbf{x}}_{t+1} = \tilde{\mathbf{f}}(\tilde{\mathbf{x}}_t, \mathbf{u}_t), \quad \tilde{\mathbf{x}}_1 = \tilde{\mathbf{x}}_{\text{Initial}}, \quad \forall t \in \{1, \dots, T\}, \quad (5.4)$$

The state of the building $\tilde{\mathbf{x}}_t$ in time step t is given by:

$$\tilde{\mathbf{x}}_t = (\tilde{E}_{\text{BESS},t}, \tilde{\vartheta}_{\text{HWT},t})^\top, \quad \forall t \in \{2, \dots, T+1\}, \quad (5.5)$$

$$\tilde{\mathbf{x}}_1 = (\tilde{E}_{\text{BESS},\text{Initial}}, \tilde{\vartheta}_{\text{HWT},\text{Initial}})^\top, \quad (5.6)$$

$\tilde{E}_{\text{BESS},t}$ is the energy that is stored in the BESS in time step t and $\tilde{\vartheta}_{\text{HWT},t}$ is the temperature of the HWT in time step t . The control inputs $\tilde{\mathbf{u}}_t$ in time step t are given by:

$$\tilde{\mathbf{u}}_t = (\tilde{u}_{\text{BESS},\text{C},t}, \tilde{u}_{\text{BESS},\text{D},t}, \tilde{\mathbf{u}}_{\text{Appliances},t}, \tilde{u}_{\text{CHP},t})^\top, \quad \forall t \in \{1, \dots, T\}, \quad (5.7)$$

where $\tilde{u}_{\text{BESS},\text{C},t} \in [0, 1]$ and $\tilde{u}_{\text{BESS},\text{D},t} \in [0, 1]$ are the charge and discharge control inputs for the BESS in time step t , $\tilde{\mathbf{u}}_{\text{Appliances},t} \in \{0, 1\}$ are the control inputs for the appliances in

time step t and $\tilde{u}_{\text{CHP},t} \in \{0, 1\}$ is the control input of the micro-CHP in time step t . The control inputs are determined by the rolling horizon optimization (see Section 5.5) or by a rule-based controller in case of the benchmark scenarios.

The parameters $\tilde{P}_{\text{Ex},t}$, $\tilde{P}_{\text{Im},t}$ and $\tilde{G}_{\text{CHP},t}$ that define the operating costs of the building (see Equations 5.1 and 5.3) are calculated by:

$$\tilde{P}_{\text{Ex},t} = \begin{cases} -1 \cdot \tilde{P}_{\text{Grid},t} & \text{if } \tilde{P}_{\text{Grid},t} \leq 0 \\ 0 & \text{otherwise} \end{cases}, \quad \forall t \in \{1, \dots, T\}, \quad (5.8)$$

$$\tilde{P}_{\text{Im},t} = \begin{cases} \tilde{P}_{\text{Grid},t} & \text{if } 0 < \tilde{P}_{\text{Grid},t} \\ 0 & \text{otherwise} \end{cases}, \quad \forall t \in \{1, \dots, T\} \quad (5.9)$$

and

$$\tilde{G}_{\text{CHP},t} = \tilde{u}_{\text{CHP},t} \cdot G_{\text{CHP},\text{Nom}}, \quad \forall t \in \{1, \dots, T\}. \quad (5.10)$$

$\tilde{P}_{\text{Grid},t}$ is the power that is exchanged with the grid, i. e., the sum of all power flows in the building. Depending on the sign of $\tilde{P}_{\text{Grid},t}$, the variable represents the power fed into the grid or drawn from the grid:

$$\tilde{P}_{\text{Grid},t} = \sum_{j=1}^J \tilde{P}_{\text{Appliances},j,t} + \tilde{P}_{\text{Base},t} + \tilde{P}_{\text{BESS},\text{C},t} - \tilde{P}_{\text{PV},t} - \tilde{P}_{\text{CHP},t} - \tilde{P}_{\text{BESS},\text{D},t}, \quad \forall t \in \{1, \dots, T\}. \quad (5.11)$$

where $\tilde{P}_{\text{BESS},\text{C},t}$ and $\tilde{P}_{\text{BESS},\text{D},t}$ are the charge and discharge powers of the BESS in time step t , $\tilde{P}_{\text{Base},t}$ is the base load in time step t , $\tilde{P}_{\text{Appliances},j,t}$ is the power consumption of appliance j in time step t , $\tilde{P}_{\text{CHP},t}$ is the power generation by the micro-CHP in time step t and $\tilde{P}_{\text{PV},t}$ is the generation by the PV system in time step t . The power flows and energy states of the building simulation are listed in Table 5.3. The charge and discharge powers of the BESS, i. e., $\tilde{P}_{\text{BESS},\text{C},t}$ and $\tilde{P}_{\text{BESS},\text{D},t}$, the power consumption of the appliances, i. e., $\tilde{P}_{\text{Appliances},j,t}$, and the power generation of the micro-CHP are dependent on the corresponding control inputs. The control inputs that are defined by the optimization are listed in Table 5.4. The definitions of the power generation or consumption of particular devices, i. e., the simulation models of the individual devices, are presented in the corresponding subsections of Section 5.6.

The process of the building simulation is presented in Algorithm 5.1. The functions that are applied therein are defined as follows:

adjustOptimizationInputs($\tilde{u}_{\text{CHP},t-1}$, $\tilde{E}_{\text{BESS},t-1}$, $\tilde{v}_{\text{HWT},t-1}$, $\underline{\mathbf{k}}_{\text{Appliances}}$, $\overline{\mathbf{k}}_{\text{Appliances}}$, $\mathbf{b}_{\text{Appliances}}$, t): This function calculates the parameters that have to be passed to the optimization. The parameters include the status of the appliances the $\underline{\mathbf{k}}_{\text{Appliances}}$, $\overline{\mathbf{k}}_{\text{Appliances}}$ and $\mathbf{b}_{\text{Appliances}}$, the current status of the micro-CHP that is given by $u_{\text{CHP},\text{Initial}}$ and $k_{\text{CHP},\text{Initial}}$, the current status of the BESS $E_{\text{BESS},\text{Initial}}$ as well as the current state of the HWT $v_{\text{BESS},\text{Initial}}$. When

Table 5.3: Energy generation and consumption, and energy storage system states in the building simulation.

Parameter	Symbol	Unit
Grid exchange power in time step t	$\tilde{P}_{\text{Grid},t}$	W
Grid import power in time step t	$\tilde{P}_{\text{Im},t}$	W
Grid export power in time step t	$\tilde{P}_{\text{Ex},t}$	W
BESS charge power in time step t	$\tilde{P}_{\text{BESS,C},t}$	W
BESS discharge power in time step t	$\tilde{P}_{\text{BESS,D},t}$	W
Power consumption of appliance in time step t j	$\tilde{P}_{\text{Appliances},j,t}$	W
Electric power generation of the micro-CHP in time step t	$\tilde{P}_{\text{CHP},t}$	W
Heat generation of the micro-CHP in time step t	$\tilde{\Phi}_{\text{CHP},t}$	W
Natural gas consumption of the micro-CHP in time step t	$\tilde{G}_{\text{CHP},t}$	W
Power generation of the PV system in time step t	$\tilde{P}_{\text{PV},t}$	W
Future power generation of the PV system predicted in time step t	$\hat{P}_{\text{PV},t}$	W
Energy in the BESS in time step t	$\tilde{E}_{\text{BESS},t}$	Ws
Energy in the BESS	$\tilde{E}_{\text{BESS,Initial}}$	Ws
Temperature of the HWT in time step t	$\vartheta_{\text{HWT},t}$	K
Initial temperature of the HWT	$\vartheta_{\text{HWT,Initial}}$	K

Table 5.4: Control inputs in the building simulation. The control inputs are defined in the optimization.

Control input	Symbol	
Control input to start Appliance j in time step t	$\tilde{u}_{\text{CHP},t}$	$\in [0, 1]$
Control input to start micro-CHP in time step t	$\tilde{u}_{\text{Appliances},j,t}$	$\in [0, 1]$
Control input to charge the BESS in time step t	$\tilde{u}_{\text{BESS,C},t}$	$\in \{0, 1\}$
Control input to discharge the BESS in time step t	$\tilde{u}_{\text{BESS,D},t}$	$\in \{0, 1\}$

Algorithm 5.1: Process of the building simulation

```

1 function performBuildingSimulation(  $\tilde{\mathbf{P}}_{\text{PV}}, \tilde{\mathbf{P}}_{\text{Base}}, \tilde{\mathbf{\Phi}}_{\text{HS}}, \tilde{\mathbf{\Phi}}_{\text{DHW}}, \tilde{E}_{\text{BESS},1}, \tilde{\vartheta}_{\text{HWT},1},$ 
    $\tilde{\pi}_{\text{Ex}}, \tilde{\pi}_{\text{Im}}, \tilde{\pi}_{\text{Gas}}, \Delta_{\text{N}}, \Delta_{\text{k}});$ 
   Input : PV generation profile  $\tilde{\mathbf{P}}_{\text{PV}}$ , electricity base load profile  $\tilde{\mathbf{P}}_{\text{Base}}$ , heat
           consumption profiles  $\tilde{\mathbf{\Phi}}_{\text{HS}}, \tilde{\mathbf{\Phi}}_{\text{DHW}}$ , initial storage states  $\tilde{E}_{\text{BESS},1}, \tilde{\vartheta}_{\text{HWT},1}$ ,
           price profiles  $\tilde{\pi}_{\text{Ex}}, \tilde{\pi}_{\text{Im}}, \tilde{\pi}_{\text{Gas}}$ , optimization window  $\Delta_{\text{N}}$ , optimization time
           step duration  $\Delta_{\text{k}}$ .
   Output: Electricity costs, electricity feed-in compensation, gas costs, final storage
           states, total costs
2 for  $t \in \{1, \dots, T\}$  do
3   if  $t \bmod \frac{\Delta_{\text{k}}}{\Delta_{\text{t}}} = 0$  then
4     [ $\underline{\mathbf{k}}_{\text{Appliances}}, \overline{\mathbf{k}}_{\text{Appliances}}, \mathbf{b}_{\text{Appliances}}, k_{\text{CHP,Initial}}, u_{\text{CHP,Initial}}, E_{\text{BESS,Initial}}, \vartheta_{\text{HWT,Initial}}$ ]
       = adjustOptimizationInputs( $\tilde{u}_{\text{CHP},t-1}, \tilde{E}_{\text{BESS},t-1}, \tilde{\vartheta}_{\text{HWT},t-1},$ 
        $\underline{\mathbf{k}}_{\text{Appliances}}, \overline{\mathbf{k}}_{\text{Appliances}}, \mathbf{b}_{\text{Appliances}}, t$ );
5      $\hat{\mathbf{P}}_{\text{PV}} = \text{performPVGenerationPrediction}(\tilde{\mathbf{P}}_{\text{PV}}, \Delta_{\text{N}}, \Delta_{\text{k}});$ 
6     [ $\hat{\pi}_{\text{Im}}, \hat{\pi}_{\text{Ex}}, \hat{\pi}_{\text{Gas}}$ ] = performTariffPredictions( $\tilde{\pi}_{\text{Ex}}, \tilde{\pi}_{\text{Im}}, \tilde{\pi}_{\text{Gas}}, \Delta_{\text{N}}, \Delta_{\text{k}}$ );
7     [ $\hat{\mathbf{P}}_{\text{Base}}, \hat{\mathbf{\Phi}}_{\text{HWT}}, \hat{\mathbf{\Phi}}_{\text{DHW}}$ ] = performConsumptionPredictions( $\tilde{\mathbf{P}}_{\text{Base}}, \tilde{\mathbf{\Phi}}_{\text{DHW}},$ 
        $\tilde{\mathbf{\Phi}}_{\text{HS}}, \Delta_{\text{N}}, \Delta_{\text{k}}$ );
8      $\tilde{\mathbf{u}}_t = \text{doRollingHorizonOptimization}(\hat{\mathbf{P}}_{\text{Base}}, \hat{\mathbf{P}}_{\text{PV}}, \hat{\mathbf{\Phi}}_{\text{HS}}, \hat{\mathbf{\Phi}}_{\text{DHW}}, \hat{\pi}_{\text{Im}}, \hat{\pi}_{\text{Ex}}, \hat{\pi}_{\text{Gas}},$ 
        $E_{\text{BESS,Initial}}, \vartheta_{\text{HWT,Initial}}, \underline{\mathbf{k}}_{\text{Appliances}}, \overline{\mathbf{k}}_{\text{Appliances}}, \mathbf{b}_{\text{Appliances}}, k_{\text{CHP,Initial}},$ 
        $u_{\text{CHP,Initial}}$ );
9   end
10   $P_{\text{BESS,D,Ref}} = \tilde{u}_{\text{BESS,D},t} \cdot \overline{P}_{\text{BESS,D}};$ 
11   $P_{\text{BESS,C,Ref}} = \tilde{u}_{\text{BESS,C},t} \cdot \overline{P}_{\text{BESS,C}};$ 
12  [ $\tilde{P}_{\text{BESS,D},t}, \tilde{P}_{\text{BESS,C},t}$ ] = performUnderlyingBESSControl( $P_{\text{BESS,D,Ref}}, P_{\text{BESS,C,Ref}},$ 
        $\tilde{E}_{\text{BESS},t}, \tilde{P}_{\text{PV},t}, \tilde{P}_{\text{CHP},t}, \tilde{P}_{\text{Appliances},t}, \tilde{P}_{\text{Base},t}, \eta_{\text{BESS}}, \Delta_{\text{t}}$ );
13   $\tilde{P}_{\text{Grid},t} = \sum_{j=1}^J \tilde{P}_{\text{Appliances},j,t} + \tilde{P}_{\text{Base},t} + \tilde{P}_{\text{BESS,C},t} - \tilde{P}_{\text{PV},t} - \tilde{P}_{\text{CHP},t} - \tilde{P}_{\text{BESS,D},t};$ 
14  if  $\tilde{P}_{\text{Grid},t} \leq 0$  then
15     $\tilde{P}_{\text{Ex},t} = -1 \cdot \tilde{P}_{\text{Grid},t};$ 
16     $\tilde{P}_{\text{Im},t} = 0;$ 
17  end
18  else
19     $\tilde{P}_{\text{Ex},t} = 0;$ 
20     $\tilde{P}_{\text{Im},t} = \tilde{P}_{\text{Grid},t};$ 
21  end
22   $\tilde{G}_{\text{CHP},t} = \tilde{u}_{\text{CHP},t} \cdot G_{\text{CHP,Nom}};$ 
23   $\tilde{u}_{\text{BESS,D},t} = \tilde{P}_{\text{BESS,D},t} / \overline{P}_{\text{BESS,D}};$ 
24   $\tilde{u}_{\text{BESS,C},t} = \tilde{P}_{\text{BESS,C},t} / \overline{P}_{\text{BESS,C}};$ 
25   $\tilde{\mathbf{x}}_{t+1} = f(\tilde{\mathbf{x}}_t, \tilde{\mathbf{u}}_t);$ 
26 end
27  $\tilde{C}_{\text{T}} = \text{calculateOperatingCosts}(\tilde{\pi}_{\text{Im}}, \tilde{\pi}_{\text{Ex}}, \tilde{\pi}_{\text{Gas}}, \tilde{P}_{\text{Ex}}, \tilde{P}_{\text{Im}}, \tilde{G}_{\text{CHP}}, \Delta_{\text{t}});$ 
28 return  $\tilde{C}_{\text{T}};$ 

```

passed to the optimization, the current states of the micro-CHP, the BESS and HWT are the initial states in the optimization model.

performPVGenerationPrediction($\tilde{\mathbf{P}}_{\text{PV}}, \Delta_N, \Delta_k$): This function calculates the forecast of the PV generation for the given optimization horizon. The forecast uses historic PV generation values as input. The forecast algorithm works as described in Section 5.6.3.

performTariffPredictions($\tilde{\pi}_{\text{Ex}}, \tilde{\pi}_{\text{Im}}, \tilde{\pi}_{\text{Gas}}, \Delta_N, \Delta_k$): This function calculates the forecast of the tariffs, i. e., the prices for the electricity imports, the electricity export compensation and the gas prices, for the given optimization horizon. In this thesis, these parameters are defined to be known. Thus, a perfect prediction is assumed. However, the parameters have to be in the temporal resolution that is used in the optimization, i. e., N time steps that represent a time period of Δ_k .

performConsumptionPredictions($\tilde{\mathbf{P}}_{\text{Base}}, \tilde{\mathbf{\Phi}}_{\text{DHW}}, \tilde{\mathbf{\Phi}}_{\text{HS}}, \Delta_N, \Delta_k$): This function calculates the forecast of the electricity and heat consumption for the given optimization horizon. In this thesis, a perfect forecast is used. However, any prediction algorithm can be used in combination with the approach presented in this thesis, e. g., using historic consumption values.

doRollingHorizonOptimization($\hat{\mathbf{P}}_{\text{Base}}, \hat{\mathbf{P}}_{\text{PV}}, \hat{\mathbf{\Phi}}_{\text{HS}}, \hat{\mathbf{\Phi}}_{\text{DHW}}, \hat{\pi}_{\text{Im}}, \hat{\pi}_{\text{Ex}}, \hat{\pi}_{\text{Gas}}, \tilde{E}_{\text{BESS}}, \tilde{v}_{\text{HWT}}, \underline{\mathbf{k}}_{\text{Appliances}}, \overline{\mathbf{k}}_{\text{Appliances}}, \mathbf{b}_{\text{Appliances}}, k_{\text{CHP,Initial}}, \Delta_N, \Delta_k$): This function calculates the control inputs for the devices. The calculation is done by applying the rolling horizon approach as defined in Section 5.5. The function uses the PV generation forecast, the energy consumption forecast, the current state values of the BESS $\tilde{E}_{\text{BESS},t}$ and the HWT $\tilde{v}_{\text{HWT},t}$, the variables that indicates the status of the appliances $\underline{\mathbf{k}}_{\text{Appliances}}, \overline{\mathbf{k}}_{\text{Appliances}}$ and $\mathbf{b}_{\text{Appliances}}$ as well as the current status of the micro-CHP derived from $u_{\text{CHP,Initial}}$ and $k_{\text{CHP,Initial}}$ as input.

performUnderlyingBESSControl($P_{\text{BESS,D,Ref}}, P_{\text{BESS,C,Ref}}, \tilde{E}_{\text{BESS},t}, \tilde{P}_{\text{PV},t}, \tilde{P}_{\text{CHP},t}, \tilde{P}_{\text{Appliances},t}, \tilde{P}_{\text{Base},t}, \eta_{\text{BESS}}, \Delta_t$): This function performs the underlying BESS control as defined in Algorithm 5.3 in Section 5.6.1. It calculates the BESS charge and discharge control inputs in dependence of the BESS state $\tilde{E}_{\text{BESS},t}$, the PV generation $\tilde{P}_{\text{PV},t}$, the micro-CHP generation $\tilde{P}_{\text{CHP},t}$, the base load consumption $\tilde{P}_{\text{Base},t}$, the appliance consumption $\tilde{P}_{\text{Appliances},t}$ and the reference (dis-)charge powers defined by the optimization $P_{\text{BESS,D,Ref}}, P_{\text{BESS,C,Ref}}$.

calculateOperatingCosts($\tilde{\pi}_{\text{Im}}, \tilde{\pi}_{\text{Ex}}, \tilde{\pi}_{\text{Gas}}, \tilde{\mathbf{P}}_{\text{Ex}}, \tilde{\mathbf{P}}_{\text{Im}}, \tilde{\mathbf{G}}_{\text{CHP}}, \Delta_t, \tilde{E}_{\text{HWT},T+1}, \tilde{E}_{\text{BESS},T+1}$): This function calculates the operating costs of the building that occur in the simulation period of $\Delta_t \cdot T$. The operating costs are calculated according to Equation 5.3. The inputs are $\tilde{\pi}_{\text{Ex}}, \tilde{\mathbf{P}}_{\text{Ex}}, \tilde{\pi}_{\text{Im}}, \tilde{\mathbf{P}}_{\text{Im}}, \tilde{\pi}_{\text{Gas}}, \tilde{\mathbf{G}}_{\text{CHP}}, \tilde{E}_{\text{HWT},T+1}$ and $\tilde{E}_{\text{BESS},T+1}$.

5.5 Rolling Horizon Optimization Approach

As stated in Section 5.3, the overall goal is to find an approach to the operation of a building energy system to minimize the operating costs of the building energy system. As

Algorithm 5.2: Process of the rolling horizon optimization to calculate the vector of control variables.

- 1 function doRollingHorizonOptimization($\hat{P}_{\text{Base}}, \hat{P}_{\text{PV}}, \hat{\Phi}_{\text{HWT}}, \hat{\Phi}_{\text{DHW}}, \hat{\pi}_{\text{Im}}, \hat{\pi}_{\text{Ex}}, \hat{\pi}_{\text{Gas}}, \tilde{E}_{\text{BESS}}, \tilde{\vartheta}_{\text{HWT}}, \underline{k}_{\text{Appliances}}, \bar{k}_{\text{Appliances}}, \mathbf{b}_{\text{Appliances}}, k_{\text{CHP,Initial}}, \Delta_{\text{N}}, \Delta_{\text{k}}$);
Input : $\hat{P}_{\text{Base}}, \hat{P}_{\text{PV}}, \hat{\Phi}_{\text{HWT}}, \hat{\Phi}_{\text{DHW}}, \hat{\pi}_{\text{Im}}, \hat{\pi}_{\text{Ex}}, \hat{\pi}_{\text{Gas}}, \tilde{E}_{\text{BESS},t}, \tilde{\vartheta}_{\text{HWT},t}, \underline{k}_{\text{Appliances}}, \bar{k}_{\text{Appliances}}, \mathbf{b}_{\text{Appliances}}, k_{\text{CHP,Initial}}, \Delta_{\text{N}}, \Delta_{\text{k}}$
Output: Vector of control variables $\mathbf{u}_0 = (u_{\text{BESS,C},0}, u_{\text{BESS,D},0}, \mathbf{u}_{\text{Appliances},0}, u_{\text{CHP},0})^T$
 - 2 $[\mathbf{x}, \mathbf{u}, \mathbf{a}] = \text{solveOptimizationProblem}(\hat{P}_{\text{Base}}, \hat{P}_{\text{PV}}, \hat{\Phi}_{\text{HWT}}, \hat{\Phi}_{\text{DHW}}, \hat{\pi}_{\text{Im}}, \hat{\pi}_{\text{Ex}}, \hat{\pi}_{\text{Gas}}, \vartheta_{\text{HWT,Initial}}, E_{\text{BESS,Initial}}, \underline{k}_{\text{Appliances}}, \bar{k}_{\text{Appliances}}, \mathbf{b}_{\text{Appliances}}, k_{\text{CHP,Initial}}, u_{\text{CHP,Initial}})$;
 - 3 return \mathbf{u}_0 ;
-

its main contribution, this thesis presents a rolling horizon optimization approach that uses a stochastic two-stage optimization.

As stated in Section 4.3, rolling horizon optimization approaches that optimize the operation of a building energy system have already been presented in the literature. These approaches have shown comparatively good results. However, the related work presented in Section 4.3 shows that the explicit consideration of the uncertainties of the energy generation and consumption forecasts in the optimization by means of stochastic optimization is expected to further improve the performance of rolling horizon optimization approaches. This thesis takes up this idea and further investigates the application of a stochastic optimization in a rolling horizon optimization approach to the optimization of building energy systems. As stated in Section 4.3.4, the formulation of a stochastic multi-stage problem (see Section 3.11.2) is expected to be the best choice to include the forecast uncertainties. However, the related work states that a stochastic multi-stage optimization leads to a high computational effort causing optimization times that are inappropriate for the optimization of building energy systems. To reduce the computational effort, stochastic two-stage problems have been investigated in the literature as an approximation to a full multi-stage stochastic program (see Section 4.3.4). They show an increase of performance compared to deterministic state-of-the-art formulations that do not respect uncertainties explicitly while still having reasonable computation times. However, there are only a few approaches presented in the literature (see Table 4.3) which are either limited in the devices they include or in the temporal resolution.

The rolling horizon approach performs an optimization to achieve optimal control inputs for the controllable devices for a given optimization horizon of N time steps. The optimization includes forecasts of the energy consumption and generation in the building. A rolling horizon optimization run is performed with a time step duration of Δ_{k} . This means that in the optimization, a new optimization run is performed after $\frac{\Delta_{\text{k}}}{\Delta_{\text{t}}}$ time steps. Or in other words, an optimization run of the rolling horizon optimization is performed in every time step $t \in \{1, \dots, T\}$ in which $t \bmod \frac{\Delta_{\text{k}}}{\Delta_{\text{t}}} = 0$ holds true. The temporal duration of the optimization horizon is $\Delta_{\text{N}} = \Delta_{\text{k}} \cdot N$.

In the building simulation and in particular in Algorithm 5.1, the rolling horizon optimization is executed in function *doRollingHorizonOptimization* that is presented in Algorithm 5.2. The used inputs are calculated using the following functions:

- *adjustOptimizationInputs*,
- *performPVGenerationPrediction*,
- *performTariffPredictions*,
- *performConsumptionPredictions*,
- *doRollingHorizonOptimization*.

They include the forecasts of the PV generation and energy consumption, the forecasts of the prices as well as the initial states of the appliances, the micro-CHP and the energy storage systems. These parameters are then used to instantiate the optimization problem with the model presented in Section 5.8. The optimization problem is then passed to a solver that solves the problem. These steps are done in function *solveOptimizationProblem*, which gives the optimal values of the decision values as output. The exact process and its implementation are described in Section 5.9. Since the purpose of the optimization is to find the optimal control inputs for the building energy system, the optimal value of the objective function is not important. The optimal values of the control variables that correspond to the first time step are then returned to the simulation and used to calculate the temporal progression of the building energy system.

To evaluate the performance of the rolling horizon optimization approach, it is compared to rule-based control approaches (see Chapter 6). In addition, the performance of the stochastic two stage approach is evaluated by a comparison to a rolling horizon optimization approach that uses a state-of-the-art one-stage approach. More precisely, a one-stage rolling horizon optimization approach that uses a perfect forecast of the PV generation and an approach that uses an uncertain point forecast are used in a benchmark scenario. The evaluation of the approaches is presented in Chapter 6.

5.6 Model of the Energy System

In this section, the mathematical models of the devices contained in the smart building configuration (see Section 5.2.1) are presented. Each model is used in the rolling horizon optimization approach as well as in the simulation of the building.

5.6.1 Batteries Energy Storage System

The building energy system includes an electrical energy storage system, i. e., a BESS. The model presented in this section can be used to model various battery technologies, e. g., lead-acid or lithium-ion batteries. However, different technologies lead to different choices in the parameters. The battery is connected via a power converter to the electricity grid of the building (see Figure 5.2), forming the BESS. The power converter losses are combined with the battery (dis-)charge efficiency (see Section 4.1.2). Here, both efficiencies

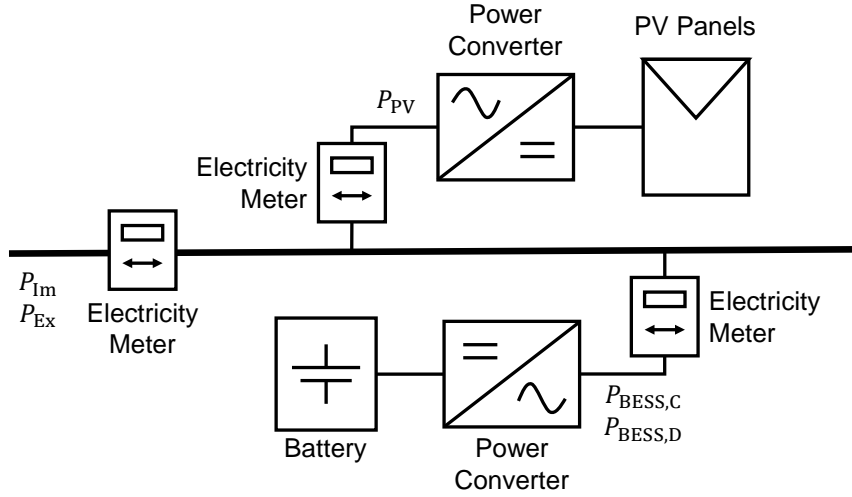


Figure 5.2: Overview of the PV system and the BESS.

Table 5.5: Parameters of the BESS model.

Parameter	Symbol	Value	Unit
(Dis-)Charge efficiencies	η_{BESS}	0.92	–
Maximum amount of energy in the BESS	\bar{E}_{BESS}	7	kWh
Minimum amount of energy in the BESS	$\underline{E}_{\text{BESS}}$	0	Ws
Energy stored in the BESS initially	$E_{\text{BESS,Initial}}$	varies	Ws
Maximum charge power	$\bar{P}_{\text{BESS,C}}$	7	kW
Minimum charge power	$\underline{P}_{\text{BESS,C}}$	0	kW
Maximum discharge power	$\bar{P}_{\text{BESS,D}}$	7	kW
Minimum discharge power	$\underline{P}_{\text{BESS,D}}$	0	kW

are assumed to be constant. This is in line with other approaches (cf. [3, 14, 59]). A list of the parameters of the BESS model is presented in Table 5.5.

The energy that is stored in the BESS is given by:

$$E_{\text{BESS},k+1} = E_{\text{BESS},k} + \Delta_k \cdot (\eta_{\text{BESS}} \cdot P_{\text{BESS},\text{C},k} - \eta_{\text{BESS}}^{-1} P_{\text{BESS},\text{D},k}) \quad \forall k \in \{1, \dots, N\}, \quad (5.12a)$$

$$E_{\text{BESS},1} = E_{\text{BESS,Initial}} + \Delta_k \cdot (\eta_{\text{BESS}} \cdot P_{\text{BESS},\text{C},0} - \eta_{\text{BESS}}^{-1} P_{\text{BESS},\text{D},0}). \quad (5.12b)$$

$E_{\text{BESS,Initial}}$ is the initial state of the battery that is measured in the system¹. The (dis-)charge efficiencies of the BESS is denoted by η_{BESS} and the time step length is denoted by Δ_k . In this thesis, charge and the discharge efficiencies have been chosen to be $\eta_{\text{BESS}} = 0.92$. This leads to an overall efficiency of 85% which resembles an average commercially available BESS [82, 182]. The usable capacity of the BESS is 7 kWh and minimum and maximum limits of the energy stored in the BESS are assumed to be $\underline{E}_{\text{BESS}} = 0$ kWh and $\overline{E}_{\text{BESS}} = 7$ kWh, respectively. [82]. The maximum charge power and discharge power of the BESS is $\overline{P}_{\text{BESS},\text{C}} = 7$ kW and $\overline{P}_{\text{BESS},\text{D}} = 7$ kW. This relates to a C rate of 1, which is typically used in BESS [41]. Hereby, no additional constraints on the maximum charge power introduced by the power converter are considered. The capacity of the BESS is chosen to be 7 kWh. In a large scale study of 16.000 BESS in Germany, Figgenger et al. state that 7 kWh is the average lithium-ion BESS capacity of the investigated BESSs [82, p. 45]. The capacity is chosen to be 2 kWh per 1 kW peak of the PV system. This reflects a slightly over-sized BESS that provides a high flexibility, which can be harnessed by the optimization approach. However, the sizing of the BESS is dependent on the tariff structures [117].

The energy that is stored in the BESS is given by $\mathbf{E}_{\text{BESS}} = (E_{\text{BESS},1}, \dots, E_{\text{BESS},N})^\top$. The amount of energy that is stored in the BESS is limited by the maximum amount of energy $\overline{E}_{\text{BESS}}$ and the minimum amount of energy $\underline{E}_{\text{BESS}}$ that can be stored in the BESS. This is ensured by the following constraints:

$$\underline{E}_{\text{BESS}} \leq E_{\text{BESS},k} \leq \overline{E}_{\text{BESS}}, \quad \forall k \in \{1, \dots, N\}. \quad (5.13)$$

The charge $P_{\text{BESS},\text{C},k}$ and the discharge powers $P_{\text{BESS},\text{D},k}$ of the BESS are defined as a function of the control inputs $\mathbf{u}_{\text{BESS},\text{C}} = (u_{\text{BESS},\text{C},0}, \dots, u_{\text{BESS},\text{C},N-1})^\top$ and $\mathbf{u}_{\text{BESS},\text{D}} = (u_{\text{BESS},\text{D},0}, \dots, u_{\text{BESS},\text{D},N-1})^\top$ as well as the maximum charge and discharge powers.

$$P_{\text{BESS},\text{C},k} = u_{\text{BESS},\text{C},k} \cdot \overline{P}_{\text{BESS},\text{C}}, \quad \forall k \in \{0, \dots, N-1\}, \quad (5.14a)$$

$$P_{\text{BESS},\text{D},k} = u_{\text{BESS},\text{D},k} \cdot \overline{P}_{\text{BESS},\text{D}}, \quad \forall k \in \{0, \dots, N-1\}. \quad (5.14b)$$

¹The initial state $E_{\text{BESS,Initial}}$ can be seen as the state in time step $k = 0$. However, the notation $E_{\text{BESS,Initial}}$ is chosen over $E_{\text{BESS},0}$ to emphasize that the initial state is no decision variable in the optimization.

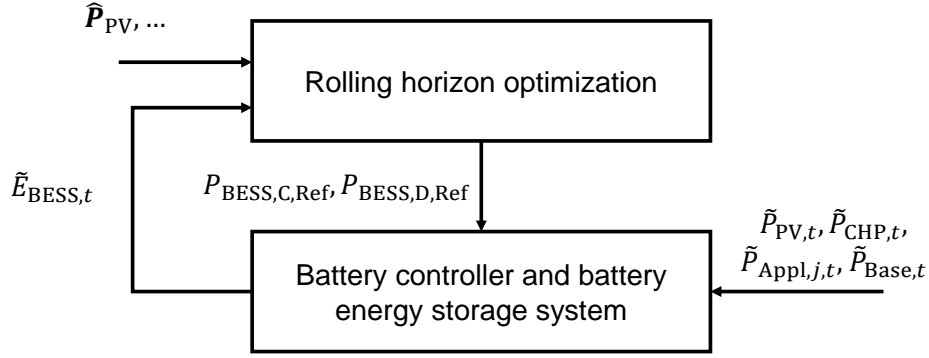


Figure 5.3: Schema of the interaction of the rolling horizon optimization and the BESS controller.

The control inputs are decision variables with $\mathbf{u}_{BESS,C} \in [0, 1]^N$ and $\mathbf{u}_{BESS,D} \in [0, 1]^N$. The charge and discharge powers are constrained to be between a minimum and a maximum value:

$$\underline{P}_{BESS,C} \leq P_{BESS,C,k} \leq \bar{P}_{BESS,C}, \quad \forall k \in \{0, \dots, N-1\}, \quad (5.15a)$$

$$\underline{P}_{BESS,D} \leq P_{BESS,D,k} \leq \bar{P}_{BESS,D}, \quad \forall k \in \{0, \dots, N-1\}. \quad (5.15b)$$

After each optimization run in the rolling horizon optimization approach the optimal values $P_{BESS,C,0}^*$ and $P_{BESS,D,0}^*$ are communicated to an underlying rule-based controller. The underlying controller uses the optimal charge and discharge powers as reference values:

$$P_{BESS,C,Ref} = P_{BESS,C,k}^* \quad (5.16a)$$

$$P_{BESS,D,Ref} = P_{BESS,D,k}^* \quad (5.16b)$$

The underlying controller uses the reference values to define the charge and discharge powers (see next section, Figures 5.3 and Algorithm 5.3). After every optimization run, the reference values $P_{BESS,C,Ref}$ and $P_{BESS,D,Ref}$ are updated.

The formulation presented in Equation 5.15 is only capable of modeling minimum charge and discharge powers that are equal to zero. If the BESS has minimum charge and discharge powers that are greater than zero, typically an additional off-state or stand-by mode has to be included. This can be achieved by the addition of one binary decision variable $u_{BESS,0}$ for every time step. This leads to N additional decision variables. Hence, Equation 5.15 would become:

$$\underline{P}_{BESS,C} \cdot u_{BESS,0,k} \leq P_{BESS,C,k} \leq \bar{P}_{BESS,C} \cdot u_{BESS,0,k}, \quad \forall k \in \{0, \dots, N-1\}, \quad (5.17a)$$

$$\underline{P}_{BESS,D} \cdot u_{BESS,0,k} \leq P_{BESS,D,k} \leq \bar{P}_{BESS,D} \cdot u_{BESS,0,k}, \quad \forall k \in \{0, \dots, N-1\}. \quad (5.17b)$$

This thesis only considers the case where $\underline{P}_{BESS,C} = \underline{P}_{BESS,D} = 0$. However, minimum charge and discharge powers that are greater than zero can easily be added to the model as shown above.

It has to be noted that the model does not explicitly prohibit a simultaneous charging and discharging of the BESS even though this is physically not possible. In the model, a simultaneous charging and discharging of the BESS actually results in a waste of energy. This is a consequence of the energy loss based on the efficiency of the BESS. In the presented scenarios, a waste of energy is never beneficial. Thus, control inputs that lead to a simultaneous charging and discharging of the BESS are not results of the rolling horizon optimization. Consequently, the simultaneous charging and discharging does not have to be prohibited explicitly, because it would lead to non-optimal solutions of the optimization problem anyway. This has been proven in [93].

A simultaneous charging and discharging of the BESS can be explicitly prohibited by the introduction of additional binary decision variables $\mathbf{b}_{\text{BESS}} = (b_{\text{BESS},0}, \dots, b_{\text{BESS},N-1})^\top$ with $\mathbf{b}_{\text{BESS}} \in \{0, 1\}^N$ [132, 133]. Equation 5.15 would then change to:

$$\underline{P}_{\text{BESS},C} \cdot b_{\text{BESS},k} \leq P_{\text{BESS},C,k} \leq \overline{P}_{\text{BESS},C} \cdot b_{\text{BESS},k}, \quad \forall k \in \{0, \dots, N-1\}, \quad (5.18a)$$

$$\underline{P}_{\text{BESS},D} \cdot (1 - b_{\text{BESS},k}) \leq P_{\text{BESS},D,k} \leq \overline{P}_{\text{BESS},D} \cdot (1 - b_{\text{BESS},k}), \quad \forall k \in \{0, \dots, N-1\}. \quad (5.18b)$$

In the case of a quadratic optimization problem, the following constraint can be introduced instead:

$$P_{\text{BESS},C,k} \cdot P_{\text{BESS},D,k} = 0, \quad \forall k \in \{0, \dots, N-1\}. \quad (5.19)$$

For the sake of simplicity and to ease the model, the simultaneous charging and discharging of the BESS is not prohibited explicitly in this thesis. This is also expected to lower the time to solve the optimization problem [93].

The model presented above is similar but not equal to other models that are presented in the literature on the optimization of the operation of a building energy system (cf. [3, 14, 93, 132, 222]).

Beyond the scope of this thesis, scenarios exist in which a waste of energy could be beneficial. Examples are scenarios with a negative electricity price $\pi_{\text{Im},k}$:

$$\exists k \in \{0, \dots, N-1\} : \pi_{\text{Im},k} < 0. \quad (5.20)$$

In this case, the consumption of energy is rewarded. At the European energy markets this case rarely occurs based on an underestimation of the electricity generation by renewables. Even though end-user prices differ from market prices, for example because of additional fees like the network fees, market prices are reflected in the end-user prices. This is expected to become more relevant in the future (see Section 2.9). In the sense of ancillary services, negative electricity prices can be used to encourage a change in behavior to resolve short time deviations in the balance of generation and consumption (see Sections 2.9 and 2.15).

Another example is a scenario with a negative feed-in compensation, i. e.. a positive feed-in price² $\pi_{\text{Ex},k}$:

$$\exists k \in \{0, \dots, N-1\} : 0 < \pi_{\text{Ex},k}. \quad (5.21)$$

²In this thesis, positive prices lead to costs while negative prices lead to earnings, i. e., a compensation.

Algorithm 5.3: Underlying BESS control algorithm

```

1 function performUnderlyingBESSControl( $P_{\text{BESS,D,Ref}}$ ,  $P_{\text{BESS,C,Ref}}$ ,  $\tilde{E}_{\text{BESS},t}$ ,  $\tilde{P}_{\text{PV},t}$ ,
    $\tilde{P}_{\text{CHP},t}$ ,  $\tilde{P}_{\text{Appliances},t}$ ,  $\tilde{P}_{\text{Base},t}$ ,  $\eta_{\text{BESS}}$ ,  $\Delta_t$ ) ;
   Input : BESS discharge power reference value  $P_{\text{BESS,D,Ref}}$ , BESS charge power
           reference value  $P_{\text{BESS,C,Ref}}$ , BESS state  $\tilde{E}_{\text{BESS},t}$ , PV generation  $\tilde{P}_{\text{PV},t}$ ,
           micro-CHP generation  $\tilde{P}_{\text{CHP},t}$ , base load consumption  $\tilde{P}_{\text{Base},t}$ , appliances
           consumption  $\tilde{P}_{\text{Appliances},t}$ , BESS efficiency  $\eta_{\text{BESS}}$ , time step duration  $\Delta_t$ 
   Output: BESS charge power  $\tilde{P}_{\text{BESS,C},t}$  and BESS discharge power  $\tilde{P}_{\text{BESS,D},t}$ 
2  $\tilde{P}_{\text{BESS,D},t} = P_{\text{BESS,D,Ref}}$ ;
3  $\tilde{P}_{\text{BESS,C},t} = P_{\text{BESS,C,Ref}}$ ;
4 if  $P_{\text{BESS,D,Ref}} > \tilde{P}_{\text{Appliances},t} + \tilde{P}_{\text{Base},t}$  then
5 |    $\tilde{P}_{\text{BESS,D},t} = \tilde{P}_{\text{Appliances},t} + \tilde{P}_{\text{Base},t}$ ;
6 end
7 if  $\tilde{E}_{\text{BESS},t} - \Delta_t \cdot \eta_{\text{BESS}}^{-1} \cdot \tilde{P}_{\text{BESS,D},t} < \underline{E}_{\text{BESS}}$  then
8 |    $\tilde{P}_{\text{BESS,D},t} = \Delta_t \cdot \eta_{\text{BESS}} \cdot (\tilde{E}_{\text{BESS},t} - \underline{E}_{\text{BESS}})$ ;
9 end
10 if  $P_{\text{BESS,C,Ref}} > \tilde{P}_{\text{CHP},t} + \tilde{P}_{\text{PV},t}$  then
11 |    $\tilde{P}_{\text{BESS,C},t} = \tilde{P}_{\text{CHP},t} + \tilde{P}_{\text{PV},t}$ ;
12 end
13 if  $\tilde{E}_{\text{BESS},t} + \Delta_t \cdot \eta_{\text{BESS}} \cdot \tilde{P}_{\text{BESS,C},t} > \overline{E}_{\text{BESS}}$  then
14 |    $\tilde{P}_{\text{BESS,C},t} = \Delta_t \cdot \eta_{\text{BESS}}^{-1} \cdot (\overline{E}_{\text{BESS}} - \tilde{E}_{\text{BESS},t})$ ;
15 end
16 return  $\tilde{P}_{\text{BESS,D},t}$ ,  $\tilde{P}_{\text{BESS,C},t}$ ;

```

In this case, the feed-in of energy is penalized. This case is connected to the one described above (see Equation 5.20). It rarely occurs at the European energy markets and is based on an underestimation of the electricity generation from renewables. In the sense of ancillary services, the prices can express an overload of the electricity grid based on a too large electricity generation (see Sections 2.9 and 2.15) and hence encourage a change in behavior to lower the electricity feed-in. This can be done by raising the local consumption or lowering the local generation.

Underlying BESS Controller

It is proposed that the BESS uses an underlying rule-based controller in addition to the rolling horizon optimization. The BESS controller handles processes that happen on shorter timescales than the rolling horizon optimization. It ensures that no energy from the BESS is fed into the grid and that the battery is not charged by taking energy from the grid while considering the (dis-)charge powers defined by the optimization. This approach is based on [174, 179]. This combination of optimization and rule-based controllers is becoming more popular in the field of energy management [14, 59] (see Section 4.3.3). The system schematic

of the BESS controller is shown in Figure 5.3. The BESS controller computes the current (dis-)charge powers in dependence on the current electricity generation and consumption that is measured in the building and if necessary, overwrites the outcomes of the rolling horizon optimization. The underlying control algorithm is presented in Algorithm 5.3. It uses the BESS discharge power reference value $P_{\text{BESS,D,Ref}}$, BESS charge power reference value $P_{\text{BESS,C,Ref}}$, the BESS state $\tilde{E}_{\text{BESS},t}$, the PV generation $\tilde{P}_{\text{PV},t}$, the micro-CHP generation $\tilde{P}_{\text{CHP},t}$, the base load consumption $\tilde{P}_{\text{Base},t}$, the appliances consumption $\tilde{P}_{\text{Appliances},t}$, the BESS efficiency η_{BESS} and the time step duration Δ_t to determine the BESS charge power $\tilde{P}_{\text{BESS,C},t}$ and BESS discharge power $\tilde{P}_{\text{BESS,D},t}$. Certainly, the controller can be adapted to suit different application cases, e. g., to support the feed-in of electricity from the BESS into the grid.

Rule-based BESS Operation

In addition to the optimized operation of the BESS in which the charge and discharge powers are determined by the rolling horizon optimization, this thesis investigates a rule-based control algorithm. It is defined in Algorithm 5.4. The rule-based control algorithm only uses the current BESS state $\tilde{E}_{\text{BESS},t}$, the PV generation $\tilde{P}_{\text{PV},t}$, the micro-CHP generation $\tilde{P}_{\text{CHP},t}$, the base load consumption $\tilde{P}_{\text{Base},t}$, and the appliance consumption $\tilde{P}_{\text{Appliances},t}$ as inputs. No predictions of the electricity consumption or generation are considered. The BESS discharge power $\tilde{P}_{\text{BESS,D},t}$ and the BESS charge power $\tilde{P}_{\text{BESS,C},t}$ are set according to current electricity consumption and generation. Whenever a surplus of generation occurs, the battery is charged and whenever a surplus of consumption occurs, the BESS is discharged. This is done while complying with the constraints given in Equations 5.13 and 5.15. When the rule-based control algorithm is applied, the underlying BESS controller (see Algorithm 5.3) is not used.

5.6.2 Micro Combined Heat and Power Plant

The micro-CHP that is considered in this thesis is based on the Senertec Dachs G5.5 with a nominal electric power generation of 5.5 kW and a nominal heat generation of 12.5 kW. The micro-CHP consumes 20.5 kW of input power, which is provided by natural gas. The Senertec Dachs G5.5 can be integrated into a BEMS via a REST interface. This is demonstrated in the ESHL at the KIT [9, 135, 163, 165, 174, 179] and the FZI HoLL [22, 163]. The Senertec Dachs G5.5 serves as an exemplary micro-CHP that is designed for the operation in buildings and has proven to work with a BEMS. This has been investigated in various publications [9, 22, 135, 163, 165, 174, 179].

The MILP model that is presented in the following equations has been developed based on the generic approaches presented in [43, 172]. The details of the Senertec Dachs G5.5 and the corresponding MILP model are presented in the following section. A list of all parameters of the micro-CHP model is given in Table 5.6.

The electric power generation $P_{\text{CHP},k}$, the heat generation $\Phi_{\text{CHP},k}$ and the power provided by the natural gas $G_{\text{CHP},k}$ in time step k are modeled as a product of the corresponding

Algorithm 5.4: Rule-based BESS control algorithm

```

1 function performRule-basedBESSControl( $\tilde{E}_{\text{BESS},t}$ ,  $\tilde{P}_{\text{PV},t}$ ,  $\tilde{P}_{\text{CHP},t}$ ,  $\tilde{P}_{\text{Base},t}$ ,
    $\tilde{P}_{\text{Appliances},t}$ ,  $\tilde{P}_{\text{Appliances},t}$ ,  $\Delta_k$ );
   Input : BESS state  $\tilde{E}_{\text{BESS},t}$ , PV generation  $\tilde{P}_{\text{PV},t}$ , micro-CHP generation  $\tilde{P}_{\text{CHP},t}$ ,
     base load consumption  $\tilde{P}_{\text{Base},t}$ , appliance consumption  $\tilde{P}_{\text{Appliances},t}$ , BESS
     efficiency  $\tilde{P}_{\text{Appliances},t}$ , time step duration  $\Delta_k$ 
   Output: BESS discharge power  $\tilde{P}_{\text{BESS},\text{D},t}$ , BESS charge power  $\tilde{P}_{\text{BESS},\text{C},t}$ 
2  $\tilde{P}_{\text{BESS},\text{D},t} = 0$ ;
3  $\tilde{P}_{\text{BESS},\text{C},t} = 0$ ;
4 if  $0 \leq \tilde{P}_{\text{Appliances},t} + \tilde{P}_{\text{Base},t} - \tilde{P}_{\text{CHP},t} - \tilde{P}_{\text{PV},t}$  then
5 |  $\tilde{P}_{\text{BESS},\text{D},t} = \tilde{P}_{\text{Appliances},t} + \tilde{P}_{\text{Base},t} - \tilde{P}_{\text{CHP},t} - \tilde{P}_{\text{PV},t}$ ;
6 end
7 else
8 |  $\tilde{P}_{\text{BESS},\text{C},t} = \tilde{P}_{\text{CHP},t} + \tilde{P}_{\text{PV},t} - \tilde{P}_{\text{Appliances},t} - \tilde{P}_{\text{Base},t}$ ;
9 end
10 if  $\bar{P}_{\text{BESS},\text{C}} < \tilde{P}_{\text{BESS},\text{C},t}$  then
11 |  $\tilde{P}_{\text{BESS},\text{C},t} = \bar{P}_{\text{BESS},\text{C}}$ ;
12 end
13 if  $\bar{P}_{\text{BESS},\text{D}} < \tilde{P}_{\text{BESS},\text{D},t}$  then
14 |  $\tilde{P}_{\text{BESS},\text{D},t} = \bar{P}_{\text{BESS},\text{D}}$ ;
15 end
16 if  $\tilde{E}_{\text{BESS},t} - \Delta_k \cdot \eta_{\text{BESS}}^{-1} \cdot \tilde{P}_{\text{BESS},\text{D},t} < \underline{E}_{\text{BESS}} \wedge \tilde{P}_{\text{BESS},\text{D},t} \neq 0$  then
17 |  $\tilde{P}_{\text{BESS},\text{D},t} = \Delta_k \cdot \eta_{\text{BESS}} \cdot (\tilde{E}_{\text{BESS},t} - \underline{E}_{\text{BESS}})$ ;
18 end
19 if  $\tilde{E}_{\text{BESS},t} + \Delta_k \cdot \eta_{\text{BESS}} \cdot \tilde{P}_{\text{BESS},\text{C},t} > \bar{E}_{\text{BESS}} \wedge \tilde{P}_{\text{BESS},\text{C},t} \neq 0$  then
20 |  $\tilde{P}_{\text{BESS},\text{C},t} = \Delta_k \cdot \eta_{\text{BESS}}^{-1} \cdot (\bar{E}_{\text{BESS}} - \tilde{E}_{\text{BESS},t})$ ;
21 end
22 return  $\tilde{P}_{\text{BESS},\text{D},t}$ ,  $\tilde{P}_{\text{BESS},\text{C},t}$ ;

```

Table 5.6: Parameters of the micro-CHP model.

Parameter	Symbol	Value	Unit
Nominal electricity generation	$P_{\text{CHP},\text{Nom}}$	5.5	kW
Nominal heat generation	$\Phi_{\text{CHP},\text{Nom}}$	12.5	kW
Nominal gas consumption	$G_{\text{CHP},\text{Nom}}$	20.5	kW
Minimum run-time after start	$k_{\text{CHP},\text{Min}}$	varies	–
Initial state of the micro-CHP in the optimization run	$u_{\text{CHP},\text{Initial}}$	varies	–
Initial forced run-time based on earlier starts	$k_{\text{CHP},\text{Initial}}$	varies	–
Penalty costs per start	$\pi_{\text{CHP},\text{Start}}$	1	cent

binary control variable $u_{\text{CHP},k}$ and the respective nominal powers $P_{\text{CHP,Nom}}$, $\Phi_{\text{CHP,Nom}}$ and $G_{\text{CHP,Nom}}$. This is expressed by the following shorthand notations:

$$P_{\text{CHP},k} = u_{\text{CHP},k} \cdot P_{\text{CHP,Nom}} \quad \forall k \in \{0, \dots, N-1\}, \quad (5.22a)$$

$$\Phi_{\text{CHP},k} = u_{\text{CHP},k} \cdot \Phi_{\text{CHP,Nom}} \quad \forall k \in \{0, \dots, N-1\}, \quad (5.22b)$$

$$G_{\text{CHP},k} = u_{\text{CHP},k} \cdot G_{\text{CHP,Nom}} \quad \forall k \in \{0, \dots, N-1\}. \quad (5.22c)$$

Hence, the micro-CHP is operating in all time steps $k \in \{0, \dots, N-1\}$ in which $u_{\text{CHP},k} = 1$. The control variables $\mathbf{u}_{\text{CHP}} = (u_{\text{CHP},0}, \dots, u_{\text{CHP},N-1})^\top$ are decision variables with $\mathbf{u}_{\text{CHP}} \in \{0, 1\}^N$. This model is extended by the addition of a minimum number of consecutive operating time steps $k_{\text{CHP,Min}}$. Thus, it has to be taken into account if the minimal number of consecutive operating time steps leads to a forced on-time in the first time steps in the operating horizon. The initial number of time steps in which the micro-CHP is forced to run based on earlier starts is given by $k_{\text{CHP,Initial}}$. This number of time steps is determined before the optimization and treated as a fixed parameter. The value of the control variable in the time step previous to the optimization is given by $u_{\text{CHP,Initial}}$.

The minimum number of consecutive time steps the micro-CHP has to run is taken into account by the following constraints. Here, it is important to repeat that the optimization problem that is solved in the rolling horizon optimization depends on the time and the states of the system in the simulation. When the approach is applied in a real building, the states that are measured in the real building are used in contrast to the states of the simulation. In the case of the micro-CHP, the choice of constraints is dependent on the operation of the micro-CHP before the start of the rolling horizon operation, i. e., if the micro-CHP has been running and how long it has been running.

If $k_{\text{CHP,Initial}} \neq 0$ the optimization problem contains the following constraints:

$$k_{\text{CHP,Min}} \cdot (u_{\text{CHP},k} - u_{\text{CHP},k-1}) \leq \sum_{i=k}^{k+k_{\text{CHP,Min}}-1} u_{\text{CHP},i}, \quad \forall k \in \{k_{\text{CHP,Initial}}, \dots, N - k_{\text{CHP,Min}}\} \quad (5.23)$$

and

$$k_{\text{CHP,Initial}} - \sum_{i=0}^{k_{\text{CHP,Initial}}-1} u_{\text{CHP},i} = 0. \quad (5.24)$$

The constraint presented in Equation 5.24 ensures that the micro-CHP runs in the number of time steps $k_{\text{CHP,Initial}}$ in which the micro-CHP is forced to run based on earlier starts.

If $k_{\text{CHP,Initial}} = 0$ the optimization problem contains the following constraints instead of the ones presented in Equations 5.23 and 5.24:

$$k_{\text{CHP,Min}} \cdot (u_{\text{CHP},k} - u_{\text{CHP},k-1}) \leq \sum_{i=k}^{k+k_{\text{CHP,Min}}-1} u_{\text{CHP},i}, \quad \forall k \in \{1, \dots, N - k_{\text{CHP,Min}}\}, \quad (5.25a)$$

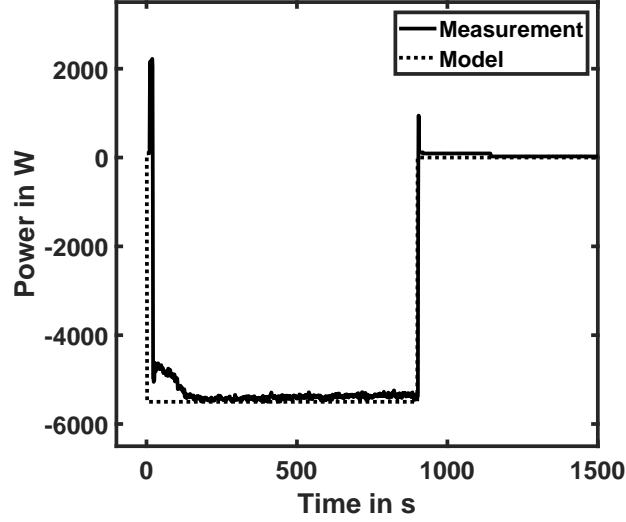


Figure 5.4: Visualization of the electricity generation and consumption of the micro-CHP. The solid black line indicates a measurement performed in the Senertec Dachs G5.5 in the ESHL and the dashed line indicates the derived model used in this thesis. Here, negative power values indicate an electricity generation while positive power values indicate an electricity consumption.

$$k_{\text{CHP,Min}} \cdot (u_{\text{CHP},0} - u_{\text{CHP,Initial}}) \leq \sum_{i=0}^{k_{\text{CHP,Min}}-1} u_{\text{CHP},i} \quad (5.25b)$$

To ensure the minimum number of consecutive time steps at the end of the optimization horizon, the following constraints are introduced independently of the value of $k_{\text{CHP,Initial}}$:

$$0 \leq \sum_{i=k}^N u_{\text{CHP},i} - (N - k) \cdot (u_{\text{CHP},k} - u_{\text{CHP},k-1}), \quad \forall k \in \{N - k_{\text{CHP,Min}} + 1, \dots, N\}. \quad (5.26)$$

In Figure 5.4, the electric power generation that results from the MILP model is shown in comparison to the electric power generation that is generated by a real Senertec Dachs G5.5 and measured in the ESHL. The comparison shows a good agreement between the model and the measurement overall. However, the model overrates the electricity generation at the beginning of the operation. To regard this as well as the fact that the wear of the micro-CHP raises with the number of starts, a price $\pi_{\text{CHP,Start}}$ per start of the micro-CHP is introduced. A start of the micro-CHP in time step k occurs when $u_{\text{CHP},k} - u_{\text{CHP},k-1} = 1$. The binary variable $s_{\text{CHP},k}$ indicates if the micro-CHP starts in time step k . The penalty cost c_{CHP} resulting from the starts of the micro-CHP over the optimization horizon are given by:

$$c_{\text{CHP}} = \sum_{i=0}^{N-1} \pi_{\text{CHP,Start}} \cdot s_{\text{CHP},i}. \quad (5.27)$$

Algorithm 5.5: Heat-led micro-CHP control algorithm

```

1 function performCHPControl( $\cdot$ );
   Input : Hot water tank temperature  $\tilde{\vartheta}_{\text{HWT},t}$ , Last micro-CHP control input
            $\tilde{u}_{\text{CHP},t-1}$ 
   Output: Micro-CHP control input  $\tilde{u}_{\text{CHP},t}$ 
2 if  $\tilde{\vartheta}_{\text{HWT},t} \leq \underline{\vartheta}_{\text{HWT}}$  then
3   |  $\tilde{u}_{\text{CHP},t} = 1$ ;
4 end
5 else if  $\tilde{\vartheta}_{\text{HWT},t} < \bar{\vartheta}_{\text{HWT}} \wedge \tilde{u}_{\text{CHP},t-1} = 1$  then
6   |  $\tilde{u}_{\text{CHP},t} = 1$ ;
7 end
8 else if  $\bar{\vartheta}_{\text{HWT}} \leq \tilde{\vartheta}_{\text{HWT},t}$  then
9   |  $\tilde{u}_{\text{CHP},t} = 0$ ;
10 end
11 return  $\tilde{u}_{\text{CHP},t}$ ;

```

It is important to note that $\mathbf{s}_{\text{CHP}} = (s_{\text{CHP},0}, \dots, s_{\text{CHP},N-1})^\top$ is defined as a decision variable with $\mathbf{s}_{\text{CHP}} \in \{0, 1\}^N$. The number of starts of the micro-CHP is minimized with respect to the following constraints:

$$(u_{\text{CHP},k} - u_{\text{CHP},k-1}) \leq s_{\text{CHP},k}, \quad \forall k \in \{1, \dots, N-1\}, \quad (5.28a)$$

$$(u_{\text{CHP},0} - u_{\text{CHP,Initial}}) \leq s_{\text{CHP},0}. \quad (5.28b)$$

This model can be extended to include other constraints, e. g., ramping constraints. This can be done by the use of the extensive amount of modeling approaches that are for example presented in [43, 172].

Heat-led Micro-CHP Operation

In addition to the optimized operation of the micro-CHP as described above, this thesis investigates a rule-based control algorithm that operates in a heat-led mode. The rule-based control algorithm loosely follows the one presented in [111].

Since this thesis assumes the existence of a heat storage, i. e., an HWT, the heat load of the building is supplied by the HWT instead of being directly supplied by the micro-CHP. Thus, the heat load that has to be provided by the micro-CHP is related to the state of the heat storage. A common approach to the operation of the micro-CHP is to completely charge the heat storage whenever it is empty. In the case of the HWT, this means: If the temperature falls beneath a given minimal value, the water is heated up until it reaches a given value. This control scheme is also known as bang–bang control or hysteresis control. The rule-based control algorithm is presented in Algorithm 5.5.

5.6.3 PV System

As defined in Section 5.2.1, this thesis considers buildings with a local electricity generation by a PV system. As described in Section 4.1.4, this thesis uses a data-driven approach to model the electricity generation of the PV system. This generation is modeled using a PV generation profile that has been measured in the FZI HoLL in Karlsruhe, Germany [22]. The profile has been measured in the year 2013. The electricity generation profile is scaled to match a given capacity of the PV system. The resolution of the measured profiles is one minute and reflects seasonal as well as short-term intermittency.

The generated electric power in the optimization horizon, i. e., the electric generation profile, is given by $\mathbf{P}_{\text{PV}} = (P_{\text{PV},0}, \dots, P_{\text{PV},N-1})^\top$. These values are not assumed to be known exactly but with some uncertainty. Hence, the electric generation profile is modeled as a vector of random variables in the optimization.

In the optimization, predicted electricity generation profiles $\hat{\mathbf{P}}_{\text{PV}} = (\hat{P}_{\text{PV},0}, \dots, \hat{P}_{\text{PV},N-1})^\top$ are used to describe the electricity generation profiles:

$$P_{\text{PV},k} := \hat{P}_{\text{PV},k}, \quad \forall k \in \{0, \dots, N-1\} \quad (5.29)$$

It is assumed that the PV system cannot be controlled by the BEMS. In addition, no remote control is considered. However, a potential control of the PV system can be included in the model easily. It can be achieved by the introduction of additional decision variables $\mathbf{u}_{\text{PV}} = (u_{\text{PV},0}, \dots, u_{\text{PV},N-1})^\top$ with $\mathbf{u}_{\text{PV}} \in [0, 1]^N$. The variables \mathbf{u}_{PV} are defined as control inputs of the PV system. The electric generation profile \mathbf{P}_{PV} is then given by:

$$P_{\text{PV},k} = u_{\text{PV},k} \cdot \hat{P}_{\text{PV},k}, \quad \forall k \in \{0, \dots, N-1\} \quad (5.30)$$

In the simulation of the building, the realization of the electricity generation in time step t is given by $\tilde{P}_{\text{PV},t}$. The values of $\tilde{P}_{\text{PV},t}$ are given by the measured electricity generation profiles. These are used in the forecast of the PV described in the following section.

Probabilistic PV Generation Forecast

To provide a probabilistic PV generation forecast, this thesis uses quantile regression as described in Section 4.1.5. The approach used in this thesis follows the one presented in [192]. It differs from the approach presented in [192] by not using a (k)-NN approach to determine the training data. Instead, this thesis uses the last 30 days to train the model, i. e., estimate the model parameters.

As described in Section 4.1.5, day-ahead PV generation forecasts typically use resolutions of 1 h. However, publications that use higher resolutions exist in the literature. In [192], a resolution of 15 min is used while good prediction quality is achieved. Based on this knowledge, in this thesis a forecast resolution of 30 min is used, being in the middle between 1 h and 15 min.

As stated in [192], it is beneficial to erase night values to only use non-trivial values in the training of the model. Hence, only day times have been used to train the forecast model. Therefore, time steps that have no PV generation in the corresponding time of day in the last 30 days are removed from the training data. In the used data set, this leads to 33 time steps of day time with each having a duration of 30 min.

In this thesis, the prediction function is a polynomial of degree one with four features. In [192], this approach shows slightly worse results compared to more complicated approaches like higher order polynomials, support vector regressions or ANNs. Thus, the simplest approach is used. The approach used in this thesis is also used in other publications in the domain of building energy management, for example in [14].

The models have been trained using the MATLAB data mining toolbox *SciXMiner* [170]. The selection of the features has been performed automatically by SciXMiner. One model is trained for each season in the evaluation scenarios, i. e., winter, spring and summer. The resulting model for the summer scenario is:

$$\hat{P}_{\text{PV},t_0+k} = \theta_1 + \theta_2 \cdot P_{\text{PV},t_0+k-132} + \theta_3 \cdot P_{\text{PV},t_0+k-115} + \theta_4 \cdot P_{\text{PV},t_0+k-50} + \theta_5 \cdot P_{\text{PV},t_0+k-33}, \quad \forall k \in \{1, \dots, 33\}, \quad (5.31)$$

with $(\theta_1, \theta_2, \theta_3, \theta_4, \theta_5) = (756.271, -0.372553, -0.309879, 0.146567, 0.108794)$. This selection of features is also used in the quantile regressions.

The quantile regressions are performed as described in [192]. A training set with 30 days and H_{Tr} time steps is used. As described above, $S = 4$ features are used. The automatically detected features are: $P_{\text{PV},t-33}$, $P_{\text{PV},t-132}$, $P_{\text{PV},t-115}$ and $P_{\text{PV},t-50}$ with $(s_1, s_2, s_3, s_4) = (-132, -115, -50, -33)$. The prediction model forecasts $H_{\text{For}} = 33$ time periods, i. e., the number of time steps in 24 hours with PV generation.

As described in Section 4.1.5, the prediction model for every quantile q is given by:

$$\hat{P}_{\text{PV},q,t+H} = f_q(P_{\text{PV},t}, \dots, P_{\text{PV},t-H}, \boldsymbol{\theta}_q). \quad (5.32)$$

In this thesis, the functional relation $f_q(\cdot)$ is a polynomial of degree one. Hence, five parameters $\boldsymbol{\theta}_q = (\theta_{1,q}, \theta_{2,q}, \theta_{3,q}, \theta_{4,q}, \theta_{5,q})^\top$ have to be determined. The parameters are determined by minimizing the distance between the predicted PV generation $\hat{\mathbf{P}}_{\text{PV},q}$ and the quantiles in the training set $\mathbf{P}_{\text{PV},q}$. Here, $\hat{\mathbf{P}}_{\text{PV},q}$ is given by:

$$\hat{\mathbf{P}}_{\text{PV},q} = \begin{pmatrix} 1, P_{\text{PV},H_{\text{For}}+1-s_1}, \dots, P_{\text{PV},H_{\text{For}}+1-s_4} \\ \vdots \\ 1, P_{\text{PV},H_{\text{For}}+H_{\text{Tr}}-s_1}, \dots, P_{\text{PV},H_{\text{For}}+H_{\text{Tr}}-s_4} \end{pmatrix} \begin{pmatrix} \theta_{1,q} \\ \vdots \\ \theta_{5,q} \end{pmatrix}. \quad (5.33)$$

Thus, determining the parameters done by solving the following optimization problem for

every $q \in \{0.01, 0.02, \dots, 0.99\}$:

$$\begin{aligned} & \underset{\boldsymbol{\theta}_q}{\text{minimize}} && \|\mathbf{P}_{\text{PV},q} - \mathcal{P}_{\text{PV}}\boldsymbol{\theta}_q\|^2 \\ & \text{subject to} && \begin{cases} 0 \leq \mathcal{P}_{\text{PV}}\boldsymbol{\theta}_q & \text{if } q = 0.01 \\ \mathcal{P}_{\text{PV}}\boldsymbol{\theta}_{(q-0.01)} \leq (\mathbf{1}_{\text{HT}}, \mathcal{P}_{\text{PV}})\boldsymbol{\theta}_q & \text{otherwise} \end{cases} \end{aligned} \quad (5.34)$$

As introduced in [192], „the constraint avoids the problem of quantile crossing [74], in which a quantile regression delivers values which are smaller than the ones provided by a model representing a lower quantile [192]”. This approach results in a prediction model for every quantile prediction. In Figure 4.6, interval forecasts of the PV generation for three exemplary days are visualized. The figure shows four different predicted intervals with a coverage of 20 %, 40 %, 60 % and 80 %. The figure only shows day times. Before the quantiles can be used in the rolling horizon optimization, the night values, 15 zeros, have to be added again. This results in 48 time steps each representing a 30 min time period. In the optimization, the time step duration of 30 min has to be adjusted to Δ_k by using every time step value $\frac{30 \text{ min}}{\Delta_k}$ times.

For the stochastic two-stage approach that is presented in this thesis, M PV generation forecast scenarios are needed. Using the quantile regressions, probabilistic scenarios can be constructed using sampling methods [38, 262]. However, this approach leads to prediction scenarios with a high volatility. In order to cover the whole probability space of possible prediction scenarios a high number of scenarios is needed [38]. When targeting a stochastic optimization approach as it is done in this thesis, the use of a high number of scenarios may lead to very high optimization times (see Section 3.11.2) and thus may be unfeasible. To reduce the number of scenarios, a selection of the PV generation quantile regressions described above is used. Each generation forecast scenario is assumed to have an equal probability of occurrence. This is motivated by assuming that only the clear sky generation and possible decreases in the generation based on a total cloudiness can be predicted by the chosen prediction model (as described in Sections 4.1.5 and Figure 4.3). Both effects are predicted by the prediction model described in this section (cf. Figures 4.3 and 4.6). Furthermore, it is assumed that the information of the possible amount of energy generated by the PV system as well as possible variations based on random processes have a higher effect on the performance of the rolling horizon optimization than information considering the possible volatility.

The first generation forecast scenario with $m = 1$ is given by the quantile regression with $q = 0.5$. This represents the median PV generation forecast. The other $M - 1$ PV generation forecasts are given by the quantile regressions with q_m :

$$q_m = 0.01 \cdot m \cdot \left\lceil \frac{99}{M + 1} \right\rceil, \quad \forall m \in \{2, \dots, M\}. \quad (5.35)$$

This sampling method of the profiles provided by the quantile regressions ensures an approximation of the PDF of the PV generation.

Here, it is important to note that the PV generation forecast as well as the sampling method of the possible PV generation scenarios should be chosen in order to maximize the performance of the rolling horizon optimization. The approaches that are the best with respect to the performance of the rolling horizon optimization do not necessarily have to be optimal with respect to other evaluation functions typically used in time series analysis, for example the Mean Absolute Percent Error (MAPE) or the Root Mean Square Error (RMSE).

When looking at the two-stage stochastic programming approach presented in this thesis, the M PV generation forecast scenarios are in particular needed for the second stage. As described in Section 3.11.1, the first-stage is assumed to have no uncertainty. Hence, only one PV generation forecast scenario is needed in the first stage. This is given by the quantile regression with $q = 0.5$. Thus, the forecast is equal to a point forecast when choosing $M = 1$. The PV generation profile forecast has $M \cdot (N - 1) + 1$ parameters.

5.6.4 Appliances

As defined in Section 5.2.1, this thesis investigates energy management in a building that is equipped with appliances, which are a washing machine, a dryer, a dish washer, an induction hob and an oven. The washing machine, the dryer and the dish washer are controllable by the BEMS while the oven and the induction hob are not. In this thesis, controllable means deferrable as defined in Section 4.1.6 and depicted in Figure 4.7. The starting times of the appliances are simulated according to typical statistical values that are based on data by [205, 238]. The corresponding PDFs are presented in Figures 5.5 and 5.6. This approach follows the one presented in [163, p. 139]. More precisely, the starting times of the non-controllable appliances, i. e., the oven and the induction hob, are simulated according to the PDFs. The starting times of the controllable devices, i. e., the washing machine, the dryer and the dish washer are simulated according to the PDFs if they are not scheduled, i. e., not controlled by the optimization. If the starting times are determined by the optimization, the earliest ($\underline{k}_{\text{Appliances},j}$) and the latest possible starting time ($\bar{k}_{\text{Appliances},j}$) of appliance j are chosen to have 24 h in between. More precisely, 24 h minus the duration of the operation of the appliance. Devices that have been started according to a scheduling of the optimization are scheduled again at midnight. This choice leads to the largest load shifting potential while neglecting the realistic use of the appliances. However, this approach allows for an evaluation of the energy management approaches and reduces the complexity of the simulation. In addition, this choice allows for a simpler comparison to the results from the literature [48, 223] which also use a scheduling time of 24 h.

In the following sections the modeling of the appliances is described in detail.

Deferrable Appliances

This thesis includes deferrable loads as defined in Section 4.1.6 and depicted in Figure 4.7. The starting times of the appliances can be defined by the optimization. Deferrable appliances are an example of general shiftable loads.

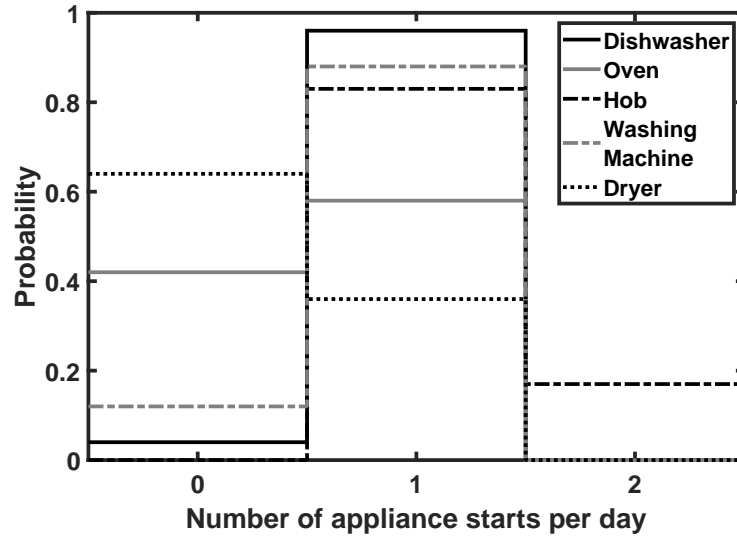


Figure 5.5: PDFs of the number of starts of the appliances.

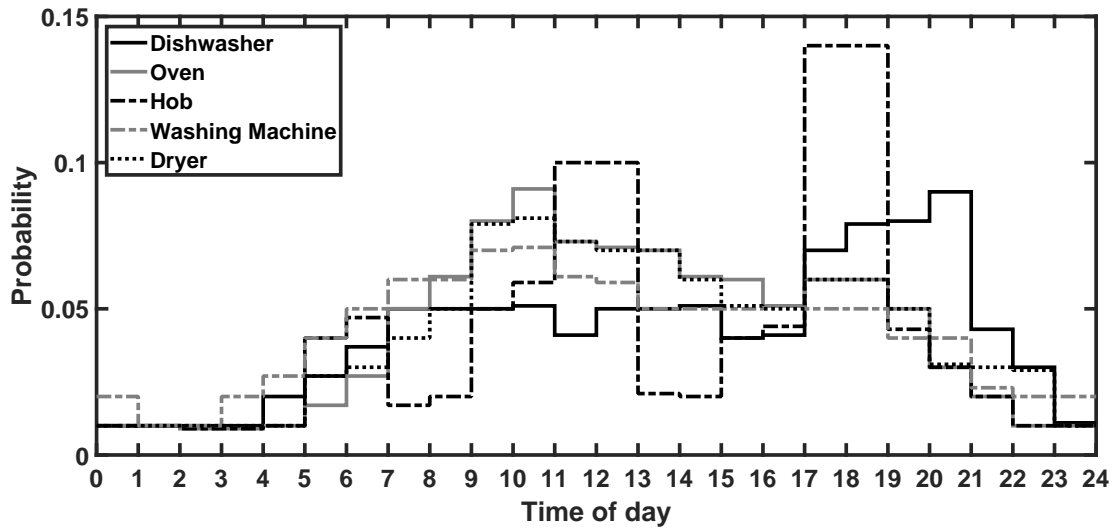


Figure 5.6: PDFs of the times of usage the appliances.

Table 5.7: Parameters of the deferrable appliances.

Parameter	Symbol	Value	Unit
Number of appliances	J	varies	–
On-off parameter of appliance j	$b_{\text{Appliances},j}$	varies	–
Earliest possible starting time of appliance j	$\underline{k}_{\text{Appliances},j}$	varies	–
Latest possible starting time of appliance j	$\bar{k}_{\text{Appliances},j}$	varies	–
Duration of the operating of appliance j	$l_{\text{Appliances}}(j)$	varies	–
Nominal electricity consumption of appliance j	$P_{\text{Appliances,Nom},j}$	varies	W

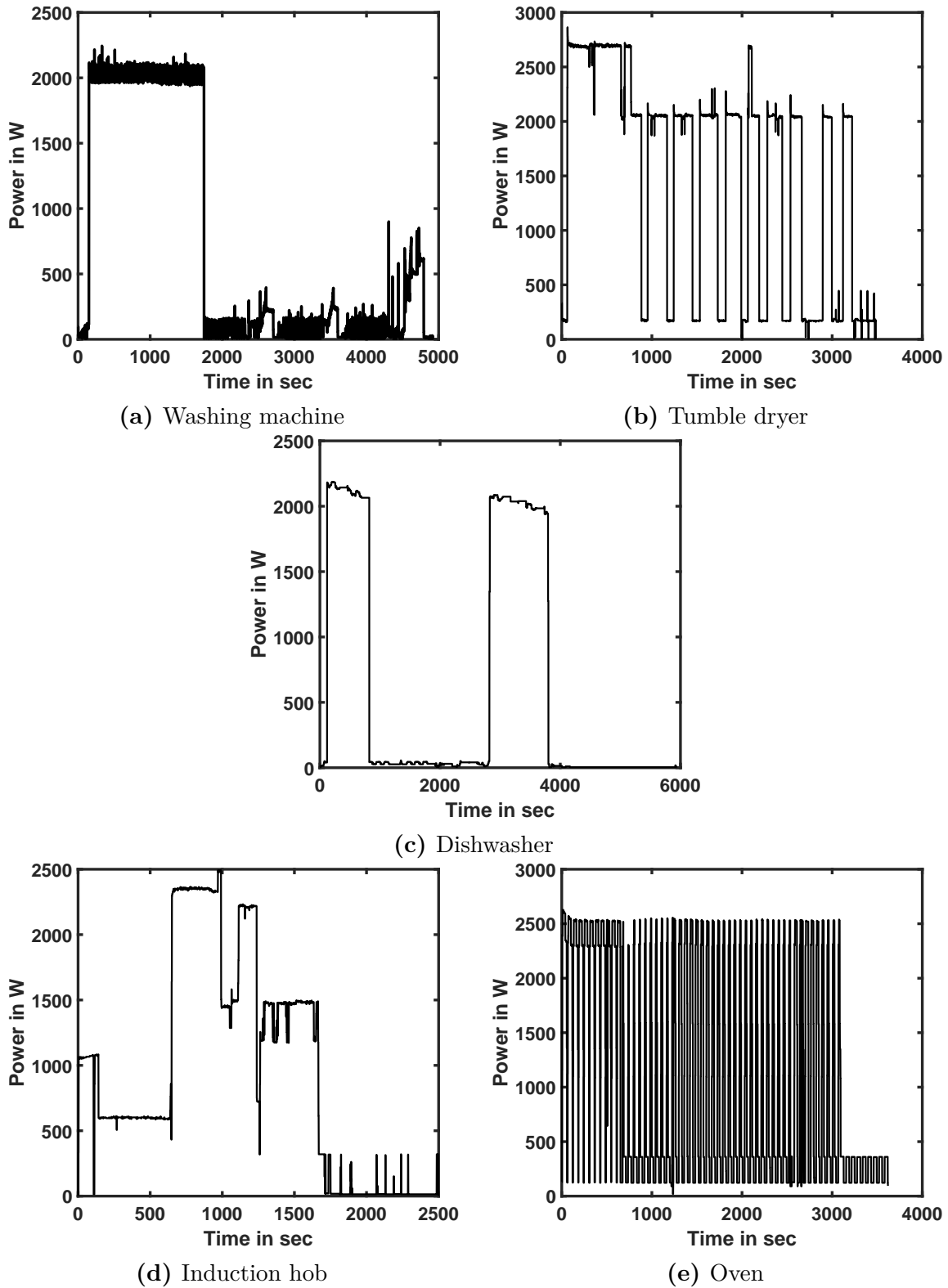


Figure 5.7: Load profiles of the five appliances. The figures show the measured electric power consumption for the washing machine (a), the tumble dryer (b) the dishwasher (c), the induction hob (d) and the oven (e) that are used in the evaluation [163].

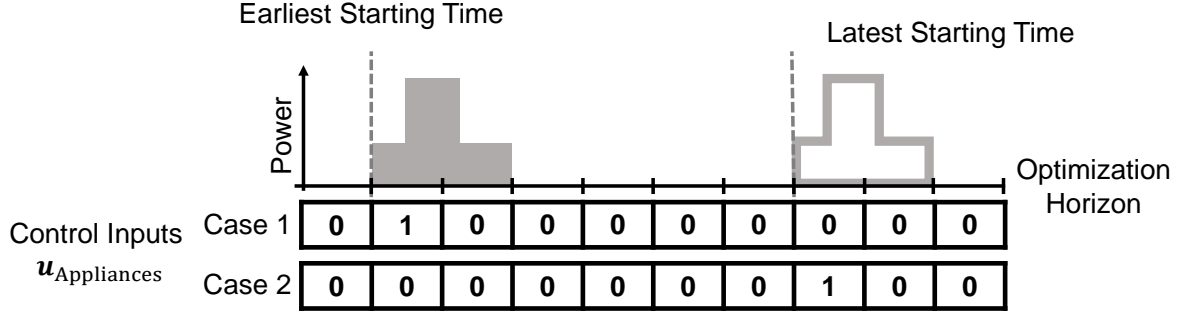


Figure 5.8: Visualization of the connection of the control inputs and the resulting load profiles. The control inputs for case 1 lead to the earliest possible start of the appliance and thus the load profile depicted in solid gray. In case 2 the latest possible time step has been chosen to start the optimization. The resulting load profile is depicted by the gray line.

For each appliance one real consumption profile has been recorded (see Figure 5.7) using a resolution of one second [163]. These load profiles are used to model the nominal load profiles $\mathbf{P}_{\text{Appliances,Nom},j}$, where j is the index of the appliance, i. e., the dishwasher, the washing machine or the tumble dryer. In the evaluation, only one profile per appliance is used in the evaluation. Different operation modes, for example, washing programs or temperatures, are not considered. The nominal load profiles in the model have a time step duration of Δ_k . A visualization of the measured load profile and the model of the washing machine is presented in Figure 5.9

If a control variable is equal to one, the respective appliance is started in this time step (see Figure 5.8). The control variables $\mathbf{u}_{\text{Appliances},j} = (u_{\text{Appliances},j,0}, \dots, u_{\text{Appliances},j,N-1})^\top$, $\forall j \in \{1, \dots, J\}$ are binary decision variables with $\mathbf{u}_{\text{Appliances},j} \in \{0, 1\}^N$, $\forall j \in \{1, \dots, J\}$ and $\mathbf{u}_{\text{Appliances}} = (\mathbf{u}_{\text{Appliances},1}, \dots, \mathbf{u}_{\text{Appliances},J})^\top$ with $\mathbf{u}_{\text{Appliances}} \in \{0, 1\}^{N \times J}$. In addition, the following vector can be defined $\mathbf{u}_{\text{Appliances},k} = (u_{\text{Appliances},1,k}, \dots, u_{\text{Appliances},J,k})^\top$, $\forall k \in \{0, \dots, N-1\}$ with $\mathbf{u}_{\text{Appliances},k} \in \{0, 1\}^J$, $\forall k \in \{0, \dots, N-1\}$.

Consequently, only one of the control inputs can be equal to one for each appliance. This is ensured by:

$$\sum_{i=0}^{N-1} u_{\text{Appliances},j,i} = b_{\text{Appliances},j}, \quad \forall j \in \{1, \dots, J\}. \quad (5.36)$$

$b_{\text{Appliances},j} \in \{0, 1\}$, $\forall j \in \{1, \dots, J\}$ is a parameter that defines whether appliance j is scheduled within the optimization horizon. It is important to clarify that $b_{\text{Appliances},j}$ is determined before the optimization and constant within the optimization. If $b_{\text{Appliances},j} = 1$, appliance j is scheduled and Equation 5.36 ensures that exactly one control input $u_{\text{Appliances},k}$ is equal to one. In contrast, a choice of $b_{\text{Appliances},j} = 0$ means that appliance j is not scheduled or has already been started. Hence, Equation 5.36 ensures that $u_{\text{Appliances},k} = 0$, $\forall k \in \{0, \dots, N-1\}$. Consequently, all decision variables $\mathbf{u}_{\text{Appliances}}$ are fixed.

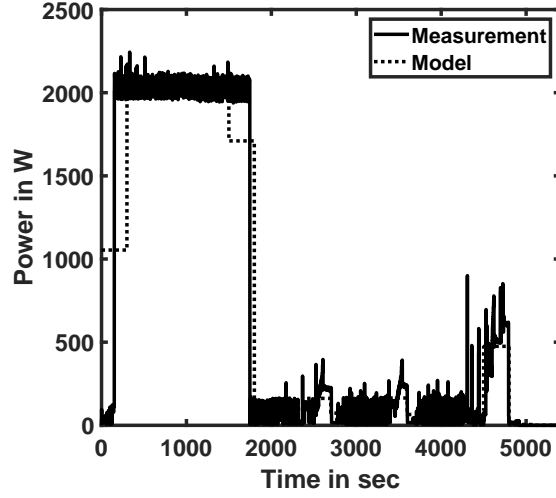


Figure 5.9: Visualization of the washing machine model (dashed black line) in comparison to the measurement (solid black line).

The electric power $P_{\text{Appliances},j,k}$ that is consumed in time step k by appliance j is given by:

$$P_{\text{Appliances},j,k} = \sum_{i=k-l_{\text{Appliances},j}+1}^k u_{\text{Appliances},j,i} \cdot P_{\text{Appliances},\text{Nom},j,k-i+1}, \quad \forall k \in \{l_{\text{Appliances},j}, \dots, N-1\}, \forall j \in \{1, \dots, J\}, \quad (5.37a)$$

$$P_{\text{Appliances},j,k} = \sum_{i=0}^k u_{\text{Appliances},j,i} \cdot P_{\text{Appliances},\text{Nom},j,k-i+1}, \quad \forall k \in \{0, \dots, l_{\text{Appliances},j}-1\}, \forall j \in \{1, \dots, J\}. \quad (5.37b)$$

$l_{\text{Appliances},j}$ is the duration of the operation of appliance j in time steps. The duration is equal to the dimension of the vector resembling the given nominal load profile $\mathbf{P}_{\text{Appliances},\text{Nom},j} \in \mathbb{R}^{l_{\text{Appliances},j}}$, $\forall j \in \{1, \dots, J\}$ of appliance j .

It is assumed that each appliance j has to be started between a given earliest starting time $\underline{k}_{\text{Appliances},j}$ and a given latest starting time $\bar{k}_{\text{Appliances},j}$:

$$\underline{k}_{\text{Appliances},j} \leq \sum_{i=0}^{N-1} u_{\text{Appliances},j,i} \cdot i \leq \bar{k}_{\text{Appliances},j}, \quad \forall j \in \{1, \dots, J\}. \quad (5.38)$$

Here, the earliest starting time $\underline{k}_{\text{Appliances},j}$ and the latest starting time $\bar{k}_{\text{Appliances},j}$ are elements of the set $\{0, \dots, N-1\}$. The latest starting time has to be larger than the earliest starting time:

$$\underline{k}_{\text{Appliances},j} \leq \bar{k}_{\text{Appliances},j}, \quad \forall j \in \{1, \dots, J\}. \quad (5.39)$$

The constraints in Equations 5.36 and 5.38 fix the values of decision variables based on the time of optimization. Because of this, several models can be introduced each with a different number of decision variables. However, the approach presented in this section aims at defining a general model that holds in all cases. Typically, fixed decision variables are identified by the solver and are dealt with accordingly. In Section 5.9 more details of the implementation of this are presented.

When an appliance j has been started, the parameter $b_{\text{Appliances},j}$ that indicates whether appliance j is scheduled will be set to 0. An appliance j is started when $u_{\text{Appliances,Nom},j,0}^* = 1$. In addition, the remaining nominal load profile $\mathbf{P}_{\text{Appliances,Nom}}$ of the appliance, i. e., components 2 to $l_{\text{Appliances},j}$, are added to the base load prediction. When the appliance j is scheduled again, the parameter $b_{\text{Appliances},j}$ is set to 1 and the parameters $\underline{k}_{\text{Appliances},j}$ and $\bar{k}_{\text{Appliances},j}$ are updated as chosen by the user.

Non-Deferrable Appliances

In addition to the deferrable appliances that can be controlled by the BEMS, non-deferrable appliances are considered. They cannot be controlled by the BEMS. The non-deferrable appliances are treated as started by the inhabitants. The times of use are defined according to the PDFs presented in Figures 5.5 and 5.6. However, as described in Section 5.4, in this thesis a perfect forecast is used. Thus, the starting times are assumed to be known by the BEMS.

The electricity consumption profiles of the non-deferrable appliances are added to the base load profile (see Figure 5.7).

5.6.5 Electric Base Load

This thesis uses the approach presented in [163, p. 127]. The remaining electrical load, which is not caused by the simulated major appliances, is simulated using the German standard load profile of households H0. In particular, the representative load profiles that have been developed by the *Verband der Elektrizitätswirtschaft e. V. (VDEW)* (English: The Association of the German Electricity Industry) [250]. The VDEW representative load profiles contain individual load profiles for workdays, Saturdays and Sundays. Each class of day is varied three times to represent the winter, the summer, and a season in between, resulting in nine different load profiles. In addition, the consumption in each day is scaled by a factor $\alpha(d)$ that reflects seasonal influences on the electricity consumption. The factor is given by a fourth-order polynomial equation that is dependent on the day of the year $d \in \{1, \dots, 365\}$ [163, p. 128]:

$$\alpha(d) = -3.92 \cdot 10^{-10} \cdot d^4 + 0.00000032 \cdot d^3 - 0.0000702 \cdot d^2 + 0.0021 \cdot d + 1.24. \quad (5.40)$$

This function results in a factor $\alpha(d)$ that is between 0.78 and 1.25. All profiles used in the simulations have a resolution of 15 min. The same approach has been used in [9, 163, 164, 165, 174, 179].

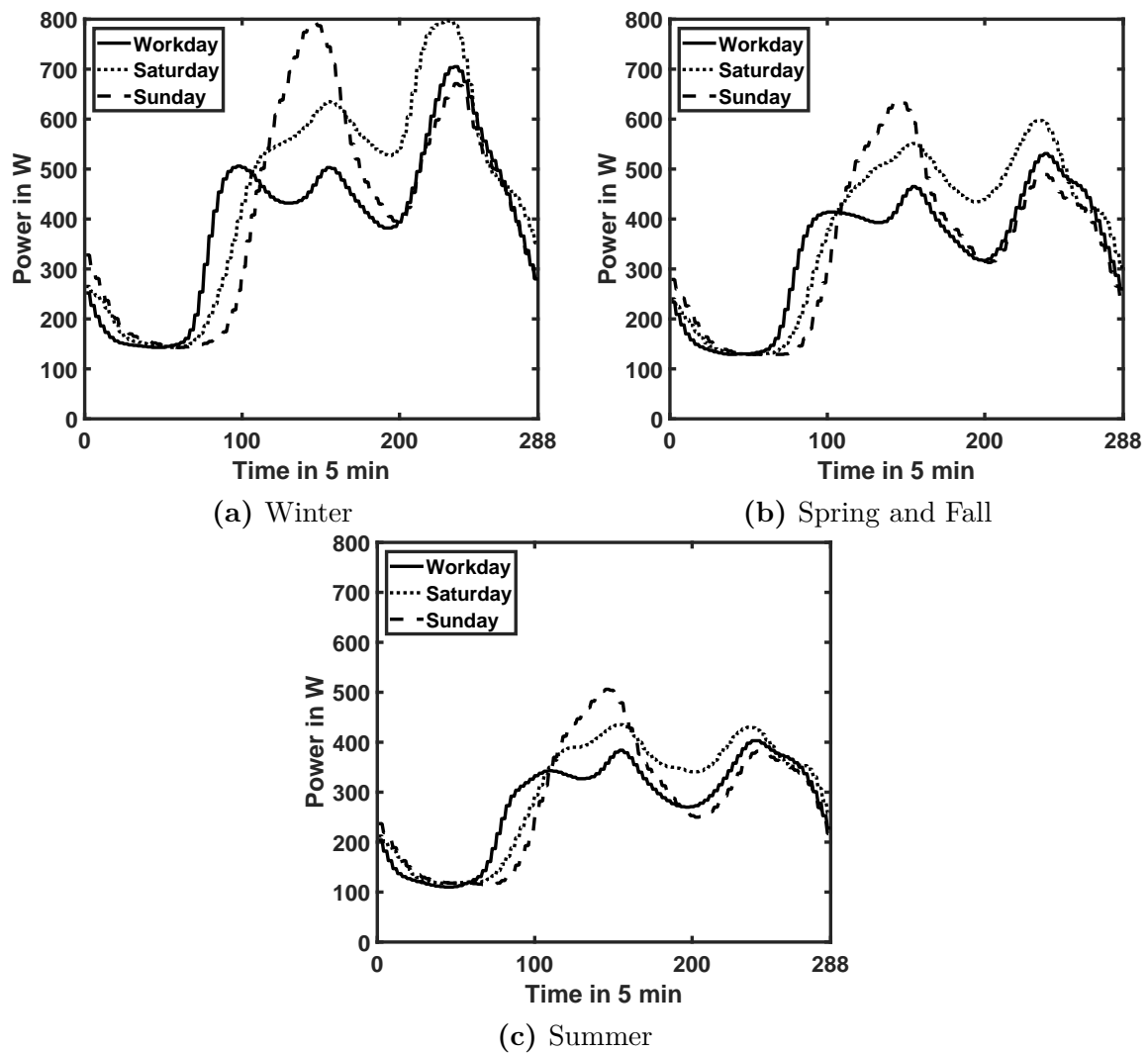


Figure 5.10: Electricity consumption profiles for a workday, a Saturday and a Sunday in the winter (a), in the spring and in the fall (b) as well as in the summer (c).

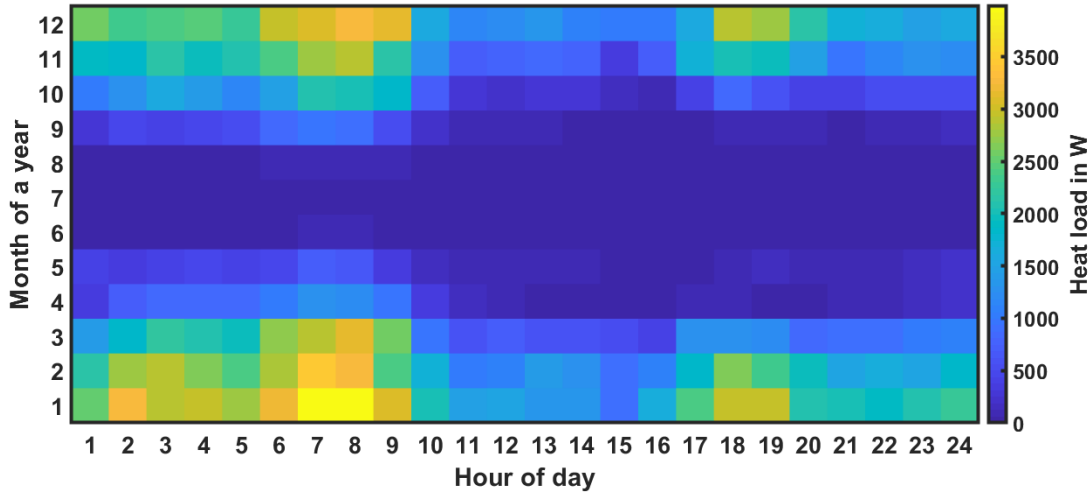


Figure 5.11: Visualization of the average heating system heat consumption in every hour in every month in a year.

Rule-based Appliance Operation

In the evaluation presented in Chapter 6, a rule-based operation approach is compared to the two-stage stochastic rolling horizon approach. In the rule-based scenario, the deferrable appliances are started at 12:00. This is done without considering any predictions. This simple approach targets the operation of the appliance at times of high PV generation.

5.6.6 Space Heating

This thesis uses a static heat load profile to simulate the space heating of the building. The heat load profile has been obtained by a thermal simulation of a building that resembles the ESHL. The simulation has been performed by Gräßle et al. [101] using TRANSYS. In [9], this load profile has been used to evaluate the performance of the OSH. Mauser [163, p. 130] introduced further variations in the load profiles presented by Gräßle. The resulting approach has then been implemented in the OSH framework to enable a realistic simulation of a thermal building energy system. The approach has been presented and evaluated in [163, 165]. This thesis uses the approach introduced by Mauser [163, p. 130]. More precisely, the OSH has been used to obtain a heat load profile for a household with four persons. This process leads to an individual heat load profile for every day in the year. The obtained load profile has a resolution of 1 h. The space heating heat load profile is scaled to an annual heat consumption of 2000 kWh per person in the household. It is assumed that the yearly Heating System (HS) heat load profiles include all losses in the DHW system. A visualization of the average HS heat consumption in every hour in every month in a year is presented in Figure 5.11.

The HS heat load in the simulation is given by $\tilde{\Phi}_{\text{HS}} = (\tilde{\Phi}_{\text{HS},1}, \dots, \tilde{\Phi}_{\text{HS},T})^\top$. To translate these parameters to the domain of the optimization, the time step lengths have to be

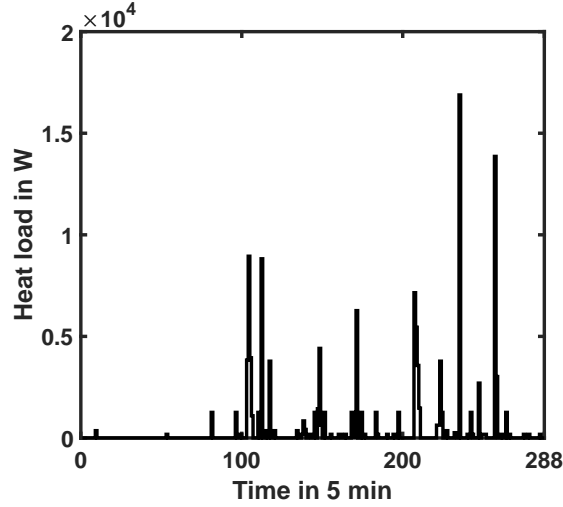


Figure 5.12: Visualization of a DHW exemplary heat load profile in a day.

adjusted from Δ_t in the simulation to Δ_k in the rolling horizon optimization. For an optimization that starts in the simulation time step t_0 , the HS heat load is given by:

$$\Phi_{\text{HS},k} = \tilde{\Phi}_{\text{HS},\left(\lfloor t_0+k \cdot \frac{\Delta_k}{\Delta_t} \rfloor\right)}, \quad \forall k \in \{0, \dots, N-1\} \quad (5.41)$$

Where the HS heat load $\tilde{\Phi}_{\text{HS},t}$ is known for the simulation period with $t \in \{1, \dots, T\}$. In the rolling horizon optimization, the heat loads from the HS $\Phi_{\text{HS},k}$ are treated as fixed parameters.

5.6.7 Domestic Hot Water Consumption

Similarly to the space heating, the DHW consumption is simulated using static heat load profiles. They are taken from the OSH, which uses an approach that is presented in [163, p. 130]. The heat load profiles represent a household with four persons.

The simulation in the OSH uses 13 draw off profiles that are partially based on typical draw off profiles provided in the regulation of the energy labeling of space heaters by the European Commission [73]. Each draw off profile has a duration between 9 and 506 s, an average heat load between 6.0 and 50.4 kW and a total energy consumption between 0.015 and 6.524 kWh per draw off period. Based on [73], every draw off profile has an assigned probability of occurrence that is dependent on the hour of the day and the day of the week. The DHW heat load profiles are computed by drawing draw off profiles according to these probabilities. The resulting DHW heat load profiles are then corrected to include seasonal changes according to [252, Figure D1] and daily changes according to [252, Figure D2]. A detailed description of the simulation process of the DHW heat load profiles is given in [163, p. 130]. The yearly DHW heat load profile is scaled to represent a yearly consumption of 700 kWh per person in the household. It assumed that the yearly DHW heat load profiles

Table 5.8: Parameters of the hot water tank model.

Parameter	Symbol	Value	Unit
Maximum temperature	$\bar{\vartheta}_{\text{HWT}}$	80	°C
Minimum temperature	ϑ_{HWT}	60	°C
Volume of the HWT	V_{HWT}	0.75	m ³
Volumetric mass density of water	ρ_{Water}	1000	kg m ⁻³
Specific heat capacity of water	c_{Water}	4182	W s kg ⁻¹ K ⁻¹
Ambient temperature of the HWT	$\vartheta_{\text{HWT,Ambient}}$	20	°C
Heat loss factor 1	a_{HWT}	12	W
Heat loss factor 2	b_{HWT}	5.93	W
Heat loss factor 3	c_{HWT}	1000	m ⁻³
Heat loss factor 4	d_{HWT}	40	K

include all losses in the DHW system. An exemplary DHW heat load profile is given in Figure 5.12.

The DHW heat load in the simulation is given by $\tilde{\Phi}_{\text{DHW}} = (\tilde{\Phi}_{\text{DHW},1}, \dots, \tilde{\Phi}_{\text{DHW},T})$. To translate these parameters to the domain of the optimization, the time step lengths have to be adjusted from Δ_t in the simulation to Δ_k in the rolling horizon optimization. For an optimization that starts in the simulation time step t_0 , the DHW heat load for the HS is given by:

$$\Phi_{\text{DHW},k} = \tilde{\Phi}_{\text{DHW}, \lfloor t_0 + k \cdot \frac{\Delta_k}{\Delta_t} \rfloor}, \quad \forall k \in \{0, \dots, N-1\}, \quad (5.42)$$

where the DHW heat loads $\tilde{\Phi}_{\text{DHW},t}$ are known for the simulation period with $t \in \{1, \dots, T\}$. In the rolling horizon optimization, the DHW heat loads $\Phi_{\text{DHW},k}$ are treated as fixed parameters.

5.6.8 Hot Water Tank

This thesis considers an HWT that is used as a thermal energy storage. The amount of stored energy can be expressed by the temperature of the stored water. In this thesis, the temperature of the stored water $\vartheta_{\text{HWT},k+1}$ in time step $k+1$ is modeled as a linear function of the temperature in the previous time step as well as the heat loss $\Phi_{\text{HWT,Loss},k}$, the heat generated by the micro-CHP $\Phi_{\text{CHP},k}$, the heat consumed by the HS $\Phi_{\text{HS},k}$ and the heat consumed by the domestic hot water system $\Phi_{\text{DHW},k}$ in the previous time step k :

$$\begin{aligned} \vartheta_{\text{HWT},k+1} = & \vartheta_{\text{HWT},k} + \Delta_k \cdot [\Phi_{\text{CHP},k} - \Phi_{\text{HWT,Loss},k} \\ & - \Phi_{\text{HS},k} - \Phi_{\text{DHW},k}] / (V_{\text{HWT}} \cdot \rho_{\text{Water}} \cdot c_{\text{Water}}), \quad \forall k \in \{1, \dots, N\}, \end{aligned} \quad (5.43a)$$

$$\begin{aligned} \vartheta_{\text{HWT},1} = & \vartheta_{\text{HWT,Initial}} + \Delta_k \cdot [\Phi_{\text{CHP},0} - \Phi_{\text{HWT,Loss},0} \\ & - \Phi_{\text{HS},0} - \Phi_{\text{DHW},0}] / (V_{\text{HWT}} \cdot \rho_{\text{Water}} \cdot c_{\text{Water}}). \end{aligned} \quad (5.43b)$$

$\vartheta_{\text{HWT,Initial}}$ is the value of the tank temperature in time step 0. It is equal to the tank temperature in the simulation or the tank temperature that is measured in a real system before the start of the optimization. In order to calculate the temperature change, the generated and consumed heat has to be divided by the volume of the HWT V_{HWT} , the volumetric mass density of water ρ_{Water} and the specific heat capacity of water c_{Water} . The values of the tank temperature are given by $\vartheta_{\text{HWT}} = (\vartheta_{\text{HWT},1}, \dots, \vartheta_{\text{HWT},N})^T$.

The temperature of the water in the tank is not allowed to exceed a given maximum temperature $\bar{\vartheta}_{\text{HT}}$ or fall below a given minimum temperature $\underline{\vartheta}_{\text{HT}}$. This is modeled by the introduction of the following constraints:

$$\underline{\vartheta}_{\text{HWT}} \leq \vartheta_{\text{HWT},k} \leq \bar{\vartheta}_{\text{HWT}}, \quad \forall k \in \{1, \dots, N\}. \quad (5.44)$$

It is assumed that the micro-CHP generates a suitable amount of heat that Equation 5.44 holds in all cases. In real systems, extreme circumstances, for example very low ambient temperatures for a long time or a very high domestic hot water consumption, can lead to a violation of the constraint given in Equation 5.44. This causes the optimization problem to be infeasible, which means that no solution can be found that meet the constraints. To include a possible violation of the limits of the tank temperature Equation 5.44 has to be changed to a soft constraint that can be violated at a certain cost [260, p. 31]. This can be done by the introduction of additional decision variables. These variables are called slack variables [260, p. 31].

The model used in this thesis does not include constraints on maximum thermal energy that can be drawn or stored in the HWT in one time step (cf. Equation 5.15). The use of recorded heat consumption profiles allows the assumption that all thermal energy needs and all the thermal energy that has been generated by the micro-CHP can be stored. However, constraints on the maximum thermal energy exchange with the HWT can easily be added using the approach presented in Equation 5.15.

Standing Loss

In this thesis, the standing loss of the HWT $\Phi_{\text{HWT,Loss}}$ is modeled according to the EU regulation of the energy efficiency classes of HWT classes [73, Annex II]. The regulation provides a model that provides a heat loss depending solely on the volume of the tank V_{HWT} in m^3 :

$$\Phi_{\text{HWT,Loss},k} = (a_{\text{HWT}} + b_{\text{HWT}} \cdot (c_{\text{HWT}} \cdot V_{\text{HWT}})^{0.4}), \quad \forall k \in \{0, \dots, N-1\}. \quad (5.45)$$

a_{HWT} and b_{HWT} are the parameters that define the heat loss in the respective energy efficiency class while c_{HWT} is a fixed parameter [73, Annex II]. Mauser [163, p. 157] extended this model to integrate the dependency of the water temperature in the tank on the heat loss according to Equation 4.6. In this thesis, the heat loss of the HWT uses the

same model as presented by Mauser. It is given by the following shorthand notation:

$$\Phi_{\text{HWT,Loss},k} = (a_{\text{HWT}} + b_{\text{HWT}} \cdot (c_{\text{HWT}} \cdot V_{\text{HWT}})^{0.4}) \cdot \frac{(\vartheta_{\text{HWT},k} - \vartheta_{\text{HWT,Ambient}})}{d_{\text{HWT}}}, \quad \forall k \in \{1, \dots, N - 1\}, \quad (5.46a)$$

$$\Phi_{\text{HWT,Loss},0} = (a_{\text{HWT}} + b_{\text{HWT}} \cdot (c_{\text{HWT}} \cdot V_{\text{HWT}})^{0.4}) \cdot \frac{(\vartheta_{\text{HWT,Initial}} - \vartheta_{\text{HWT,Ambient}})}{d_{\text{HWT}}}. \quad (5.46b)$$

This model is similar to other optimization approaches in the literature [164, 222]. The parameters a_{HWT} and b_{HWT} are chosen to represent an HWT that resembles the transition from energy efficiency classes B to C [73, Annex II]. The parameter c_{HWT} is chosen based on the assumption of a minimum temperature difference between the ambient temperature of the HWT and the minimum water temperature of 40 K. The ambient temperature $\vartheta_{\text{HWT,Ambient}}$ is chosen to be constant and equal to 20 °C. This choice of parameters results in an average standing heat loss of 2.3 kWh per day when assuming a constant tank temperature of 60 °C. For an HWT with a size of 750 L, this results in a temperature decrement of about 2.5 K. This is comparable to real HWTs commonly used in combination with the Senertec Dachs G5.5 micro-CHP [225, p. 47 & 89]. A list of the HWT model parameters and the chosen values is presented in Table 5.8.

5.6.9 Tariffs

Future energy systems are assumed to have a high penetration of RESs (see Section 2.3). Based on the volatility and intermittency of the electricity generation of RESs, the prices of electric energy are assumed to become more time-dependent to mirror the time-dependent generation. Often, it is assumed that these time-dependent prices will be offered to end users. As described in Section 2.9.2, TOU electricity tariffs are tariffs with a time-dependent electricity price. In this thesis, the presence of TOU electricity tariffs is assumed.

In addition, TOU electricity tariffs can be seen as a measure of DSM (see Sections 2.9.5 and 2.15). Following this viewpoint, TOU electricity tariffs can be used by demand side managers to communicate with end users (see Figure 2.9c). The tariffs incentivize the end users to shape their electricity consumption in order to minimize their costs. Hence, the TOU electricity tariffs are not limited to represent the electricity prices in the wholesale market but can also include other factors. Electricity tariffs can also be used as a measure of DSM, for example to solve a temporary congestion of the grid. In summary, TOU electricity tariffs reward the electricity consumption in steps of low prices and punish the consumption at times of high prices.

In addition to time-dependent electricity prices, time-dependent feed-in compensations are assumed (see Section 2.9.2). Time dependent feed-in compensations can be justified in an analogous manner to the time-dependent electricity prices.

In this thesis, the electricity consumption price in each time step t in the simulation of the building is given by $\tilde{\pi}_{\text{Im},t}$. The index Im stands for import, relating to the amount of

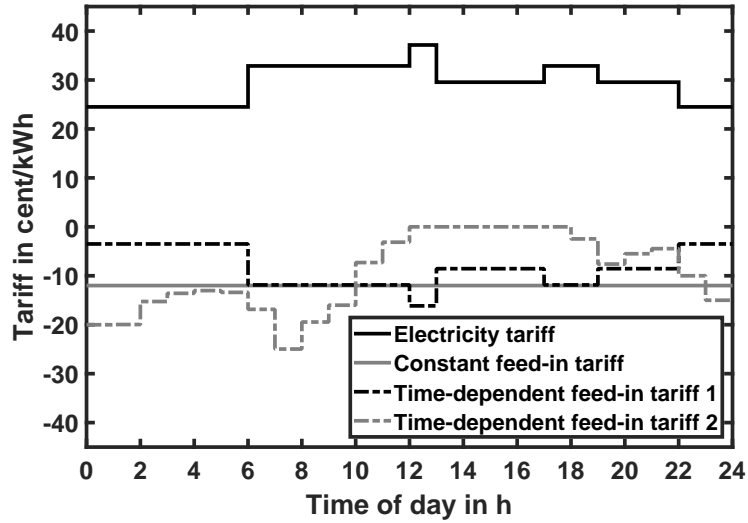


Figure 5.13: Electricity consumption and feed-in tariffs.

energy that is imported from the grid into the build. In contrast, the index Ex stands for export, relating to the amount of energy that is exported from the building to the grid. It is important to note that this thesis uses a convention in which prices are positive and rewards are negative. This is in-line with formulating the optimization problem as a minimization problem that targets the minimization of costs.

In this thesis, it is assumed that the electricity consumption price is always higher than the absolute value of the feed-in compensation (see also Section 5.6.10):

$$|\tilde{\pi}_{\text{Ex},t}| \leq \tilde{\pi}_{\text{Im},t}, \quad \forall t \in \{1, \dots, T\}. \quad (5.47)$$

This can be motivated by assuming that the commodity electric energy at a given time in a given spatial point has a given value. Then, the import price should be larger since it includes grid fees, market fees, payment fees, etc. This assumption does not incorporate any possible valuation of the source of the electric energy. An example of such a valuation can be that electric energy from renewables is more valuable than the electric energy from fossil resources based on being more environmentally friendly.

In the following sections, the time-dependent electricity prices and feed-in compensations that are used in this thesis are described in detail. In Figure 5.13 all the electricity consumption and feed-in tariffs used in this thesis are displayed.

Electricity Tariff

The TOU electricity tariff that is used in this thesis has originally been presented in [143]. It has been created to provide a realistic scenario to enable work in the field of future energy systems, smart grids, economic optimization of energy systems (see Section 2.12) and energy management. The temporal sequence of prices resembles the shape of the yearly

average electricity price at the German day ahead auction at the EPEX SPOT market as well as the German standard load profile of households H0 [250]. However, the absolute prices are assumed to be close to the ones common in Germany in the year 2015. This price is assumed to include all fees, e. g., grid connection fees.

In this thesis, an average price of 30 cent/kWh is assumed. Hence, the TOU electricity tariff presented in [163] is rescaled to have a daily average price of 30 cent/kWh.

The electricity consumption tariff is constant for the duration of each hour in the day. However, each hour can have a different consumption price. In addition, the electricity consumption tariff is assumed to be equal in each day of the year. The electricity consumption tariff is displayed by the solid black line in Figure 5.13.

To translate these parameters to the domain of the optimization, the time step lengths have to be adjusted from Δ_t in the simulation to Δ_k in the rolling horizon optimization. For an optimization starting in the simulation time step t_0 , the electricity consumption prices are given by:

$$\pi_{\text{Im},k} = \tilde{\pi}_{\text{Im},\left(\lfloor t_0+k \cdot \frac{\Delta_k}{\Delta_t} \rfloor\right)}, \quad \forall k \in \{0, \dots, N-1\}. \quad (5.48)$$

The electricity consumption prices $\tilde{\pi}_{\text{Im},t}$ are known for the simulation period with $t \in \{1, \dots, T\}$. In the rolling horizon optimization, the electricity consumption prices $\pi_{\text{Im},k}$ are treated as fixed parameters.

Feed-in Tariff

In addition to the TOU tariff for the electricity consumption, the electricity feed-in, i. e., export, to the grid is also assumed to be billed based on a time-dependent tariff. Since time-dependent feed-in tariffs are not widely spread amongst end users and examples of feed-in tariffs that can be used in this thesis are rare, this thesis uses two different artificial time-dependent feed-in tariffs plus one feed-in tariff with a constant compensation. They are chosen to represent three different scenarios: a scenario based on the current state-of-the-art, a scenario that represents a realistic future feed-in tariff and an extreme scenario. All three feed-in tariffs are given in Figure 5.13.

The constant feed-in tariff has a compensation of 12 cent/kWh. This resembles the current situation in Germany for PV systems on residential buildings having a maximum power of 10 kW [39]. The first time-dependent tariff resembles a possible future feed-in tariff. It is created by multiplying the TOU electricity tariff by -1 and performing a linear shift of 21 cent/kWh to obtain an average compensation of 9 cent/kWh. The second time-dependent tariff resembles an extreme feed-in tariff. It is based on an extreme day at the intra-day market at the European Power Exchange in September 2015. The same choice of tariffs has also been used in [174, 179].

For the sake of simplicity, this thesis assumes that the feed-in compensation does not depend on the source of the energy that is fed into the grid. In addition, it is assumed

that there are no compensations for the self-consumption of electricity generated by the micro-CHP or the PV system. Furthermore, power prices and power limits as defined in Section 2.9.2 are not considered in this thesis. However, power limits can be included in the model by introducing additional decision variables following the approach presented in [129, 132].

To translate these parameters to the domain of the optimization, the time step lengths have to be adjusted from Δ_t in the simulation to Δ_k in the rolling horizon optimization. For an optimization that starts in the simulation time step t_0 , the electricity consumption prices are given by:

$$\pi_{\text{Ex},k} = \tilde{\pi}_{\text{Ex},\left(\lceil t_0+k \cdot \frac{\Delta_k}{\Delta_t} \rceil\right)}, \quad \forall k \in \{0, \dots, N-1\}. \quad (5.49)$$

The electricity feed-in compensations $\tilde{\pi}_{\text{Ex},t}$ are known for the simulation period with $t \in \{1, \dots, T\}$. In the rolling horizon optimization, the electricity feed-in compensations $\pi_{\text{Im},k}$ are treated as fixed parameters.

Gas Tariff

The scenario that is investigated in this thesis (see Section 5.2) includes a micro-CHP that is run by natural gas. This thesis assumes a constant gas price of $\pi_{\text{Gas,Flat}} = 9$ cent/kWh. This choice resembles the current situation in Germany.

Since the gas consumption price is not dependent on the time, the prices in the simulation $\tilde{\pi}_{\text{Gas},t}$ and the rolling horizon optimization $\pi_{\text{Gas},k}$, respectively, are given by:

$$\tilde{\pi}_{\text{Gas},t} = \pi_{\text{Gas,Flat}}, \quad \forall t \in \{1, \dots, T\}, \quad (5.50)$$

$$\pi_{\text{Gas},k} = \pi_{\text{Gas,Flat}}, \quad \forall k \in \{0, \dots, N-1\}. \quad (5.51)$$

5.6.10 Device Interaction Model and Grid Interaction Model

In addition to the individual devices in the building energy system, the interaction of the devices as well as the interaction with the electricity grid have to be modeled. Therefore, the following constraints have been introduced.

The power balance has to be ensured in every time step. This means that the electricity generation has to be equal to the electricity consumption. This requires that the sum of all power flows to devices that consume electricity plus the grid export power is equal to the sum of all power flows from devices that generate energy plus the grid import power in all time steps k . This is addressed in the following constraints:

$$\sum_{j=1}^J P_{\text{Appliances},j,k} + P_{\text{Base},k} + P_{\text{BESS},\text{C},k} + P_{\text{Ex},k} = P_{\text{Im},k} + P_{\text{PV},k} + P_{\text{CHP},k} + P_{\text{BESS},\text{D},k}, \quad \forall k \in \{0, \dots, N-1\} \quad (5.52)$$

$P_{\text{Im},k}$ and $P_{\text{Ex},k}$ are the power that is imported from the grid and the power that is exported to the grid, respectively. The imported power is treated as electricity generation while the exported power is treated as electricity consumption. Both power flows, $\mathbf{P}_{\text{Im}} = (P_{\text{Im},0}, \dots, P_{\text{Im},N-1})^\top$ and $\mathbf{P}_{\text{Ex}} = (P_{\text{Ex},0}, \dots, P_{\text{Ex},N-1})^\top$, are modeled to be decision variables with $\mathbf{P}_{\text{Im}} \in \mathbb{R}^N$ and $\mathbf{P}_{\text{Ex}} \in \mathbb{R}^N$.

The interaction with the grid is assumed to have no constraints. This means there are no maximum or minimum import and export powers. Hence, the following constraints are used:

$$0 \leq P_{\text{Im},k}, \quad \forall k \in \{0, \dots, N-1\} \quad (5.53)$$

and

$$0 \leq P_{\text{Ex},k}, \quad \forall k \in \{0, \dots, N-1\}. \quad (5.54)$$

In general, feed-in from the BESS is only beneficial in case of a time-varying feed in compensation that has a spread between the different feed-in compensations that is so high that it compensates the energy losses based on the non-perfect efficiency of the BESS. Thus, the amount of energy that is fed into the grid from the BESS as well as the point in time this is done is heavily dependent on the tariff structures.

However, the local government of Victoria, Australia, introduced a time-dependent feed-in tariff [72] and explicitly encourages the feed-in from all sources, including a BESS, in particular time steps of the day. In their opinion, the feed-in supports the grid operation independently of its source.

Similarly to the feed-in from the BESS, the charging of the BESS using power that is drawn from the grid can be beneficial in special cases. However, the amount of power that is drawn from the grid to charge the BESS as well as the point in time this is done is heavily dependent on the tariff structures.

In this thesis, only scenarios are evaluated, in which feed-in from the BESS into the grid as well as power import from the grid to charge the BESS are not allowed. This allows for a comparison to a state-of-the-art rule based approach that is used in commercially available BESSs (see Section 5.6.1 and Algorithm 5.4). The feed-in from the BESS is prevented by the following constraint:

$$0 \leq P_{\text{Ex},k} \leq P_{\text{PV},k} + P_{\text{CHP},k}, \quad \forall k \in \{0, \dots, N-1\}. \quad (5.55)$$

The power that is exported to the grid $P_{\text{Ex},k}$ is limited to the sum of the local generation $P_{\text{PV},k} + P_{\text{CHP},k}$ in every time step k . This has the same result as limiting the discharge power of the BESS to the sum of the local electricity consumption $\sum_{j=1}^J P_{\text{Appliances},j,k} + P_{\text{Base},k}$ in every time step k :

$$P_{\text{BESS,D},k} \leq \sum_{j=1}^J P_{\text{Appliances},j,k} + P_{\text{Base},k}, \quad \forall k \in \{0, \dots, N-1\}. \quad (5.56)$$

To prohibit charging the BESS by taking power from the grid, the following constraints are introduced similarly to Equation 5.55:

$$0 \leq P_{\text{Im},k} \leq \sum_{j=1}^J P_{\text{Appliances},j,k} + P_{\text{Base},k}, \quad \forall k \in \{0, \dots, N-1\}. \quad (5.57)$$

Here, the power that is imported from the grid $P_{\text{Im},k}$ is limited to the sum of the local consumption $\sum_{j=1}^J P_{\text{Appliances},j,k} + P_{\text{Base},k}$ in every time step k . Analogously to Equation 5.56, the following constraint can be introduced instead:

$$P_{\text{BESS},C,k} \leq P_{\text{PV},k} + P_{\text{CHP},k}, \quad \forall k \in \{0, \dots, N-1\}. \quad (5.58)$$

A simultaneous import and export of electricity is not explicitly prohibited by the model even though this is physically not possible. This is based on the assumption that the absolute value of the feed-in compensation $\pi_{\text{Ex},k}$ is lower than the electricity price $\pi_{\text{Im},k}$ (see Sections 5.6.9 and Equation 5.47). When this assumption holds true, electricity export or feed-in is always preferred over import. Because of that, electricity import will only happen when feed in is not possible.

In scenarios in which the absolute value of the feed-in compensation $\pi_{\text{Ex},k}$ is higher than the electricity price $\pi_{\text{Im},k}$:

$$\exists k \in \{0, \dots, N-1\} : \pi_{\text{Im},k} \leq |\pi_{\text{Ex},k}|, \quad (5.59)$$

a simultaneous electricity import and export occurs in the model. This happens because the optimization takes cheaper electricity out of the grid and feeds it directly back into the grid to create revenues. This is physically not possible and makes no sense economically (see Section 5.6.9). In addition, the optimization problem becomes unconstrained when P_{Im} and P_{Ex} are not constrained individually (see Equation 5.55 and 5.57).

A simultaneous import and export of electricity can be explicitly prohibited by the introduction of additional binary decision variables $\mathbf{b}_{\text{Grid}} = (b_{\text{Grid},0}, \dots, b_{\text{Grid},N-1})^\top$ with $\mathbf{b}_{\text{Grid}} \in \{0, 1\}^N$. Equation 5.15 would then change to:

$$0 \leq P_{\text{Im},k} \leq \bar{P}_{\text{Im}} \cdot b_{\text{Grid},k}, \quad \forall k \in \{0, \dots, N-1\}, \quad (5.60a)$$

$$0 \leq P_{\text{Ex},k} \leq \bar{P}_{\text{Ex}} \cdot (1 - b_{\text{Grid},k}), \quad \forall k \in \{0, \dots, N-1\}. \quad (5.60b)$$

Here, \bar{P}_{Im} and \bar{P}_{Ex} are the maximum powers that can be drawn from the grid and fed into the grid, respectively. Both parameters can be chosen to resemble physical limits of the grid connection or to be very large compared to the actual powers.

5.7 Formulation of the State-of-the-art One-stage Rolling Horizon Optimization Problem

As described in Section 5.5, the goal of the rolling horizon optimization problem is to determine the control inputs for the devices that are set to minimize the operating costs.

Table 5.9: List of decision variables in the state-of-the-art one-stage rolling horizon optimization problem

Decision variable	Symbol	Domain	Unit	Description
micro-CHP control inputs	\mathbf{u}_{CHP}	$\{0, 1\}^N$	–	Control input
Appliances control inputs	$\mathbf{u}_{\text{Appliances}}$	$\{0, 1\}^{N \times J}$	–	Control input
BESS charge control inputs	$\mathbf{u}_{\text{BESS,C}}$	$[0, 1]^N$	–	Control input
BESS discharge control inputs	$\mathbf{u}_{\text{BESS,D}}$	$[0, 1]^N$	–	Control input
Grid import power	P_{Im}	\mathbb{R}^N	kW	Auxiliary variable
Grid export power	P_{Ex}	\mathbb{R}^N	kW	Auxiliary variable
Number of micro-CHP starts	s_{CHP}	$\{0, 1\}^N$	–	Auxiliary variable

The controlled devices are the BESS, the appliances and the micro-CHP. In the one-stage rolling horizon optimization problem, the control inputs relate to the control variables:

$$\mathbf{u}_k = (u_{\text{BESS,C},k}, u_{\text{BESS,D},k}, \mathbf{u}_{\text{Appliances},k}, u_{\text{CHP},k})^\top, \quad \forall k \in \{0, \dots, N-1\}. \quad (5.61)$$

In the optimization problem, the control variables are decision variables.

The auxiliary variables are additional decision variables. They are the grid export power, the grid import power and the number of starts of the micro-CHP:

$$\mathbf{a}_k = (P_{\text{Ex},k}, P_{\text{Im},k}, s_{\text{CHP},k})^\top, \quad \forall k \in \{0, \dots, N-1\}. \quad (5.62)$$

The state variables are defined for the time steps $\{1, \dots, N\}$ while control and auxiliary variables are defined for the time steps $\{0, \dots, N-1\}$. This definition enables the usage of the discrete time model as defined in Sections 3.4 and Equation 3.3.

Even though only the control variables are of interest in order to control the devices, the other decision variables are needed to formulate the optimization problem as a mixed-integer linear program. When using a different modeling approach, the additional decision variables may be omitted. A detailed list of the decision variables that are used in the optimization problem is presented in Table 5.9.

In addition to the decision variables, the optimization problem contains various parameters that are fixed during the optimization. However, as described in Sections 3.5 and 5.5 the parameters can change between the individual optimization runs of the rolling horizon approach. This leads to a different optimization problem in every optimization run of the rolling horizon optimization. However, the structure of the problem remains unchanged, but the values of the parameters change. A list of all model parameters is presented in Table 6.7.

When solving the optimization problem, it is assumed that a solution exists for all realistic parameter combinations, i. e., parameter combinations that represent realistic scenarios. This can be motivated by the fact that the building is always connected to the electricity

grid as well as to the gas grid and the power import and export are not limited. For the HS it is assumed that the heat load can always be satisfied by the combination of micro-CHP and HWT.

5.7.1 Objective Function

The operating costs consist of three parts: the cost of importing the electricity from the grid, the gas cost, and the compensation of the electricity that is fed into the grid. As described in Section 5.6.9, this thesis assumes a time-dependent electricity tariff and a time-dependent feed-in compensation. This leads to time variable stage costs as defined in Section 3.6:

$$l(P_{\text{Ex},k}, P_{\text{Im},k}, G_{\text{CHP},k}, s_{\text{CHP},k}) = \Delta_k \cdot [\pi_{\text{Ex},k} \cdot P_{\text{Ex},k} + \pi_{\text{Im},k} \cdot P_{\text{Im},k} + \pi_{\text{Gas},k} \cdot G_{\text{CHP},k}] + \pi_{\text{CHP,Start}} \cdot s_{\text{CHP},k} \quad (5.63)$$

The objective function $J_N(\mathbf{P}_{\text{Ex}}, \mathbf{P}_{\text{Im}}, \mathbf{G}_{\text{CHP}}, \mathbf{s}_{\text{CHP}})$ for the optimization window of N time steps is given by:

$$J_N(\mathbf{P}_{\text{Ex}}, \mathbf{P}_{\text{Im}}, \mathbf{G}_{\text{CHP}}, \mathbf{s}_{\text{CHP}}) = \sum_{k=0}^{N-1} \Delta_k \cdot [\pi_{\text{Ex},k} \cdot P_{\text{Ex},k} + \pi_{\text{Im},k} \cdot P_{\text{Im},k} + \pi_{\text{Gas},k} \cdot G_{\text{CHP},k}] + \pi_{\text{CHP,Start}} \cdot s_{\text{CHP},k} \quad (5.64)$$

Here, $\pi_{\text{Ex},k}$ is the compensation for the electricity export in time step k , $\pi_{\text{Im},k}$ is the price for the electricity import in time step k and $\pi_{\text{Gas},k}$ is the price for gas in time step k . Since $\pi_{\text{Ex},k}$, $\pi_{\text{Im},k}$ and $\pi_{\text{Gas},k}$ are given in cent/kWh, the grid import power P_{Im} , the grid export power P_{Ex} and the gas consumption power G_{CHP} have to be multiplied by the time step length Δ_k in any time step k . The variables $s_{\text{CHP},k}$ are the number of starts of the micro-CHP. It is important to note that the optimization problem in the rolling horizon approach does not necessarily have to be equal to the optimization of the operating costs of the building (see Section 3.5). The costs for starting the micro-CHP can be seen as penalty costs that encourage specific solutions (see Sections 3.4 and Equation 3.7). Even though a start of the micro-CHP does not directly lead to costs, a higher number of starts is not desired by the designer of the system. This is a consequence of the dependence between the wear and the number of starts of the micro-CHP. Furthermore, terminal costs, i. e., a term in the objective function that is dependent on the final time step $k = N$, can be added to the objective function (Section 3.5) to encourage specific solutions. The specific solutions are chosen by the designer of the planning and optimization system. Based on his knowledge of the expected future behavior of the building energy system beyond the optimization horizon, the specific solutions are expected to lead to a high performance of the rolling horizon optimization approach over a time period longer than the optimization window. However, no terminal costs as defined in Section 3.5 are assumed in this thesis.

5.7.2 Constraints

The constraints of the optimization problem result from the device and interaction models presented in Section 5.6. In this section, the constraints that are described in detail in Section 5.6 are summarized and recapitulated. A list of the decision variables is given in Table 5.9 and a list of all the model parameters is presented in Table 6.7.

The state equations (see Section 3.3) of the BESS are given by

$$E_{\text{BESS},k+1} = E_{\text{BESS},k} + \Delta_k \cdot (\eta_{\text{BESS}} \cdot P_{\text{BESS},\text{C},k} + \eta_{\text{BESS}}^{-1} P_{\text{BESS},\text{D},k}) \quad \forall k \in \{1, \dots, N\}, \quad (5.65a)$$

$$E_{\text{BESS},1} = E_{\text{BESS,Initial}} + \Delta_k \cdot (\eta_{\text{BESS}} \cdot P_{\text{BESS},\text{C},0} + \eta_{\text{BESS}}^{-1} P_{\text{BESS},\text{D},0}). \quad (5.65b)$$

The constraints limiting the BESS state variable to its maximum and minimum are:

$$\underline{E}_{\text{BESS}} \leq E_{\text{BESS},k} \leq \bar{E}_{\text{BESS}}, \quad \forall k \in \{1, \dots, N\}. \quad (5.66)$$

The control variables of the BESS are constrained by:

$$P_{\text{BESS},\text{C}} \leq P_{\text{BESS},\text{C},k} \leq \bar{P}_{\text{BESS},\text{C}}, \quad \forall k \in \{0, \dots, N-1\}, \quad (5.67a)$$

$$P_{\text{BESS},\text{D}} \leq P_{\text{BESS},\text{D},k} \leq \bar{P}_{\text{BESS},\text{D}}, \quad \forall k \in \{0, \dots, N-1\}, \quad (5.67b)$$

using the following shorthand notations:

$$P_{\text{BESS},\text{C},k} = u_{\text{BESS},\text{C},k} \cdot \bar{P}_{\text{BESS},\text{C}}, \quad \forall k \in \{0, \dots, N-1\}, \quad (5.68a)$$

$$P_{\text{BESS},\text{D},k} = u_{\text{BESS},\text{D},k} \cdot \bar{P}_{\text{BESS},\text{D}}, \quad \forall k \in \{0, \dots, N-1\}. \quad (5.68b)$$

The state equations of the HWT are given by:

$$\vartheta_{\text{HWT},k+1} = \vartheta_{\text{HWT},k} + \Delta_k \cdot [\Phi_{\text{CHP},k} - \Phi_{\text{HWT,Loss},k} - \Phi_{\text{HS},k} - \Phi_{\text{DHW},k}] / (V_{\text{HWT}} \cdot \rho_{\text{Water}} \cdot c_{\text{Water}}), \quad \forall k \in \{1, \dots, N\}, \quad (5.69a)$$

$$\vartheta_{\text{HWT},1} = \vartheta_{\text{HWT,Initial}} + \Delta_k \cdot [\Phi_{\text{CHP},0} - \Phi_{\text{HWT,Loss},0} - \Phi_{\text{HS},0} - \Phi_{\text{DHW},0}] / (V_{\text{HWT}} \cdot \rho_{\text{Water}} \cdot c_{\text{Water}}), \quad (5.69b)$$

using the following shorthand notations:

$$\Phi_{\text{HWT,Loss},k} = (a_{\text{HWT}} + b_{\text{HWT}} \cdot (c_{\text{HWT}} \cdot V_{\text{HWT}})^{0.4}) \cdot \frac{(\vartheta_{\text{HWT},k} - \vartheta_{\text{HWT,Ambient}})}{d_{\text{HWT}}}, \quad \forall k \in \{1, \dots, N-1\}, \quad (5.70a)$$

$$\Phi_{\text{HWT,Loss},0} = (a_{\text{HWT}} + b_{\text{HWT}} \cdot (c_{\text{HWT}} \cdot V_{\text{HWT}})^{0.4}) \cdot \frac{(\vartheta_{\text{HWT,Initial}} - \vartheta_{\text{HWT,Ambient}})}{d_{\text{HWT}}}. \quad (5.70b)$$

The control variables of the micro-CHP are constrained by:

$$0 \leq \sum_{i=k}^N u_{\text{CHP},i} - (N - k) \cdot (u_{\text{CHP},k} - u_{\text{CHP},k-1}), \quad \forall k \in \{N - k_{\text{CHP,Min}} + 1, \dots, N\}. \quad (5.71)$$

If the parameter $k_{\text{CHP,Initial}} \neq 0$, the optimization problem contains the following constraints:

$$k_{\text{CHP,Min}} \cdot (u_{\text{CHP},k} - u_{\text{CHP},k-1}) \leq \sum_{i=k}^{k+k_{\text{CHP,Min}}-1} u_{\text{CHP},i}, \quad \forall k \in \{k_{\text{CHP,Initial}}, \dots, N - k_{\text{CHP,Min}}\} \quad (5.72)$$

and

$$k_{\text{CHP,Initial}} - \sum_{i=0}^{k_{\text{CHP,Initial}}-1} u_{\text{CHP},i} = 0. \quad (5.73)$$

If $k_{\text{CHP,Initial}} = 0$, the optimization problem contains the following constraints:

$$k_{\text{CHP,Min}} \cdot (u_{\text{CHP},k} - u_{\text{CHP},k-1}) \leq \sum_{i=k}^{k+k_{\text{CHP,Min}}-1} u_{\text{CHP},i}, \quad \forall k \in \{1, \dots, N - k_{\text{CHP,Min}}\}, \quad (5.74a)$$

$$k_{\text{CHP,Min}} \cdot (u_{\text{CHP},0} - u_{\text{CHP,Initial}}) \leq \sum_{i=0}^{k_{\text{CHP,Min}}-1} u_{\text{CHP},i}. \quad (5.74b)$$

To ease the handling of the control variables of the micro-CHP, the following shorthand notations are introduced:

$$P_{\text{CHP},k} = u_{\text{CHP},k} \cdot P_{\text{CHP,Nom}}, \quad \forall k \in \{0, \dots, N - 1\}, \quad (5.75a)$$

$$\Phi_{\text{CHP},k} = u_{\text{CHP},k} \cdot \Phi_{\text{CHP,Nom}}, \quad \forall k \in \{0, \dots, N - 1\}, \quad (5.75b)$$

$$G_{\text{CHP},k} = u_{\text{CHP},k} \cdot G_{\text{CHP,Nom}}, \quad \forall k \in \{0, \dots, N - 1\}. \quad (5.75c)$$

The auxiliary variables which consider the number of starts of the micro-CHP are constrained by:

$$(u_{\text{CHP},k} - u_{\text{CHP},k-1}) \leq s_{\text{CHP},k}, \quad \forall k \in \{1, \dots, N - 1\}, \quad (5.76a)$$

$$(u_{\text{CHP},0} - u_{\text{CHP,Initial}}) \leq s_{\text{CHP},0}. \quad (5.76b)$$

$$(5.76c)$$

The control variables of the appliances are constrained by:

$$\sum_{i=0}^{N-1} u_{\text{Appliances},j,i} = b_{\text{Appliances},j}, \quad \forall j \in \{1, \dots, J\} \quad (5.77)$$

and

$$\underline{k}_{\text{Appliances},j} \leq \sum_{i=0}^{N-1} u_{\text{Appliances},j,i} \cdot i \leq \bar{k}_{\text{Appliances},j}, \quad \forall j \in \{1, \dots, J\}. \quad (5.78)$$

To ease the handling of the control variables of the appliances, the following shorthand notations are introduced:

$$P_{\text{Appliances},j,k} = \sum_{i=k-l_{\text{Appliances},j}}^k u_{\text{Appliances},j,i} \cdot P_{\text{Appliances},\text{Nom},j,k-i+1}, \quad \forall k \in \{l_{\text{Appliances},j}, \dots, N-1\}, \forall j \in \{1, \dots, J\}, \quad (5.79a)$$

$$P_{\text{Appliances},j,k} = \sum_{i=0}^k u_{\text{Appliances},j,i} \cdot P_{\text{Appliances},\text{Nom},j,k-i+1}, \quad \forall k \in \{0, \dots, l_{\text{Appliances},j} - 1\}, \forall j \in \{1, \dots, J\}. \quad (5.79b)$$

The balance of the power flows is ensured by:

$$\sum_{j=1}^J P_{\text{Appliances},j,k} + P_{\text{Base},k} + P_{\text{BESS},\text{C},k} + P_{\text{Ex},k} = P_{\text{Im},k} + P_{\text{PV},k} + P_{\text{CHP},k} + P_{\text{BESS},\text{D},k}, \quad \forall k \in \{0, \dots, N-1\}. \quad (5.80)$$

The relationships between the auxiliary variables $P_{\text{Ex},k}$ and $P_{\text{Im},k}$ and the control variables are given by:

$$0 \leq P_{\text{Ex},k} \leq P_{\text{PV},k} + P_{\text{CHP},k}, \quad \forall k \in \{0, \dots, N-1\} \quad (5.81)$$

and

$$0 \leq P_{\text{Im},k} \leq \sum_{j=1}^J P_{\text{Appliances},j,k} + P_{\text{Base},k}, \quad \forall k \in \{0, \dots, N-1\}. \quad (5.82)$$

5.7.3 Summary of the Optimization Problem

The optimization problem that has to be solved in every optimization in the rolling horizon optimization approach is:

$$\begin{aligned} & \text{minimize} && \sum_{k=0}^{N-1} l(\mathbf{P}_{\text{Ex}}, P_{\text{Im},k}, G_{\text{CHP},k}, s_{\text{CHP},k}) \\ & \mathbf{u}_{\text{BESS},\text{D}} \in [0,1]^N && \\ & \mathbf{u}_{\text{BESS},\text{C}} \in [0,1]^N && \\ & \mathbf{u}_{\text{CHP}} \in \{0,1\}^N && \\ & \mathbf{u}_{\text{Appliances}} \in \{0,1\}^{J \times N} && \\ & \mathbf{P}_{\text{Im}} \in \mathbb{R}^N && \\ & \mathbf{P}_{\text{Ex}} \in \mathbb{R}^N && \\ & \mathbf{s}_{\text{CHP}} \in \mathbb{R}^N && \\ & \text{subject to} && (5.65) - (5.82) \end{aligned} \quad (5.83)$$

Here, it is important to note that the parameters N and Δ_k are tuning parameters that have to be chosen by the designer of the planning and optimization system. The choice of the parameters in the evaluation scenario is motivated in Section 6.6.2.

5.8 Formulation of the Stochastic Two-stage Rolling Horizon Optimization Problem

The stochastic two-stage rolling horizon optimization problem is formulated according to the definition presented in Sections 3.11.1 and Equation 3.40. The first stage relates to the first time step of the state-of-the-art optimization problem defined in Section 5.7. In case of the control and the auxiliary variables, the first time step is given by $k = 0$ and in case of the state variables the first time step is given by $k = 1$. The second stage includes all other time steps. For the control and the auxiliary variables, these are defined by $k \in \{1, \dots, N - 1\}$ and for the state variables these are defined by $k \in \{2, \dots, N\}$. In the first stage, no uncertainties are considered, while the second stage includes uncertain parameters. In this thesis, the uncertain parameters are the forecasts of the PV generation. The formulation of the problem allows for an easy integration of other uncertainties, e. g., the uncertainties in the forecast of the electricity or heat consumptions. However, the influence of the performance of the optimization approach are hard to estimate.

As defined in Section 3.11.1 and Equation 3.40, the objective function of the stochastic two-stage rolling horizon optimization problem consists of the sum of the objective function for the first-stage and the expected value of the optimal solution for the second-stage problem. For a given realization of the uncertain parameters, the optimal solution for the second-stage problem is found by minimizing the objective function of the second-stage problem. For a number $M \in \mathbb{N}$ of possible realizations of the uncertain parameters, the expected value of the optimal solution for the second-stage problem is given by the sum over the optimal solutions for the second-stage problem for all possible realizations of the uncertain parameters where every term is weighted by the probability of occurrence of the respective possible realization (see Section 3.11.3 and Equation 3.49). In general, M gives the number of forecast scenarios. In this thesis, the forecast scenarios relate to possible PV generation scenarios.

As a consequence, the number of decision variables increases with respect to the formulation of the state-of-the-art one-stage rolling horizon optimization problem as defined in Section 5.7. More accurately, $(M - 1) \cdot (N - 1)$ additional decision variables are necessary with respect to the state-of-the-art one-stage rolling horizon optimization problem. A list of all decision variables in the stochastic two-stage rolling horizon optimization problem is presented in Table 5.10. Here, it is important to note that for $M = 1$, the stochastic two-stage rolling horizon optimization problem becomes equal to the one-stage rolling horizon optimization problem.

The control variables in the stochastic two-stage rolling horizon optimization problem are given by (cf. Equation 5.61):

$$\mathbf{u}^{1\text{ST}} = (u_{\text{BESS,C}}^{1\text{ST}}, u_{\text{BESS,D}}^{1\text{ST}}, \mathbf{u}_{\text{Appliances}}^{1\text{ST}}, u_{\text{CHP}}^{1\text{ST}})^{\top}, \quad (5.84)$$

$$\mathbf{u}_{m,k}^{2\text{ST}} = (u_{\text{BESS,C},m,k}^{2\text{ST}}, u_{\text{BESS,D},m,k}^{2\text{ST}}, \mathbf{u}_{\text{Appliances},m,k}^{2\text{ST}}, u_{\text{CHP},m,k}^{2\text{ST}})^{\top}, \quad \forall k \in \{1, \dots, N - 1\}, \forall m \in \{1, \dots, M\}. \quad (5.85)$$

Table 5.10: List of decision variables in the stochastic two-stage rolling horizon optimization problem

Decision variable	Symbol	Domain	Unit	Description
1. stage micro-CHP control inputs	$u_{\text{CHP}}^{1\text{ST}}$	$\{0, 1\}$	–	Control input
2. stage micro-CHP control inputs	$u_{\text{CHP}}^{2\text{ST}}$	$\{0, 1\}^{N-1 \times M}$	–	Control input
1. stage appliances control inputs	$u_{\text{Appliances}}^{1\text{ST}}$	$\{0, 1\}$	–	Control input
2. stage appliances control inputs	$u_{\text{Appliances}}^{2\text{ST}}$	$\{0, 1\}^{N-1 \times M \times J}$	–	Control input
1. stage BESS charge control inputs	$u_{\text{BESS,C}}^{1\text{ST}}$	$[0, 1]$	–	Control input
2. stage BESS charge control inputs	$u_{\text{BESS,C}}^{2\text{ST}}$	$[0, 1]^{N-1 \times M}$	–	Control input
1. stage BESS discharge control inputs	$u_{\text{BESS,D}}^{1\text{ST}}$	$[0, 1]$	–	Control input
2. stage BESS discharge control inputs	$u_{\text{BESS,D}}^{2\text{ST}}$	$[0, 1]^{N-1 \times M}$	–	Control input
1. stage grid import power	$P_{\text{Im}}^{1\text{ST}}$	\mathbb{R}	kW	Auxiliary variable
2. stage grid import power	$P_{\text{Im}}^{2\text{ST}}$	$\mathbb{R}^{N-1 \times M}$	kW	Auxiliary variable
1. stage grid export power	$P_{\text{Ex}}^{1\text{ST}}$	\mathbb{R}	kW	Auxiliary variable
2. stage grid export power	$P_{\text{Ex}}^{2\text{ST}}$	$\mathbb{R}^{N-1 \times M}$	kW	Auxiliary variable
1. stage number of micro-CHP starts	$s_{\text{CHP}}^{1\text{ST}}$	$\{0, 1\}$	–	Auxiliary variable
2. stage number of micro-CHP starts	$s_{\text{CHP}}^{2\text{ST}}$	$\{0, 1\}^{N-1 \times M}$	–	Auxiliary variable

The superscripts 1ST and 2ST are introduced for ease of reading. They refer to the first and second stage, respectively. This nomenclature is applied to all variables. Hence, the auxiliary variables are given by (cf. Equation 5.62):

$$\mathbf{a}^{1\text{ST}} = (P_{\text{Ex}}^{1\text{ST}}, P_{\text{Im}}^{1\text{ST}}, s_{\text{CHP}}^{1\text{ST}})^\top, \quad (5.86)$$

$$\mathbf{a}_k^{2\text{ST}} = (P_{\text{Ex},m,k}^{2\text{ST}}, P_{\text{Im},m,k}^{2\text{ST}}, s_{\text{CHP},m,k}^{2\text{ST}})^\top, \quad \forall k \in \{1, \dots, N-1\}, \forall m \in \{1, \dots, M\}. \quad (5.87)$$

Similarly to the state-of-the-art one-stage rolling horizon optimization problem, the optimization problem has various parameters that are fixed during the optimization but can change between the individual optimization runs of the rolling horizon approach. The difference between the parameters of the state-of-the-art one-stage rolling horizon optimization problem and the stochastic two-stage rolling horizon optimization problem is the handling of the PV generation forecast. While the state-of-the-art one-stage rolling horizon optimization problem considers only one predicted power value in every time step k , the stochastic two-stage rolling horizon optimization problem considers M values $P_{\text{PV},m,k}^{2\text{ST}}$ with $m \in \{1, \dots, M\}$, i. e., the possible generation scenarios, in every time step in the second stage $k \in \{1, \dots, N-1\}$. All other parameters are equal to those in the state-of-the-art one-stage rolling horizon optimization problem (see Table 6.7).

For the stochastic two-stage rolling horizon optimization problem, the same assumptions on the existence of a solution are made as in the case of the state-of-the-art one-stage rolling horizon optimization problem (see Section 5.7).

5.8.1 Objective Function

The introduction of the stochastic two-stage approach changes the objective function. In addition to the objective function defined in the state-of-the-art one-stage rolling horizon optimization problem, the objective function of the stochastic two-stage rolling horizon optimization problem does not only include stage costs that are dependent on the time step $k \in \{0, \dots, N-1\}$ but also those that are dependent on the PV generation scenario $m \in \{1, \dots, M\}$. The costs in time step $k = 0$, i. e., the first stage of the stochastic two-stage rolling horizon optimization, are given by:

$$l^{1\text{ST}}(P_{\text{Ex}}^{1\text{ST}}, P_{\text{Im}}^{1\text{ST}}, G_{\text{CHP}}^{1\text{ST}}, s_{\text{CHP}}^{1\text{ST}}) = \Delta_k \cdot [\pi_{\text{Ex},0} \cdot P_{\text{Ex}}^{1\text{ST}} + \pi_{\text{Im},0} \cdot P_{\text{Im}}^{1\text{ST}} + \pi_{\text{Gas},0} \cdot G_{\text{CHP}}^{1\text{ST}}] + \pi_{\text{CHP,Start}} \cdot s_{\text{CHP}}^{1\text{ST}} \quad (5.88)$$

The costs in every time step of the second stage are given by:

$$l^{2\text{ST}}(P_{\text{Ex},k}^{2\text{ST}}, P_{\text{Im},k}^{2\text{ST}}, G_{\text{CHP},k}^{2\text{ST}}, s_{\text{CHP},k}^{2\text{ST}}, m) = \Delta_k \cdot [\pi_{\text{Ex},k} \cdot P_{\text{Ex},m,k}^{2\text{ST}} + \pi_{\text{Im},m,k} \cdot P_{\text{Im},m,k}^{2\text{ST}} + \pi_{\text{Gas},k} \cdot G_{\text{CHP},m,k}^{2\text{ST}}] + \pi_{\text{CHP,Start}} \cdot s_{\text{CHP},m,k}^{2\text{ST}} \quad (5.89)$$

The objective function for the optimization window of N time steps is given by:

$$\begin{aligned}
 J_N^{1+2ST}(P_{\text{Ex}}^{1ST}, P_{\text{Im}}^{1ST}, G_{\text{CHP}}^{1ST}, s_{\text{CHP}}^{1ST}, \mathbf{P}_{\text{Ex}}^{2ST}, \mathbf{P}_{\text{Im}}^{ST}, \mathbf{G}_{\text{CHP}}^{2ST}, \mathbf{s}_{\text{CHP}}^{2ST}) \\
 = \Delta_k \cdot [\pi_{\text{Ex},0} \cdot P_{\text{Ex}}^{1ST} + \pi_{\text{Im},0} \cdot P_{\text{Im}}^{1ST} + \pi_{\text{Gas},0} \cdot G_{\text{CHP}}^{1ST}] + \pi_{\text{CHP,Start}} \cdot s_{\text{CHP}}^{1ST} \\
 + \frac{1}{M} \sum_{k=1}^{N-1} \sum_{m=1}^M \Delta_k \cdot [\pi_{\text{Ex},k} \cdot P_{\text{Ex},m,k}^{2ST} + \pi_{\text{Im},k} \cdot P_{\text{Im},m,k}^{2ST} \\
 + \pi_{\text{Gas},k} \cdot G_{\text{CHP},m,k}^{2ST}] + \pi_{\text{CHP,Start}} \cdot s_{\text{CHP},m,k}^{2ST} \quad (5.90)
 \end{aligned}$$

When using the stage costs defined in Equations 5.88 and 5.89 the objective function becomes:

$$\begin{aligned}
 J_N^{1+2ST}(P_{\text{Ex}}^{1ST}, P_{\text{Im}}^{1ST}, G_{\text{CHP}}^{1ST}, s_{\text{CHP}}^{1ST}, \mathbf{P}_{\text{Ex}}^{2ST}, \mathbf{P}_{\text{Im}}^{ST}, \mathbf{G}_{\text{CHP}}^{2ST}, \mathbf{s}_{\text{CHP}}^{2ST}) \\
 = l^{1ST}(P_{\text{Ex}}^{1ST}, P_{\text{Im}}^{1ST}, G_{\text{CHP}}^{1ST}, s_{\text{CHP}}^{1ST}) \\
 + \frac{1}{M} \sum_{k=1}^{N-1} \sum_{m=1}^M l^{2ST}(P_{\text{Ex},k}^{2ST}, P_{\text{Im},k}^{2ST}, G_{\text{CHP},k}^{2ST}, s_{\text{CHP},k}^{2ST}, m) \quad (5.91)
 \end{aligned}$$

5.8.2 Constraints

In addition to the number of decision variables, the number of constraints increases as well. In this section all constraints are listed and the corresponding constraints of the state-of-the-art one-stage rolling horizon optimization problem are referenced.

The state equations of the BESS are (cf. Equation 5.65):

$$E_{\text{BESS}}^{1ST} = E_{\text{BESS,Initial}} + \Delta_k \cdot (\eta_{\text{BESS}} \cdot P_{\text{BESS,C}}^{1ST} + \eta_{\text{BESS}}^{-1} P_{\text{BESS,D}}^{1ST}), \quad (5.92)$$

and

$$\begin{aligned}
 E_{\text{BESS},m,k+1}^{2ST} = E_{\text{BESS},m,k}^{2ST} + \Delta_k \cdot (\eta_{\text{BESS}} \cdot P_{\text{BESS,C},m,k}^{2ST} \\
 + \eta_{\text{BESS}}^{-1} P_{\text{BESS,D},m,k}^{2ST}) \quad \forall k \in \{2, \dots, N\}, \forall m \in \{1, \dots, M\}, \quad (5.93a)
 \end{aligned}$$

$$\begin{aligned}
 E_{\text{BESS},m,2}^{2ST} = E_{\text{BESS}}^{1ST} + \Delta_1 \cdot (\eta_{\text{BESS}} \cdot P_{\text{BESS,C},m,1}^{2ST} \\
 + \eta_{\text{BESS}}^{-1} P_{\text{BESS,D},m,1}^{2ST}), \quad \forall m \in \{1, \dots, M\}. \quad (5.93b)
 \end{aligned}$$

The constraints limiting the BESS state variable to its maximum and minimum are (cf. Equation 5.66):

$$\underline{E}_{\text{BESS}} \leq E_{\text{BESS}}^{1ST} \leq \bar{E}_{\text{BESS}} \quad (5.94)$$

and

$$\underline{E}_{\text{BESS}} \leq E_{\text{BESS},m,k}^{2ST} \leq \bar{E}_{\text{BESS}}, \quad \forall k \in \{2, \dots, N\}, \forall m \in \{1, \dots, M\}. \quad (5.95)$$

The control variables of the BESS are constrained by (cf. Equation 5.67):

$$\underline{P}_{\text{BESS,C}} \leq P_{\text{BESS,C}}^{1\text{ST}} \leq \overline{P}_{\text{BESS,C}}, \quad (5.96\text{a})$$

$$\underline{P}_{\text{BESS,D}} \leq P_{\text{BESS,D}}^{1\text{ST}} \leq \overline{P}_{\text{BESS,D}} \quad (5.96\text{b})$$

and

$$\underline{P}_{\text{BESS,C}} \leq P_{\text{BESS,C},m,k}^{2\text{ST}} \leq \overline{P}_{\text{BESS,C}}, \quad \forall k \in \{1, \dots, N-1\}, \forall m \in \{1, \dots, M\}, \quad (5.97\text{a})$$

$$\underline{P}_{\text{BESS,D}} \leq P_{\text{BESS,D},m,k}^{2\text{ST}} \leq \overline{P}_{\text{BESS,D}}, \quad \forall k \in \{1, \dots, N-1\}, \forall m \in \{1, \dots, M\}, \quad (5.97\text{b})$$

using the following shorthand notations (cf. Equation 5.68):

$$P_{\text{BESS,C}}^{1\text{ST}} = u_{\text{BESS,C}}^{1\text{ST}} \cdot \overline{P}_{\text{BESS,C}}, \quad (5.98\text{a})$$

$$P_{\text{BESS,D}}^{1\text{ST}} = u_{\text{BESS,D}}^{1\text{ST}} \cdot \overline{P}_{\text{BESS,D}} \quad (5.98\text{b})$$

and

$$P_{\text{BESS,C},m,k}^{2\text{ST}} = u_{\text{BESS,C},m,k}^{2\text{ST}} \cdot \overline{P}_{\text{BESS,C}}, \quad \forall k \in \{1, \dots, N-1\}, \forall m \in \{1, \dots, M\}, \quad (5.99\text{a})$$

$$P_{\text{BESS,D},m,k}^{2\text{ST}} = u_{\text{BESS,D},m,k}^{2\text{ST}} \cdot \overline{P}_{\text{BESS,D}}, \quad \forall k \in \{1, \dots, N-1\}, \forall m \in \{1, \dots, M\}. \quad (5.99\text{b})$$

The state equations of HWT are given by (cf. Equation 5.69):

$$\vartheta_{\text{HWT}}^{1\text{ST}} = \vartheta_{\text{HWT,Initial}}^{1\text{ST}} + \Delta_k \cdot [\Phi_{\text{CHP}}^{1\text{ST}} - \Phi_{\text{HWT,Loss}}^{1\text{ST}} - \Phi_{\text{HS},0} - \Phi_{\text{DHW},0}] / (V_{\text{HWT}} \cdot \rho_{\text{Water}} \cdot c_{\text{Water}}). \quad (5.100)$$

and

$$\begin{aligned} \vartheta_{\text{HWT},m,k+1}^{2\text{ST}} = & \vartheta_{\text{HWT},m,k}^{2\text{ST}} + \Delta_k \cdot [\Phi_{\text{CHP},m,k}^{2\text{ST}} - \Phi_{\text{HWT,Loss},m,k}^{2\text{ST}} \\ & - \Phi_{\text{HS},k} - \Phi_{\text{DHW},k}] / (V_{\text{HWT}} \cdot \rho_{\text{Water}} \cdot c_{\text{Water}}), \\ & \forall k \in \{2, \dots, N-1\}, \forall m \in \{1, \dots, M\}, \end{aligned} \quad (5.101\text{a})$$

$$\begin{aligned} \vartheta_{\text{HWT},m,2}^{2\text{ST}} = & \vartheta_{\text{HWT}}^{1\text{ST}} + \Delta_k \cdot [\Phi_{\text{CHP},m,1}^{2\text{ST}} - \Phi_{\text{HWT,Loss},m,1}^{2\text{ST}} \\ & - \Phi_{\text{HS},1} - \Phi_{\text{DHW},1}] / (V_{\text{HWT}} \cdot \rho_{\text{Water}} \cdot c_{\text{Water}}), \\ & , \forall m \in \{1, \dots, M\}. \end{aligned} \quad (5.101\text{b})$$

The following shorthand notations are used (cf. Equation 5.70):

$$\Phi_{\text{HWT,Loss}}^{1\text{ST}} = (a_{\text{HWT}} + b_{\text{HWT}} \cdot (c_{\text{HWT}} \cdot V_{\text{HWT}})^{0.4}) \cdot \frac{(\vartheta_{\text{HWT,Initial}} - \vartheta_{\text{HWT,Ambient}})}{d_{\text{HWT}}} \quad (5.102)$$

and

$$\begin{aligned} \Phi_{\text{HWT,Loss},m,k}^{2\text{ST}} = & (a_{\text{HWT}} + b_{\text{HWT}} \cdot (c_{\text{HWT}} \cdot V_{\text{HWT}})^{0.4}) \cdot \frac{(\vartheta_{\text{HWT},m,k}^{2\text{ST}} - \vartheta_{\text{HWT,Ambient}})}{d_{\text{HWT}}}, \\ & \forall k \in \{2, \dots, N-1\}, \forall m \in \{1, \dots, M\}, \end{aligned} \quad (5.103\text{a})$$

$$\Phi_{\text{HWT, Loss}, m, 1}^{2\text{ST}} = (a_{\text{HWT}} + b_{\text{HWT}} \cdot (c_{\text{HWT}} \cdot V_{\text{HWT}})^{0.4}) \cdot \frac{(\vartheta_{\text{HWT}}^{1\text{ST}} - \vartheta_{\text{HWT, Ambient}})}{d_{\text{HWT}}},$$

$$, \quad \forall m \in \{1, \dots, M\}. \quad (5.103b)$$

The control variables of the micro-CHP are constrained by (cf. Equation 5.71):

$$0 \leq \sum_{i=k}^N u_{\text{CHP}, m, k}^{2\text{ST}} - (N - k) \cdot (u_{\text{CHP}, m, k}^{2\text{ST}} - u_{\text{CHP}, m, k-1}^{2\text{ST}}),$$

$$\forall k \in \{N - k_{\text{CHP, Min}} + 1, \dots, N\}, \forall m \in \{1, \dots, M\}. \quad (5.104)$$

If $2 \leq k_{\text{CHP, Initial}}$ the optimization problem contains the following constraints (cf. Equations 5.72 and 5.73):

$$k_{\text{CHP, Min}} \cdot (u_{\text{CHP}, m, k}^{2\text{ST}} - u_{\text{CHP}, m, k-1}^{2\text{ST}}) \leq \sum_{i=k}^{k+k_{\text{CHP, Min}}-1} u_{\text{CHP}, m, i}^{2\text{ST}},$$

$$\forall k \in \{k_{\text{CHP, Initial}}, \dots, N - k_{\text{CHP, Min}}\}, \forall m \in \{1, \dots, M\}, \quad (5.105a)$$

$$k_{\text{CHP, Initial}} - u_{\text{CHP}}^{1\text{ST}} - \sum_{i=1}^{k_{\text{CHP, Initial}}-1} u_{\text{CHP}, m, i}^{2\text{ST}} = 0, \quad \forall m \in \{1, \dots, M\}. \quad (5.105b)$$

If $k_{\text{CHP, Initial}} = 1$ the optimization problem contains the following constraints:

$$k_{\text{CHP, Min}} \cdot (u_{\text{CHP}, m, k}^{2\text{ST}} - u_{\text{CHP}, m, k-1}^{2\text{ST}}) \leq \sum_{i=k}^{k+k_{\text{CHP, Min}}-1} u_{\text{CHP}, m, i}^{2\text{ST}},$$

$$\forall k \in \{k_{\text{CHP, Initial}} + 1, \dots, N - k_{\text{CHP, Min}}\}, \forall m \in \{1, \dots, M\}, \quad (5.106a)$$

$$k_{\text{CHP, Min}} \cdot (u_{\text{CHP}, m, k}^{2\text{ST}} - u_{\text{CHP}}^{1\text{ST}}) \leq \sum_{i=k}^{k+k_{\text{CHP, Min}}-1} u_{\text{CHP}, m, i}^{2\text{ST}},$$

$$\forall k \in \{k_{\text{CHP, Initial}}\}, \forall m \in \{1, \dots, M\}, \quad (5.106b)$$

$$k_{\text{CHP, Initial}} - u_{\text{CHP}}^{1\text{ST}} - \sum_{i=1}^{k_{\text{CHP, Initial}}-1} u_{\text{CHP}, m, i}^{2\text{ST}} = 0, \quad \forall m \in \{1, \dots, M\}. \quad (5.106c)$$

If $k_{\text{CHP, Initial}} = 0$ the optimization problem contains the following constraints (cf. Equation 5.74):

$$k_{\text{CHP, Min}} \cdot (u_{\text{CHP}, m, k}^{2\text{ST}} - u_{\text{CHP}, m, k-1}^{2\text{ST}}) \leq \sum_{i=k}^{k+k_{\text{CHP, Min}}-1} u_{\text{CHP}, m, i}^{2\text{ST}},$$

$$\forall k \in \{2, \dots, N - k_{\text{CHP, Min}}\}, \quad \forall m \in \{1, \dots, M\}, \quad (5.107a)$$

$$k_{\text{CHP,Min}} \cdot (u_{\text{CHP},m,1}^{2\text{ST}} - u_{\text{CHP}}^{1\text{ST}}) \leq \sum_{i=k}^{1+k_{\text{CHP,Min}}-1} u_{\text{CHP},m,i}^{2\text{ST}}, \quad \forall m \in \{1, \dots, M\}, \quad (5.107\text{b})$$

$$k_{\text{CHP,Min}} \cdot (u_{\text{CHP}}^{1\text{ST}} - u_{\text{CHP,Initial}}) \leq u_{\text{CHP}}^{1\text{ST}} + \sum_{i=1}^{k_{\text{CHP,Min}}-1} u_{\text{CHP},m,i}^{2\text{ST}}, \quad \forall m \in \{1, \dots, M\}. \quad (5.107\text{c})$$

To ease the handling of the control variables of the micro-CHP, the following shorthand notations are introduced (cf. Equation 5.75):

$$P_{\text{CHP}}^{1\text{ST}} = u_{\text{CHP}}^{1\text{ST}} \cdot P_{\text{CHP,Nom}}, \quad (5.108\text{a})$$

$$\Phi_{\text{CHP}}^{1\text{ST}} = u_{\text{CHP}}^{1\text{ST}} \cdot \Phi_{\text{CHP,Nom}}, \quad (5.108\text{b})$$

$$G_{\text{CHP}}^{1\text{ST}} = u_{\text{CHP}}^{1\text{ST}} \cdot G_{\text{CHP,Nom}}. \quad (5.108\text{c})$$

and

$$P_{\text{CHP},m,k}^{2\text{ST}} = u_{\text{CHP},m,k}^{2\text{ST}} \cdot P_{\text{CHP,Nom}}, \quad \forall k \in \{1, \dots, N-1\}, \forall m \in \{1, \dots, M\}, \quad (5.109\text{a})$$

$$\Phi_{\text{CHP},m,k}^{2\text{ST}} = u_{\text{CHP},m,k}^{2\text{ST}} \cdot \Phi_{\text{CHP,Nom}}, \quad \forall k \in \{1, \dots, N-1\}, \forall m \in \{1, \dots, M\}, \quad (5.109\text{b})$$

$$G_{\text{CHP},m,k}^{2\text{ST}} = u_{\text{CHP},m,k}^{2\text{ST}} \cdot G_{\text{CHP,Nom}}, \quad \forall k \in \{1, \dots, N-1\}, \forall m \in \{1, \dots, M\}. \quad (5.109\text{c})$$

The auxiliary variables which consider the number of starts of the micro-CHP are constrained by (cf. Equation 5.76):

$$(u_{\text{CHP},m,k}^{2\text{ST}} - u_{\text{CHP},m,k-1}^{2\text{ST}}) \leq s_{\text{CHP},m,k}^{2\text{ST}}, \quad \forall k \in \{2, \dots, N-1\}, \forall m \in \{1, \dots, M\}, \quad (5.110\text{a})$$

$$(u_{\text{CHP},m,1}^{2\text{ST}} - u_{\text{CHP}}^{1\text{ST}}) \leq s_{\text{CHP},m,1}^{2\text{ST}}, \quad \forall m \in \{1, \dots, M\}, \quad (5.110\text{b})$$

$$(u_{\text{CHP}}^{1\text{ST}} - u_{\text{CHP,Initial}}) \leq s_{\text{CHP}}^{1\text{ST}}. \quad (5.110\text{c})$$

The control variables of the appliances are constrained by (cf. Equations 5.77 and 5.78):

$$u_{\text{Appliances},j}^{1\text{ST}} + \sum_{i=1}^{N-1} u_{\text{Appliances},j,m,i}^{2\text{ST}} = b_{\text{Appliances},j}, \quad \forall j \in \{1, \dots, J\}, \forall m \in \{1, \dots, M\} \quad (5.111)$$

and

$$\bar{k}_{\text{Appliances},j} \leq \sum_{i=1}^{N-1} u_{\text{Appliances},j,m,i}^{2\text{ST}} \cdot i \leq \bar{k}_{\text{Appliances},j}, \quad \forall j \in \{1, \dots, J\}, \forall m \in \{1, \dots, M\}. \quad (5.112)$$

To ease the handling of the control variables of the appliances, the following shorthand notations are introduced (cf. Equation 5.79):

$$P_{\text{Appliances},j}^{1\text{ST}} = u_{\text{Appliances},j,i}^{1\text{ST}} \cdot P_{\text{Appliances,Nom},j,1}, \quad \forall j \in \{1, \dots, J\}. \quad (5.113\text{a})$$

$$P_{\text{Appliances},j,m,k}^{2\text{ST}} = \sum_{i=k-l_{\text{Appliances},j}}^k u_{\text{Appliances},j,m,i}^{2\text{ST}} \cdot P_{\text{Appliances},\text{Nom},j,k-i+1},$$

$$\forall k \in \{l_{\text{Appliances},j}, \dots, N-1\}, \forall j \in \{1, \dots, J\}, \forall m \in \{1, \dots, M\}, \quad (5.113b)$$

$$P_{\text{Appliances},j,m,k}^{2\text{ST}} = \sum_{i=0}^k u_{\text{Appliances},j,m,i}^{2\text{ST}} \cdot P_{\text{Appliances},\text{Nom},j,k-i+1}^{2\text{ST}},$$

$$\forall k \in \{1, \dots, l_{\text{Appliances},j} - 1\}, \forall j \in \{1, \dots, J\}, \forall m \in \{1, \dots, M\}. \quad (5.113c)$$

The balance of the power flows is ensured by (cf. Equation 5.80):

$$\sum_{j=1}^J P_{\text{Appliances},j}^{1\text{ST}} + P_{\text{Base},0} + P_{\text{BESS},\text{C}}^{1\text{ST}} + P_{\text{Ex}}^{1\text{ST}} = P_{\text{Im}}^{1\text{ST}} + P_{\text{PV}}^{1\text{ST}} + P_{\text{CHP}}^{1\text{ST}} + P_{\text{BESS},\text{D}}^{1\text{ST}}, \quad (5.114a)$$

$$\sum_{j=1}^J P_{\text{Appliances},j,m,k}^{2\text{ST}} + P_{\text{Base},k} + P_{\text{BESS},\text{C},m,k}^{2\text{ST}} + P_{\text{Ex},m,k}^{2\text{ST}} = P_{\text{Im},m,k}^{2\text{ST}} + P_{\text{PV},m,k}^{2\text{ST}}$$

$$+ P_{\text{CHP},m,k}^{2\text{ST}} + P_{\text{BESS},\text{D},m,k}^{2\text{ST}}, \quad \forall k \in \{1, \dots, N-1\}, \forall m \in \{1, \dots, M\}. \quad (5.114b)$$

The relationships between the auxiliary variables and the control variables are given by (cf. Equations 5.81 and 5.82):

$$0 \leq P_{\text{Ex}}^{1\text{ST}} \leq P_{\text{PV}}^{1\text{ST}} + P_{\text{CHP}}^{1\text{ST}}, \quad (5.115a)$$

$$0 \leq P_{\text{Ex},m,k}^{2\text{ST}} \leq P_{\text{PV},m,k}^{2\text{ST}} + P_{\text{CHP},m,k}^{2\text{ST}},$$

$$\forall k \in \{1, \dots, N-1\}, \forall m \in \{1, \dots, M\} \quad (5.115b)$$

and

$$0 \leq P_{\text{Im}}^{1\text{ST}} \leq \sum_{j=1}^J P_{\text{Appliances},j}^{1\text{ST}} + P_{\text{Base},0}, \quad (5.116a)$$

$$0 \leq P_{\text{Im},m,k}^{2\text{ST}} \leq \sum_{j=1}^J P_{\text{Appliances},j,m,k}^{2\text{ST}} + P_{\text{Base},k}, \quad \forall k \in \{1, \dots, N-1\}, \forall m \in \{1, \dots, M\}.$$

$$(5.116b)$$

5.8.3 Summary of the Optimization Problem

The optimization problem that has to be solved in every optimization in the rolling horizon optimization approach is:

$$\begin{aligned}
 & \text{minimize} && J_N^{1+2ST}(P_{\text{Ex}}^{1ST}, P_{\text{Im}}^{1ST}, G_{\text{CHP}}^{1ST}, s_{\text{CHP}}^{1ST}, P_{\text{Ex}}^{2ST}, P_{\text{Im}}^{ST}, G_{\text{CHP}}^{2ST}, s_{\text{CHP}}^{2ST}) \\
 & u_{\text{CHP}}^{1ST} \in \{0,1\} \\
 & u_{\text{CHP}}^{2ST} \in \{0,1\}^{N-1 \times M} \\
 & u_{\text{Appliances}}^{1ST} \in \{0,1\} \\
 & u_{\text{Appliances}}^{2ST} \in \{0,1\}^{N-1 \times M \times J} \\
 & u_{\text{BESS,C}}^{1ST} \in [0,1] \\
 & u_{\text{BESS,C}}^{2ST} \in [0,1]^{N-1 \times M} \\
 & u_{\text{BESS,D}}^{1ST} \in [0,1] \\
 & u_{\text{BESS,D}}^{2ST} \in [0,1]^{N-1 \times M} \\
 & P_{\text{Im}}^{1ST} \in \mathbb{R} \\
 & P_{\text{Im}}^{2ST} \in \mathbb{R}^{N-1 \times M} \\
 & P_{\text{Ex}}^{1ST} \in \mathbb{R} \\
 & P_{\text{Ex}}^{2ST} \in \mathbb{R}^{N-1 \times M} \\
 & s_{\text{CHP}}^{1ST} \in \mathbb{R} \\
 & s_{\text{CHP}}^{2ST} \in \mathbb{R}^{N-1 \times M} \\
 & \text{subject to} && (5.92) - (5.116)
 \end{aligned} \tag{5.117}$$

Here it is important to note that the parameters N , M and Δ_k are tuning parameters that have to be chosen by the designer of the planning and optimization system. The choice of the parameters in the evaluation scenario is motivated in Section 6.6.2.

5.9 Implementation

The simulation of the building energy system has been implemented using MATLAB 2018a. It is implemented as described in Algorithm 5.1. The optimization problem has been formulated using the YALMIP framework [147] in version R20181012. The YALMIP framework allows for a formulation of the optimization problem in a language close to a mathematical formulation as shown in Sections 5.7 and 5.8. The exact formulation of the problem using the YALMIP framework is displayed in Appendix A. The YALMIP framework also provides an interface to various solvers. In this thesis, the solver CPLEX 12.8.0 has been used in the evaluation of the approach.

In the *solveOptimizationProblem*(\cdot) function, the CPLEX solver is interfaced from MATLAB via the YALMIP framework. In this process, the formulation in the YALMIP language has to be converted to a numerical format used by CPLEX. This conversion takes time. In the case of the optimization problems that have to be solved in this thesis, the time is in the magnitude of minutes. To reduce the number of conversions, the YALMIP framework allows to compile the numerical models once and save it in order to reuse it in every optimization run.

After that, only the parameters of the optimization have to be inserted into the optimization model for every optimization run. However, this is only possible when the structure of

the optimization problem does not change over time. The structure of Equations 5.23 and 5.24 is dependent on $k_{\text{CHP,Initial}}$, which changes over time. Hence, several optimization problems have to be solved and thus several numerical models have to be compiled and used in the particular time steps. More precisely $k_{\text{CHP,Min}}$ numerical models have to be compiled. In general, other frameworks, programming languages or solvers can be used in the implementation.

This thesis does not focus on the development of a BEMS that can be deployed to the market. When doing so, the device abstraction as well as further data interfaces have to be added. This is described in Section 2.14 and presented in Figure 2.8. An example for such an interface is a Graphical User Interface (GUI) that allows the inhabitants to input user preferences and provides visualization.

5.10 Adaptivity of the Approach

The optimization problem defined in Sections 5.7 and 5.8 represents a specific device composition. However, devices that only differ in the choice of the parameters, e. g., BESSs with different capacities, can be included by adapting the parameters of the model. The inclusion of new devices, i. e., devices that have to be modeled differently from the ones described in Section 5.6, for example heat pumps, in the stochastic rolling horizon approach is possible in general. This leads to the inclusion of new constraints. In some cases, the device interactions have to be adapted additionally. In the sum of power flows (see Equation 5.52), new terms have to be added. There, it has to be respected whether the new device generates or consumes power. If necessary, the power import and export constraints have to be adapted in order to consider the new devices (see Equations 5.57 and 5.55). In addition, the objective function (see Equation 5.90) has to be adapted by the addition of new terms if necessary. In the case of heat generating or consuming devices, the heat flows have to be adapted. This can be done by adapting the HWT state equation (see Equation 5.43) or by adding a new constraint that considers the sum of heat flows similarly to the sum of power flows presented in Equation 5.52. When a new type of energy carrier, e. g., cold water, or other parameters, for example user comfort, should additionally be respected in the optimization, new flow constraints (see Equation 5.52) have to be added.

In general, this process can be automated in a BEMS as it is described in [165] and [163]. However, this is not further discussed and analyzed in this thesis.

Even though an extension of the stochastic rolling horizon approach to the optimization of the operation of building energy systems presented in this thesis is in general possible, it is important to note that depending on the new devices, the performance of the optimization approach can deviate from the one presented in this thesis (see Chapter 6). It is not possible to make a statement on the performance of the stochastic rolling horizon approach to the optimization of the operation of building energy systems presented in this thesis when new devices are added. Thus, when adding new devices, the performance of the approach has to be assessed newly and the tuning parameters of the approach have to be adapted when necessary.

6. Evaluation

In this chapter, the performance of the presented stochastic two-stage rolling horizon optimization approach is evaluated by means of simulation-based case studies. Therein, a smart building equipped with a BEMS is simulated, which uses the stochastic two-stage rolling horizon optimization approach. The simulation is performed over a defined simulation period and the resulting operating costs are calculated. To assess the performance of the stochastic two-stage rolling horizon approach, smart buildings that use other control schemes are simulated as well and the resulting costs are compared to each other.

The chapter starts with a detailed description of the evaluation scenarios. Then simulation results are presented that motivate the choice of the parameters of the stochastic two-stage rolling horizon optimization approach. Based on this, simulation results related to the performance of the stochastic rolling horizon optimization approach and the benchmark approaches are presented. The chapter ends with a discussion of the obtained results.

6.1 Smart Building Configuration

The investigated smart building configuration is presented in Section 5.2.1, Figure 5.1 presents a visualization. It comprises a smart building equipped with a BEMS that controls a micro-CHP, a BESS and a deferrable washing machine. In addition, a PV system and an HWT are present. Electricity consumption unrelated to the deferrable washing machine is combined into a base load. The heat consumption is separated into a DHW consumption and a heating system consumption. An overview of the smart building configuration which is used in all evaluation scenarios is presented in Figure 5.1 and Table 6.1. The individual devices are modeled according to the descriptions given in Section 5.6.

6.2 Smart Building Simulation

The evaluation process is based on the simulation of a building energy system. A detailed description of the simulation is presented in Section 5.4 and Algorithm 5.1. For the

Table 6.1: Overview of the evaluation scenario.

Annual electricity consumption	4700 kWh
Annual HS consumption	8000 kWh
Annual DHW consumption	2800 kWh
PV system	Maximum generation: 3.7 kW Yearly generation: 4000 kWh
Simulated appliances	Non-controlled: tumble dryer, dishwasher, induction hob, oven Controlled: washing machine
BESS	Capacity: 7 kWh Max. charge power: 7 kW Efficiency: 0.92
Micro-CHP	Nominal electricity generation: 5.5 kW Nominal heat generation: 12.5 kW Nominal gas consumption: 20.5 kW
Hot water tank	Volume of the HWT: 0.75 m ³ Max. temperature: 80 °C Min. temperature: 60 °C Standing loss: see Eq. 5.46
Electricity tariff	Time-dependent: see Figure 5.13
Feed-in tariff	Time-dependent: see Figure 5.13
Gas tariff	8 cent/kWh

Table 6.2: Parameters of the building energy system simulation. The given values are used in all evaluation scenarios.

Parameter	Symbol	Value	Unit
Simulation period	Δ_T	7	d
Time step duration	Δ_t	1	s
BESS initial state	$\tilde{E}_{\text{BESS,Initial}}$	0	kWh
HWT initial state	$\tilde{\vartheta}_{\text{HWT,Initial}}$	60	°C

Table 6.3: Overview of the load profile resolutions used in the building energy system simulation in the evaluation scenarios.

Load profile	Profile resolution in s
Appliances	1
DHW consumption	1
HS consumption	1
PV system	60
Base load	900

evaluation process, the duration of the simulation Δ_T and the time step duration Δ_t in the simulation have to be defined. A longer simulation period is beneficial to reduce the influence of uncertainty in the PV generation forecasts based on an increased sample size, where sample size refers to the number of days. However, to keep the simulation time¹, i. e., the processing time needed to perform the individual simulations, manageable and enable the investigation of multiple scenarios, the simulation period is limited to $\Delta_T = 7$ d. This is the same simulation period as in [223]. A time step duration of $\Delta_t = 1$ s is chosen, to represent the lowest resolution that is present in the used load profiles (see Table 6.3). The initial state values of the energy storage systems, i. e., the BESS and the HWT, are chosen to correspond to the minimal energy storage charge as defined in Sections 5.6.1 and 5.6.8. This means the initial state of the BESS is $\tilde{E}_{\text{BESS,Initial}} = \underline{E}_{\text{BESS}} = 0$ kWh and the initial state of the HWT is $\tilde{\vartheta}_{\text{HWT,Initial}} = \underline{\vartheta}_{\text{HWT}} = 60$ °C.

A list of the simulation parameters and the corresponding values is given in Table 6.2. A list of the load profile resolutions used in the simulation of the building energy system is presented in Table 6.3. The load profile resolutions resemble the available load profiles as defined in Section 5.6.

During the simulation of the building energy system, the rolling horizon optimization is performed repetitively (see Sections 5.4 and 5.5). The parameters of the optimization model correspond to the values given in Section 5.6. A list of the model parameters is

¹A time step duration of 3 min leads to 3360 optimization runs. When each optimization takes 1 min this results in a simulation time of 2.3 days.

presented in Table 6.7.

6.3 Overview of the Evaluation Scenarios

To evaluate the stochastic two-stage rolling horizon optimization approach presented in Section 5.8, several simulations are carried out. Each simulation is performed in a different scenario. The scenarios differ in:

- the feed-in tariff (see Table 6.4, Figure 5.13 and Section 5.6.9) and
- the month of the year (see Table 6.5).

The resulting total number of scenarios is:

$$3 \text{ feed-in tariffs} \times 3 \text{ seasons} = 9 \text{ scenarios.}$$

As defined in Section 5.3, the goal of the optimized operation of building energy systems investigated in this thesis is the minimization of operating costs. Consequently, the performance of the approaches is dependent on the tariff structure present in the evaluation scenario. However, future tariff structures in future energy systems are not known today. As a consequence, specific feed-in tariffs have to be predefined in order to evaluate the performance of the control schemes for different tariff structures. Thus, the range of all possible future feed-in tariffs is approximated by defining three different feed-in tariffs: the Constant Feed-in Tariff (FT-1), the Time-dependent Feed-in Tariff 1 (FT-2) and the Time-dependent Feed-in Tariff 2 (FT-3). FT-1 resembles the current state of the art. It has no time dependence. FT-2 resembles a possible time-dependent future tariff structure that is inspired by the literature (cf. [143]). FT-3 is a time-dependent feed-in tariff with a large spread. In the evaluation, it serves as a test case of an extreme feed-in tariff. A list of the electricity and feed-in tariffs is presented in Table 6.4, a visualization is presented in Figure 5.13. A detailed description is presented in Section 5.6.9.

To evaluate the effects of seasonal changes, three different simulations are carried out, each starting in a different month of the year, i. e., January, March and July (Table 6.5).

To assess the performance of the stochastic two-stage optimization approach compared to other approaches, it is compared to four other control schemes. These four control schemes are: a reference control scheme, a state-of-the-art control scheme, a rule-based micro-CHP control scheme and a rule-based control scheme.

The reference control scheme, the state-of-the-art control scheme and the stochastic control scheme use the rolling horizon optimization as defined in Section 5.5. However, the reference control scheme uses a perfect forecast of the electricity generation of the PV system, whereas the state-of-the-art control scheme uses a single point forecast. The presented approach uses a scenario-based probabilistic forecast. It is referred to as the stochastic control scheme in the following. The rule-based micro-CHP control scheme uses a rule-based control of

Table 6.4: Overview of the electricity tariffs that are used in the evaluations. A detailed description is presented in Section 5.6.9.

Abbreviation	Description	Spread in cent/kWh
ET	TOU electricity consumption tariff. The tariff resembles a possible future tariff structure [143].	12.65
FT-1	Feed-in tariff without time dependence. The tariff resembles the current state of the art.	0
FT-2	Time-dependent feed-in tariff. The tariff resembles a possible future tariff structure.	12.65
FT-3	Time-dependent feed-in tariff with large spread. The tariff resembles a test scenario that encourages load and generation shifting.	24.97

Table 6.5: Overview of the starting times of the simulations.

Season	Month of the year
Summer	July
Transitional season, spring	March
Winter	January

the micro-CHP in combination with an optimization-based control of the BESS and the washing machine. The rule-based control scheme uses a rule-based control for every device. These different control schemes allow for an estimation of a possible performance gain of the approach presented in this thesis over other approaches presented in the literature in the evaluation scenarios. In addition, the performance can be estimated in comparison to a system with an artificial perfect forecast, which cannot be realized in a real building. However, the perfect forecast scenario is expected to provide a high performance and thus serves as a reference. The results of the simulations using the reference control scheme are used as a benchmark in the evaluation of the investigated control schemes (see Table 6.6). They are also used to choose the tuning parameters of the optimization approach in the state-of-the-art, the stochastic and the rule-based micro-CHP control schemes.

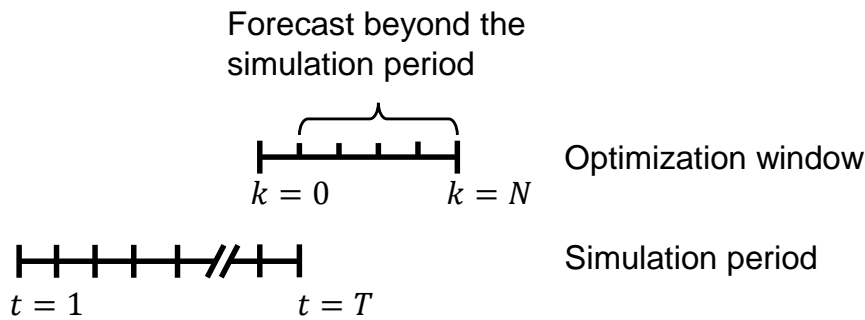
The five control schemes are investigated in each scenario. This leads to:

$$3 \text{ feed-in tariffs} \times 5 \text{ control schemes} \times 3 \text{ seasons} = 45 \text{ simulations.}$$

This number does not include the variations in the tuning parameters of the optimization approach.

Table 6.6: Overview of the different device control schemes in the evaluation. The control schemes of the devices are either Rule-based Control (RBC) or Optimization-based Control (OBC)

Scenarios	Device control			PV generation forecast
	BESS	Micro-CHP	Appliances	
Reference control scheme	OBC	OBC	OBC	perfect
State-of-the-art control scheme	OBC	OBC	OBC	single point
Stochastic control scheme	OBC	OBC	OBC	probabilistic
Rule-based micro-CHP control scheme	OBC	RBC	OBC	probabilistic
Rule-based control scheme	RBC	RBC	RBC	–

**Figure 6.1:** Visualization of an optimization window that exceeds the simulation period.

6.4 Simulation Process

All simulations are performed by using the BwUniCluster, a high performance computing resource provided by the state of Baden-Württemberg. The simulations use 4 cores of an Intel Xeon E5-2670 with 2.60 GHz and 24 GB of RAM.

In case of the optimization-based control of the devices, a rolling horizon optimization is repeatedly carried out. Each rolling horizon optimization uses a specific optimization window Δ_N . The optimization uses the parameters and the values presented in Tables 6.7 and 6.8. The parameters for which the values are indicated by the word “varies” vary for different optimization runs. Examples are the initial state of the micro-CHP and the on-off parameter of the washing machine.

Each rolling horizon optimization run determines the optimal device control inputs with respect to the forecasts. The rolling horizon optimization runs are performed repeatedly during the simulation of the building energy system. Since the simulation period is finite, this leads to the situation that the forecast and optimization horizon exceeds the simulation period. A visualization of this case is presented in Figure 6.1.

This case does not occur in a real building. It only occurs in the artificial evaluation scenario

Table 6.7: Parameters of the state-of-the-art and stochastic two-stage rolling horizon optimization approach. The given values for the smart building configuration apply to all evaluation scenarios.

Parameter	Symbol	Value	Unit
Micro-CHP model parameters			
Nominal electricity generation	$P_{\text{CHP,Nom}}$	5500	W
Nominal heat generation	$\Phi_{\text{CHP,Nom}}$	12500	W
Nominal gas consumption	$G_{\text{CHP,Nom}}$	20500	W
Minimum run-time after start	$k_{\text{CHP,Min}}$	15 min/ Δ_k	–
Initial state of the micro-CHP	$u_{\text{CHP,Initial}}$	varies	–
Initial forced run-time based on earlier starts	$k_{\text{CHP,Initial}}$	varies	–
Costs per start	π_{CHP}	1	cent
BESS model parameters			
Efficiency	η_{BESS}	0.92	–
Maximum amount of energy stored in the BESS	\bar{E}_{BESS}	7000	Wh
Minimum amount of energy stored in the BESS	$\underline{E}_{\text{BESS}}$	0	Wh
Energy stored in the BESS initially	$E_{\text{BESS,Initial}}$	varies	Wh
Maximum charge power	$\bar{P}_{\text{BESS,C}}$	7000	W
Minimum charge power	$\underline{P}_{\text{BESS,C}}$	0	W
Maximum discharge power	$\bar{P}_{\text{BESS,D}}$	7000	W
Minimum discharge power	$\underline{P}_{\text{BESS,D}}$	0	W
Appliances model parameters			
Number of appliances	J	1	–
On-off parameter of appliance j	$b_{\text{Appliances},j}$	varies	–
Earliest possible start time of appliance j	$\underline{k}_{\text{Appliances},j}$	varies	–
Latest possible start time of appliance j	$\bar{k}_{\text{Appliances},j}$	varies	–
Duration of the operation of appliance j	$l_{\text{Appliances}}(j)$	varies	–
Nominal electricity consumption of appliance j	$P_{\text{Appliances,Nom},j}$	Figure 5.7	W
PV system model parameters			
PV generation in time step k	$P_{\text{PV}}(k)$	varies	W

Table 6.8: Continuation of Table 6.7.

Parameter	Symbol	Value	Unit
HWT model parameters			
Maximum temperature	$\bar{\vartheta}_{\text{HWT}}$	80	$^{\circ}\text{C}$
Minimum temperature	ϑ_{HWT}	60	$^{\circ}\text{C}$
Volume of the HWT	V_{HWT}	0.75	m^3
Volumetric mass density of water	ρ_{Water}	1000	kg m^{-3}
Specific heat capacity of water	c_{Water}	4182	$\text{W s kg}^{-1} \text{K}^{-1}$
Ambient temperature of the HWT	$\vartheta_{\text{HWT,Ambient}}$	20	$^{\circ}\text{C}$
Heat loss factor 1	a_{HWT}	12	W
Heat loss factor 2	b_{HWT}	5.93	W
Heat loss factor 3	c_{HWT}	1000	m^{-3}
Heat loss factor 4	d_{HWT}	40	K
Tariff model parameters			
Electricity import tariff in time step k	$\pi_{\text{Im}}(k)$	varies	$\text{cent W}^{-1} \text{s}^{-1}$
Electricity export tariff in time step k	$\pi_{\text{Ex}}(k)$	varies	$\text{cent W}^{-1} \text{s}^{-1}$
Gas import tariff in time step k	$\pi_{\text{Gas}}(k)$	varies	$\text{cent W}^{-1} \text{s}^{-1}$

that is needed in the scientific evaluation. However, the case in which the forecast and optimization horizon surpasses the simulation horizon has to be addressed in the evaluation. In this thesis, each forecast value that targets a point in time after the simulation horizon is defined to be equal to zero. This applies to the forecast of the electricity tariff, the feed-in tariff, the gas tariff, the PV generation, the heat consumption and the electricity consumption. In so doing, a low amount of energy stored in the ESS, i. e., the BESS and the HWT, at the end of the simulation period is expected as a result of the optimization. This allows for an easier comparison of the simulation runs as the value of the stored energy is not straight forward to be estimated in the presence of time-dependent tariffs. Nevertheless, the energy stored in the ESS at the end of the simulation can be non-zero. This has two reasons. Firstly, the rule-based control approaches are not influenced by the forecasts. They solely use instantaneous values and do not consider any knowledge of the future. Secondly, the non-perfect forecast introduces uncertainty into the system that leads to a non-optimal operation of the building energy system. This can lead to non-zero final states of the energy storage systems. Finally, the averaging effects caused by different time step durations in the optimization (see Section 4.2.2), the forecasts and the simulation can introduce a non optimal behavior that can lead to a non-zero final states of the ESSs. Thus, the operating costs calculated in the simulations have to be corrected in order to account for the energy stored in the BESS and the HWT at the end of the simulation. The correction is done as defined in Section 5.3 and Equation 5.3.

As described in Section 5.7, in each optimization run a different optimization problem has

to be solved. Thus, it is hard to estimate the run-time of the optimization process, i. e., the time that is needed to find the optimal control inputs. In order to limit the simulation times, the CPLEX solver is used with a time limit of 1 min. The time limit is chosen in a way that the majority of the optimization problems in the state-of-the-art control scheme are solved within the time limit (see Section 6.6.3). In doing so, the results that are obtained for the state-of-the-art control scheme can be used as a benchmark for the stochastic control scheme.

Choosing a time limit smaller than the time between two optimization runs also enables a possible application in a real building. In addition, the time limit is introduced to limit the time that is needed to carry out a simulation to enable the investigation of several scenarios. The following sections that describe the evaluation of the approaches to the operation of the building energy system provide a more detailed description of the duration of the optimization processes. All other parameters of the CPLEX solver are left in their standard configuration.

6.5 Parameter Tuning

The stochastic two-stage rolling horizon optimization approach uses two tuning parameters that are free to choose. They have to be chosen by the designer of the system. As described in Section 3.5, one approach to estimate suitable values is to choose an optimization window Δ_N that is large enough that a further increment has no significant effect on the performance of the rolling horizon approach. This holds for the resolution of the optimization window, i. e., the reciprocal time step duration $1/\Delta_k$. However, the choice of the optimization window and the time step duration is limited by the resulting optimization times. Longer optimization windows and shorter time step duration lead to more time steps in the optimization window and thus to more decision variables. This is expected to increase the optimization time.

To find suitable values for the optimization window and the time step duration, a hyperparameter optimization is carried out by applying a grid search. Here, the grid points are chosen to approximately cover the domain of sensible choices in the domain of the optimization of the operation of building energy systems (see Section 4.3). The investigated tuning parameters are chosen as follows:

$$N \in \left\{ \frac{18 \text{ h}}{\Delta_k}, \frac{24 \text{ h}}{\Delta_k}, \frac{30 \text{ h}}{\Delta_k}, \frac{36 \text{ h}}{\Delta_k}, \frac{42 \text{ h}}{\Delta_k}, \frac{48 \text{ h}}{\Delta_k} \right\},$$

$$\Delta_k \in \{3 \text{ min}, 5 \text{ min}, 15 \text{ min}\}.$$

The parameter tuning is performed by performing a simulation in the reference control scheme for every parameter combination of N and Δ_k . Then the resulting total costs as well as the optimization times are compared.

6.6 Evaluation Results

In the following sections, the results of the simulations described in Section 6.3 are presented. The results are listed and interesting observations are briefly discussed. In Section 6.7, the results are discussed in detail and conclusions on the stochastic two-stage rolling horizon approach presented in this thesis are made. In this section the results in the summer scenario with FT-2 are presented in detail, whereas the tables and figures for the other scenarios can be found in Appendix B and are referenced in the corresponding sections. The results of the other scenarios are described and differences between the scenarios are analyzed.

6.6.1 Reference Control Scheme

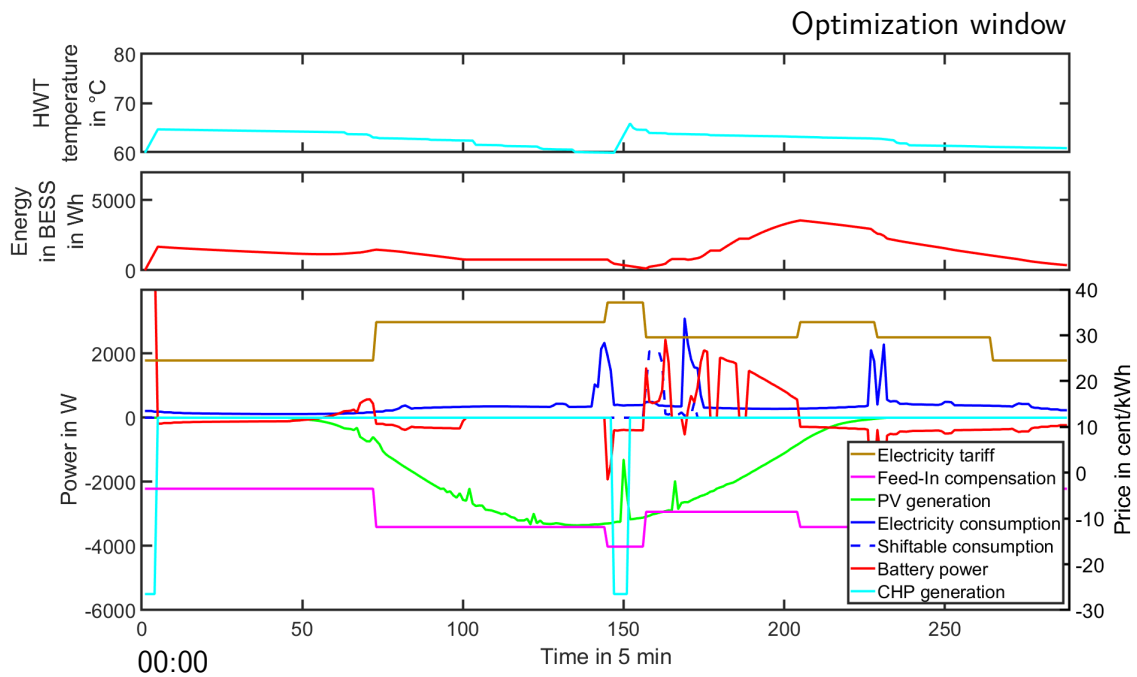
The reference control scheme uses a perfect PV generation forecast. This forecast is used in a rolling horizon optimization to determine the perfect control inputs for the devices. Figure 6.2 shows the results of two exemplary optimization runs, one started at 00:00 and one started at 12:00. More precisely, the graphs display the predicted behavior of the building energy system with the control inputs determined by the optimization. Here, negative power values indicate an electricity generation while positive power values indicate an electricity consumption. This convention applies to all figures in this chapter.

Figure 6.2 shows that the BESS is planned to be charged using electricity generated by the PV system in a time period with a relatively low feed-in compensation. Moreover, the charging and discharging of the BESS are scheduled so that the energy stored in the BESS in the final time step in the optimization window is $E_{\text{BESS},N} = 0$. This behavior is a result of not considering terminal costs in the optimization (see Section 5.7.1). The micro-CHP is scheduled to start in the time period with the maximum feed-in compensation. Furthermore, the micro-CHP is scheduled to achieve a water temperature of the HWT of $\vartheta_{\text{HWT},N} = \vartheta_{\text{HWT}} = 60^\circ\text{C}$ in the final time step in the optimization window.

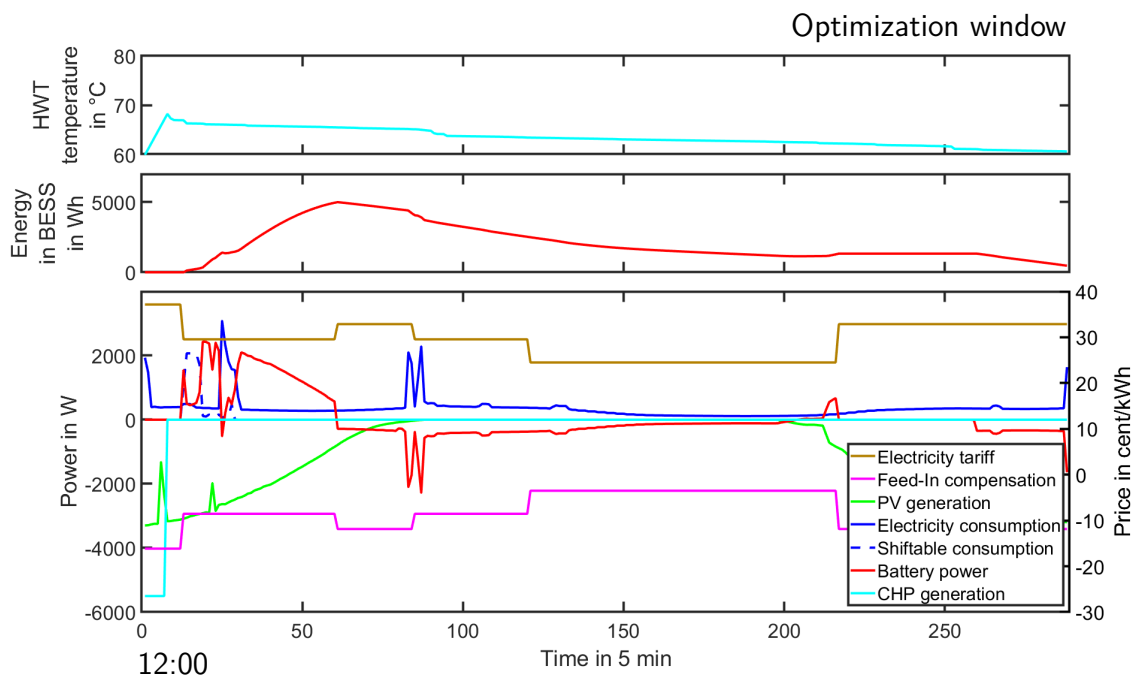
Total Costs

The results of the summer scenario with FT-2 are listed in Table 6.9. The table lists the electricity costs and the gas costs in the simulation period, the final states of the BESS and the HWT and the total costs in the simulation period. The total costs are defined in Section 5.3 and Equation 5.3. The results of the simulations of all other scenarios are listed in Tables B.1 to B.9.

The corresponding visualizations of the total costs in dependence of the optimization window and time step duration are shown in Figures 6.3, 6.4 and 6.5. The figures show the trend that the total costs decrease with increasing optimization window Δ_N . In addition, the total costs decrease with decreasing time step duration. The total costs for $\Delta_k = 3$ min and $\Delta_k = 5$ min are similar. These observations are made in all scenarios, i. e., for all feed-in tariffs and all starting times of the simulations. However, single simulations deviate from these observations. For example in the summer scenario with FT-2, the total costs for



(a) Started at 00:00.



(b) Started at 12:00.

Figure 6.2: Visualization of the electrical loads and ESS states in the building energy system using the reference control scheme. Exemplary results of two optimization runs. The upper graph (a) shows the result of an optimization run started 00:00 and the lower graph (b) shows the result of an optimization run started 12:00.

Table 6.9: Simulation results of the reference control scheme in the summer scenario with FT-2.

Δ_k in min	Δ_N in h	Electricity cost in cent	Gas cost in cent	$\tilde{E}_{\text{BESS},T+1}$ in Ws	$\tilde{\vartheta}_{\text{HWT},T+1}$ in °C	Total costs in cent
3	18	-1408	902	317	63	-643
3	24	-1425	943	315	66	-739
3	30	-1435	910	334	63	-668
3	36	-1428	927	988	65	-711
3	42	-1438	935	312	66	-739
3	48	-1439	968	1058	68	-820
5	18	-1370	888	359	62	-564
5	24	-1408	916	577	64	-659
5	30	-1401	929	1031	65	-689
5	36	-1420	929	345	65	-707
5	42	-1410	943	1154	66	-729
5	48	-1435	943	353	67	-762
15	18	-1338	902	437	63	-552
15	24	-1357	943	437	66	-668
15	30	-1366	943	440	66	-669
15	36	-1385	943	436	66	-686
15	42	-1378	943	436	66	-688
15	48	-1383	943	293	66	-690

$\Delta_k = 3$ min and an optimization window of 24 h is lower than the total costs for $\Delta_k = 3$ min and an optimization window of 30 h (see Figure 6.4c). This is caused by the 24-hour periodicity of the energy consumption and generation caused by the day-night cycle.

When looking at the total costs in each scenario, it can be observed that the total costs in the simulation period are dependent on the design parameters Δ_k , the time step duration, and N , the number of time steps in the optimization window. The dependence on the optimization window Δ_N can be explained by the use of additional information about the future behavior of the building energy system leading to different device schedules. The dependence on the time step duration Δ_k can be explained by averaging effects.

The simulation results show non-zero final states of the BESS $\tilde{E}_{\text{BESS},T+1}$ (see Tables B.1 to B.9), even though $\tilde{E}_{\text{BESS},T+1} = 0$ is expected. In the simulations that use a perfect forecast of the PV generation, $\tilde{E}_{\text{BESS},T+1}$ is expected to be zero. This results from not valuing the energy stored in the ESSs at the end of the optimization window. This mismatch is caused by time averaging effects. They lead to a behavior in the simulation that is different to the one in the optimization. Another effect occurs in the scenarios with FT-3. These scenarios have time steps with a feed-in compensation equal to zero. Thus, the feed-in of electricity generated in this time interval, for example by the PV system, is not economical. Consequently, the BESS is charged and the amount of energy can exceed the amount that is expected to be needed in the optimization window. This can lead to a non-zero final state of the BESS (see Figures B.3, B.6 and B.9). In the summer scenarios with FT-3, the results of the simulations with $\Delta_k = 15$ min deviate from the ones with $\Delta_k = 3$ min and 5 min (see Figure 6.5c). For $\Delta_k = 15$ min, the results for $\Delta_N = 36$ h and 42 h are worse than the results for $\Delta_N = 24$ h and 48 h. This is based on a combination of the effects described above. A detailed visualization of the resulting load profiles of the simulations are presented in Figure B.1. The figure shows that for $\Delta_N = 42$ h the BESS is charged more often in times of low feed-in compensation than for $\Delta_N = 48$ h, in particular during the third day of the simulation period.

In order to find the optimal device schedules in the simulation, an optimization with a time step duration of $\Delta_k = \Delta_t = 1$ s and an optimization window of $\Delta_N = \Delta_T = 7$ d has to be performed (see Section 3.4). However, this problem could not be solved due to very high memory requirements. Therefore, the minimal total costs of the reference control scheme are used as a benchmark in the comparison of the control schemes presented in Section 6.6.6.

Optimization Times

Figure 6.6 shows a visualization of the times the individual optimization runs need to find the optimal results in the simulation of the summer scenario with FT-2 over seven days². To limit the simulation time, i. e., the time that is needed to perform the simulation, the

²The figure shows box plots: The black pluses are outliers that have a value greater than $q_3 + 1.5 \cdot (q_3 - q_1)$ or less than $q_1 - 1.5 \cdot (q_3 - q_1)$, where q_1 and q_3 are the 25th and 75th percentiles of the sample data, respectively. The lower and the upper whisker show the minimum and the maximum value of the data

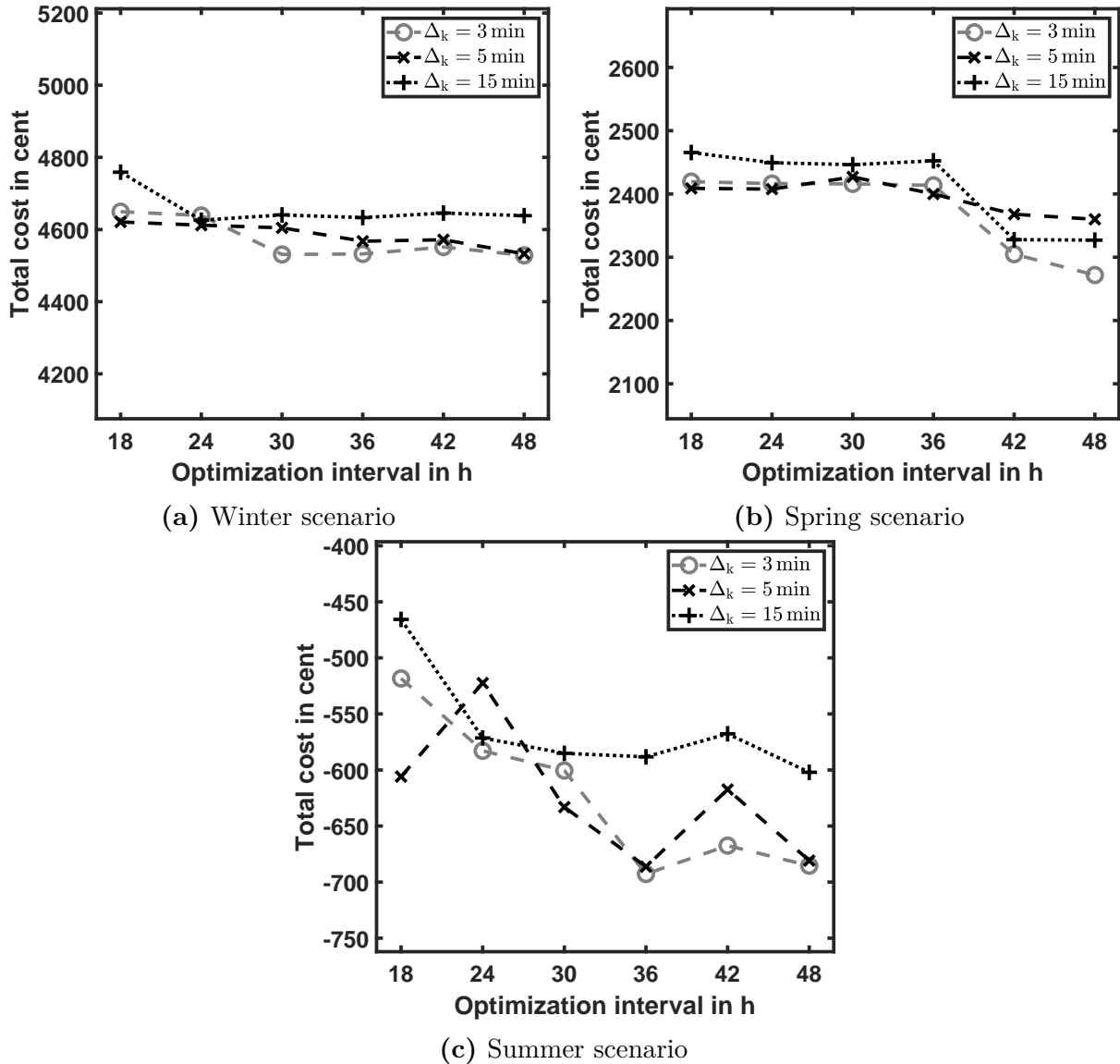


Figure 6.3: Visualization of the dependence of the total costs on the optimization window in the reference control scheme with FT-1. The gray circles indicate an optimization time step duration of $\Delta_k = 3$ min, the black Xs indicate $\Delta_k = 5$ min and the black crosses indicate $\Delta_k = 15$ min. (a) shows the winter, (b) shows the spring, and (c) shows the summer scenario. The lines are a guide to the eye.

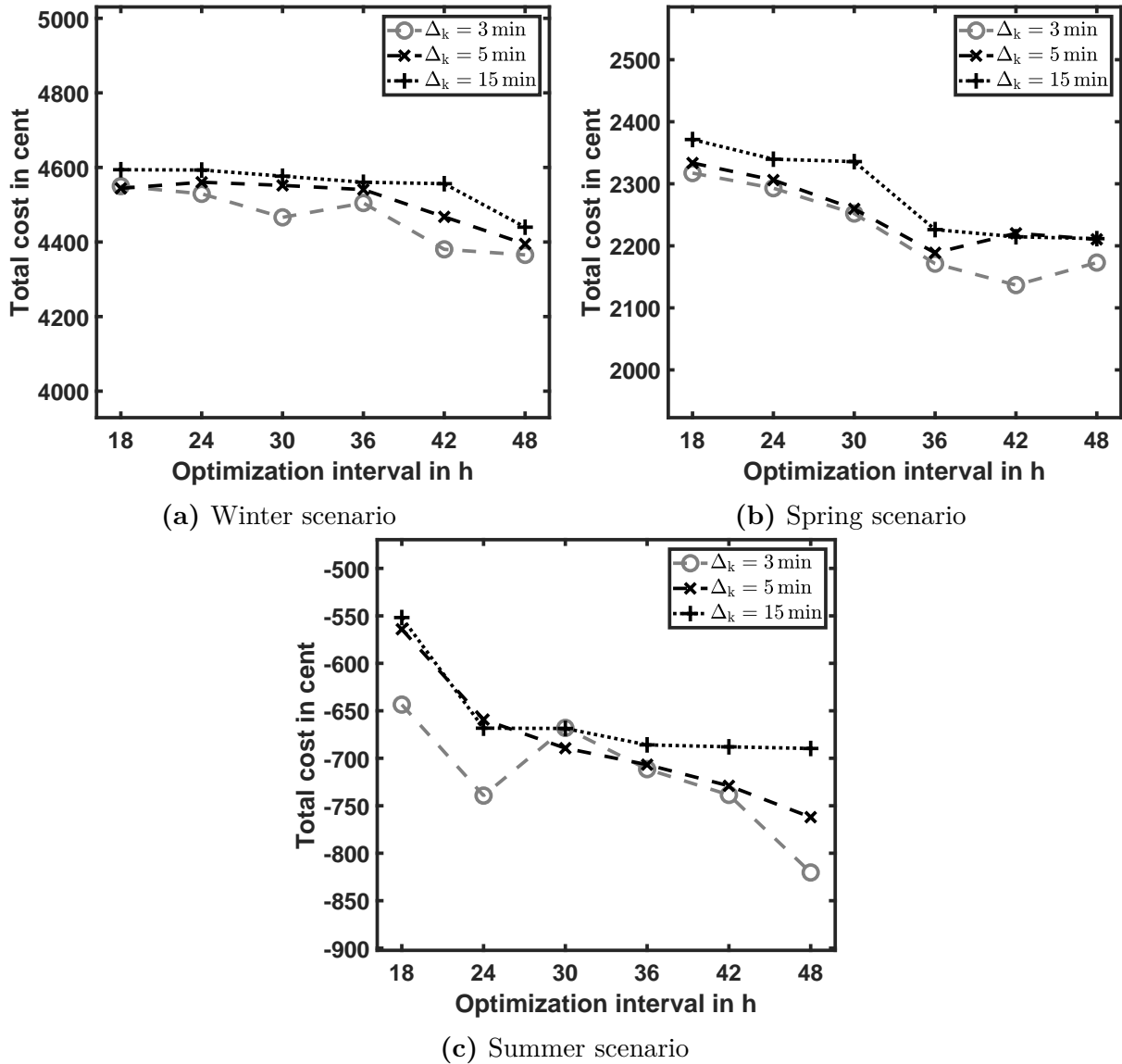


Figure 6.4: Visualization of the dependence of the total costs on the optimization window in the reference control scheme with FT-2. The gray circles indicate an optimization time step duration of $\Delta_k = 3$ min, the black Xs indicate $\Delta_k = 5$ min and the black crosses indicate $\Delta_k = 15$ min. (a) shows the winter, (b) shows the spring, and (c) shows the summer scenario. The lines are a guide to the eye.

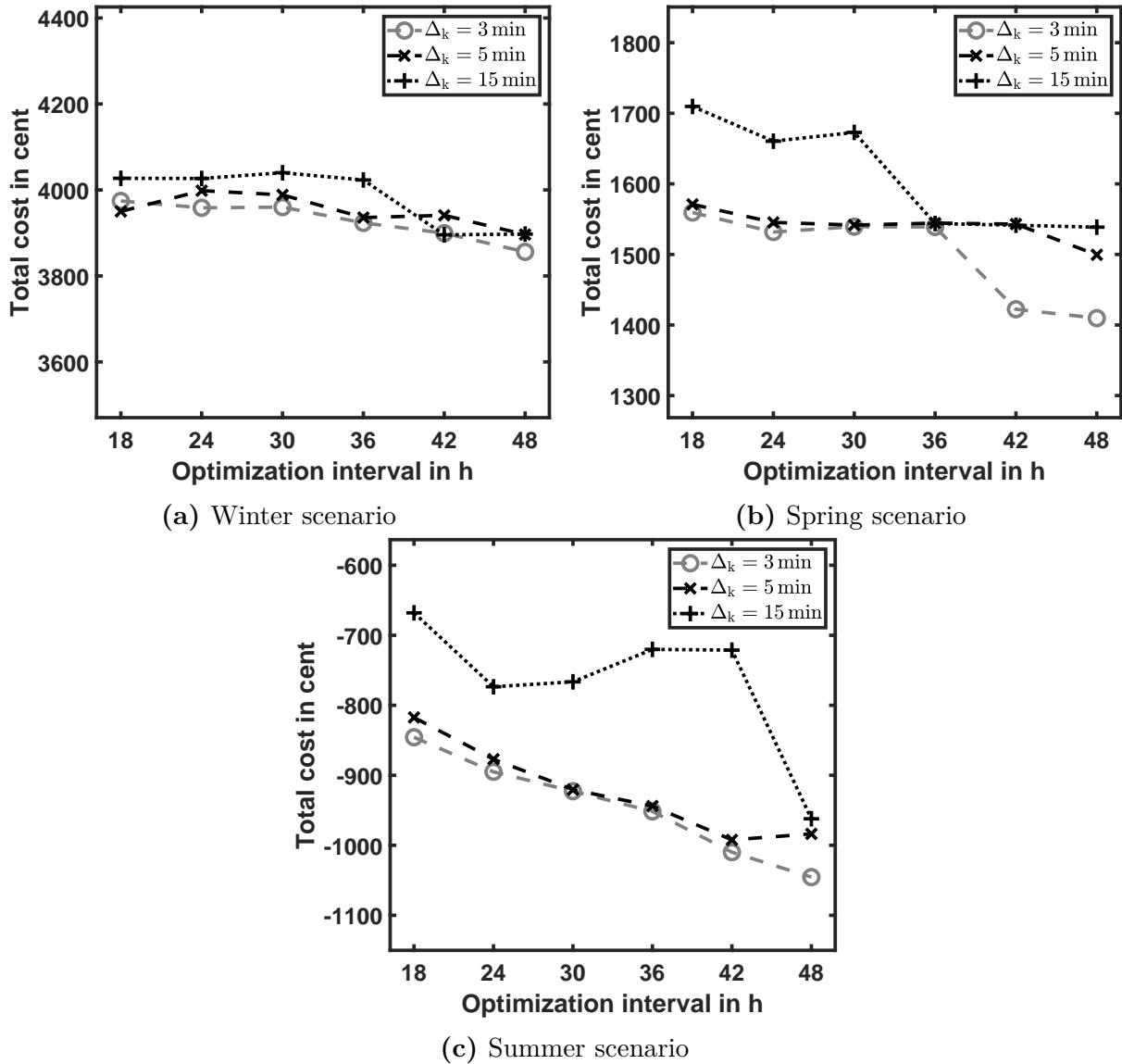


Figure 6.5: Visualization of the dependence of the totals costs on the optimization window in the reference control scheme with FT-3. The gray circles indicate an optimization time step duration of $\Delta_k = 3$ min, the black Xs indicate $\Delta_k = 5$ min and the black crosses indicate $\Delta_k = 15$ min. (a) shows the winter, (b) shows the spring, and (c) shows the summer scenario. The lines are a guide to the eye.

optimization time is limited to one minute. The optimization time varies between the optimization runs because in each optimization run a different optimization problem has to be solved (see Section 3.6). In case of $\Delta_k = 3$ min (see Figure 6.6a), the optimization time increases with increasing optimization window. For an increasing optimization window, the 75th percentile gets closer to optimization time limit of 1 min. For an optimization window of 48 h, the 75th percentile is equal to the optimization time limit of 1 min. Here, it can be assumed that the optimization time is limited by the optimization time limit and the resulting solutions are not proven to be optimal.

In case of $\Delta_k = 5$ min (see Figure 6.6b) and $\Delta_k = 15$ min (see Figure 6.6c), most of the optimization times are smaller than 1 min. In general, the median of the optimization times decrease when the time step durations increase. This is caused by the decreasing number of decision variables in the case of an increasing time step duration. In case of $\Delta_k = 15$ min (see Figure 6.6c), the median optimization times decrease from an optimization window of 42 to 48 h.

The graphs displaying the optimization times in the other scenarios are presented in Figure B.2 to Figure B.10. The observations described above can also be seen in the other scenarios. In addition, the following two observations are made: Firstly, the optimization times decrease from FT-1 to FT-2 to FT-3. Secondly, the optimization times increase from summer to spring to winter. This indicates that the different feed-in tariffs as well as the different generation and consumption profiles lead to different optimization problems. A qualitative assessment of the dependency of the optimization time on the feed-in tariff gives the following possible explanation: FT-1 has a time-independent tariff structure while FT-2 and FT-3 have time-dependent tariff structures. FT-3 has a feed-in compensation minimum that is equal to a feed-in compensation of zero. In case of FT-3, the feed-in at times of no feed-in compensation is minimized. In case of PV generation, this is expected to lead to an increase of consumption in the respective time period. Consequently, a distinct device schedule is expected to be determined by the BEMS. In case of FT-1, no minimum or maximum feed-in compensations exist and thus no distinct action of the BEMS is clearly favorable. Consequently, many possible device schedules are expected to lead to similar or even equal total costs. This ambiguity of an optimal device schedule is the source of the increased optimization times in the reference control scheme with FT-1.

6.6.2 Choice of Tuning Parameters

Based on the results presented in Figures 6.3, 6.4 and 6.5, a time step duration of $\Delta_k = 5$ min is chosen for the state-of-the-art and stochastic two-stage rolling horizon approach. In addition, the optimization window is chosen to be $\Delta_N = 24$ h and $\Delta_N = 30$ h. These values are chosen based on the total costs to optimization time ratio.

set excluding the outliers, respectively. The lower and the upper end of the box show the 25th and 75th percentiles, respectively. The middle line shows the median.

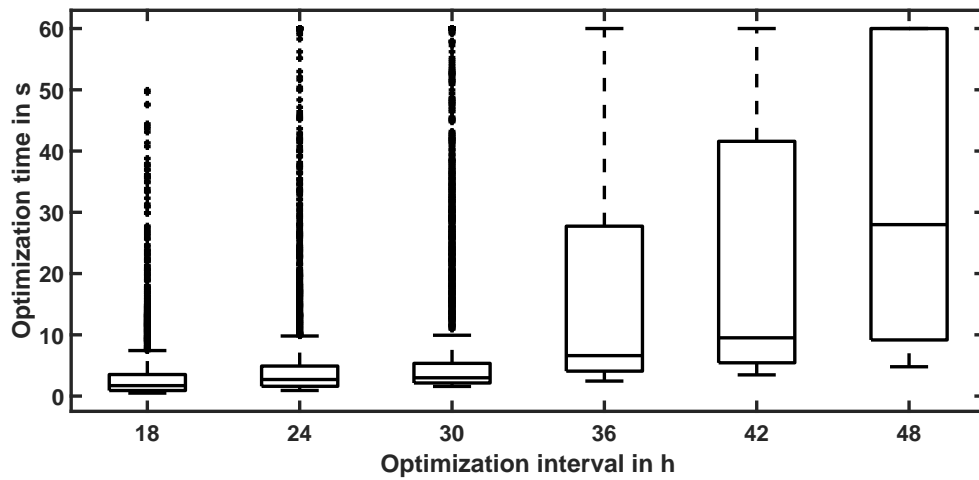
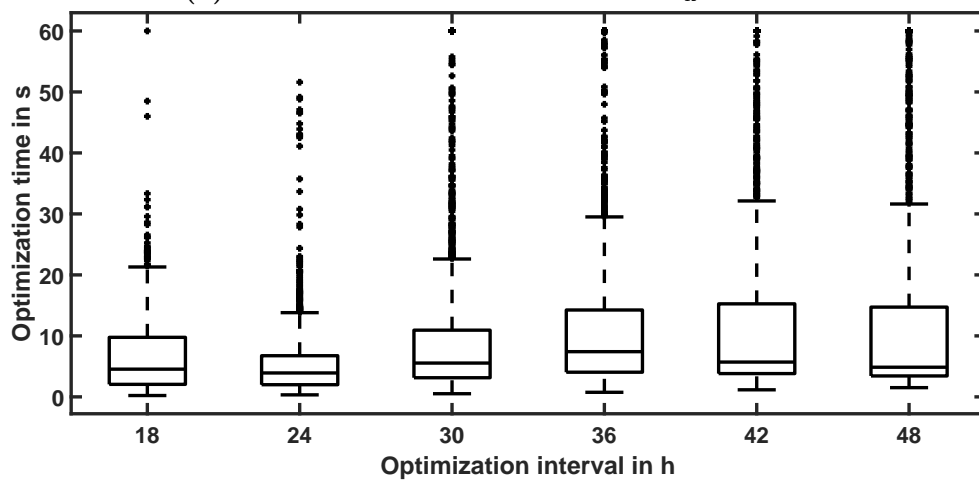
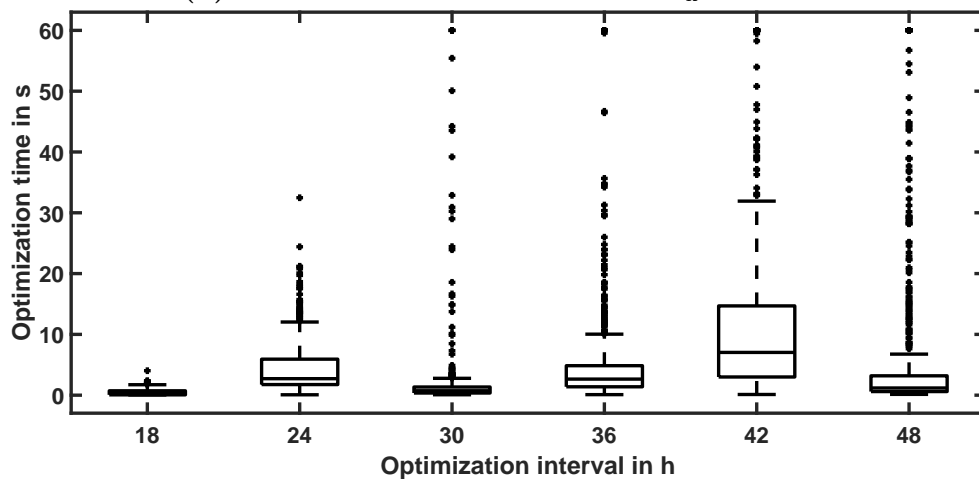
(a) Summer scenario with FT-2 and $\Delta_k = 3$ min.(b) Summer scenario with FT-2 and $\Delta_k = 5$ min.(c) Summer scenario with FT-2 and $\Delta_k = 15$ min.

Figure 6.6: Visualization of the optimization times in dependence on the optimization window and the time step duration in the reference control scheme in the summer scenario with FT-2. (a) shows the optimization times in the simulations with a time step duration of $\Delta_k = 3$ min, (b) shows $\Delta_k = 5$ min and (c) shows $\Delta_k = 15$ min.

6.6.3 State-of-the-art and Stochastic Control Scheme

The state-of-the-art control scheme uses a single point forecast of the PV generation while the stochastic control scheme uses a scenario-based probabilistic forecast of the PV generation (see Section 5.6.3). While in the state-of-the-art control scheme the state-of-the-art one-stage rolling horizon optimization approach presented in Section 5.7 is used, the stochastic two-stage rolling horizon optimization approach presented in Section 5.8 is used in the stochastic control scheme. As described in Section 5.8, the stochastic two-stage rolling horizon optimization approach contains a design parameter that has to be chosen by the designer of the system, which is the number of forecast scenarios M . In this thesis, the forecast scenarios relate to possible PV generation scenarios. Here, no choice of the number of forecast scenarios M is obvious. Therefore, several choices are evaluated using simulations. The investigated choices of the tuning parameter M are:

$$M \in \{1, 3, 5, 7, 9, 11, 13\}.$$

For $M = 1$ the stochastic two-stage rolling horizon optimization approach is equal to the state-of-the-art one-stage rolling horizon optimization approach. To ease the reading, the state-of-the-art control scheme will be denoted by $M = 1$.

Figure 6.7 shows the results of an exemplary optimization run in the state-of-the-art control scheme started at 00:00. The graphs show that the optimization chooses the control variables similar to the reference control scheme (see Section 6.6.1 and Figure 6.2). One can clearly see the different time resolutions of the PV system generation forecast compared to the perfect forecast in the reference control scheme presented in Figure 6.2. The BESS is planned to be charged using electricity generated by the PV system in a time period with a relatively low feed-in compensation. Moreover, the charging and discharging of the BESS is scheduled to achieve that the BESS is empty, $E_{\text{BESS},N} = \underline{E}_{\text{BESS}} = 0$, in the final time step in the optimization window. The micro-CHP is scheduled to start in the time period with the maximum feed-in compensation. Moreover, the schedule of the micro-CHP leads to a water temperature of the HWT of $\vartheta_{\text{HWT},N} = \underline{\vartheta}_{\text{HWT}} = 60^\circ\text{C}$ in the final time step in the optimization window.

Figure 6.8 shows the nine PV generation forecast scenarios provided by the probabilistic PV generation forecasts with $M = 9$ on an exemplary day. Moreover, the schedules for the controlled devices and the resulting energy stored in the BESS are shown for all nine forecast scenarios. The figures show that the individual devices are scheduled adjusted to the 9 different generation forecasts. In case of the BESS (see Figures 6.8b and c), the differences in schedules, which are dependent on the forecast scenario of the PV generation, can be distinguished. In the presented optimization run and the run-times of the micro-CHP (see Figure 6.8d) and the washing machine do not differ between the forecast scenarios. In general, the run-times of the micro-CHP and the washing machine can differ as well.

Total Costs

The results for the summer scenario with the feed-in tariff FT-2 are presented in Table 6.10. The table lists the electricity costs and the gas costs in the simulation period, the final

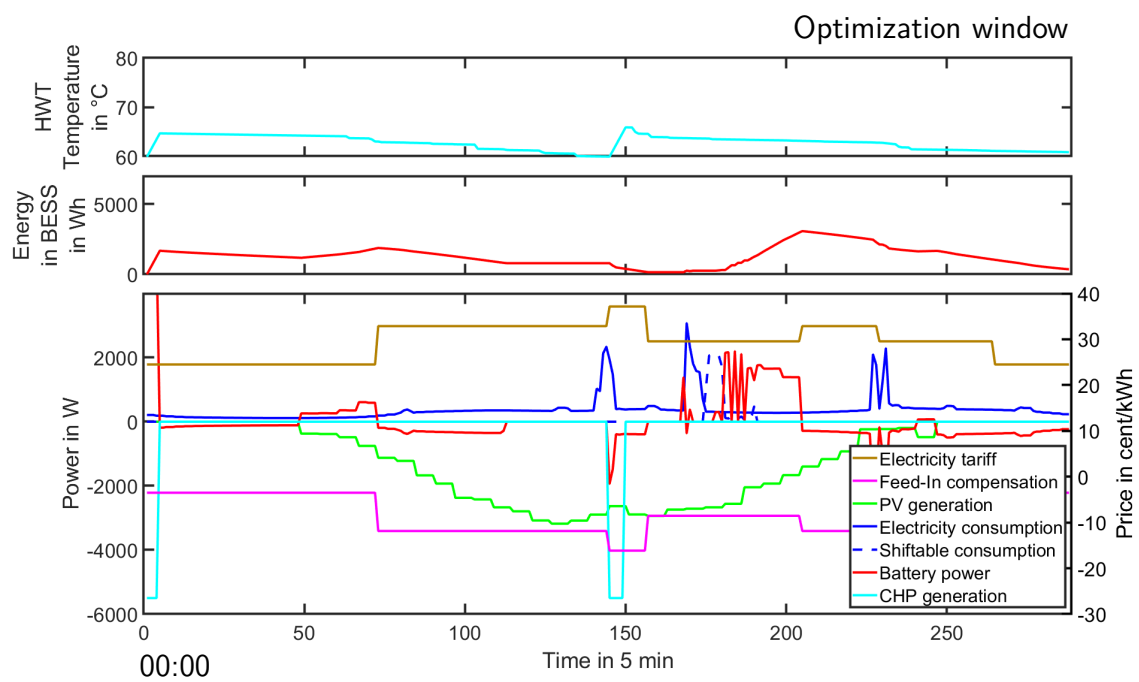
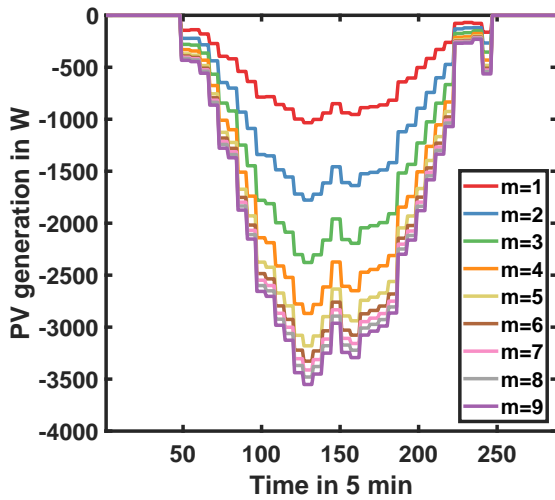
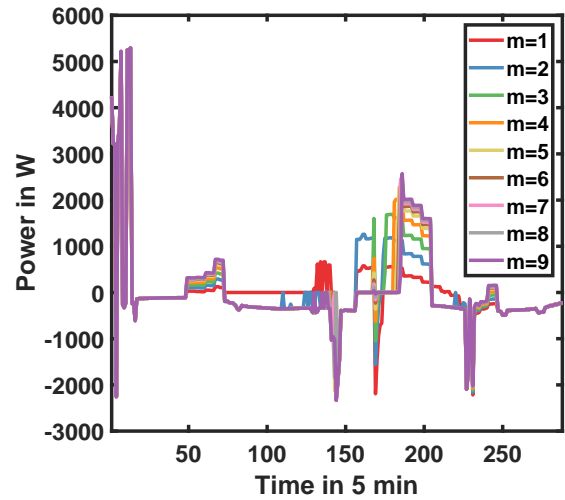


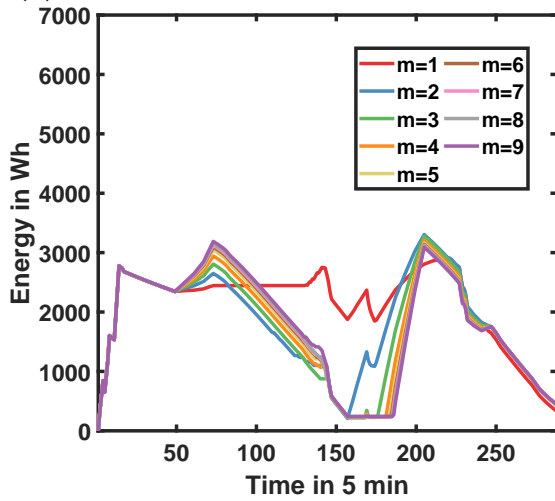
Figure 6.7: Visualization of the electrical loads and ESS states in the building energy system with the state-of-the-art control scheme. The graph shows the result of an optimization run started at 00:00.



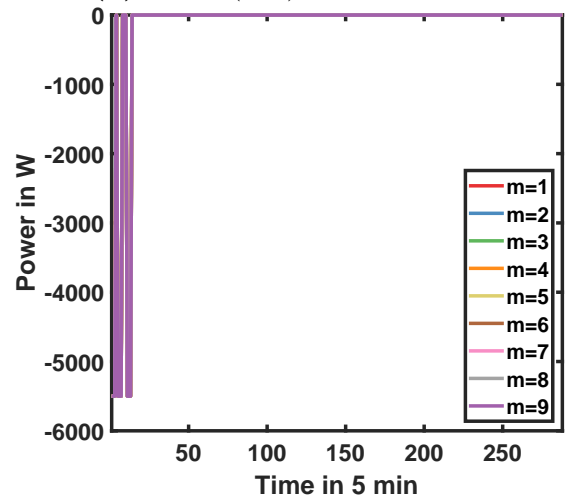
(a) Probabilistic PV generation forecasts.



(b) BESS (dis-)charge powers.



(c) Energy in the BESS



(d) Micro-CHP generation.

Figure 6.8: Exemplary probabilistic PV generation forecasts (a) and resulting BESS charge and discharge powers (b), energy stored in the BESS (c) and the micro-CHP generation (d) for $M = 9$ on an exemplary day.

Table 6.10: Simulation results of the state-of-the-art and stochastic control schemes in the summer scenarios with FT-2.

Δ_N in h	M	Electricity cost in cent	Gas cost in cent	$\tilde{E}_{\text{BESS},T+1}$ in W	$\tilde{\vartheta}_{\text{HWT},T+1}$ in °C	Total costs in cent
24	1	-1213	916	0	64	-455
24	3	-1248	929	0	65	-525
24	5	-1234	943	0	66	-546
24	7	-1234	916	13	65	-505
24	9	-1226	929	67	64	-478
24	11	No valid solution found				
30	1	-1219	929	0	65	-493
30	3	-1249	929	0	65	-522
30	5	-1242	929	0	65	-532
30	7	-1243	916	0	64	-484
30	9	No valid solution found				
30	11	No valid solution found				

states of the BESS and the HWT and the total costs in the simulation period. The total costs are defined in Section 5.3 and Equation 5.3. They include the feed-in compensation and thus are negative in the summer scenario. The results of the simulations of all other scenarios are listed in Tables B.10 to B.15. The corresponding visualizations of the total costs in dependence of the optimization window and number of forecast scenarios are shown in Figures 6.9, 6.10 and 6.11. In some simulations, for at least one of the emerging optimization problems no valid solution has been found within the optimization time limit. This happened for optimization problems with a high number of forecast scenarios and longer optimization windows. In the tables listing the results, these simulations are marked with the line: No valid solution found. In the Figures 6.9, 6.10 and 6.11 these simulations are not presented.

The figures show that, in effect of increasing the numbers of forecast scenarios depends on the season. In winter and spring, the total costs increase with increasing M . In summer, the total costs decrease with increasing M and then increase again. In the scenarios with FT-1 and FT-2, the total costs increase after $M = 5$. In the scenarios with FT-3, the total costs increase after $M = 9$. The dependence on the duration of the optimization window Δ_N is inconsistent. In some scenarios, the total costs increase with increasing Δ_N , in others the total costs decrease.

Optimization Times

Figure 6.12 shows a visualization of the times the individual optimization runs need to find the optimal results in the simulation over seven days. The optimization times in the other scenarios are presented in Figure B.12 and Figure B.13. To limit the simulation time, i. e., the time that is needed to perform the simulation, the optimization time is limited to one

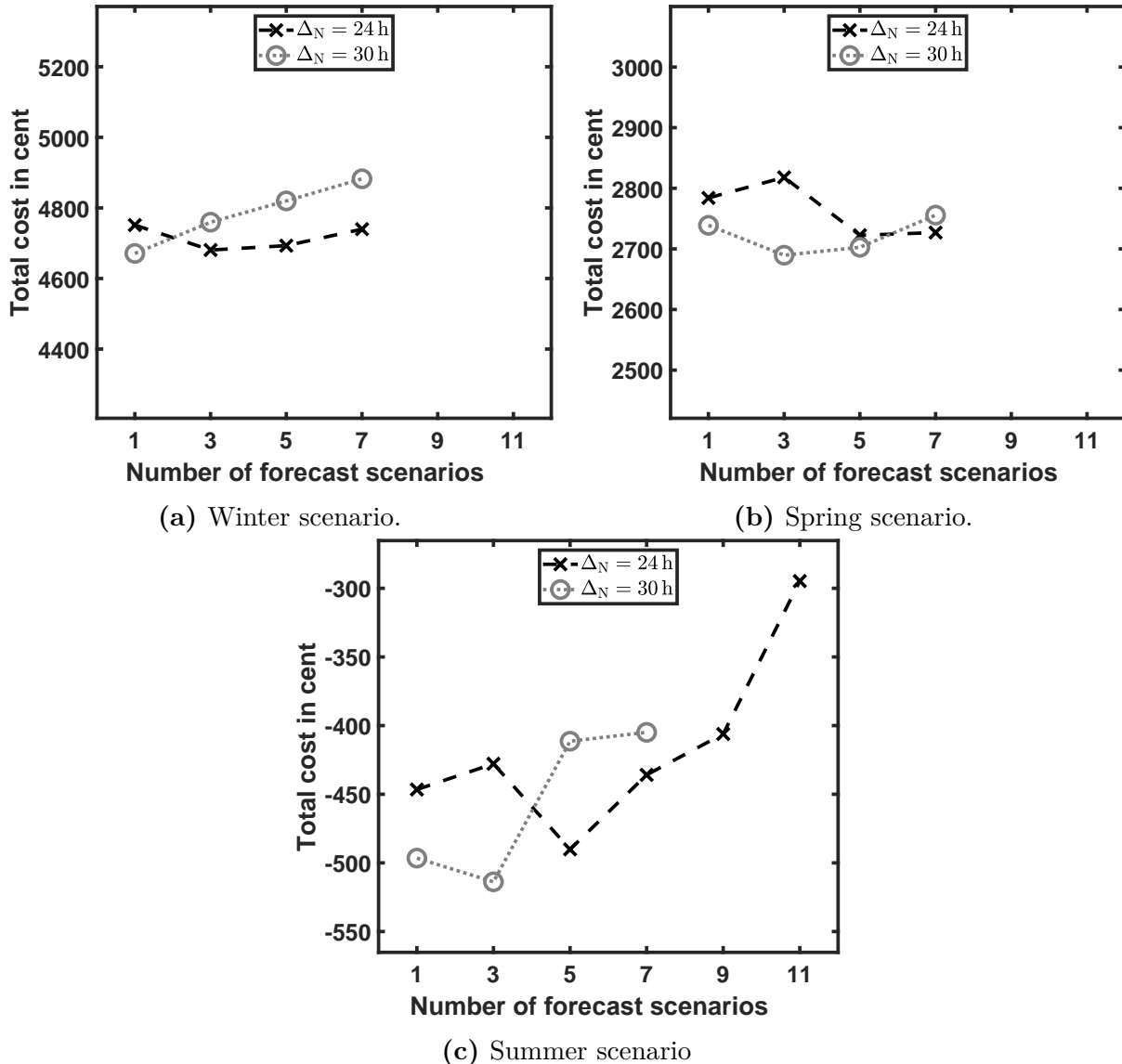


Figure 6.9: Visualization of the dependence of the total costs on the optimization window and the number of forecast scenarios in the state-of-the-art and stochastic control schemes in the scenarios with FT-1. The black Xs indicate an optimization window duration of $\Delta_N = 24$ h the gray circles indicate $\Delta_N = 30$ h. (a) shows the winter, (b) shows the spring, and (c) shows the summer scenario. The lines are a guide to the eye.

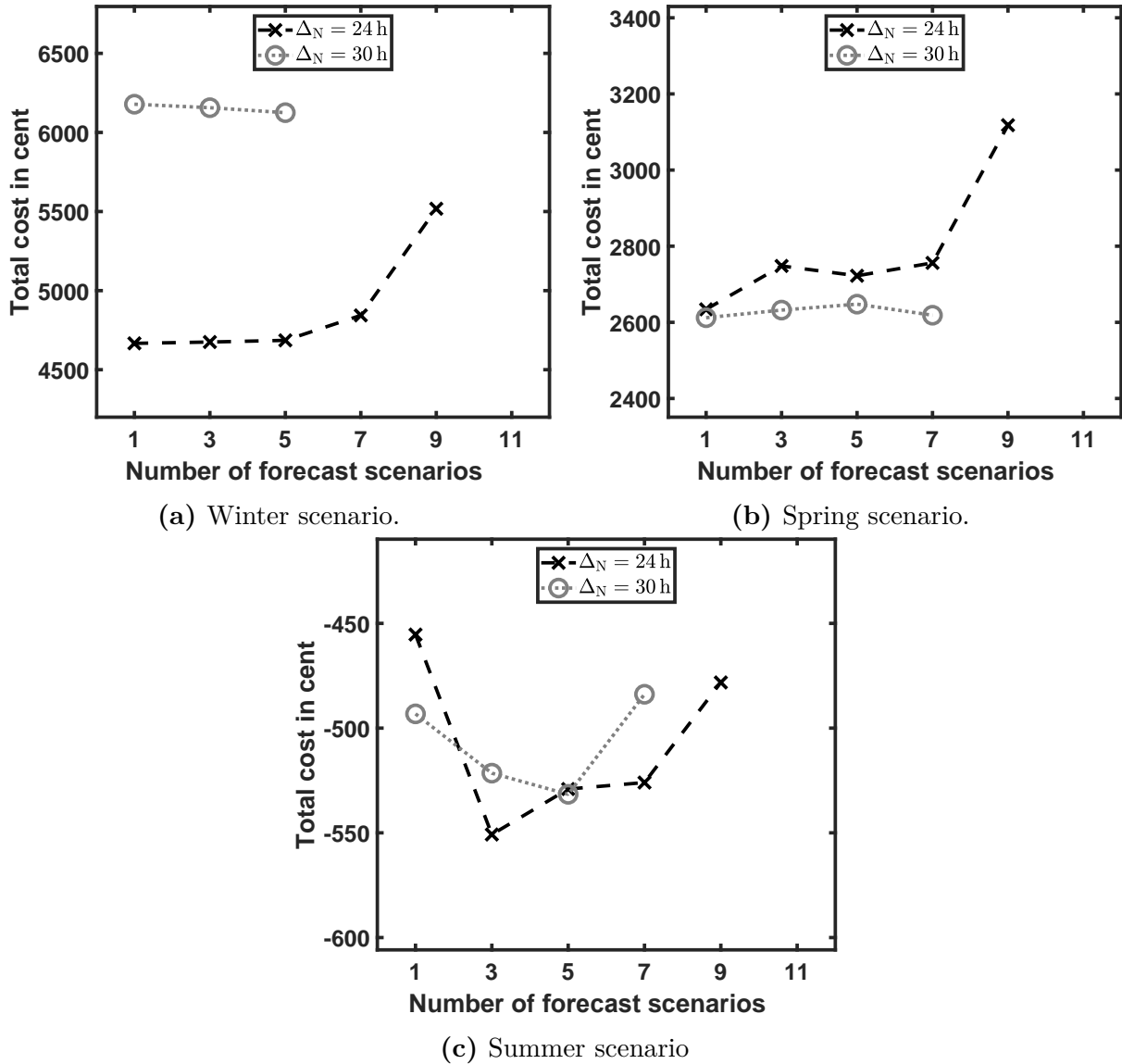


Figure 6.10: Visualization of the dependence of the total costs on the optimization window and the number of forecast scenarios in the state-of-the-art and stochastic control schemes in the scenarios with FT-2. The black Xs indicate an optimization window duration of $\Delta_N = 24$ h the gray circles indicate $\Delta_N = 30$ h. (a) shows the winter, (b) shows the spring, and (c) shows the summer scenario. The lines are a guide to the eye.

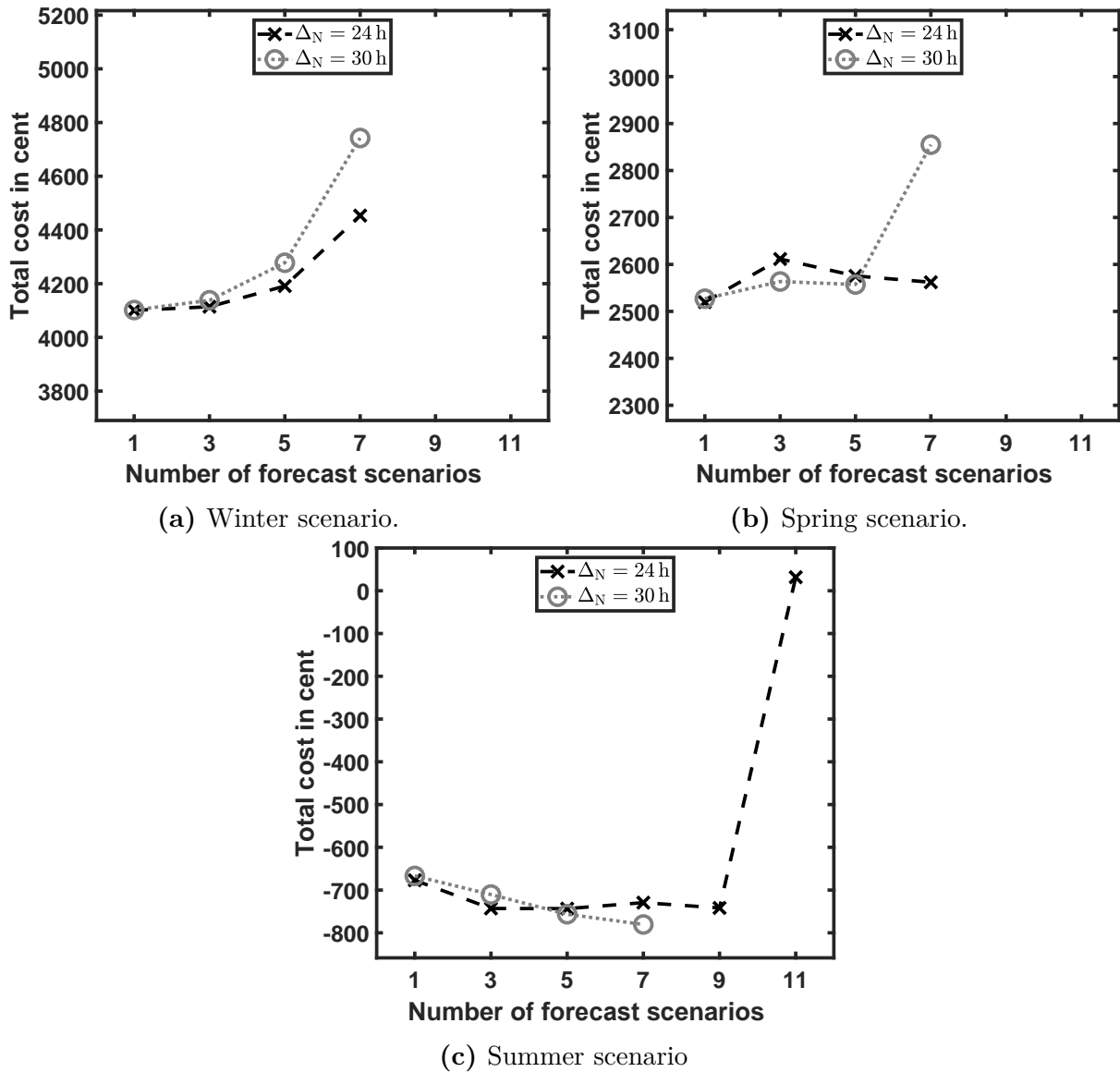
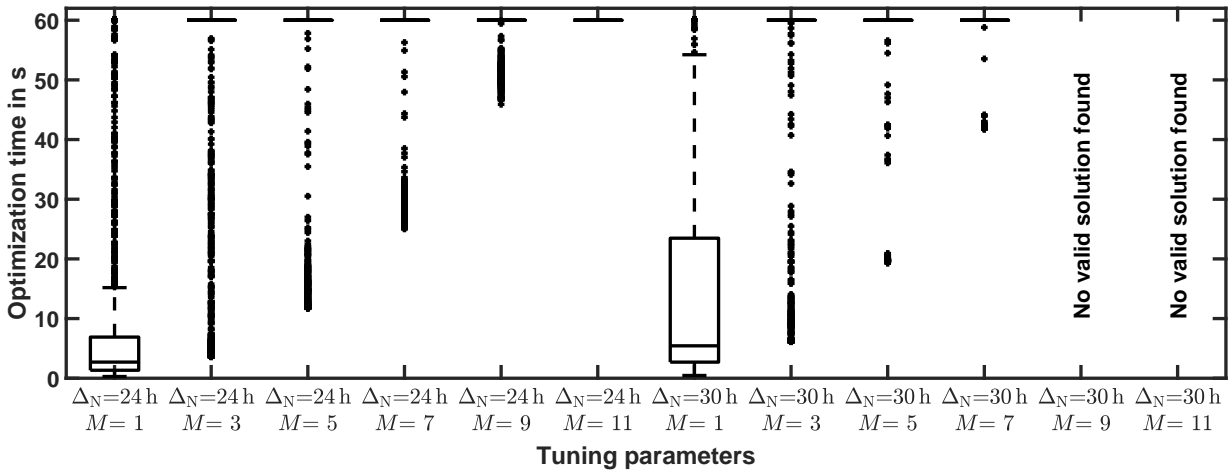
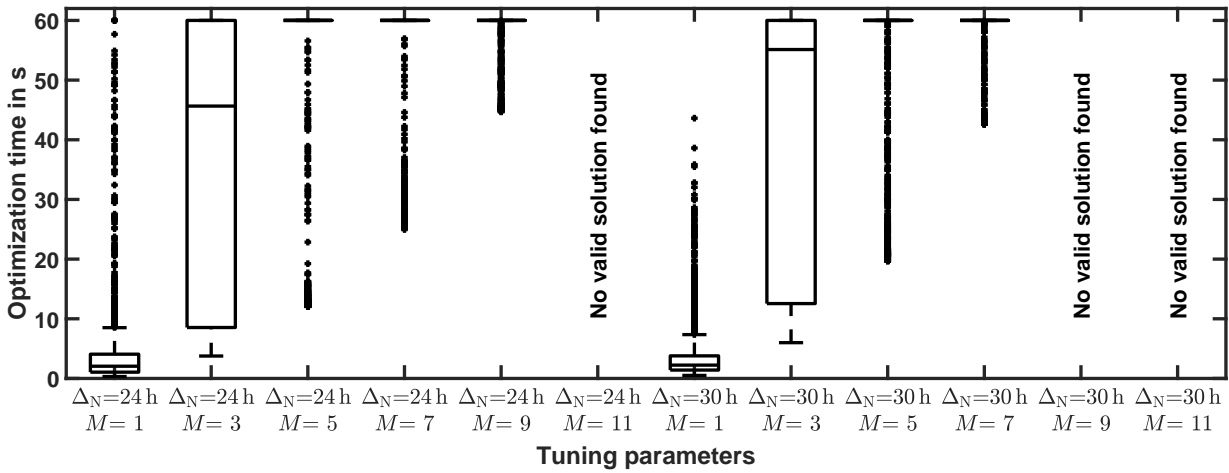


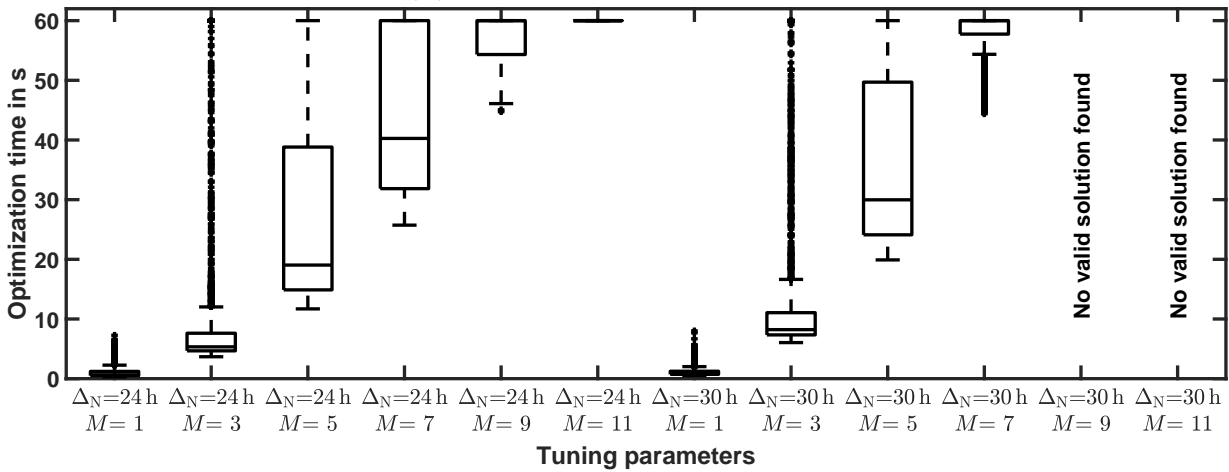
Figure 6.11: Visualization of the dependence of the total costs on the optimization window and the number of forecast scenarios in the state-of-the-art and stochastic control schemes in the scenarios with FT-3. The black Xs indicate an optimization window duration of $\Delta_N = 24$ h the gray circles indicate $\Delta_N = 30$ h. (a) shows the winter, (b) shows the spring, and (c) shows the summer scenario. The lines are a guide to the eye.



(a) Summer scenario with FT-1.



(b) Summer scenario with FT-2.



(c) Summer scenario with FT-3.

Figure 6.12: Visualization of the optimization times in dependence on the optimization window and the time step duration in the state-of-the-art and stochastic control schemes in the summer scenarios with FT-1 (a), FT-2 (b) and FT-3 (c).

minute. Similar to the reference control scheme, the optimization time varies between the optimization runs. This is based on the different optimization problems that have to be solved in the optimization runs (see Section 3.6). In general, the median of the optimization times increase with increasing number of forecast scenarios M . For $M = 1$ all optimization runs can be solved within the time limit, while in the simulations with a higher M some optimization runs have to be stopped at the time limit. This is caused by the increasing number of decision variables in the case of increasing M and Δ_N . The optimization time is also dependent on the feed-in tariff and the time for the year. The optimization times decrease from FT-1 to FT-2 to FT-3. The same observations are also made in the reference control scheme (see Section 6.6.1). Here, the same possible explanations as in the reference control scheme can be made (see Section 6.6.1). In general, the optimization times are higher than in the reference control scheme. However, the majority of the optimization problems in the state-of-the-art control scheme are solved within the time limit, whereas a large part of the optimizations in the stochastic control scheme are stopped because of the time limit. Consequently, making a statement on the absolute performance of the stochastic control scheme is problematic. However, the observed increase in performance in some scenarios demonstrates the potential of the stochastic control scheme with respect to the state-of-the-art control scheme.

6.6.4 Rule-based Micro-CHP Control Scheme

The rule-based micro-CHP control scheme uses the same forecasts as the state-of-the-art and stochastic control schemes (see Section 6.6.3). They differ in the control of the micro-CHP. In the rule-based micro-CHP control scheme, the micro-CHP is controlled using the heat-led rule-based control defined in Section 5.6.2. The BESS and the appliance scheduled according to the optimization. The optimization problem in the rule-based micro-CHP control scheme is the same as defined in Section 5.8, however, all decision variables and constraints which consider the micro-CHP and the HWT are omitted. This reduces the number of decision variables, in particular the number of binary decision variables, as well as the number of constraints. Similar to the stochastic control scheme, the rule-based micro-CHP control scheme has the number of forecast scenarios M as a design parameter. Here, the same choices of the tuning parameter M are investigated:

$$M \in \{1, 3, 5, 7, 9, 11, 13\}.$$

Figure 6.13 shows the results of an exemplary optimization run started at 00:00. The graphs show that the optimization chooses the control variables similar to the stochastic control scheme (see Section 6.6.3 and Figure 6.2). The BESS is scheduled to be charged using electricity generated by the PV system in a time period with a relatively low feed-in compensation. Moreover, the charging and discharging of the BESS is scheduled so that the energy stored in the BESS in the final time step in the optimization window is $E_{\text{BESS},N} = 0$. This behavior is a result of not considering terminal costs in the optimization (see Section 5.7.1). The micro-CHP is scheduled using the heat-led rule based-control. This

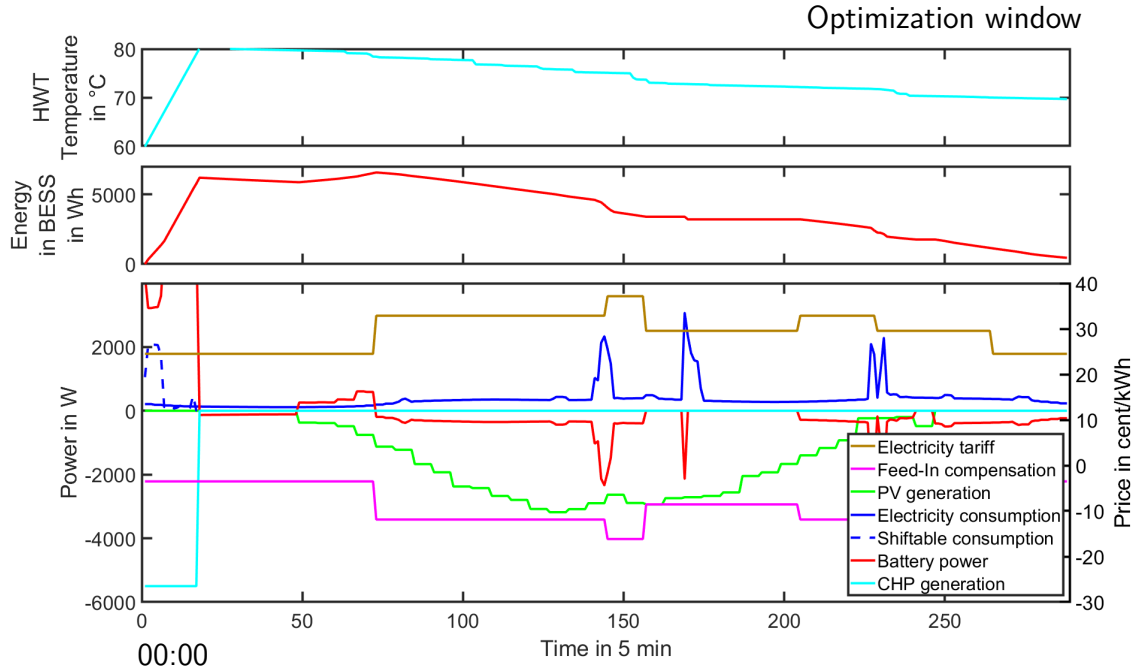


Figure 6.13: Visualization of the electrical loads and ESSs states in the building energy system in the rule-based micro-CHP control scheme. The graph shows a result of an exemplary optimization run started at 00:00.

means the micro-CHP is started whenever the HWT temperature is equal to or below its minimum temperature, i. e., $\tilde{\vartheta}_{\text{HWT},t} \leq \underline{\vartheta}_{\text{HWT}}$. The micro-CHP is stopped when the HWT temperature is equal to or above its maximum temperature, i. e., $\vartheta_{\text{HWT},\text{Max}} \leq \tilde{\vartheta}_{\text{HWT},t}$. This leads to an HWT temperature above the minimum HWT temperature at the end of the simulation period. In the optimization, a forecast of the run-times of the micro-CHP is used. The washing machine is started at a point in time when the micro-CHP runs. Thus, the electricity generated by the micro-CHP is used to run the washing machine.

Total Costs

The results of the simulations in the summer scenario with FT-2 are presented in Table 6.11. The table lists the electricity costs and the gas costs in the simulation period, the final states of the BESS and the HWT and the resulting total costs in the simulation period. The results of the simulations of all other scenarios are listed in Tables B.19 to B.24. The corresponding visualizations of the total costs in dependence of the optimization window and number of forecast scenarios are shown in Figures 6.14, 6.15 and 6.16. Similar to the observations in Section 6.6.3, for at least one of the emerging optimization problems no valid solution has been found within the optimization time limit. This happened for problems with high number of forecast scenarios and high optimization windows. In the

Table 6.11: Simulation results of the rule-based micro-CHP control scheme in the summer scenario with FT-2.

Δ_N in h	M	Electricity cost in cent	Gas cost in cent	$\tilde{E}_{\text{BESS},T+1}$ in Ws	$\tilde{\vartheta}_{\text{HWT},T+1}$ in °C	Total costs in cent	
24	1	-1091	938	0	64	-318	
24	3	-1159	938	0	64	-386	
24	5	-1164	938	113	64	-392	
24	7	-1158	938	113	64	-385	
24	9	-1152	938	106	64	-379	
24	11	-1144	938	155	64	-371	
30	1	-1092	938	0	64	-320	
30	3	-1167	938	0	64	-394	
30	5	-1158	938	114	64	-385	
30	7	-1166	938	116	64	-393	
30	9	-1102	938	474	64	-329	
30	11	No valid solution found					

tables listing the results, these simulations are marked with the line: No valid solution found. In the Figures 6.9, 6.10 and 6.11 these simulations are not presented. In almost all scenarios, the total costs decrease with increasing M . The only exception are the winter and spring scenarios with FT-3. In the other scenarios, the total costs decrease from $M = 1$ to $M = 3$. For an increasing M the total costs stay at the same level. The dependence on the optimization window is small and inconsistent through the scenarios. In general, the total costs in simulations with $\Delta_N = 24$ h are very similar to the total costs in simulations with $\Delta_N = 30$ h.

Optimization Times

Figure 6.17 shows a visualization of the times the individual optimization runs need to find the optimal results in the simulation over seven days. The figures displaying the optimization times in the other scenarios are presented in Figure B.15 and Figure B.16. Similar to the reference control scheme, the optimization time varies between the optimization runs. In general, the median of the optimization times increase with increasing M . In the simulations with $\Delta_N = 30$ h and $M = 11$, in at least one optimization run no valid solution has been found within the optimization time limit. In the simulations with $\Delta_N = 24$ h and $M = 11$ and the simulations with $\Delta_N = 30$ h and $M = 9$ some optimizations have to be stopped at the time limit. In all other scenarios, optimal results could be found in all optimization runs. This is expected to be caused by the increasing number of decision variables in the case of increasing M and Δ_N . However, the optimization times are lower than for the state-of-the-art and stochastic control scheme. This is based on the reduced number of decision variables compared to the state-of-the-art and stochastic control scheme.

The optimization time is also dependent on the feed-in tariff and the season. In the

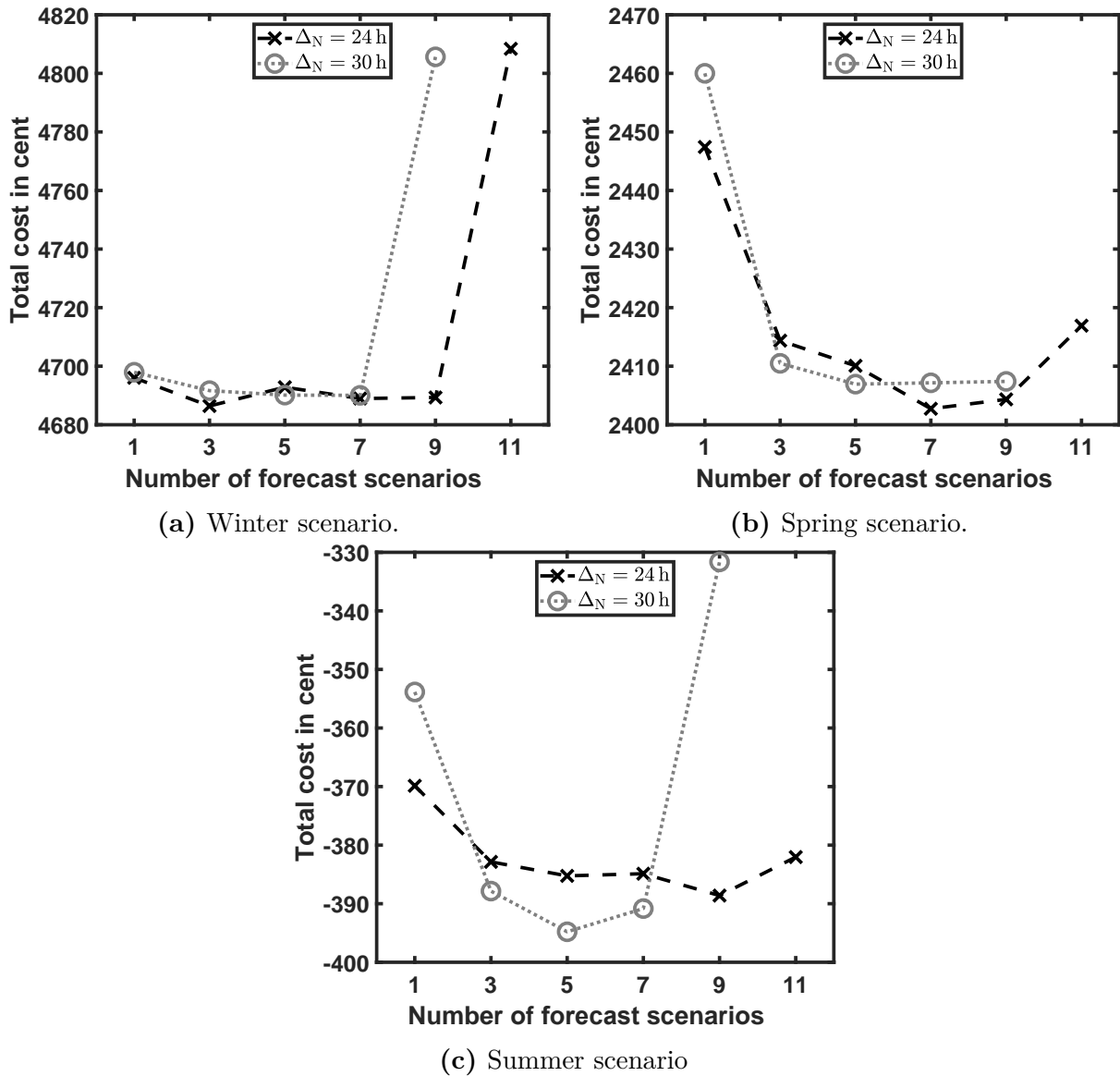


Figure 6.14: Visualization of the dependence of the total costs on the optimization window and the number of forecast scenarios in the rule-based micro-CHP control scheme in the scenarios with FT-1. The black Xs indicate an optimization window duration of $\Delta_N = 24$ h the gray circles indicate $\Delta_N = 30$ h. (a) shows the winter, (b) shows the spring, and (c) shows the summer scenario. The lines are a guide to the eye.

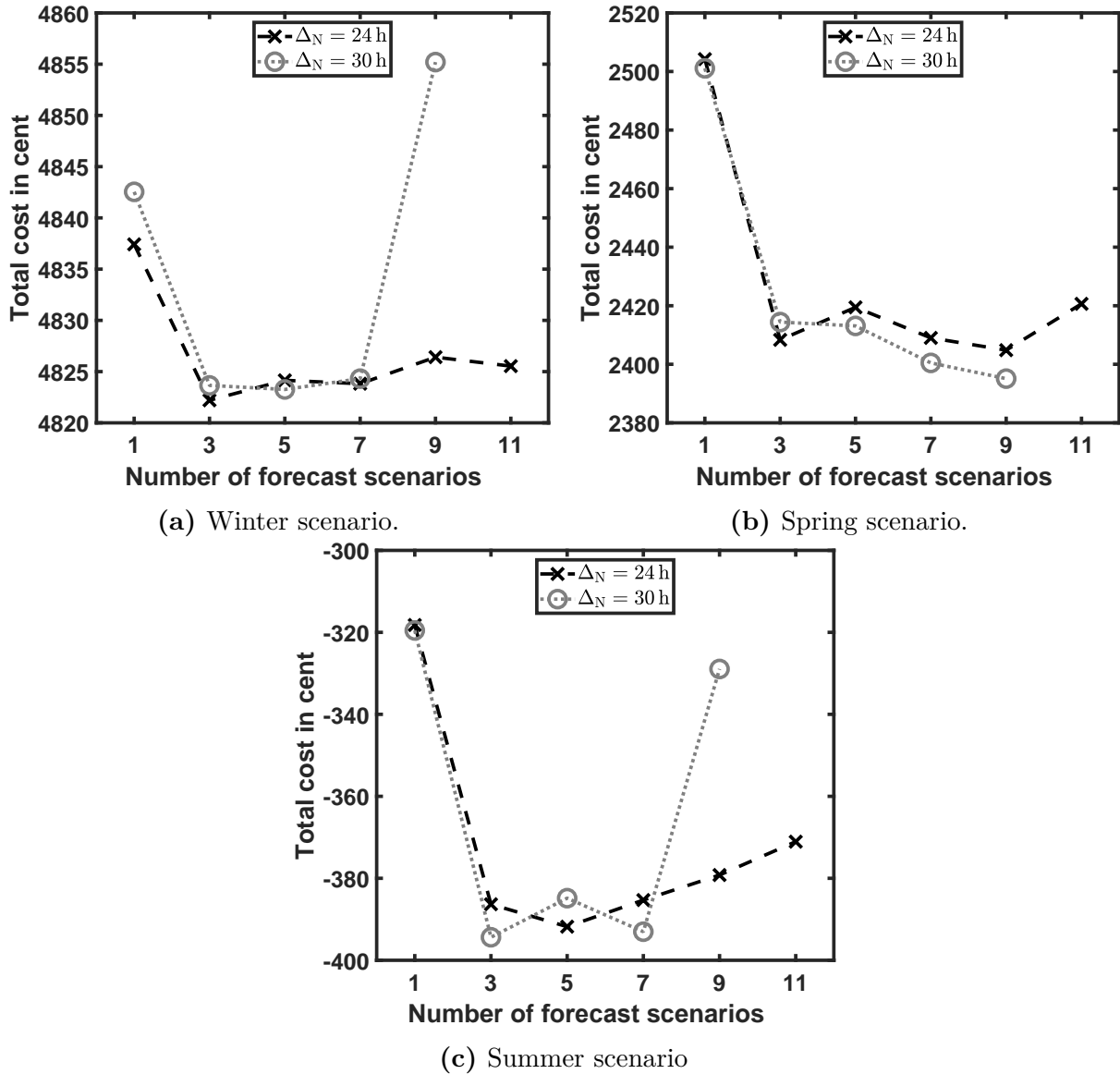


Figure 6.15: Visualization of the dependence of the total costs on the optimization window and the number of forecast scenarios in the rule-based micro-CHP control scheme in the scenarios with FT-2. The black Xs indicate an optimization window duration of $\Delta_N = 24$ h the gray circles indicate $\Delta_N = 30$ h. (a) shows the winter, (b) shows the spring, and (c) shows the summer scenario. The lines are a guide to the eye.

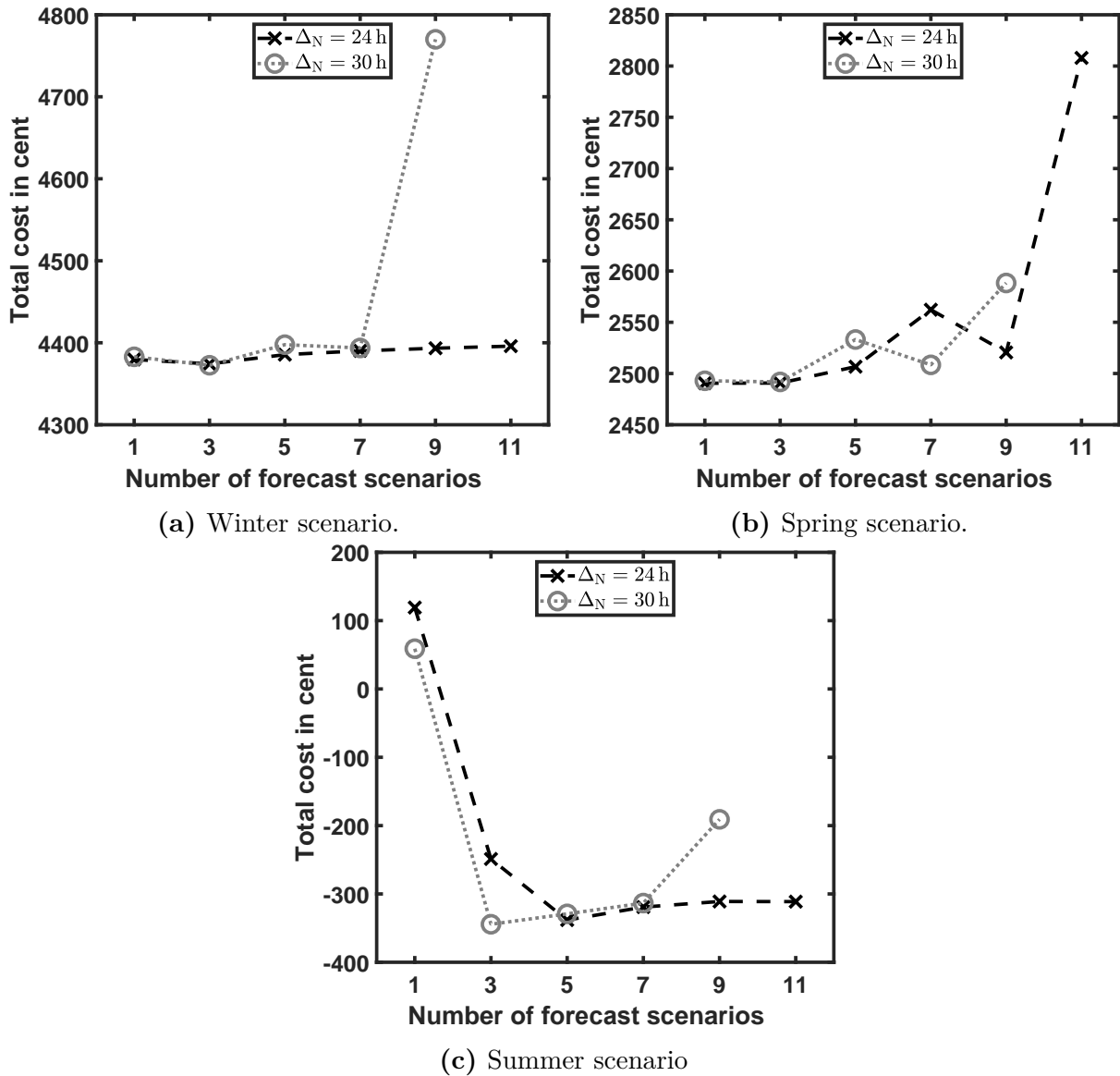
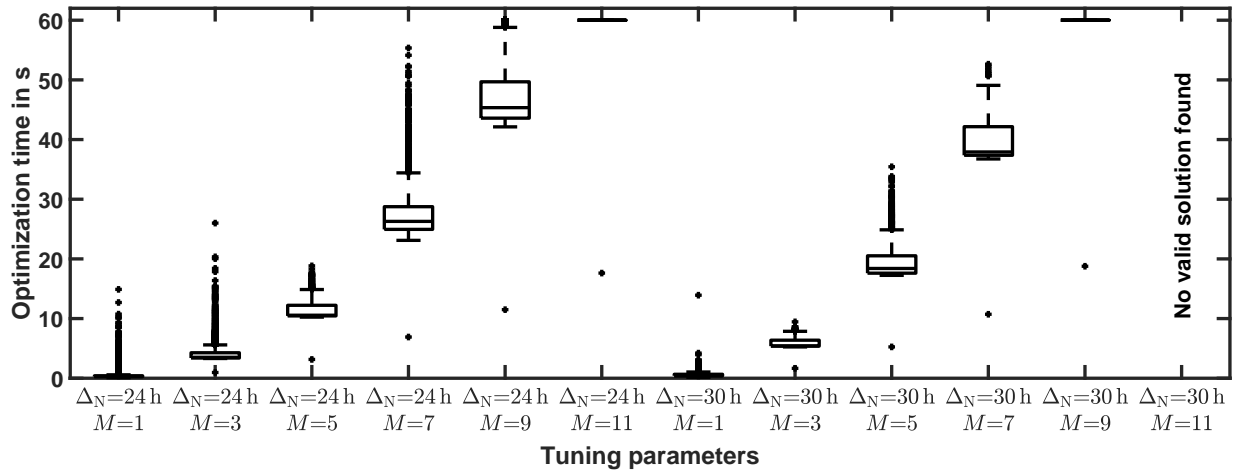
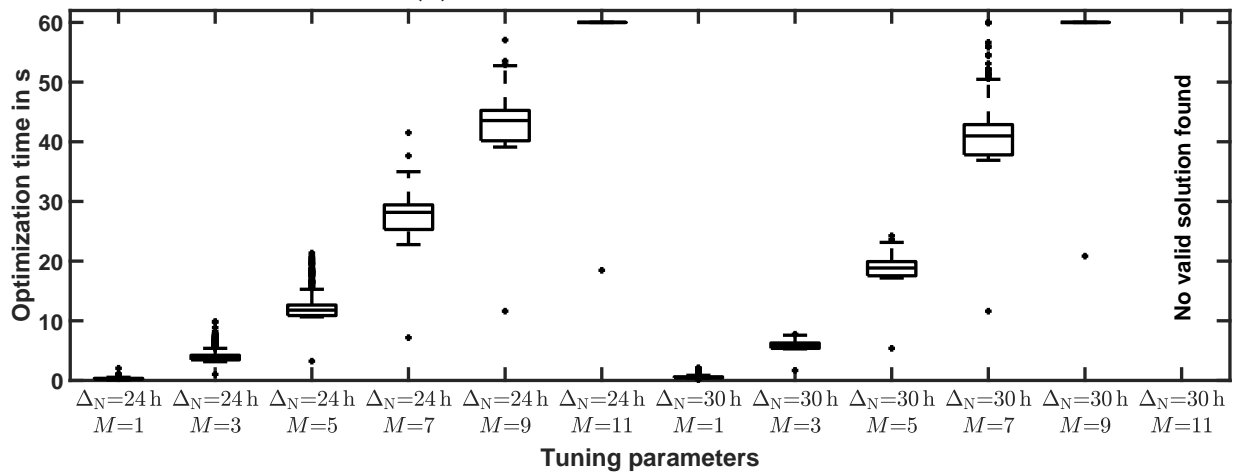


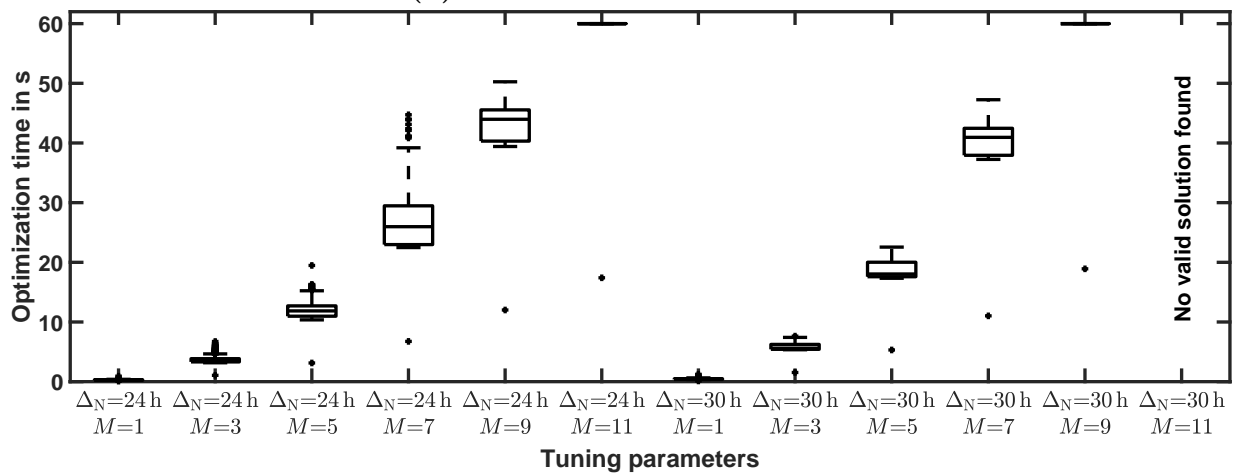
Figure 6.16: Visualization of the dependence of the total costs on the optimization window and the number of forecast scenarios in the rule-based micro-CHP control scheme in the scenarios with FT-3. The black Xs indicate an optimization window duration of $\Delta_N = 24$ h the gray circles indicate $\Delta_N = 30$ h. (a) shows the winter, (b) shows the spring, and (c) shows the summer scenario. The lines are a guide to the eye.



(a) Summer scenario with FT-1.



(b) Summer scenario with FT-2.



(c) Summer scenario with FT-3.

Figure 6.17: Visualization of the optimization times in dependence on the optimization window and the time step duration in the rule-based micro-CHP control scheme summer scenarios with FT-1 (a), FT-2 (b) and FT-3 (c).

rule-based micro-CHP control scheme, the variations are not as high as in the reference, state-of-the-art and stochastic control schemes. The dependence of the optimization time on the feed-in tariffs is small. The same observation is made for the dependence of the optimization time on the season year.

6.6.5 Rule-based Control Scheme

A visualization of the electrical loads and ESSs states in the building energy system in the rule-based control scheme during one day is presented in Figure 6.18. The graph shows that the HWT is charged whenever the temperature in the HWT falls below the given minimum temperature of 60°C. This means that the micro-CHP is started whenever the HWT temperature is equal to or below its minimum temperature, i. e., $\tilde{\vartheta}_{\text{HWT},t} \leq \vartheta_{\text{HWT}}$. The micro-CHP is stopped when the HWT temperature is equal to or above its maximum temperature, i. e., $\bar{\vartheta}_{\text{HWT}} \leq \tilde{\vartheta}_{\text{HWT},t}$. The BESS is charged whenever power at the grid connection point minus the (dis-)charge power of the BESS is negative and discharged whenever the grid connection point minus the (dis-)charge power of the BESS is positive. This leads to a non-zero charging level of the ESSs, i. e., the BESS and the HWT, at the end of the simulation period. The washing machine is started at 12:00. In summary, the simulation shows the expected behavior defined in Sections 5.6.1, 5.6.4 and 5.6.2. The rule-based control scheme does not use an optimization. Hence, no optimization times are analyzed. The time to perform the rule based control can be neglected.

Total Costs

The results of the simulations in the rule based control scheme are listed in Table 6.12. The dependence of the total costs on the starting times of the simulations as well as the feed-in tariffs is visualized in Figure 6.19. For all three feed-in tariffs, the total costs decrease from winter to summer. As described in Section 6.6.1, this is expected because of the increasing PV generation. In the winter scenario, all three feed-in tariffs lead to similar total cost. This is caused by the low PV generation. In the spring and summer scenario, FT-1 leads to higher costs than FT-2 and FT-3.

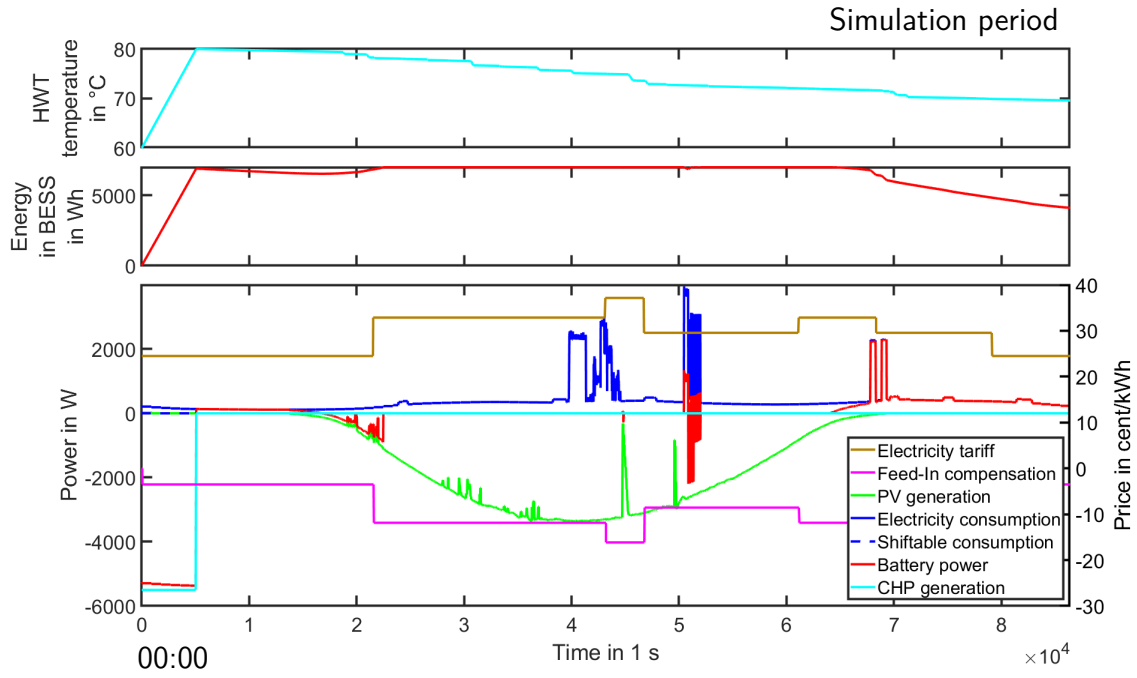


Figure 6.18: Visualization of the electrical loads and ESSs states in the building energy system with the rule-based control scheme.

Table 6.12: Results of the simulations performed to evaluate the rule-based operation.

Season	Feed-in Tariff	Electricity cost in cent	Gas cost in cent	$\tilde{E}_{\text{BESS},T+1}$ in Ws	$\tilde{\vartheta}_{\text{HWT},T+1}$ in °C	Total costs in cent
Winter	1	-785	5756	5411	69	4598
Spring	1	-1263	4046	6279	76	2114
Summer	1	-1350	938	1960	64	-578
Winter	2	-541	5756	5411	69	4842
Spring	2	-1115	4046	6279	76	2262
Summer	2	-1246	938	1960	64	-474
Winter	3	-845	5756	5411	69	4537
Spring	3	-801	4046	6279	76	2576
Summer	3	-648	938	1960	64	125

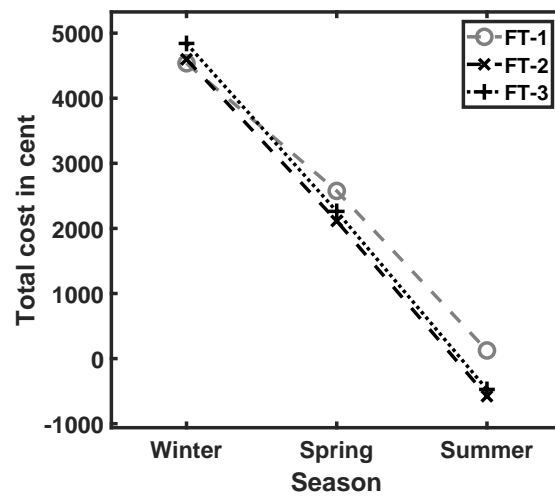


Figure 6.19: Results of the rule-based operation. The lines are a guide to the eye.

6.6.6 Scenario Comparison

Figure 6.20 shows a comparison of the absolute evaluation results in the different scenarios. Therein, Figure 6.20a shows the total costs in simulations with the five different control schemes in the winter scenarios. Figure 6.20b shows the results in spring scenarios and Figure 6.20c shows the results in the summer scenarios. Each figure shows the total costs in dependence on the control scheme and the feed-in tariff. In the figures, each bar shows the best value, i. e., the lowest total cost, for all investigated tuning parameter combinations. Here, lower values, i. e., lower total cost, indicate a higher performance. In Figure 6.21, a comparison of the relative change in the results in the different scenarios is shown. Each bar shows the relative change of the total costs with respect to the reference control scheme³. Here, negative values mean that the respective control scheme performs better than the reference control scheme in the respective scenario, positive values indicate a worse performance with respect to the reference control scheme. Hence, higher values indicate a better performance. Table 6.13 lists all scenario and control scheme combinations with their best tuning parameter combinations.

When investigating the results, the following general observations can be made:

1. As expected, the winter scenarios have the highest total costs and the summer scenarios have the lowest total costs for all three feed-in tariffs.
2. In all three season scenarios, the total costs slightly decrease from FT-1 to FT-2 to FT-3.
3. The reference control scheme leads to the minimal total costs in every scenario except in the spring scenario with FT-1.
4. No best tuning parameter combination can be found.
5. The majority of the optimization problems in the state-of-the-art control scheme are solved within the time limit, whereas a large part of the optimizations in the stochastic control scheme are stopped because of the time limit.
6. In the summer scenario, the stochastic control scheme outperforms the state-of-the-art control scheme. In all other scenarios they perform similarly.

Based on the different energy consumption and PV generation profiles, the results for each season are analyzed individually. This is also needed for the results of the three feed-in tariffs. In the following sections, the results in the three season scenarios are discussed.

Winter Scenario

The results in the winter scenarios are visualized in Figures 6.20a and 6.21a. In the winter scenarios with FT-1, the reference control scheme performs best, followed by the rule-based,

³Each bar shows the relative change of the total costs obtained in the simulation C to the total costs obtained by the reference control scheme C_{Ref} . The relative change is defined by: $\frac{C - C_{\text{Ref}}}{|C_{\text{Ref}}|}$.

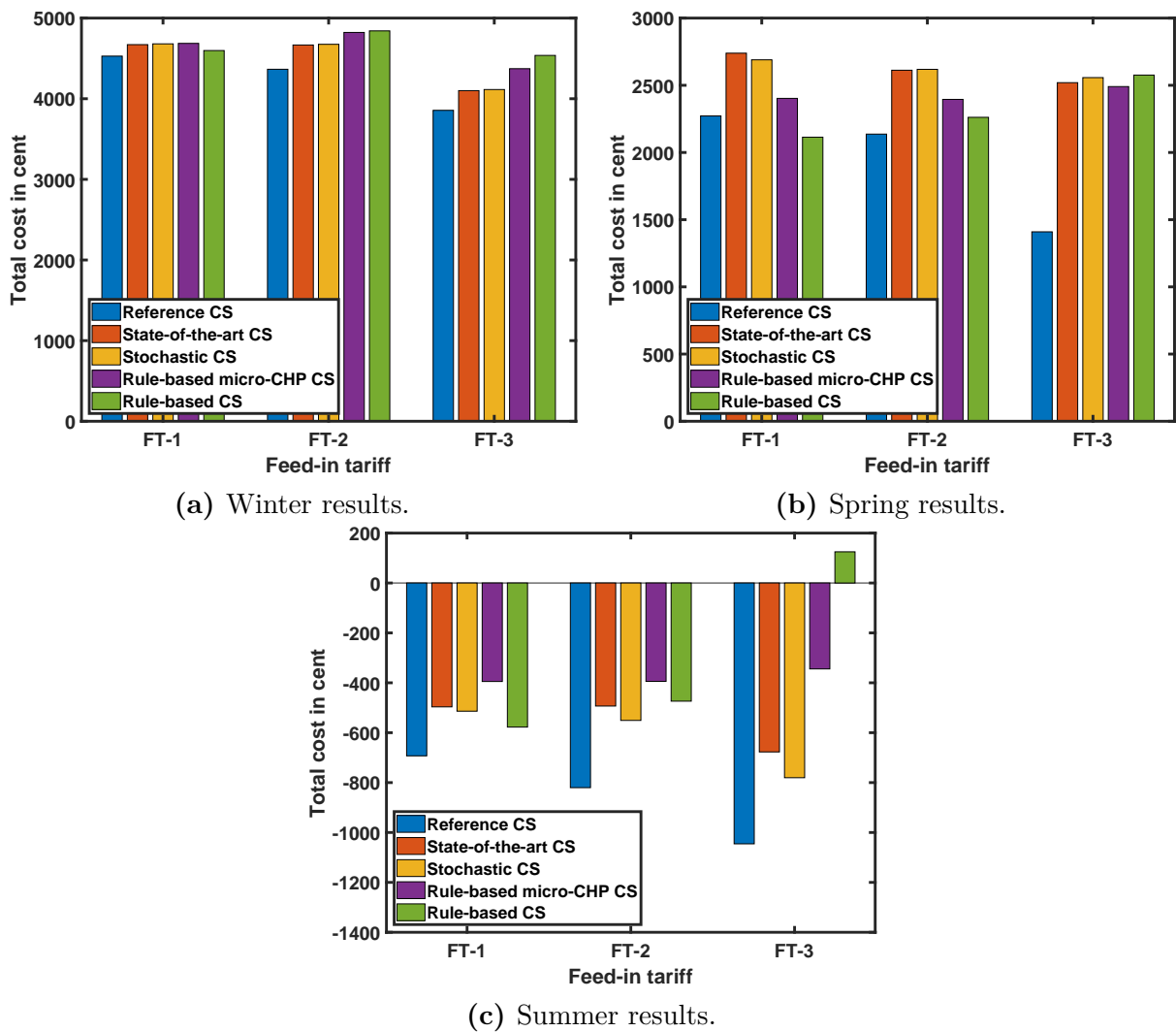


Figure 6.20: Comparison of the evaluation results for the different control schemes (CS) in the different scenarios for winter (a), spring (b) and summer (c).

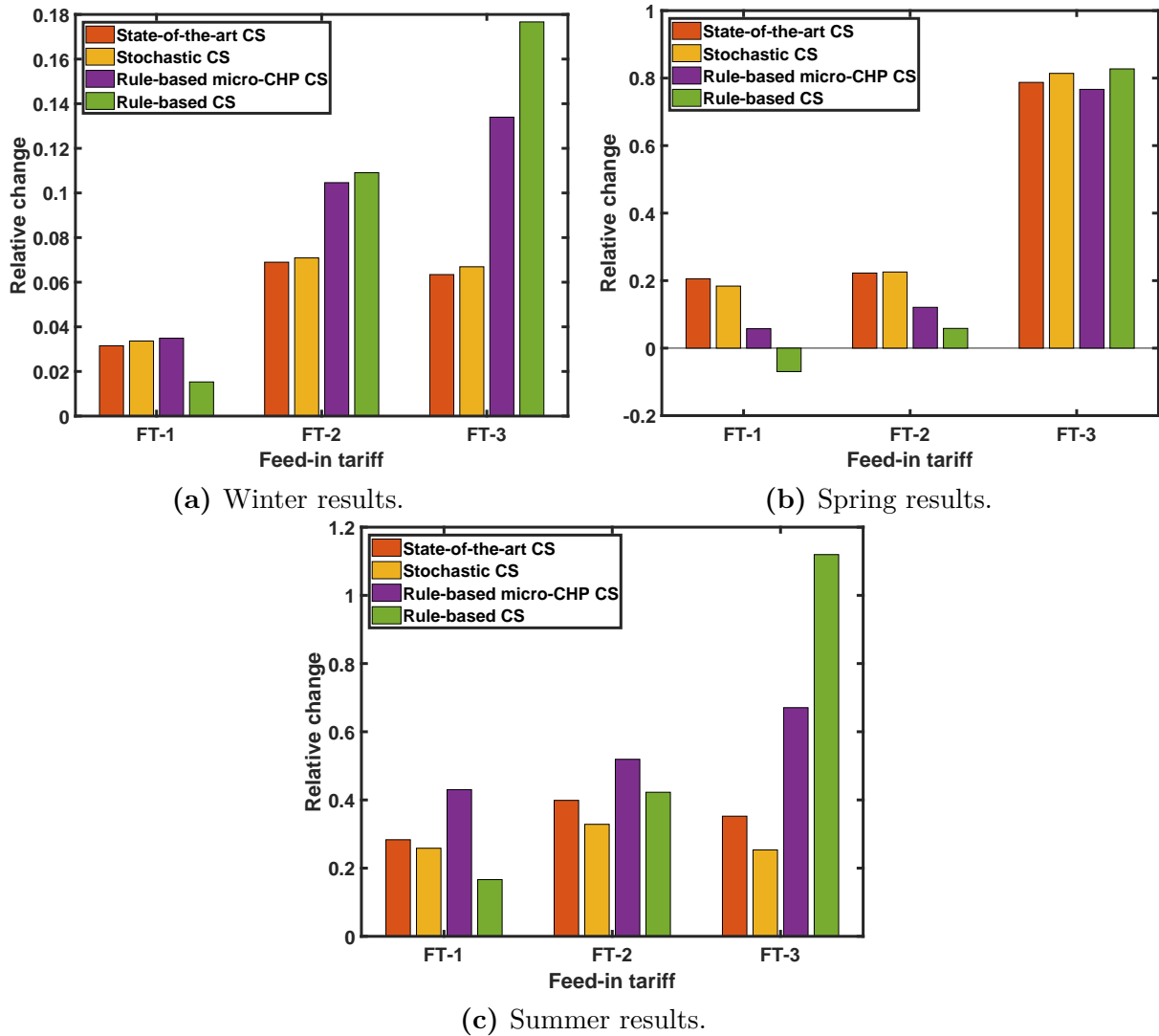


Figure 6.21: Comparison of the evaluation results for the different control schemes (CS) in the different scenarios for winter (a), spring (b) and summer (c).

Table 6.13: List of the best tuning parameter combinations in the evaluation scenarios for all control schemes.

Control scheme	Scenario		Tuning parameters		
	Season	Feed-in tariff	Δ_k in min	Δ_N in h	M
Reference	Winter	FT-1	3	48	–
Reference	Winter	FT-2	3	36	–
Reference	Winter	FT-3	3	48	–
Reference	Spring	FT-1	3	48	–
Reference	Spring	FT-2	3	30	–
Reference	Spring	FT-3	3	48	–
Reference	Summer	FT-1	3	36	–
Reference	Summer	FT-2	3	36	–
Reference	Summer	FT-3	3	48	–
State-of-the-art	Winter	FT-1	5	30	1
State-of-the-art	Winter	FT-2	5	24	1
State-of-the-art	Winter	FT-3	5	24	1
State-of-the-art	Spring	FT-1	5	30	1
State-of-the-art	Spring	FT-2	5	30	1
State-of-the-art	Spring	FT-3	5	24	1
State-of-the-art	Summer	FT-1	5	30	1
State-of-the-art	Summer	FT-2	5	30	1
State-of-the-art	Summer	FT-3	5	24	1
Stochastic	Winter	FT-1	5	24	3
Stochastic	Winter	FT-2	5	24	3
Stochastic	Winter	FT-3	5	24	3
Stochastic	Spring	FT-1	5	30	3
Stochastic	Spring	FT-2	5	30	5
Stochastic	Spring	FT-3	5	30	5
Stochastic	Summer	FT-1	5	30	3
Stochastic	Summer	FT-2	5	24	3
Stochastic	Summer	FT-3	5	30	7
Rule-based micro-CHP	Winter	FT-1	5	24	3
Rule-based micro-CHP	Winter	FT-2	5	24	3
Rule-based micro-CHP	Winter	FT-3	5	30	3
Rule-based micro-CHP	Spring	FT-1	5	24	7
Rule-based micro-CHP	Spring	FT-2	5	30	9
Rule-based micro-CHP	Spring	FT-3	5	24	1
Rule-based micro-CHP	Summer	FT-1	5	30	5
Rule-based micro-CHP	Summer	FT-2	5	30	3
Rule-based micro-CHP	Summer	FT-3	5	30	3

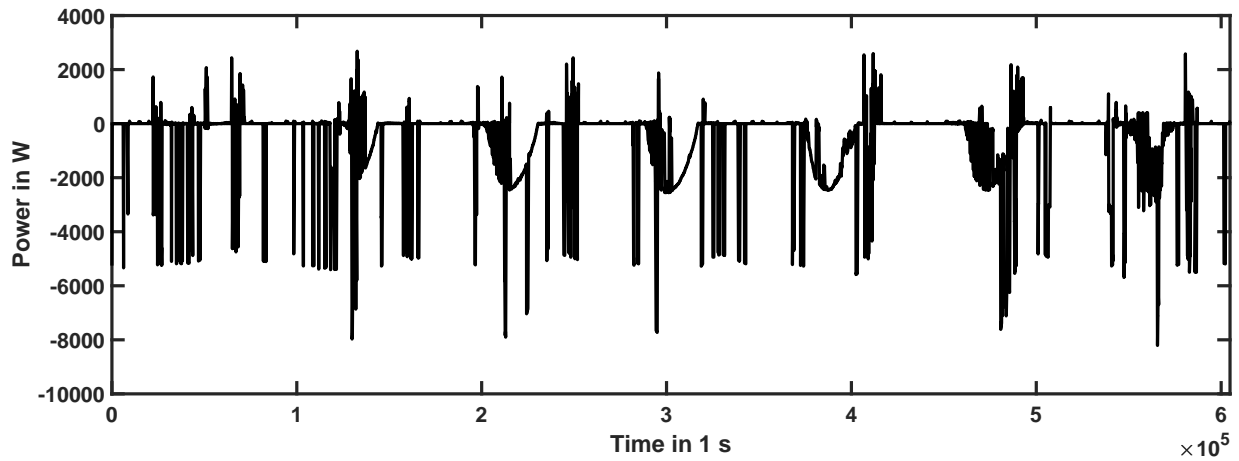
the rule-based micro-CHP, the stochastic and lastly state-of-the-art control scheme. The high performance of the rule-based control scheme is described in detail in the next section. However, the relative changes are small compared to the other scenarios. This is caused by the time-independent feed-in tariff.

In the winter scenarios with FT-2 and FT-3, the reference control scheme performs best followed by the state-of-the-art, stochastic, rule-based micro-CHP and the rule-based control scheme. Here, the state-of-the-art and the stochastic control schemes have a very similar performance that is better than the rule-based micro-CHP and the rule-based control schemes. Thus, it can be concluded that in these scenarios, the advantages of the optimization-based control surpasses their disadvantages from averaging effects. The stochastic control scheme yields no benefits over the state-of-the-art control scheme. This is caused by the low PV generation in the winter scenario.

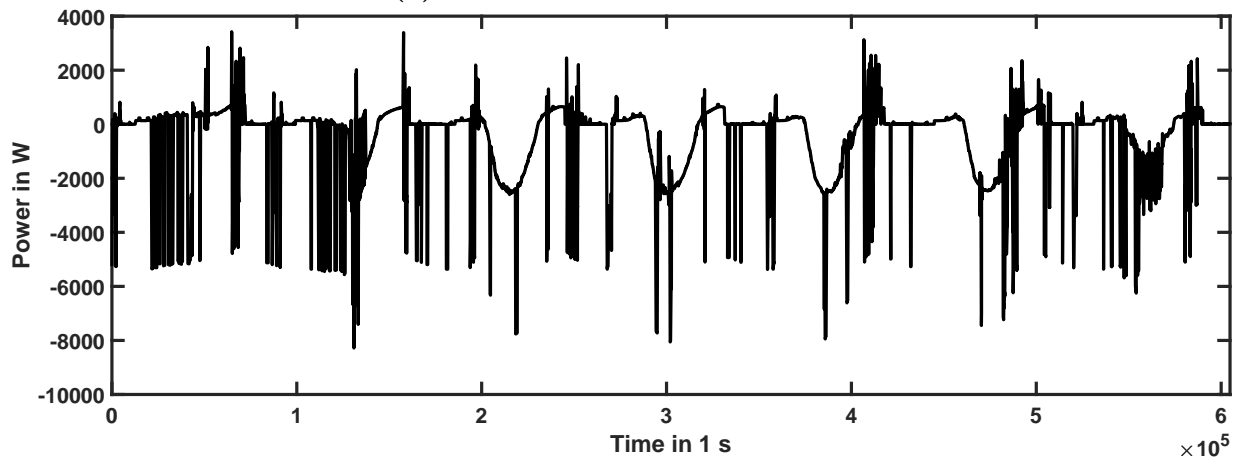
Spring Scenario

The results in the spring scenarios are visualized in Figures 6.20b and 6.21b. In the spring scenario with FT-1, the rule-based control scheme performs better than the reference control scheme. This can be explained by investigating the self-consumption and self-sufficiency rates (see Section 2.8) as well as the grid exchange powers. Table 6.14 shows the self-consumption and self-sufficiency rates for the reference and rule-based control schemes in the spring scenario with FT-1. The self-consumption and self-sufficiency rates for the state-of-the-art and stochastic control schemes are lower than the ones in the reference and the rule-based control schemes. The self-consumption and the self-sufficiency rates for the reference control scheme are higher than for the rule-based control scheme. Figure 6.22 shows a visualization of the resulting grid exchange powers in the simulations with state-of-the-art, stochastic and rule-based control schemes in the spring scenario with FT-1. However, the time steps in which an energy import from the grid occurs differ. In the optimization, the BESS schedule matches the energy consumption profile perfectly. However, in the simulation, the integrated energy consumption and generation in the 5 min time steps are equal to the optimization, the absolute values in the 1 s time steps can differ. This is the case when appliances run and an additional energy import from the grid is needed. The time-dependent electricity tariff penalizes the energy import from the grid that occurs by applying the reference control scheme. This is caused by averaging effects. This effect is higher than for the rule-based control scheme, even though, the absolute energy import from the grid is smaller. The same effect occurs in the spring scenario with FT-2 and the summer scenario with FT-1.

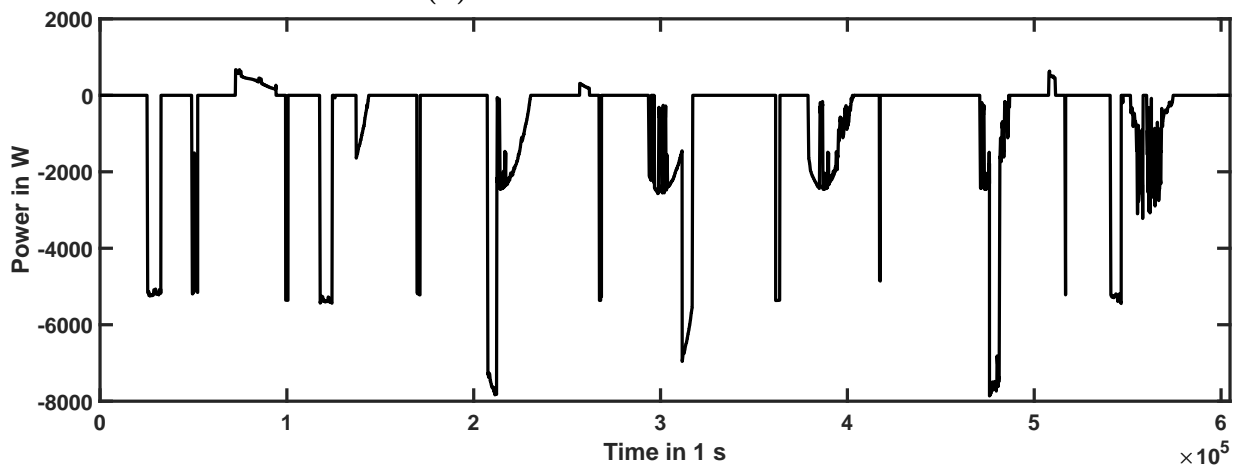
Furthermore, in the spring scenario with FT-1, FT-2 and FT-3, the rule-based micro-CHP and the rule-based control scheme perform better than the state-of-the-art and the stochastic control schemes. This can be explained by a bad PV generation forecast in the simulation period in the spring scenario, which leads to a large deviation between predicted and the actual behavior of the building energy system. In the spring scenario with FT-3, all control schemes except for the reference control scheme perform similarly. Here, the



(a) State-of-the-art control scheme.



(b) Stochastic control scheme.



(c) Rule-based control scheme.

Figure 6.22: Visualization of the grid exchange powers in the spring scenario with FT-1 and selected control schemes. (a) shows the reference control scheme, (b) shows the state-of-the-art and (c) the rule-based control scheme.

Table 6.14: Self-consumption and self-sufficiency rates for different control schemes in the spring scenario with FT-1. The stochastic control scheme uses $M = 3$.

Control scheme	Self-consumption rate	Self-sufficiency rate
Reference	0.47	0.98
State-of-the-art	0.36	0.77
Stochastic	0.37	0.77
Rule-based	0.47	0.97

Table 6.15: Self-consumption and self-sufficiency rates for different control schemes in the summer scenario with FT-1. The stochastic control scheme uses $M = 3$.

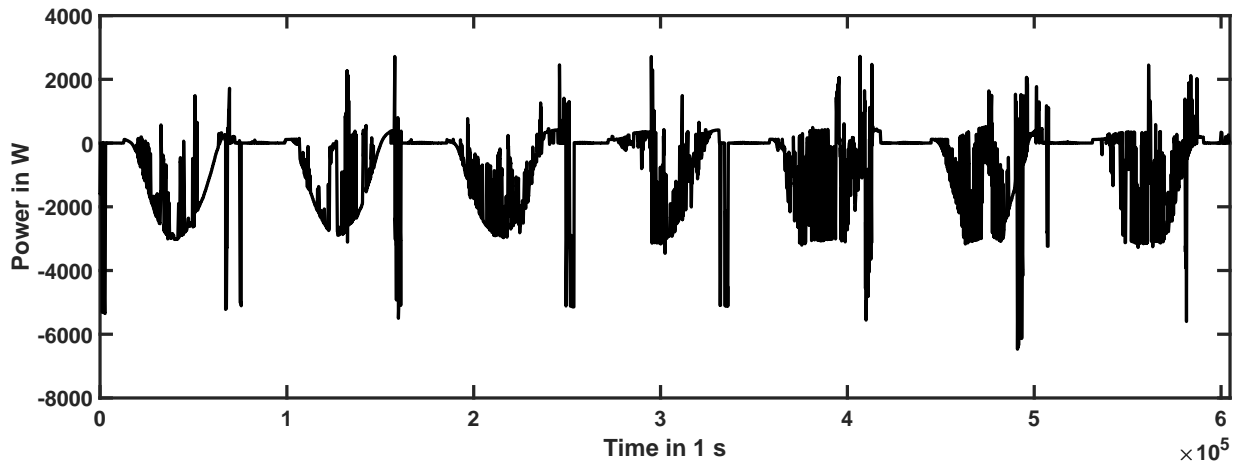
Control scheme	Self-consumption rate	Self-sufficiency rate
Reference	0.40	0.96
State-of-the-art	0.3534	0.86
Stochastic	0.36	0.87
Rule-based	0.42	0.99

disadvantages of the optimization-based control schemes induced by the bad PV generation forecasts are canceled out by the advantages induced by the extreme nature of the feed-in tariff FT-3 that rewards load shifting.

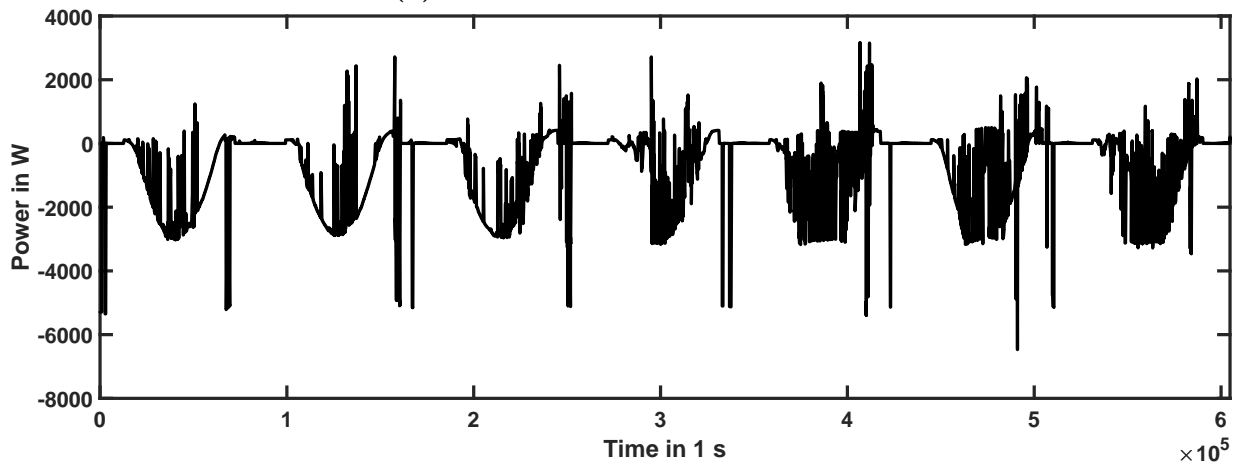
In the spring scenarios, the state-of-the-art and the stochastic control schemes have a very similar performance that is better than the rule-based micro-CHP and the rule-based control schemes. A similar performance of the stochastic and state-of-the-art control schemes are observed. This is caused the bad PV generation forecasts.

Summer Scenario

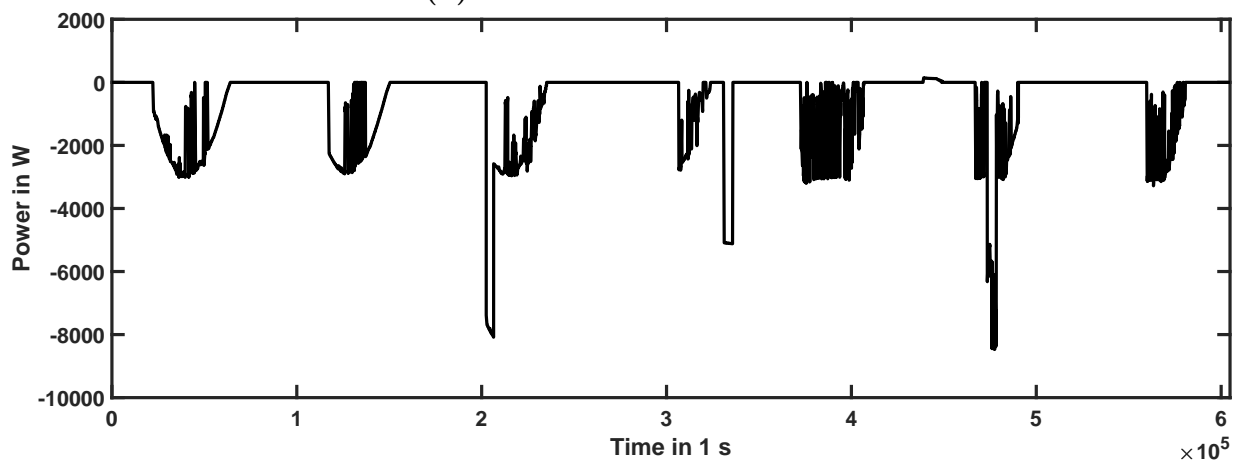
The results in the summer scenarios are visualized in Figures 6.20c and 6.21c. In the summer scenario with FT-1, the rule-based control scheme performs better than the state-of-the-art and the stochastic control scheme. This can be explained by investigating the self-consumption and self-sufficiency rates (see Section 2.8). Table 6.15 shows the self-consumption and self-sufficiency rates for the reference and rule-based control schemes in the summer scenario with FT-1. Here, the stochastic control scheme uses $M = 3$. The self-consumption and the self-sufficiency rates for the rule-based control are higher than for the other two optimization-based control schemes. This is caused by the higher energy import from the grid in the two optimization-based control schemes. This results from averaging effects as described in the last section discussing the spring scenarios with FT-1 and FT-2. In the optimization, the BESS schedule matches the energy consumption profile perfectly. It can also be observed by investigating the resulting grid exchange powers. Figure 6.23 shows a visualization of the resulting grid exchange powers in the simulations



(a) State-of-the-art control scheme.



(b) Stochastic control scheme.



(c) Rule-based control scheme.

Figure 6.23: Visualization of the grid exchange powers in the summer scenario with FT-1 and selected control schemes. (c) shows the rule based control scheme, (a) shows the state-of-the-art and (b) the stochastic rolling horizon approach with $M = 3$.

with state-of-the-art, stochastic and rule-based control schemes in the summer scenario with FT-1.

In summary, the gain by performing load shifting is not enough compared to the loss introduced by the averaging effects. This is, in particular, the case in the scenarios with FT-1. Since FT-1, caused by the time-independent feed-in compensation, does not incentivize load shifting. The effect of the time-averaging caused by the different time step durations in the simulation and optimization, $\Delta_t \neq \Delta_k$, occurs in all scenarios. However, in the scenarios with FT-2 and FT-3 the gains from load shifting exceed the losses introduced by the averaging effects.

The rule-based micro-CHP performs the worst in the summer scenarios with FT-1 and FT-2. In the summer scenario with FT-3, it performs the second worst, performing better than the rule-based control. In all summer scenarios, the stochastic control scheme outperforms the state-of-the-art control scheme. This effect increases from FT-1 to FT-2 to FT-3. Here, FT-1 does not reward any load shifting, while FT-2 and FT-3 do. However, the feed-in compensation profile of FT-3 yields higher rewards than the one of FT-2.

6.7 Discussion of the Results

The evaluation presented in this chapter targeted the assessment of the performance of the stochastic two-stage rolling horizon approach presented in Section 5.8. To do so, simulations of a smart building, which uses different control schemes, have been performed. The performance of the control schemes is measured by total costs defined in Section 5.3. To evaluate the dependence of the total costs on the season as well as the feed-in tariff, both parameters are varied in the simulations.

The stochastic control scheme that uses the stochastic two-stage rolling horizon optimization approach presented in this thesis (see Section 5.8) provides an increase in performance with respect to the other control schemes in the evaluated smart building configuration (see Figures 6.20 and 6.21). However, these improvements are limited to the summer scenarios with time-dependent feed-in tariffs. In addition, the optimization problem that has to be solved in the stochastic control scheme has more decision variables than the one in the state-of-the-art control scheme (cf, Sections 5.7 and 5.8). This leads to a higher computational effort to solve the optimization and thus longer optimization times (see Figures 6.12, B.12 and B.13).

Additionally, the dependence of the performance of the control schemes on the tuning parameters is investigated. In total there are three tuning parameters: the time step duration, the duration of the optimization window and the number of forecast scenarios. Here, the evaluation shows that shorter time step durations and longer optimization windows lead to lower total cost. However, both, shorter time step durations and longer optimization windows, lead to more decision variables and consequently the optimization times increase. Here, the performance increases by decreasing the time step durations and

increasing the duration of the optimization windows can be observed even if these measures lead to optimization runs that are stopped by the time limit of the optimization.

In case of the number of forecast scenarios, no simple dependence can be observed (see Table 6.13). In six scenarios, three forecast scenarios perform best, in three scenarios five forecast scenarios perform best and in one scenario seven forecast scenarios perform best. A similar result is observed for the rule-based micro-CHP control scheme. Here, three reasons could be identified: Firstly, the computational effort that is introduced by increasing the number of uncertainty parameters in combination with the time limit leads to poor optimization results. Secondly, the simulation period is too short and the uncertainty in the PV generation forecasts by chance leads to inferior results. Finally, the chosen PV generation method leads to a specific number of forecast scenarios being optimal. Here, other choices could be too pessimistic or too optimistic. This means that the performance of the stochastic control scheme depends on the PV generation forecast.

In summary, when designing an optimization-based control scheme for smart buildings, the designer of the system has to define three tuning parameters, ideally maximizing the optimization window and minimizing the time step duration until no further improvement of the performance of the optimization-based control scheme occurs. Additionally, the number of forecast scenarios has to be chosen. In a real building, the computation power is typically limited. Thus, the computing budget has to be utilized optimally and not all values can be chosen optimally. When looking at the presented building configuration and evaluation scenarios, the improvements gained by the stochastic control scheme are limited to the summer scenarios with time-dependent feed-in tariffs while increasing the computational effort significantly. Thus, the designer of the system has to weigh up the potential performance increase and the increasing computational effort that results from applying the stochastic control scheme instead of the state-of-the-art control scheme.

A similar observation has been made by Scott et al. [223]. They state that the stochastic control scheme does not perform better than the state-of-the-art control scheme. Furthermore, they state that the optimization-based control schemes always outperform the rule-based control schemes in their evaluation. However, they only investigate time step durations of 30 min.

To sum up, the stochastic control scheme that utilizes the stochastic two-stage rolling horizon approach presented in this thesis (see Section 5.8) provides an increase in performance with respect to the other control schemes in the evaluated smart building configuration. However, these improvements are limited to the summer scenario with a time-dependent feed-in tariff. This means that the presented approach is in particular suitable in scenarios in which the full load shifting potential of a BESS can be utilized. These scenarios have high electricity generation from a photovoltaic system, which are either results from a large photovoltaic system or a high solar irradiation. Furthermore, they have time dependent electricity consumption and feed-in tariffs.

6.7.1 Limitations

The presented control scheme, the used models, the building configuration and the evaluation scenarios are subject to limitations which are summarized in this section.

First of all, only the uncertainties in the PV generation are investigated. The uncertainty of the energy consumption has not been addressed. Furthermore, a limited optimization time, which limits the analysis of the full potential of the stochastic control scheme, has been used in the evaluation. The optimization runs in the optimization-based control schemes are coupled, which means the result of one optimization run influences the inputs for the next optimization run. If one of the optimization run is not solved optimally, for example due to the optimization time limit, the non-optimal result creates an input for the next optimization run. Even if these next optimization runs are solved optimally, the error that is made in the optimization run with a non-optimal solution can become larger over several optimization runs, creating a chain reaction that is hard to investigate.

Moreover, due to the high optimization times, only a limited number of forecast scenarios is used in the stochastic control scheme. Additionally, the specific tariff schemes are discussed and specific relations are required (see Section 5.6.9). For example, a feed-in to the grid from the BESS or power limits have not been investigated. Furthermore, only one building configuration has been analyzed.

6.7.2 Future Opportunities

As described above, a suitable control scheme has to be chosen in every scenario. Thus, an on-line choice on the control schemes could be beneficial. This means that an overlaying control mechanism could choose a suitable control scheme for a specific situation during the run-time of the building energy system. One example is a rule-based decision that chooses different control schemes based on the season. However, more advanced approaches could be used, for example optimization-based control mechanisms. Such an approach has been proposed and investigated as part of this doctoral project [174]. Here, on-line choice of the control schemes has been proposed in combination with a simulation-based optimization that uses a Genetic Algorithm (GA).

The long optimization times that are needed to solve the optimization problems could be reduced by applying a heuristic to solve the optimization problems. For example, a GA has been successfully applied in the domain of smart buildings [165, 174, 179]. However, a GA is not suitable to solve the optimization problems that arise from the building energy system model that is presented in this thesis. Initial experiments showed that a GA hardly finds valid solutions of the optimization problem due to the large number of constraints that have to be defined in order to formulate a MILP model. Consequently, GAs should be used with different models, for example with non-linear models as it is done in [165, 174, 179]. This can reduce the number of decision variables and reduce the limitations which are introduced by the use of MILP models, e.g., additional constraints. For example, when using a MILP model, the starting time of an appliance that can only be switched on or

off has to be modeled using several binary or integer decision variables. In the case of non-linear models, this can be modeled using one integer or real-valued decision variable (cf. [9, 163, 165]). However, comparing an optimization-based control scheme that is using a MILP model to one that is using a non-linear model is challenging. Assuming that suitable optimization algorithms are available, it has to be ensured that both models lead to the same behavior of the energy system. To do so, the optimal solutions of all possible optimization problems that occur in the rolling horizon optimization have to be equal.

If an adapted optimization model in combination with a fast optimization algorithm can be achieved, more forecast scenarios of the PV generation could be included to potentially increase the performance of the stochastic control scheme.

In addition, the presented stochastic control scheme can be applied to other smart building configurations. These could potentially benefit more from the stochastic two-stage rolling horizon approach. The observations that are made for the rule-based micro-CHP control scheme indicate that for other smart building configurations, the optimization time can be reduced. For example, the micro-CHP considered in this thesis, i. e. the Senertec Dachs G5.5 (see Section 5.6.2), can only be switched on or off. This has to be modeled with binary decision variables, which leads to a combinatorial optimization problem. Other micro-CHPs which allow for a continuous choice of the operating power can be modeled using real-valued decision variables. This can lead to optimization problems that can be solved much faster.

Even though, the stochastic control scheme that uses the stochastic two-stage rolling horizon optimization approach does not provide a higher performance than the state-of-the-art control scheme, it generates one predicted load profile for every forecast scenario. These load profiles can be potentially used in combination with a higher-level DSM.

7. Conclusion

After the evaluation of the proposed stochastic two-stage rolling horizon optimization approach has been presented in Chapter 6, this chapter gives a final summary of the content of this thesis and a final conclusion is drawn (see Section 7.1). After that, open questions are named and potential further research is motivated (see Section 7.2).

7.1 Summary and Conclusion

The increased use of RESs as well as the introduction of DERs into the energy grids leads to a change in the energy system, changing the conventional central paradigm of electricity distribution from “supply follows demand” to “demand follows supply”. This change calls for new control and coordination mechanisms and systems that ensure a secure supply of affordable energy. BEMSs are an example for these systems. They enable smart buildings to manage their energy system to increase their efficiency, reduce the operating costs and provide DR measures.

This thesis focuses on increasing the performance of BEMSs by investigating the utilization of the knowledge of uncertainties in the forecasts of energy generation and consumption in optimization-based control schemes. To do so, three research questions have been compiled (see Section 1.1). These questions have been addressed as follows:

Research Question 1: How can uncertainties be included in the optimization in building energy management?

In Chapter 3, theoretical concepts and formulations related to the modeling of discrete time systems and their optimized operation by a rolling horizon optimization are introduced. Moreover, an introduction to decision-making under uncertainty and the respective mathematical concepts is given. The modeling of energy systems in buildings is further analyzed and related work in the literature is summarized in Chapter 4. This includes

the design of PV generation forecasts and in particular probabilistic forecasts. After that, remarks on BEMSs and implementations of such are presented. This is followed by a detailed analysis of the related work in the field of optimizing the operation of energy systems in buildings as well as the handling of uncertainties in the forecasts of the energy generation and consumption. After analyzing these topics, a stochastic two-stage rolling horizon optimization approach has been identified to yield the highest potential of including uncertainties in the optimization in building energy management. It is presented in detail in Chapter 5.

Research Question 2: How can a suitable forecast for BEMSs be achieved?

To enable the consideration of the uncertainties in the PV generation forecast in the stochastic two-stage rolling horizon optimization approach, a probabilistic PV generation forecast that generates forecast scenarios based on a quantile regression has been designed. It is presented in Section 5.6.3.

Research Question 3: What is the performance of the proposed approach?

The proposed approach is evaluated in nine evaluation scenarios using a specific building configuration assuming the presence of time-dependent electricity consumption and feed-in tariffs. In each evaluation scenario the feed-in tariff and the season are varied. The investigated building configuration comprises a controllable washing machine, a controllable battery energy storage systems and a controllable micro combined heat and power plant as well as additional electricity and heat consumption from non-controllable sources. In the evaluation, the presented approach is compared to a reference control scheme, using a perfect forecast of the electricity generation from the PV system, to a state-of-the-art rolling horizon optimization that uses a single-point forecast and to a rule-based control scheme. To identify the dependence on the tuning parameters in the optimization-based control schemes, several parameter combinations have been investigated. The performance of the control schemes is measured using the operating costs in a simulation of seven days. The evaluation of the stochastic two-stage rolling horizon optimization approach is presented in Chapter 6.

The discussion in Section 6.7 presents the results of the evaluations in detail as well as limitations and opportunities for future research. The results state that the reference control scheme performs best in all scenarios but one. In seven scenarios, the stochastic two-stage rolling horizon optimization approach performs similarly to a one-stage rolling horizon optimization approach that uses a single-point PV generation forecast. However, in two scenarios it performs better. These are the scenarios with the highest expected DR potential, or more precisely the summer scenarios with time-dependent feed-in tariffs. Here, the summer scenario is the scenario with the highest PV generation and the lowest heat consumption. However, the stochastic two-stage rolling horizon optimization approach leads to higher optimization times than the one-stage rolling horizon optimization approach.

In conclusion, the stochastic two-stage rolling horizon optimization approach yields an increase in performance with respect to the one-stage rolling horizon optimization approach

in specific scenarios. Hence, an application of the approach can be worthwhile, while the increased computational effort has to be respected.

7.2 Outlook

From the presented thesis three topics arise that lay the basis for potential future work. Firstly, an improvement of the presented approach to the optimized operation of building energy systems can be investigated. Other scenarios and other building configurations can be explored. Furthermore, the PV generation forecast can be improved and the resulting influence on the control schemes can be investigated. Moreover, the application of heuristics yields a potential to decrease the optimization times. This can be combined with a different building energy system model, for example by utilizing a non-linear model as it is done in [165, 174, 179]. In addition, more forecast scenarios, which increases the sampling quality of the PV generation, can be investigated to potentially increase the performance of the stochastic two-stage rolling horizon optimization approach. As described in the last section, a suitable control scheme as well as suitable choice of the tuning parameters has to be chosen in every scenario. Thus, an on-line choice of the control schemes could be beneficial. This approach has been proposed and investigated as part of this doctoral project [174]. Furthermore, this thesis is limited to single smart residential building configuration having a specific set of devices and to an optimization of the operating costs. Therefore, future work may investigate the performance of the proposed approach for different building configurations and optimization goals. Additionally, more uncertainty sources can be considered in the optimization, for example, the uncertainty in the energy consumption.

Secondly, this thesis only shortly discusses a possible application of the presented control scheme. Here, future work is needed to finish the proposed concepts on the adaptivity of the optimization model to enable the application in a commercial BEMS and real buildings.

The stochastic two-stage rolling horizon optimization approach as well as the other control schemes investigated in this thesis focus on reducing the operating costs of building energy systems in buildings equipped with an automated BEMS, i.e., smart buildings. The final topic addresses the coordination of these buildings and their participation in DSM measures is assumed to be realized through the use of time-dependent tariffs. However, the generation of these time-dependent tariffs is an active field of research [96, 136] and analyzing the potential application of the approaches presented in this thesis in combination with tariff-based coordination schemes would be worthwhile. In particular, the potential of generating one predicted load profile for every forecast scenario could potentially be used in DSM, for example in direct market demand response methods. To enable the coordination of DER as well as smart buildings in the sense of a smart grid, methods other than the tariff-based coordination schemes could be used. The presented approach could be adopted to allow for other coordination measures like physical or direct market demand response methods. When adopting the approach of an on-line choice of the control schemes, individual control schemes could be designed for each of these DSM methods.

Bibliography

- [1] Directive 2012/27/EU of the European Parliament and of the Council of 25 October 2012 on energy efficiency, amending Directives 2009/125/EC and 2010/30/EU and repealing Directives 2004/8/EC and 2006/32/EC Text with EEA relevance.
- [2] “Erneuerbare-Energien-Gesetz vom 21. Juli 2014 (BGBl. I S. 1066), das zuletzt durch Artikel 5 des Gesetzes vom 13. Mai 2019 (BGBl. I S. 706) geändert worden ist.”
- [3] K. Abdulla, J. de Hoog, V. Muenzel, F. Suits, K. Steer, A. Wirth, and S. Halgamuge, “Optimal Operation of Energy Storage Systems Considering Forecasts and Battery Degradation,” *IEEE Transactions on Smart Grid*, vol. 9, no. 3, pp. 2086–2096, 2018.
- [4] T. Ackermann, G. Andersson, and L. Söder, “Distributed generation: a definition,” *Electric Power Systems Research*, vol. 57, no. 3, pp. 195–204, 2001.
- [5] C. O. Adika and L. Wang, “Autonomous Appliance Scheduling for Household Energy Management,” *IEEE Transactions on Smart Grid*, vol. 5, no. 2, pp. 673–682, 2014.
- [6] C. O. Adika and L. Wang, “Smart charging and appliance scheduling approaches to demand side management,” *International Journal of Electrical Power & Energy Systems*, vol. 57, pp. 232–240, 2014.
- [7] Y. Agarwal, B. Balaji, R. Gupta, J. Lyles, M. Wei, and T. Weng, “Occupancy-driven energy management for smart building automation,” in *Proceedings of the 2nd ACM Workshop on Embedded Sensing Systems for Energy-Efficiency in Building - BuildSys '10*. ACM Press, 2010.
- [8] A. A. Akhil, G. Huff, A. B. Currier, B. C. Kaun, D. M. Rastler, S. B. Chen, A. L. Cotter, D. T. Bradshaw, and W. D. Gauntlett, *DOE/EPRI 2013 electricity storage handbook in collaboration with NRECA*. Sandia National Laboratories Albuquerque, NM, 2013.
- [9] F. Allering, *Organic Smart Home : Energiemanagement für Intelligente Gebäude*. Karlsruhe: KIT Scientific Publishing, 2014, PhD thesis.
- [10] D. Angeli, “Economic Model Predictive Control,” in *Encyclopedia of Systems and Control*. Springer London, 2014, pp. 1–9.

- [11] D. Angeli, R. Amrit, and J. B. Rawlings, “On Average Performance and Stability of Economic Model Predictive Control,” *IEEE Transactions on Automatic Control*, vol. 57, no. 7, pp. 1615–1626, 2012.
- [12] D. Angeli, A. Casavola, and F. Tedesco, “Theoretical advances on Economic Model Predictive Control with time-varying costs,” *Annual Reviews in Control*, vol. 41, pp. 218–224, 2016.
- [13] J. Antonanzas, N. Osorio, R. Escobar, R. Urraca, F. M. de Pison, and F. Antonanzas-Torres, “Review of photovoltaic power forecasting,” *Solar Energy*, vol. 136, pp. 78–111, 2016.
- [14] R. R. Appino, J. Á. G. Ordiano, R. Mikut, T. Faulwasser, and V. Hagenmeyer, “On the use of probabilistic forecasts in scheduling of renewable energy sources coupled to storages,” *Applied Energy*, vol. 210, pp. 1207–1218, 2018.
- [15] J. April, F. Glover, J. P. Kelly, and M. Laguna, “Practical Introduction to Simulation Optimization,” in *Proceedings of the 35th Conference on Winter Simulation: Driving Innovation*, ser. WSC '03. Winter Simulation Conference, 2003, pp. 71–78.
- [16] H. Bagge and D. Johansson, “Measurements of household electricity and domestic hot water use in dwellings and the effect of different monitoring time resolution,” *Energy*, vol. 36, no. 5, pp. 2943–2951, 2011.
- [17] J. Baker, “New technology and possible advances in energy storage,” *Energy Policy*, vol. 36, no. 12, pp. 4368–4373, 2008.
- [18] L. Barth, N. Ludwig, E. Mengelkamp, and P. Staudt, “A comprehensive modelling framework for demand side flexibility in smart grids,” *Computer Science - Research and Development*, vol. 33, no. 1-2, pp. 13–23, 2017.
- [19] E. M. L. Beale, “On Minimizing A Convex Function Subject to Linear Inequalities,” *Journal of the Royal Statistical Society. Series B (Methodological)*, vol. 17, no. 2, pp. 173–184, 1955.
- [20] M. Beaudin and H. Zareipour, “Home energy management systems: A review of modelling and complexity,” *Renewable and Sustainable Energy Reviews*, vol. 45, no. Supplement C, pp. 318–335, 2015.
- [21] B. Becker, A. Kellerer, and H. Schmeck, “User interaction interface for Energy Management in Smart Homes,” in *2012 IEEE PES Innovative Smart Grid Technologies (ISGT)*. IEEE, 2012.
- [22] B. Becker, F. Kern, M. Loesch, I. Mauser, and H. Schmeck, “Building Energy Management in the FZI House of Living Labs,” in *Energy Informatics, Chapter 9*, ser. Lecture Notes in Computer Science. Springer, 2015, vol. 9424.

-
- [23] R. Becker, “Optimierung thermischer Systeme in dezentralen Energieversorgungsanlagen,” PhD thesis, University of Dortmund, Dortmund, Germany, 2006.
- [24] R. Bellman, “On the Theory of Dynamic Programming,” *Proceedings of the National Academy of Sciences*, vol. 38, no. 8, pp. 716–719, 1952.
- [25] R. Bellman and E. Lee, “History and development of dynamic programming,” *IEEE Control Systems Magazine*, vol. 4, no. 4, pp. 24–28, 1984.
- [26] R. Bellman, *Dynamic Programming*. Princeton, NJ.: Princeton, University Press, 1957.
- [27] A. Ben-Tal, L. E. Ghaoui, and A. Nemirovski, *Robust Optimization (Princeton Series in Applied Mathematics)*. Princeton University Press, 2009.
- [28] M. Benichou, J. M. Gauthier, P. Girodet, G. Hentges, G. Ribiere, and O. Vincent, “Experiments in mixed-integer linear programming,” *Mathematical Programming*, vol. 1, no. 1, pp. 76–94, 1971.
- [29] D. Bertsimas and D. B. Brown, “Constructing Uncertainty Sets for Robust Linear Optimization,” *Operations Research*, vol. 57, no. 6, pp. 1483–1495, 2009.
- [30] D. Bertsimas, D. B. Brown, and C. Caramanis, “Theory and Applications of Robust Optimization,” *SIAM Review*, vol. 53, no. 3, pp. 464–501, 2011.
- [31] J. R. Birge and F. Louveaux, *Introduction to Stochastic Programming*. Springer, 2011.
- [32] N. Blaauwbroek, P. H. Nguyen, H. Shi, I. G. Kamphuis, W. L. Kling, and M. J. Kongsman, “Optimal resource allocation and load scheduling for a multi-commodity smart energy system,” in *2015 IEEE PowerTech*, 2015.
- [33] B. Bøhm, “Production and distribution of domestic hot water in selected Danish apartment buildings and institutions. Analysis of consumption, energy efficiency and the significance for energy design requirements of buildings,” *Energy Conversion and Management*, vol. 67, pp. 152–159, 2013.
- [34] G. E. Box, G. M. Jenkins, G. C. Reinsel, and G. M. Ljung, *Time series analysis: forecasting and control*. John Wiley & Sons, 2015.
- [35] S. Boyd, “Distributed Optimization and Statistical Learning via the Alternating Direction Method of Multipliers,” *Foundations and Trends® in Machine Learning*, vol. 3, no. 1, pp. 1–122, 2010.
- [36] M. C. Bozchalui, S. A. Hashmi, H. Hassen, C. A. Canizares, and K. Bhattacharya, “Optimal Operation of Residential Energy Hubs in Smart Grids,” *IEEE Transactions on Smart Grid*, vol. 3, no. 4, pp. 1755–1766, 2012.

- [37] M. Braun, T. Dengiz, I. Mauser, and H. Schmeck, “Comparison of Multi-objective Evolutionary Optimization in Smart Building Scenarios,” in *Applications of Evolutionary Computation*, G. Squillero and P. Burelli, Eds. Springer International Publishing, 2016, pp. 443–458.
- [38] J. B. Bremnes, “Probabilistic wind power forecasts using local quantile regression,” *Wind Energy*, vol. 7, no. 1, pp. 47–54, 2004.
- [39] Bundesnetzagentur, “Fördersätze für PV-Anlagen - Anzulegende Werte für Solaranlagen August bis Oktober 2018,” online, 2018, retrieved 25.10.2018 https://www.bundesnetzagentur.de/DE/Sachgebiete/ElektrizitaetundGas/Unternehmen_Institutionen/ErneuerbareEnergien/ZahlenDatenInformationen/EEG_Registerdaten/EEG_Registerdaten_node.html.
- [40] A. Buttler, J. Hentschel, S. Kahlert, and M. Angerer, “Statusbericht Flexibilitätsbedarf im Stromsektor,” Technische Universität München, Lehrstuhl für Energiesysteme, Tech. Rep., 2015.
- [41] BYD Company Limited, “Battery-Box Pro Specification,” online, 2017, retrived 21.01.2019 from <http://en.byd.com/energy/download/low-voltage/B-Box%20Low%20Voltage%20Specification.pdf>.
- [42] J. M. Carrasco, L. G. Franquelo, J. T. Bialasiewicz, E. Galvan, R. C. PortilloGuisado, M. A. M. Prats, J. I. Leon, and N. Moreno-Alfonso, “Power-Electronic Systems for the Grid Integration of Renewable Energy Sources: A Survey,” *IEEE Transactions on Industrial Electronics*, vol. 53, no. 4, pp. 1002–1016, 2006.
- [43] M. Carrion and J. M. Arroyo, “A computationally efficient mixed-integer linear formulation for the thermal unit commitment problem,” *IEEE Transactions on Power Systems*, vol. 21, no. 3, pp. 1371–1378, 2006.
- [44] M. Castillo-Cagigal, E. Caamaño-Martín, E. Matallanas, D. Masa-Bote, A. Gutiérrez, F. Monasterio-Huelin, and J. Jiménez-Leube, “PV self-consumption optimization with storage and Active DSM for the residential sector,” *Solar Energy*, vol. 85, no. 9, pp. 2338–2348, 2011.
- [45] CEN-CENELEC-ETSI Smart Grid Coordination Group, “SG-CG/M490/L Flexibility Management – Overview of the main concepts of flexibility management – Version 3.0,” 2014.
- [46] H. Chen, T. N. Cong, W. Yang, C. Tan, Y. Li, and Y. Ding, “Progress in electrical energy storage system: A critical review,” *Progress in Natural Science*, vol. 19, no. 3, pp. 291–312, 2009.
- [47] M. Chen and G. Rincon-Mora, “Accurate electrical battery model capable of predicting runtime and I-V performance,” *Energy Conversion, IEEE Transactions on*, vol. 21, no. 2, pp. 504–511, 2006.

-
- [48] Z. Chen, L. Wu, and Y. Fu, “Real-Time Price-Based Demand Response Management for Residential Appliances via Stochastic Optimization and Robust Optimization,” *IEEE Transactions on Smart Grid*, vol. 3, no. 4, pp. 1822–1831, 2012.
- [49] S. Chu, Y. Cui, and N. Liu, “The path towards sustainable energy,” *Nature Materials*, vol. 16, no. 1, pp. 16–22, 2017.
- [50] CIGRÉ C6.22 Working Group, “Microgrids 1: engineering, economics, & experience - Capabilities, Benefits, Business Opportunities, and Examples - Microgrid Evolution Roadmap,” 2015.
- [51] C. Clastres, T. H. Pham, F. Wurtz, and S. Bacha, “Ancillary services and optimal household energy management with photovoltaic production,” *Energy*, vol. 35, no. 1, pp. 55–64, 2010.
- [52] C. J. Cleveland and C. Morris, Eds., *Dictionary of Energy (Second Edition)*. Boston: Elsevier, 2015.
- [53] R. L. Conkling, *Energy Pricing*. Springer Berlin Heidelberg, 2011.
- [54] T. H. Cormen, C. E. Leiserson, R. L. Rivest, and C. Stein, *Introduction to Algorithms*. The MIT Press, 2009.
- [55] Council of the European Union, “Presidency conclusions 7224/1/07 REV 1 CONCL 1,” Brussels European Council 2007, 2007.
- [56] D. B. Crawley, J. W. Hand, M. Kummert, and B. T. Griffith, “Contrasting the capabilities of building energy performance simulation programs,” *Building and Environment*, vol. 43, no. 4, pp. 661–673, 2008, part Special: Building Performance Simulation.
- [57] D. B. Crawley, L. K. Lawrie, F. C. Winkelmann, W. Buhl, Y. Huang, C. O. Pedersen, R. K. Strand, R. J. Liesen, D. E. Fisher, M. J. Witte, and J. Glazer, “EnergyPlus: creating a new-generation building energy simulation program,” *Energy and Buildings*, vol. 33, no. 4, pp. 319–331, 2001.
- [58] G. B. Dantzig, “Linear Programming under Uncertainty,” *Management Science*, vol. 1, no. 3-4, pp. 197–206, 1955.
- [59] J. de Hoog, K. Abdulla, R. R. Kolluri, and P. Karki, “Scheduling Fast Local Rule-Based Controllers for Optimal Operation of Energy Storage,” in *Proceedings of the Ninth International Conference on Future Energy Systems - e-Energy '18*. ACM Press, 2018, pp. 68–172.
- [60] Die deutschen Übertragungsnetzbetreiber, “Netzentwicklungsplan Strom 2030, Version 2017. Zweiter Entwurf der Übertragungsnetzbetreiber,” online, retrieved 26.02.2019 www.netzentwicklungsplan.de, 2017.

- [61] DIN Deutsches Institut für Normung e. V., “ISO 50001 - Energy management systems - Requirements with guidance for use (ISO 50001:2011),” 2011.
- [62] I. Dincer, “On thermal energy storage systems and applications in buildings,” *Energy and Buildings*, vol. 34, no. 4, pp. 377–388, 2002.
- [63] Directorate-General for Energy (European Commission), *EU energy in figures: Statistical pocketbook 2017*. Luxembourg: Publications Office of the European Union, 2017.
- [64] DOE U.S. Department of Energy, Office of Electricity Delivery and Energy Reliability. Office of Electricity Delivery and Energy Reliability, “Smart Grid R&D Program: Summary: Report,” 2012 DOE Microgrid Workshop – July 30-31, – Chicago, USA, 2012.
- [65] H. Doukas, K. D. Patlitzianas, K. Iatropoulos, and J. Psarras, “Intelligent building energy management system using rule sets,” *Building and Environment*, vol. 42, no. 10, pp. 3562–3569, 2007.
- [66] A. Dounis and C. Caraiscos, “Advanced control systems engineering for energy and comfort management in a building environment - A review,” *Renewable and Sustainable Energy Reviews*, vol. 13, no. 6, pp. 1246–1261, 2009.
- [67] M. Doyle, “Modeling of Galvanostatic Charge and Discharge of the Lithium / Polymer / Insertion Cell,” *Journal of The Electrochemical Society*, vol. 140, no. 6, p. 1526, 1993.
- [68] M. Dvořák and P. Havel, “Combined heat and power production planning under liberalized market conditions,” *Applied Thermal Engineering*, vol. 43, pp. 163–173, 2012.
- [69] M. Ecker, N. Nieto, S. Käbitz, J. Schmalstieg, H. Blanke, A. Warnecke, and D. U. Sauer, “Calendar and cycle life study of Li(NiMnCo)O₂-based 18650 lithium-ion batteries,” *Journal of Power Sources*, vol. 248, pp. 839–851, 2014.
- [70] W. El-Baz, M. Seufzger, S. Lutzenberger, P. Tzscheutschler, and U. Wagner, “Impact of probabilistic small-scale photovoltaic generation forecast on energy management systems,” *Solar Energy*, vol. 165, pp. 136–146, 2018.
- [71] M. Ellis, J. Liu, and P. D. Christofides, *Economic Model Predictive Control*. Springer International Publishing, 2017.
- [72] Essential Services Commission 2018, “Minimum electricity feed-in tariffs to apply from 1 July 2018: Final decision,” 2018.

-
- [73] European Commission, “COMMISSION DELEGATED REGULATION (EU) No 812/2013 of 18 February 2013 supplementing Directive 2010/30/EU of the European Parliament and of the Council with regard to the energy labelling of water heaters, hot water storage tanks and packages of water heater and solar device,” 2013.
- [74] L. Fahrmeir, T. Kneib, and S. Lang, *Regression: Modelle, Methoden und Anwendungen*, ser. Statistik und ihre Anwendungen. Springer Berlin Heidelberg, 2009.
- [75] X. Fang, S. Misra, G. Xue, and D. Yang, “Smart Grid - The New and Improved Power Grid: A Survey,” *IEEE Communications Surveys Tutorials*, vol. 14, no. 4, pp. 944–980, 2012.
- [76] H. Farhangi, “The path of the smart grid,” *IEEE Power and Energy Magazine*, vol. 8, no. 1, pp. 18–28, 2010.
- [77] F. Farzan, M. A. Jafari, R. Masiello, and Y. Lu, “Toward Optimal Day-Ahead Scheduling and Operation Control of Microgrids Under Uncertainty,” *IEEE Transactions on Smart Grid*, vol. 6, no. 2, pp. 499–507, 2015.
- [78] M. Fast and T. Palmé, “Application of artificial neural networks to the condition monitoring and diagnosis of a combined heat and power plant,” *Energy*, vol. 35, no. 2, pp. 1114–1120, 2010.
- [79] S. Fazlollahi, P. Mandel, G. Becker, and F. Maréchal, “Methods for multi-objective investment and operating optimization of complex energy systems,” *Energy*, vol. 45, no. 1, pp. 12–22, 2012.
- [80] Federal Statistical Office (Destatis), “Fachserie 15, Heft 1, Wirtschaftsrechnungen – Einkommens- und Verbrauchsstichprobe, Ausstattung privater Haushalte mit ausgewählten Gebrauchsgütern, 2013,” 2014.
- [81] L. A. Fernandez-Jimenez, A. Muñoz-Jimenez, A. Falces, M. Mendoza-Villena, E. Garcia-Garrido, P. M. Lara-Santillan, E. Zorzano-Alba, and P. J. Zorzano-Santamaria, “Short-term power forecasting system for photovoltaic plants,” *Renewable Energy*, vol. 44, pp. 311–317, 2012.
- [82] J. Figgenger, D. Haberschusz, K.-P. Kairies, O. Wessels, B. Tepe, M. Ebbert, R. Herzog, and D. U. Sauer, “Wissenschaftliches Mess- und Evaluierungsprogramm Solarstromspeicher 2.0 Jahresbericht 2017,” 2017 Institut für Stromrichtertechnik und Elektrische Antriebe der RWTH Aachen, 2017.
- [83] J. Fleer and P. Stenzel, “Impact analysis of different operation strategies for battery energy storage systems providing primary control reserve,” *Journal of Energy Storage*, vol. 8, pp. 320–338, 2016.

- [84] Fronius, “Technical data Fronius Energy Package,” online, 2016, retrieved 14.12.2016 from https://www.fronius.com/cps/rde/xbcr/SID-F7812949-5B8F237D/fronius-international/SE_DS_Fronius_Symo_Hybrid_EN_386411_snapshot.pdf.
- [85] M. C. Fu, Ed., *Handbook of Simulation Optimization*. Springer New York, 2015.
- [86] S. F. Fux, M. J. Benz, and L. Guzzella, “Economic and environmental aspects of the component sizing for a stand-alone building energy system: A case study,” *Renewable Energy*, vol. 55, pp. 438–447, 2013.
- [87] J. García-González, E. Parrilla, and A. Mateo, “Risk-averse profit-based optimal scheduling of a hydro-chain in the day-ahead electricity market,” *European Journal of Operational Research*, vol. 181, no. 3, pp. 1354–1369, 2007.
- [88] J. L. Garriga and M. Soroush, “Model Predictive Control Tuning Methods: A Review,” *Industrial & Engineering Chemistry Research*, vol. 49, no. 8, pp. 3505–3515, 2010.
- [89] J. Geis-Schroer, S. Kochanneck, I. Mauser, and H. Schmeck, “Reference Scenarios for Low Voltage Power Systems,” in *Proceedings of the Eighth International Conference on Future Energy Systems - e-Energy '17*. ACM Press, 2017.
- [90] C. W. Gellings, “Power/energy: Demand-side load management: The rising cost of peak-demand power means that utilities must encourage customers to manage power usage,” *IEEE Spectrum*, vol. 18, no. 12, pp. 49–52, 1981.
- [91] C. W. Gellings, “The concept of demand-side management for electric utilities,” *Proceedings of the IEEE*, vol. 73, no. 10, pp. 1468–1470, 1985.
- [92] German Federal Network Agency, “EEG-in-Zahlen 2016,” online, 2017, retrieved 22.01.2018 from www.bundesnetzagentur.de/eegiz.
- [93] Y. Ghiassi-Farrokhfal, F. Kazhamiaka, C. Rosenberg, and S. Keshav, “Optimal Design of Solar PV Farms With Storage,” *IEEE Transactions on Sustainable Energy*, vol. 6, no. 4, pp. 1586–1593, 2015.
- [94] M. Giuntoli and D. Poli, “Optimized Thermal and Electrical Scheduling of a Large Scale Virtual Power Plant in the Presence of Energy Storages,” *IEEE Transactions on Smart Grid*, vol. 4, no. 2, pp. 942–955, 2013.
- [95] S. Golshannavaz, S. Afsharnia, and F. Aminifar, “Smart Distribution Grid: Optimal Day-Ahead Scheduling With Reconfigurable Topology,” *IEEE Transactions on Smart Grid*, vol. 5, no. 5, pp. 2402–2411, 2014.
- [96] S. Gottwalt, “Managing Flexible Loads in Residential Areas,” Karlsruhe Institute of Technology (KIT), Karlsruhe, Germany, 2015, PhD thesis.

-
- [97] S. Gottwalt, J. Garttner, H. Schmeck, and C. Weinhardt, “Modeling and Valuation of Residential Demand Flexibility for Renewable Energy Integration,” *IEEE Transactions on Smart Grid*, vol. 8, no. 6, pp. 2565–2574, 2017.
- [98] S. Gottwalt, W. Ketter, C. Block, J. Collins, and C. Weinhardt, “Demand side management – A simulation of household behavior under variable prices,” *Energy Policy*, vol. 39, no. 12, pp. 8163–8174, 2011.
- [99] A. Grandjean, J. Adnot, and G. Binet, “A review and an analysis of the residential electric load curve models,” *Renewable and Sustainable Energy Reviews*, vol. 16, no. 9, pp. 6539–6565, 2012.
- [100] M. Graßl, E. Vikdahl, and G. Reinhart, *A Petri-net Based Approach for Evaluating Energy Flexibility of Production Machines*. Springer, 2014, pp. 303–308, in *Enabling Manufacturing Competitiveness and Economic Sustainability*.
- [101] S. Grässle, B. Becker, T. Knapp, F. Allerdig, H. Schmeck, and A. Wagner, “Intelligent control system for chp-equipment in smart-homes,” in *Proceedings of the 2nd International Conference on Microgeneration and Related Technologies*, 2011.
- [102] L. Grüne and J. Pannek, *Nonlinear Model Predictive Control*. Springer International Publishing, 2017.
- [103] H.-M. Groscurth, T. Bruckner, and R. Kümmel, “Modeling of energy-services supply systems,” *Energy*, vol. 20, no. 9, pp. 941–958, 1995.
- [104] Gurobi Optimization, Inc., “Gurobi Optimizer Reference Manual - Version 7.5,” online, 2017, retrieved 24.04.18 from <http://www.gurobi.com/documentation/7.5/refman.pdf>.
- [105] D. L. Ha, F. F. de Lamotte, and Q. H. Huynh, “Real-time dynamic multilevel optimization for Demand-side Load management,” in *2007 IEEE International Conference on Industrial Engineering and Engineering Management*. IEEE, 2007.
- [106] D. L. Ha, H. Joumaa, S. Ploix, and M. Jacomino, “An optimal approach for electrical management problem in dwellings,” *Energy and Buildings*, vol. 45, pp. 1–14, 2012.
- [107] J. D. Hamilton, *Time series analysis*. Princeton university press Princeton, 1994, vol. 2.
- [108] C. A. Hans, V. Nenchev, J. Raisch, and C. Reincke-Collon, “Minimax Model Predictive Operation Control of Microgrids,” *IFAC Proceedings Volumes*, vol. 47, no. 3, pp. 10 287–10 292, 2014.
- [109] A. Hawkes, P. Aguiar, C. Hernandez-Aramburo, M. Leach, N. Brandon, T. Green, and C. Adjiman, “Techno-economic modelling of a solid oxide fuel cell stack for micro combined heat and power,” *Journal of Power Sources*, vol. 156, no. 2, pp. 321–333, 2006.

- [110] A. Hawkes and M. Leach, “Impacts of temporal precision in optimisation modelling of micro-Combined Heat and Power,” *Energy*, vol. 30, no. 10, pp. 1759–1779, 2005.
- [111] A. Hawkes and M. Leach, “Cost-effective operating strategy for residential micro-combined heat and power,” *Energy*, vol. 32, no. 5, pp. 711–723, 2007.
- [112] H.-M. Henning and A. Palzer, *Energiesystem Deutschland 2050*. Fraunhofer - Institut für Solare Energiesysteme ISE, 2013.
- [113] C. Hirsch, *Fahrplanbasiertes Energiemanagement in Smart Grids*. KIT Scientific Publishing, 2017, PhD thesis.
- [114] P. Hoes, J. Hensen, M. Loomans, B. de Vries, and D. Bourgeois, “User behavior in whole building simulation,” *Energy and Buildings*, vol. 41, no. 3, pp. 295–302, 2009.
- [115] T. Hong and S. Fan, “Probabilistic electric load forecasting: A tutorial review,” *International Journal of Forecasting*, vol. 32, no. 3, pp. 914–938, 2016.
- [116] T. Hong, P. Pinson, and S. Fan, “Global Energy Forecasting Competition 2012,” *International Journal of Forecasting*, vol. 30, no. 2, pp. 357–363, 2014.
- [117] J. Hoppmann, J. Volland, T. S. Schmidt, and V. H. Hoffmann, “The economic viability of battery storage for residential solar photovoltaic systems – A review and a simulation model,” *Renewable and Sustainable Energy Reviews*, vol. 39, pp. 1101–1118, 2014.
- [118] J. H. Horlock, *Combined heat and power*. United States: Pergamon Books Inc., Elmsford, NY, 1987.
- [119] M. Houwing, R. R. Negenborn, and B. D. Schutter, “Demand Response With Micro-CHP Systems,” *Proceedings of the IEEE*, vol. 99, no. 1, pp. 200–213, 2011.
- [120] K.-Y. Huang and Y.-C. Huang, “Integrating Direct Load Control With Interruptible Load Management to Provide Instantaneous Reserves for Ancillary Services,” *IEEE Transactions on Power Systems*, vol. 19, no. 3, pp. 1626–1634, 2004.
- [121] L. Hurwicz, “Optimality criteria for decision making under ignorance,” Cowles Commission Discussion Paper, Statistics, Tech. Rep., 1951.
- [122] H. Ibrahim, A. Ilinca, and J. Perron, “Energy storage systems - Characteristics and comparisons,” *Renewable and Sustainable Energy Reviews*, vol. 12, no. 5, pp. 1221–1250, 2008.
- [123] International Energy Agency (IEA), “Energy Technology Perspectives 2017 - Catalysing Energy Technology Transformations,” 2017.

-
- [124] J. Jargstorf, C. D. Jonghe, and R. Belmans, “Assessing the reflectivity of residential grid tariffs for a user reaction through photovoltaics and battery storage,” *Sustainable Energy, Grids and Networks*, vol. 1, pp. 85–98, 2015.
- [125] H. Jiayi, J. Chuanwen, and X. Rong, “A review on distributed energy resources and MicroGrid,” *Renewable and Sustainable Energy Reviews*, vol. 12, no. 9, pp. 2472–2483, 2008.
- [126] Y. Jin and J. Branke, “Evolutionary optimization in uncertain environments—a survey,” *Evolutionary Computation, IEEE Transactions on*, vol. 9, no. 3, pp. 303–317, 2005.
- [127] V. Kaczmarczyk, P. Fiedler, Z. Bradac, L. Franek, and J. Pasek, “Simulator for optimal scheduling of domestic appliances,” *IFAC-PapersOnLine*, vol. 48, no. 4, pp. 95–100, 2015.
- [128] J. Kallrath, *Gemischt-ganzzahlige Optimierung: Modellierung in der Praxis*. Springer Fachmedien Wiesbaden, 2013.
- [129] T. Kaschub, *Batteriespeicher in Haushalten unter Berücksichtigung von Photovoltaik, Elektrofahrzeugen und Nachfragesteuerung*. Karlsruhe: KIT Scientific Publishing, 2017, PhD thesis.
- [130] T. Kaschub, P. Jochem, and W. Fichtner, “Solar energy storage in German households: profitability, load changes and flexibility,” *Energy Policy*, vol. 98, pp. 520–532, 2016.
- [131] F. Katiraei, R. Iravani, N. Hatziargyriou, and A. Dimeas, “Microgrids management,” *IEEE Power and Energy Magazine*, vol. 6, no. 3, pp. 54–65, 2008.
- [132] F. Kazhamiaka, C. Rosenberg, and S. Keshav, “Practical Strategies for Storage Operation in Energy Systems: Design and Evaluation,” *IEEE Transactions on Sustainable Energy*, vol. 7, no. 4, pp. 1602–1610, 2016.
- [133] F. Kazhamiaka, P. Jochem, S. Keshav, and C. Rosenberg, “On the influence of jurisdiction on the profitability of residential photovoltaic-storage systems: A multi-national case study,” *Energy Policy*, vol. 109, pp. 428–440, 2017.
- [134] F. H. Knight and D. E. Jones, *Risk, Uncertainty and Profit*. Beard Books, 2002.
- [135] S. Kochannek, I. Mauser, B. Bohnet, S. Hubschneider, H. Schmeck, M. Braun, and T. Leibfried, “Establishing a hardware-in-the-loop research environment with a hybrid energy storage system,” in *2016 IEEE Innovative Smart Grid Technologies - Asia (ISGT-Asia)*, 2016, pp. 497–503.
- [136] S. Kochannek, “Systemdienstleistungserbringung durch intelligente Gebäude,” Karlsruhe Institute of Technology (KIT), Karlsruhe, Germany, 2019, PhD thesis.
- [137] R. Koenker, *Quantile Regression*. Cambridge University Press, 2005.

- [138] V. B. Krishna, W. S. Wadman, and Y. Kim, “NowCasting: Accurate and Precise Short-Term Wind Power Prediction using Hyperlocal Wind Forecasts,” in *Proceedings of the Ninth International Conference on Future Energy Systems - e-Energy '18*. ACM Press, 2018, pp. 63–74.
- [139] D. P. Kroese, T. Brereton, T. Taimre, and Z. I. Botev, “Why the Monte Carlo method is so important today,” *Wiley Interdisciplinary Reviews: Computational Statistics*, vol. 6, no. 6, pp. 386–392, 2014.
- [140] H. Laux, R. M. Gillenkirch, and H. Y. Schenk-Mathes, *Entscheidungstheorie*. Springer Berlin Heidelberg, 2014.
- [141] D. Lazos, A. B. Sproul, and M. Kay, “Optimisation of energy management in commercial buildings with weather forecasting inputs: A review,” *Renewable and Sustainable Energy Reviews*, vol. 39, pp. 587–603, 2014.
- [142] Y. Li, Y. Su, and L. Shu, “An ARMAX model for forecasting the power output of a grid connected photovoltaic system,” *Renewable Energy*, vol. 66, pp. 78–89, 2014.
- [143] A. Liebe, S. Schmitt, and M. Wissner, “Quantitative Auswirkungen variabler Stromtarife auf die Stromkosten von Haushalten,” WIK Wissenschaftliches Institut für Infrastruktur und Kommunikationsdienste GmbH Bericht, 2015.
- [144] P. Liu and Y. Fu, “Optimal operation of energy-efficiency building: A robust optimization approach,” in *2013 IEEE Power & Energy Society General Meeting*. IEEE, 2013.
- [145] D. Livengood and R. Larson, “The Energy Box: Locally Automated Optimal Control of Residential Electricity Usage,” *Service Science*, vol. 1, no. 1, pp. 1–16, 2009.
- [146] M. Loesch, D. Hufnagel, S. Steuer, T. Fabnacht, and H. Schmeck, “Demand side management in smart buildings by intelligent scheduling of heat pumps,” in *2014 IEEE International Conference on Intelligent Energy and Power Systems (IEPS)*. IEEE, 2014.
- [147] J. Löfberg, “YALMIP : A Toolbox for Modeling and Optimization in MATLAB,” in *In Proceedings of the CACSD Conference*, Taipei, Taiwan, 2004.
- [148] J. Löfberg, “Approximations of closed-loop MPC,” in *Proceedings of the 42nd IEEE Conference on Decision and Control*, Maui, Hawaii, 2003, pp. 1438–1442.
- [149] J. Löfberg, *Minimax approaches to robust model predictive control: Zugl.: Linköping, Univ., Diss., 2003*, ser. Linköping studies in science and technology Dissertations. Linköping: Univ, 2003, vol. 812.

-
- [150] F. Lopes and H. Coelho, Eds., *Electricity Markets with Increasing Levels of Renewable Generation: Structure, Operation, Agent-based Simulation, and Emerging Designs*. Springer International Publishing, 2018.
- [151] T. Lui., W. Stirling, and H. Marcy, “Get Smart,” *IEEE Power and Energy Magazine*, vol. 8, no. 3, pp. 66–78, 2010.
- [152] H. Lund, “Large-scale integration of wind power into different energy systems,” *Energy*, vol. 30, no. 13, pp. 2402–2412, 2005.
- [153] H. Lund, F. Arler, P. Østergaard, F. Hvelplund, D. Connolly, B. Mathiesen, and P. Karnøe, “Simulation versus Optimisation: Theoretical Positions in Energy System Modelling,” *Energies*, vol. 10, no. 7, p. 840, 2017.
- [154] R. Luthander, J. Widén, D. Nilsson, and J. Palm, “Photovoltaic self-consumption in buildings: A review,” *Applied Energy*, vol. 142, pp. 80–94, 2015.
- [155] J. Ma, J. Qin, T. Salsbury, and P. Xu, “Demand reduction in building energy systems based on economic model predictive control,” *Chemical Engineering Science*, vol. 67, no. 1, pp. 92–100, 2012, dynamics, Control and Optimization of Energy Systems.
- [156] Y. Ma, F. Borrelli, B. Hancey, B. Coffey, S. Bengea, and P. Haves, “Model Predictive Control for the Operation of Building Cooling Systems,” *IEEE Transactions on Control Systems Technology*, vol. 20, no. 3, pp. 796–803, 2012.
- [157] Y. Ma, A. Kelman, A. Daly, and F. Borrelli, “Predictive Control for Energy Efficient Buildings with Thermal Storage: Modeling, Stimulation, and Experiments,” *IEEE Control Systems*, vol. 32, no. 1, pp. 44–64, 2012.
- [158] L. Magnier and F. Haghghat, “Multiobjective optimization of building design using TRNSYS simulations, genetic algorithm, and Artificial Neural Network,” *Building and Environment*, vol. 45, no. 3, pp. 739–746, 2010.
- [159] P. Mancarella, “MES (multi-energy systems): An overview of concepts and evaluation models,” *Energy*, vol. 65, pp. 1–17, 2014.
- [160] J. F. Manwell and J. G. McGowan, “Lead acid battery storage model for hybrid energy systems,” *Solar Energy*, vol. 50, no. 5, pp. 399–405, 1993.
- [161] M. Marzband, A. Sumper, A. Ruiz-Álvarez, J. L. Domínguez-García, and B. Tomoiagă, “Experimental evaluation of a real time energy management system for stand-alone microgrids in day-ahead markets,” *Applied Energy*, vol. 106, pp. 365–376, 2013.
- [162] I. Mauser, J. Müller, K. Förderer, and H. Schmeck, “Definition, Modeling, and Communication of Flexibility in Smart Buildings and Smart Grid,” in *International ETG Congress 2017*, 2017, pp. 1–6.

- [163] I. Mauser, “Multi-modal Building Energy Management,” Karlsruhe Institute of Technology (KIT), Karlsruhe, Germany, 2017, PhD thesis.
- [164] I. Mauser, J. Feder, J. Müller, and H. Schmeck, “Evolutionary Optimization of Smart Buildings with Interdependent Devices,” in *Applications of Evolutionary Computation*, A. M. Mora and G. Squillero, Eds. Springer International Publishing, 2015, vol. 9028, pp. 239–251.
- [165] I. Mauser, J. Müller, F. Allering, and H. Schmeck, “Adaptive Building Energy Management with Multiple Commodities and Flexible Evolutionary Optimization,” *Renewable Energy*, vol. 87, Part 2, pp. 911–921, 2016.
- [166] I. Mauser, J. Müller, and H. Schmeck, “Utilizing Flexibility of Hybrid Appliances in Local Multi-modal Energy Management,” in *Proceedings of the 9th International Conference EEDAL’2017 - Energy Efficiency in Domestic Appliances and Lighting*, ser. JRC Conference and Workshop Report. Publications Office of the European Union, 2017, Inproceedings, pp. 1282–1297.
- [167] A. Mellit and A. M. Pavan, “A 24-h forecast of solar irradiance using artificial neural network: Application for performance prediction of a grid-connected PV plant at Trieste, Italy,” *Solar Energy*, vol. 84, no. 5, pp. 807–821, 2010.
- [168] E. Mengelkamp, J. Gärttner, K. Rock, S. Kessler, L. Orsini, and C. Weinhardt, “Designing microgrid energy markets,” *Applied Energy*, vol. 210, pp. 870–880, 2018.
- [169] J. Meunier, D. Knittel, P. Collet, and G. Sturtzer, “Simulation of real-time multi-objective optimization for a photovoltaic system with grid connection,” in *IECON 2016 - 42nd Annual Conference of the IEEE Industrial Electronics Society*, 2016, pp. 7101–7106.
- [170] R. Mikut, A. Bartschat, W. Doneit, J. Á. G. Ordiano, B. Schott, J. Stegmaier, S. Waczowicz, and M. Reischl, “The MATLAB Toolbox SciXMiner: User’s Manual and Programmer’s Guide,” *CoRR*, vol. abs/1704.03298, 2017.
- [171] R. Missaoui, H. Joumaa, S. Ploix, and S. Bacha, “Managing energy Smart Homes according to energy prices: Analysis of a Building Energy Management System,” *Energy and Buildings*, vol. 71, pp. 155–167, 2014.
- [172] S. Mitra, L. Sun, and I. E. Grossmann, “Optimal scheduling of industrial combined heat and power plants under time-sensitive electricity prices,” *Energy*, vol. 54, pp. 194–211, 2013.
- [173] J. Müller, “Evolutionary optimization under uncertainty in energy management systems,” *it - Information Technology*, vol. 59, no. 1, 2017.

-
- [174] J. Müller, M. Ahrens, I. Mauser, and H. Schmeck, “Achieving Optimized Decisions on Battery Operating Strategies in Smart Buildings,” in *Applications of Evolutionary Computation*. Springer International Publishing, 2018, pp. 205–221.
- [175] J. Müller, C. Gitte, M. Winter, and J. van der Geest, “Advanced configuration system for cost-effective integration of distributed energy systems,” in *2016 IEEE Innovative Smart Grid Technologies - Asia (ISGT-Asia)*. IEEE, 2016.
- [176] A. Molderink, V. Bakker, M. G. C. Bosman, J. L. Hurink, and G. J. M. Smit, “Management and Control of Domestic Smart Grid Technology,” *IEEE Transactions on Smart Grid*, vol. 1, no. 2, pp. 109–119, 2010.
- [177] A. Molina-Garcia, F. Bouffard, and D. S. Kirschen, “Decentralized Demand-Side Contribution to Primary Frequency Control,” *IEEE Transactions on Power Systems*, vol. 26, no. 1, pp. 411–419, 2011.
- [178] V. Muenzel, J. de Hoog, M. Brazil, A. Vishwanath, and S. Kalyanaraman, “A Multi-Factor Battery Cycle Life Prediction Methodology for Optimal Battery Management,” in *Proceedings of the 2015 ACM Sixth International Conference on Future Energy Systems - e-Energy '15*. ACM Press, 2015, pp. 57–66.
- [179] J. Müller, M. März, I. Mauser, and H. Schmeck, “Optimization of Operation and Control Strategies for Battery Energy Storage Systems by Evolutionary Algorithms,” in *Applications of Evolutionary Computation*, A. M. Mora and G. Squillero, Eds. Springer International Publishing, 2016, vol. 9598, pp. 507–522.
- [180] C. Müller-Schloer, H. Schmeck, and T. Ungerer, *Organic Computing – A Paradigm Shift for Complex Systems*. Springer, 2011, vol. 1.
- [181] M. Mültin, “Das Elektrofahrzeug als flexibler Verbraucher und Energiespeicher im Smart Home,” Karlsruhe Institute of Technology (KIT), Karlsruhe, Germany, 2014, PhD thesis.
- [182] N. Munzke, B. Schwarz, F. Büchle, and J. Barry, “Li-Ionen Heimspeichersysteme: Performance auf dem Prüfstand,” in *32. Symposium Photovoltaische Solarenergie, Kloster Banz, Bad Staffelstein 8.-10 März 2017*. Karlsruhe, 2017.
- [183] E. Namor, F. Sossan, R. Cherkaoui, and M. Paolone, “Load leveling and dispatchability of a medium voltage active feeder through battery energy storage systems: Formulation of the control problem and experimental validation,” in *2016 IEEE PES Innovative Smart Grid Technologies Conference Europe (ISGT-Europe)*. IEEE, 2016.
- [184] J. Neugebauer, O. Kramer, and M. Sonnenschein, “Classification Cascades of Overlapping Feature Ensembles for Energy Time Series Data,” in *2015 ECML/PKDD, 3rd Intl. DARE Workshop*, 2015.

- [185] K.-H. Ng and G. Sheble, “Direct load control-A profit-based load management using linear programming,” *IEEE Transactions on Power Systems*, vol. 13, no. 2, pp. 688–694, 1998.
- [186] T. A. Nguyen and M. Aiello, “Energy intelligent buildings based on user activity: A survey,” *Energy and Buildings*, vol. 56, pp. 244–257, 2013.
- [187] J. Niehans, “Zur Preisbildung bei ungewissen Erwartungen.” *Schweizerische Zeitschrift für Volkswirtschaft und Statistik*, no. 84, pp. 433–456, 1948.
- [188] H. A. Nielsen, H. Madsen, and T. S. Nielsen, “Using quantile regression to extend an existing wind power forecasting system with probabilistic forecasts,” *Wind Energy*, vol. 9, no. 1-2, pp. 95–108, 2006.
- [189] M. Nishio, J. Itoh, K. Shiroko, and T. Umeda, “A thermodynamic approach to steam-power system design,” *Industrial & Engineering Chemistry Process Design and Development*, vol. 19, no. 2, pp. 306–312, 1980.
- [190] B. Nordman and M. McWhinney, “Electronics Come of Age: A Taxonomy for Miscellaneous and Low Power Products,” in *ACEEE Summer Study on Energy Efficiency in Buildings*. Washington, D.C: ACEEE, 2006.
- [191] F. Oldewurtel, A. Parisio, C. N. Jones, D. Gyalistras, M. Gwerder, V. Stauch, B. Lehmann, and M. Morari, “Use of model predictive control and weather forecasts for energy efficient building climate control,” *Energy and Buildings*, vol. 45, no. Supplement C, pp. 15–27, 2012.
- [192] J. Á. G. Ordiano, W. Doneit, S. Waczowicz, L. Gröll, R. Mikut, and V. Hagenmeyer, “Nearest-neighbor based non-parametric probabilistic forecasting with applications in photovoltaic systems,” *arXiv preprint arXiv:1701.06463*, 2017.
- [193] J. Á. G. Ordiano, S. Waczowicz, M. Reischl, R. Mikut, and V. Hagenmeyer, “Photovoltaic power forecasting using simple data-driven models without weather data,” *Computer Science - Research and Development*, vol. 32, no. 1-2, pp. 237–246, 2016.
- [194] J. V. Paatero and P. D. Lund, “A model for generating household electricity load profiles,” *International Journal of Energy Research*, vol. 30, no. 5, pp. 273–290, 2006.
- [195] P. Palensky and D. Dietrich, “Demand Side Management: Demand Response, Intelligent Energy Systems, and Smart Loads,” *IEEE Transactions on Industrial Informatics*, vol. 7, no. 3, pp. 381–388, 2011.
- [196] M. Papageorgiou, M. Leibold, and M. Buss, *Optimierung (4. Auflage)*. Springer Berlin Heidelberg, 2015.

-
- [197] S. Papantoniou, S. Mangili, and I. Mangialenti, “Using Intelligent Building Energy Management System for the Integration of Several Systems to one Overall Monitoring and Management System,” *Energy Procedia*, vol. 111, pp. 639–647, 2017.
- [198] M. A. A. Pedrasa, T. D. Spooner, and I. F. MacGill, “Coordinated Scheduling of Residential Distributed Energy Resources to Optimize Smart Home Energy Services,” *IEEE Transactions on Smart Grid*, vol. 1, no. 2, pp. 134–143, 2010.
- [199] S. Pelland, G. Galanis, and G. Kallos, “Solar and photovoltaic forecasting through post-processing of the Global Environmental Multiscale numerical weather prediction model,” *Progress in Photovoltaics: Research and Applications*, vol. 21, no. 3, pp. 284–296, 2011.
- [200] G. Pepermans, J. Driesen, D. Haeseldonckx, R. Belmans, and W. D’haeseleer, “Distributed generation: definition, benefits and issues,” *Energy Policy*, vol. 33, no. 6, pp. 787–798, 2005.
- [201] R. Perez, M. David, T. E. Hoff, M. Jamaly, S. Kivalov, J. Kleissl, P. Lauret, and M. Perez, “Spatial and Temporal Variability of Solar Energy,” *Foundations and Trends in Renewable Energy*, vol. 1, no. 1, pp. 1–44, 2016.
- [202] J. Persky, “Retrospectives: The Ethology of Homo Economicus,” *Journal of Economic Perspectives*, vol. 9, no. 2, pp. 221–231, 1995.
- [203] P. Pinson, H. Madsen, H. A. Nielsen, G. Papaefthymiou, and B. Klöckl, “From probabilistic forecasts to statistical scenarios of short-term wind power production,” *Wind Energy*, vol. 12, no. 1, pp. 51–62, 2009.
- [204] S. Pohekar and M. Ramachandran, “Application of multi-criteria decision making to sustainable energy planning—A review,” *Renewable and Sustainable Energy Reviews*, vol. 8, no. 4, pp. 365–381, 2004.
- [205] D. Prior, *Nachbildung der Energiebedarfsstruktur der privaten Haushalte – Werkzeug zur Bewertung von Energiesparmaßnahmen*, ser. Fortschrittberichte VDI : Reihe 6, Energietechnik ; 379. VDI Verlag, 1997.
- [206] S. Prívará, J. Cigler, Z. Váňa, F. Oldewurtel, C. Sagerschnig, and E. Žáčková, “Building modeling as a crucial part for building predictive control,” *Energy and Buildings*, vol. 56, pp. 8–22, 2013.
- [207] J. B. Rawlings, D. Bonne, J. B. Jorgensen, A. N. Venkat, and S. B. Jorgensen, “Unreachable Setpoints in Model Predictive Control,” *IEEE Transactions on Automatic Control*, vol. 53, no. 9, pp. 2209–2215, 2008.
- [208] T. B. Reddy and D. Linden, *Linden’s handbook of batteries*. McGraw-hill New York, 2011, vol. 4.

- [209] M. Richter, “Utilities’ business models for renewable energy: A review,” *Renewable and Sustainable Energy Reviews*, vol. 16, no. 5, pp. 2483–2493, 2012.
- [210] F. H. Rios Silva, “Stigmergy-based Load Scheduling in a Demand Side Management Context,” Karlsruhe Institute of Technology (KIT), Karlsruhe, Germany, 2016, PhD thesis.
- [211] J. Rockström, O. Gaffney, J. Rogelj, M. Meinshausen, N. Nakicenovic, and H. J. Schellnhuber, “A roadmap for rapid decarbonization,” *Science*, vol. 355, no. 6331, pp. 1269–1271, 2017.
- [212] B. Roossien, “Flexines D8.1 – Mathematical quantification of near real-time flexibility for Smart Grids,” ECN, Tech. Rep., 2010.
- [213] F. Rothlauf, *Design of Modern Heuristics*. Springer Berlin Heidelberg, 2011.
- [214] N. V. Sahinidis, “Optimization under uncertainty: state-of-the-art and opportunities,” *Computers & Chemical Engineering*, vol. 28, no. 6-7, pp. 971–983, 2004.
- [215] P. Samadi, H. Mohsenian-Rad, R. Schober, and V. W. S. Wong, “Advanced Demand Side Management for the Future Smart Grid Using Mechanism Design,” *IEEE Transactions on Smart Grid*, vol. 3, no. 3, pp. 1170–1180, 2012.
- [216] L. J. Savage, “The theory of statistical decision,” *Journal of the American Statistical Association*, no. 46, pp. 55–67, 1951.
- [217] W.-P. Schill, “Residual load, renewable surplus generation and storage requirements in Germany,” *Energy Policy*, vol. 73, pp. 65–79, 2014.
- [218] H. Schmeck, Slides for the lecture “Smart Energy Distribution” at the Karlsruhe Institute of Technologie SS16, 2016.
- [219] H. Schmidt and D. Sauer, “Praxisgerechte Modellierung und Abschätzung von Wechselrichter-Wirkungsgraden,” in *Proceedings of 9. Internationales Sonnenforum Stuttgart*, 1994, pp. 550–557.
- [220] T. Schütz, R. Streblow, and D. Müller, “A comparison of thermal energy storage models for building energy system optimization,” *Energy and Buildings*, vol. 93, pp. 23–31, 2015.
- [221] A. J. Schwab, *Elektroenergiesysteme : Erzeugung, Übertragung und Verteilung elektrischer Energie (5. Auflage)*. Berlin, Heidelberg: Springer, 2017.
- [222] H. Schwarz, V. Bertsch, and W. Fichtner, “Two-stage stochastic, large-scale optimization of a decentralized energy system: a case study focusing on solar PV, heat pumps and storage in a residential quarter,” *OR Spectrum*, vol. 40, no. 1, pp. 265–310, 2017.

-
- [223] P. Scott, S. Thiébaux, M. van den Briel, and P. Van Hentenryck, *Residential Demand Response under Uncertainty*. Springer, 2013, pp. 645–660.
- [224] D. E. Seborg, D. A. Mellichamp, T. F. Edgar, and F. J. Doyle III, *Process dynamics and control*. John Wiley & Sons, 2010.
- [225] SenerTec Kraft-Wärme-Energiesysteme GmbH., “Planungshandbuch Dachs Gen1.1 – Art. Nr.: 15/4798.586.002,” 2015.
- [226] A. Shapiro, “On complexity of multistage stochastic programs,” *Operations Research Letters*, vol. 34, no. 1, pp. 1–8, 2006.
- [227] A. Shapiro, D. Dentcheva, and A. Ruszczyński, *Lectures on stochastic programming: modeling and theory*, ser. MPS-SIAM series on optimization ; 9. Philadelphia, Pa: Society for Industrial and Applied Mathematics, 2009.
- [228] A. Sharma, V. Tyagi, C. Chen, and D. Buddhi, “Review on thermal energy storage with phase change materials and applications,” *Renewable and Sustainable Energy Reviews*, vol. 13, no. 2, pp. 318–345, 2009.
- [229] P. Siano, “Demand response and smart grids—A survey,” *Renewable and Sustainable Energy Reviews*, vol. 30, pp. 461–478, 2014.
- [230] H. A. Simon and A. Newell, “Heuristic Problem Solving: The Next Advance in Operations Research,” *Operations Research*, vol. 6, no. 1, pp. 1–10, 1958.
- [231] J. Široký, F. Oldewurtel, J. Cigler, and S. Prívará, “Experimental analysis of model predictive control for an energy efficient building heating system,” *Applied Energy*, vol. 88, no. 9, pp. 3079–3087, 2011.
- [232] A. Soares, A. Gomes, C. H. Antunes, and C. Oliveira, “A Customized Evolutionary Algorithm for Multi-Objective Management of Residential Energy Resources,” *IEEE Transactions on Industrial Informatics*, vol. PP, no. 99, pp. 1–1, 2016.
- [233] A. Soares, C. H. Antunes, C. Oliveira, and Á. Gomes, “A multi-objective genetic approach to domestic load scheduling in an energy management system,” *Energy*, vol. 77, pp. 144–152, 2014.
- [234] J. Soares, H. Morais, T. Sousa, Z. Vale, and P. Faria, “Day-Ahead Resource Scheduling Including Demand Response for Electric Vehicles,” *IEEE Transactions on Smart Grid*, vol. 4, no. 1, pp. 596–605, 2013.
- [235] A. Soroudi and T. Amraee, “Decision making under uncertainty in energy systems: State of the art,” *Renewable and Sustainable Energy Reviews*, vol. 28, pp. 376–384, 2013.

- [236] K. C. Sou, M. Kordel, J. Wu, H. Sandberg, and K. H. Johansson, “Energy and CO₂ efficient scheduling of smart home appliances,” in *2013 European Control Conference (ECC)*. IEEE, 2013, pp. 4051–4058.
- [237] K. C. Sou, J. Weimer, H. Sandberg, and K. H. Johansson, “Scheduling smart home appliances using mixed integer linear programming,” in *2011 50th IEEE Conference on Decision and Control and European Control Conference (CDC-ECC)*. IEEE, 2011, pp. 5144–5149.
- [238] R. Stamminger, G. Broil, C. Pakula, H. Jungbecker, M. Braun, I. Rüdener, and C. Wendker, “Synergy Potential of Smart Domestic Appliances in Renewable Energy Systems,” University of Bonn, Tech. Rep., 2008.
- [239] T. Stetz, F. Marten, and M. Braun, “Improved Low Voltage Grid-Integration of Photovoltaic Systems in Germany,” *IEEE Transactions on Sustainable Energy*, vol. 4, no. 2, pp. 534–542, 2013.
- [240] G. Strbac, “Demand side management: Benefits and challenges,” *Energy Policy*, vol. 36, no. 12, pp. 4419–4426, 2008.
- [241] S. Sun, S. Keshav, C. Rosenberg, and M. Peloso, “Optimal Matching of Stochastic Solar Generators to Stochastic Loads,” in *Proceedings of the Ninth International Conference on Future Energy Systems - e-Energy '18*. ACM Press, 2018, pp. 33–37.
- [242] L. G. Swan and V. I. Ugursal, “Modeling of end-use energy consumption in the residential sector: A review of modeling techniques,” *Renewable and Sustainable Energy Reviews*, vol. 13, no. 8, pp. 1819–1835, 2009.
- [243] S. Teleke, M. E. Baran, S. Bhattacharya, and A. Q. Huang, “Rule-Based Control of Battery Energy Storage for Dispatching Intermittent Renewable Sources,” *IEEE Transactions on Sustainable Energy*, vol. 1, no. 3, pp. 117–124, 2010.
- [244] H. Tischer and G. Verbic, “Towards a smart home energy management system - A dynamic programming approach,” in *2011 IEEE PES Innovative Smart Grid Technologies*. IEEE, 2011.
- [245] H. A. Toersche, J. L. Hurink, and M. J. Koonsman, “Energy management with TRIANA on FPAI,” in *2015 IEEE PowerTech*, 2015.
- [246] K. M. Tsui and S. C. Chan, “Demand Response Optimization for Smart Home Scheduling Under Real-Time Pricing,” *IEEE Transactions on Smart Grid*, vol. 3, no. 4, pp. 1812–1821, 2012.
- [247] M. Uhrig, S. Koenig, M. R. Suriyah, and T. Leibfried, “Lithium-based vs. Vanadium Redox Flow Batteries – A Comparison for Home Storage Systems,” *Energy Procedia*, vol. 99, pp. 35–43, 2016, 10th International Renewable Energy Storage Conference, IRES 2016, 15-17 March 2016, Düsseldorf, Germany.

-
- [248] United Nations Framework Convention on Climate Change (UNFCCC), “Paris Agreement,” United Nations Treaty Collection Chapter XXVII 7.d., 2015.
- [249] S. Vazquez, S. M. Lukic, E. Galvan, L. G. Franquelo, and J. M. Carrasco, “Energy Storage Systems for Transport and Grid Applications,” *IEEE Transactions on Industrial Electronics*, vol. 57, no. 12, pp. 3881–3895, 2010.
- [250] VDEW Verband der Elektrizitätswirtschaft, “Repräsentative VDEW-Lastprofile, VDEW-Materialien M-28/99,” 1999.
- [251] VDI Verein Deutscher Ingenieure e.V., “VDI Guideline 6002 – Part 1 – Solar heating for potable water – Basic principles – System technology and application in residential buildings,” 2014.
- [252] VDI Verein Deutscher Ingenieure e.V., “VDI Guideline 6002 – Part 1 – Solar heating for potable water – Basic principles – System technology and application in residential buildings,” 2014.
- [253] C. Velasquez, D. Watts, H. Rudnick, and C. Bustos, “A Framework for Transmission Expansion Planning: A Complex Problem Clouded by Uncertainty,” *IEEE Power and Energy Magazine*, vol. 14, no. 4, pp. 20–29, 2016.
- [254] A. Völz, *Modellpädiktive Regelung nichtlinearer Systeme mit Unsicherheiten*. Springer Fachmedien Wiesbaden, 2016.
- [255] J. Von Appen, J. H. Braslavsky, J. K. Ward, and M. Braun, “Sizing and grid impact of PV battery systems – a comparative analysis for Australia and Germany,” in *2015 International Symposium on Smart Electric Distribution Systems and Technologies (EDST)*, 2015.
- [256] A. Wald, *Statistical decision functions*, ser. Wiley publications in statistics. New York: Wiley, 1950.
- [257] P. Whittle, *Hypothesis testing in time series analysis*. Almqvist & Wiksells, 1951, vol. 4.
- [258] J. Widén, “Improved photovoltaic self-consumption with appliance scheduling in 200 single-family buildings,” *Applied Energy*, vol. 126, pp. 199–212, 2014.
- [259] A. H. Willett, *The Economic Theory of Risk and Insurance*. Columbia University, 1901.
- [260] H. P. Williams, *Model building in mathematical programming (Fifth Edition)*. Chichester: Wiley, 2013.
- [261] W. Wojsznis, J. Gudaz, T. Blevins, and A. Mehta, “Practical approach to tuning MPC,” *ISA Transactions*, vol. 42, no. 1, pp. 149–162, 2003.

- [262] D. L. Woodruff, J. Deride, A. Staid, J.-P. Watson, G. Slevogt, and C. Silva-Monroy, “Constructing probabilistic scenarios for wide-area solar power generation,” *Solar Energy*, vol. 160, pp. 153–167, 2018.
- [263] H. Wu, M. Shahidehpour, Z. Li, and W. Tian, “Chance-Constrained Day-Ahead Scheduling in Stochastic Power System Operation,” *IEEE Transactions on Power Systems*, vol. 29, no. 4, pp. 1583–1591, 2014.
- [264] S. Wu and J.-Q. Sun, “A physics-based linear parametric model of room temperature in office buildings,” *Building and Environment*, vol. 50, pp. 1–9, 2012.
- [265] Z. Wu, H. Tazvinga, and X. Xia, “Demand side management of photovoltaic-battery hybrid system,” *Applied Energy*, vol. 148, pp. 294–304, 2015.
- [266] A. Zeh and R. Witzmann, “Operational Strategies for Battery Storage Systems in Low-voltage Distribution Grids to Limit the Feed-in Power of Roof-mounted Solar Power Systems,” *Energy Procedia*, vol. 46, pp. 114–123, 2014.
- [267] D. Zhang, N. Shah, and L. G. Papageorgiou, “Efficient energy consumption and operation management in a smart building with microgrid,” *Energy Conversion and Management*, vol. 74, pp. 209–222, 2013.
- [268] Y. Zhang, M. Beaudin, R. Taheri, H. Zareipour, and D. Wood, “Day-Ahead Power Output Forecasting for Small-Scale Solar Photovoltaic Electricity Generators,” *IEEE Transactions on Smart Grid*, vol. 6, no. 5, pp. 2253–2262, 2015.
- [269] Z. Zhao, W. C. Lee, Y. Shin, and K. B. Song, “An Optimal Power Scheduling Method for Demand Response in Home Energy Management System,” *IEEE Transactions on Smart Grid*, vol. 4, no. 3, pp. 1391–1400, 2013.
- [270] P. Zweifel, A. Praktijnjo, and G. Erdmann, *Energy Economics*. Springer Berlin Heidelberg, 2017.

A. Formulation of the Optimization Problem

Listing A.1: Matlab class that provides the optimization model.

```
1 classdef StochasticControllerBuilder
2
3 properties
4     %Constants
5     intervall;
6     horizon ;
7     numberOfDisturbances;
8     u_CHP_Initial=0;
9     P_Im_Max = 1000000000000;
10    V_HWT = 0.750; %m^3
11    rho_Water = 1000; %kg m^3
12    c_Water = 4182; %ws kg^-1 K^-1
13    a_HWT= 1; %m^2
14    Q_GH_Nominal = 15000; %W
15    eta_GH = 1;
16    theta_In =20;%C
17    pi_s_HWT = 1000000000000;
18    eta_BEES = 0.92;
19    E_BEES_max = 7 *1000; %Wh
20    E_BEES_min = 0;%Wh
21    P_BEES_Charge_max = 7000; %W
22    P_BEES_Discharge_max = 7000; %W
23    k_CHP_Min;
24    Phi_CHP_Run = 12500; %W;
```

```

25     P_CHPRun = 5500; %W
26     G_CHPRun= 20500; %W
27     P_Appliance_nom;
28     l_Appliance;
29     k_vector;
30     theta_HWT_max= 80; %C
31     theta_HWT_min = 60; %C
32
33     %Parameters
34     P_Base;
35     P_PV_Prediction;
36     Phi_HS ;
37     Phi_DHW ;
38     theta_HWT_Initial = sdpvar(1,1);
39     pi_Gas = sdpvar(1,1);
40     pi_CHP_Start= sdpvar(1,1);
41     pi_Ex ;
42     pi_Im ;
43     E_BESS_Initial = sdpvar(1,1);
44     r = sdpvar(1,1);
45     d = sdpvar(1,1);
46     k_CHP_Initail;
47     Parameters;
48     Delta_k;
49     k_Appliance_max= sdpvar(1,1);
50     k_Appliance_min= sdpvar(1,1);
51
52     %Variables
53     Objective = 0;
54     Constraints = [];
55     P_Appliance ;
56     P_CHP;
57     Phi_CHP;
58     G_CHP;
59     b_Appliance = binvar(1,1);
60     P_BESS_Charge ;
61     P_BESS_Discharge ;
62     Phi_HWT_Loss;
63
64     %Design Variables
65     u_CHP ;
66     u_Appliance;
67     u_BESS_Charge ;

```

```

68     u_BESS_Discharge ;
69     P_Im ;
70     P_Ex ;
71     E_BESS;
72     E_BESS_end;
73     theta_HWT;
74     theta_HWT_end;
75     s_CHP;
76
77     %For YALMIP
78     WantedVariables ;
79
80 end
81
82 methods
83 function obj = StochasticControllerBuilder(x,y,z,
      numberOfDisturbances)
84
85     %Constants
86     obj.k_CHP_Min = 15/ x;
87     obj.k_CHP_Initail = z;
88     obj.intervall =x;
89     obj.Delta_k = obj.intervall/60;
90     obj.numberofDisturbances=numberOfDisturbances;
91     obj.horizon = y / obj.intervall;
92     obj.P_Appliance_nom = mean(reshape(dlmread("Data/
      applianceLog.csv", ';'), obj.intervall*60, []))';
93     obj.l_Appliance = size(obj.P_Appliance_nom,1);
94     obj.k_vector = 1:obj.horizon;
95
96     %Parameters
97     obj.P_Base=sdpvar(obj.horizon,1);
98     obj.P_PV_Prediction=sdpvar(obj.horizon,obj.
      numberOfDisturbances);
99     obj.Phi_HS = sdpvar(obj.horizon,1);
100    obj.Phi_DHW = sdpvar(obj.horizon,1);
101    obj.pi_Ex = sdpvar(obj.horizon,1);
102    obj.pi_Im = sdpvar(obj.horizon,1);
103    obj.Parameters ={obj.P_Base,...
104                    obj.P_PV_Prediction,...
105                    obj.Phi_HS,...
106                    obj.Phi_DHW,...
107                    obj.theta_HWT_Initial,...

```

```

108         obj.pi_Ex , ...
109         obj.pi_Im , ...
110         obj.pi_Gas , ...
111         obj.pi_CHP_Start , ...
112         obj.E_BESS_Initial , ...
113         obj.k_Appliance_min , ...
114         obj.k_Appliance_max , ...
115         obj.b_Appliance};
116
117 %Variables
118 obj.P_Appliance= sdpvar(obj.horizon,obj.
        numberOfDisturbances);
119 obj.P_CHP= sdpvar(obj.horizon,obj.numberOfDisturbances);
120 obj.Phi_CHP= sdpvar(obj.horizon,obj.numberOfDisturbances);
121 obj.G_CHP= sdpvar(obj.horizon,obj.numberOfDisturbances);
122 obj.P_BESS_Charge = sdpvar(obj.horizon,obj.
        numberOfDisturbances);
123 obj.P_BESS_Discharge = sdpvar(obj.horizon,obj.
        numberOfDisturbances);
124 obj.Phi_HWT_Loss = sdpvar(obj.horizon,obj.
        numberOfDisturbances);
125
126 %Design Variables
127 obj.u_CHP = binvar(obj.horizon,obj.numberOfDisturbances);
128 obj.u_Appliance= binvar(obj.horizon,obj.
        numberOfDisturbances);
129 obj.u_BESS_Charge = sdpvar(obj.horizon,obj.
        numberOfDisturbances);
130 obj.u_BESS_Discharge = sdpvar(obj.horizon,obj.
        numberOfDisturbances);
131 obj.P_Im = sdpvar(obj.horizon,obj.numberOfDisturbances);
132 obj.P_Ex = sdpvar(obj.horizon,obj.numberOfDisturbances);
133 obj.E_BESS= sdpvar(obj.horizon,obj.numberOfDisturbances);
134 obj.E_BESS_end= sdpvar(1,obj.numberOfDisturbances);
135 obj.theta_HWT= sdpvar(obj.horizon,obj.numberOfDisturbances
        );
136 obj.theta_HWT_end= sdpvar(1,obj.numberOfDisturbances);
137 obj.s_CHP=binvar(obj.horizon,obj.numberOfDisturbances);
138
139 %for YALMIP
140 obj.WantedVariables = {obj.u_CHP , ...
141         obj.u_Appliance , ...
142         obj.u_BESS_Charge , ...

```

```

143         obj.u_BESS_Discharge,...
144         obj.P_Im,...
145         obj.P_Ex,...
146         obj.s_CHP,...
147         obj.P_BESS_Charge,...
148         obj.P_BESS_Discharge,...
149         obj.E_BESS,...
150         obj.theta_HWT};
151 end
152
153 function [controller,model] = BuildController(obj)
154     for k = 1:obj.horizon
155         obj.Objective=0;
156         for i=1:obj.numberofDisturbances
157             %Shorthand Notations for better reading
158             obj.Constraints = [obj.Constraints,obj.Phi_CHP(k,i)
159                 ) == obj.u_CHP(k,i)*obj.Phi_CHPRun];
159             obj.Constraints = [obj.Constraints,obj.G_CHP(k,i)
160                 == obj.u_CHP(k,i)*obj.G_CHPRun];
160             obj.Constraints = [obj.Constraints,obj.P_CHP(k,i)
161                 == obj.u_CHP(k,i)*obj.P_CHPRun];
161             obj.Constraints = [obj.Constraints,obj.
162                 P_BESS_Charge == obj.u_BESS_Charge * obj.
163                 P_BESS_Charge_max];
162             obj.Constraints = [obj.Constraints,obj.
164                 P_BESS_Discharge == obj.u_BESS_Discharge * obj.
165                 P_BESS_Discharge_max];
163
164             if k==1
165                 obj.Constraints = [obj.Constraints,obj.
166                     Phi_HWT_Loss(k,i) == obj.a_HWT *(12 + 5.93
167                         *(1000*obj.V_HWT)^(0.4)) ...
168                         * (obj.
169                             theta_HWT_Initial -
170                             obj.theta_In)/40];
167             else
168                 obj.Constraints = [obj.Constraints,obj.
169                     Phi_HWT_Loss(k,i) == obj.a_HWT *(12 + 5.93
170                         *(1000*obj.V_HWT)^(0.4)) ...
171                         * (obj.theta_HWT(k,i)
172                             - obj.theta_In)
173                             /40];
170             end

```

```

171
172 %Constraints
173 %Appliances
174 if k>obj.l_Appliance-1
175     obj.Constraints = [obj.Constraints,obj.
        P_Appliance(k,i) == obj.u_Appliance(k-obj.
        l_Appliance+1:k,i)' * obj.P_Appliance_nom(
        end:-1:1)];
176
177 else
        obj.Constraints = [obj.Constraints,obj.
        P_Appliance(k,i) == obj.u_Appliance(1:k,i)'
        * obj.P_Appliance_nom(k:-1:1)];
178
179 end
180 %Inital state of the energy storage systems
181 if k == 1
182     %HWT
183     obj.Constraints = [obj.Constraints,obj.
        theta_HWT(k,i) == obj.theta_HWT_Initial];
184     obj.Constraints = [obj.Constraints,obj.
        theta_HWT(k+1,i) == obj.theta_HWT(k,i)...
185         + obj.Delta_k*60*60*( obj.Phi_CHP(k,i)
        - obj.Phi_HWT_Loss(k,i) -obj.
        Phi_HS(k) - obj.Phi_DHW(k)) ...
186         / (obj.V_HWT * obj.rho_Water * obj.
        c_Water) ];
187
188     %BESS
189     obj.Constraints = [obj.Constraints, obj.E_BESS
        (k,i) == obj.E_BESS_Initial];
190     obj.Constraints = [obj.Constraints, obj.E_BESS
        (k+1,i) == obj.E_BESS(k,i) ...
191         + obj.Delta_k * (obj.eta_BESS *
        obj.P_BESS_Charge(k,i)...
192         - obj.P_BESS_Discharge(k,i)/( obj.
        eta_BESS))];
193
194 %States of the energy storage systems
195 elseif k==obj.horizon
196     obj.Constraints = [obj.Constraints,obj.
        theta_HWT_end(i) == obj.theta_HWT(k,i)...
197         + obj.Delta_k*60*60*( obj.Phi_CHP(k,i)
        - obj.Phi_HWT_Loss(k,i) -obj.

```

```

198         Phi_HS(k) - obj.Phi_DHW(k)) ...
           / (obj.V_HWT * obj.rho_Water * obj.
199             c_Water) ] ;
200     obj.Constraints = [obj.Constraints, obj.
           E_BESS_end(i) == obj.E_BESS(k,i) ...
201         + obj.Delta_k * (obj.eta_BESS *
           obj.P_BESS_Charge(k,i)...
202         - obj.P_BESS_Discharge(k,i)/( obj.
           eta_BESS))];
203
204     %Final state of the energy storage systems
205     else
206         obj.Constraints = [obj.Constraints,obj.
           theta_HWT(k+1,i) == obj.theta_HWT(k,i)...
207         + obj.Delta_k*60*60*( obj.Phi_CHP(k,i)
           - obj.Phi_HWT_Loss(k,i) -obj.
           Phi_HS(k) - obj.Phi_DHW(k)) ...
208         / (obj.V_HWT * obj.rho_Water * obj.
           c_Water) ];
209         obj.Constraints = [obj.Constraints, obj.E_BESS
           (k+1,i) == obj.E_BESS(k,i) ...
210         + obj.Delta_k * (obj.eta_BESS *
           obj.P_BESS_Charge(k,i)...
211         - obj.P_BESS_Discharge(k,i)/( obj.
           eta_BESS))];
212     end
213
214     %CHP
215     if obj.k_CHP_Initail ~=0
216         obj.Constraints = [obj.Constraints, obj.
           k_CHP_Initail-sum(obj.u_CHP(1:obj.
           k_CHP_Initail,i)) == 0];
217         if (k >= obj.k_CHP_Initail+1)&&(k<=obj.horizon
           -obj.k_CHP_Min+1)
218             obj.Constraints = [obj.Constraints, sum(
           obj.u_CHP(k:k+obj.k_CHP_Min-1,i),1) >=
           obj.k_CHP_Min*(obj.u_CHP(k)-obj.u_CHP(k
           -1,i))];
219         end
220     else
221         if k ==1

```

```

222         obj.Constraints = [obj.Constraints, sum(
                obj.u_CHP(k:k+obj.k_CHP_Min-1,i),1) >=
                obj.k_CHP_Min*(obj.u_CHP(k)-obj.
                u_CHP_Initial)];
223     elseif (k<=obj.horizon-obj.k_CHP_Min+1)
224         obj.Constraints = [obj.Constraints, sum(
                obj.u_CHP(k:k+obj.k_CHP_Min-1,i),1) >=
                obj.k_CHP_Min*(obj.u_CHP(k)-obj.u_CHP(k
                -1,i))];
225     end
226 end
227 if (k >= obj.horizon-obj.k_CHP_Min+2)
228     obj.Constraints = [obj.Constraints, sum(obj.
                u_CHP(k:obj.horizon,i)) - (obj.horizon-k)*(
                obj.u_CHP(k,i)-obj.u_CHP(k-1,i))>=0];
229 end
230 if k==1
231     obj.Constraints = [obj.Constraints, (obj.u_CHP
                (k,i)-obj.u_CHP_Initial)<= obj.s_CHP(k,i)];
232 else
233     obj.Constraints = [obj.Constraints, (obj.u_CHP
                (k,i)-obj.u_CHP(k-1,i))<= obj.s_CHP(k,i)];
234 end
235
236 %HWT
237 obj.Constraints = [obj.Constraints, obj.
                theta_HWT_min<=obj.theta_HWT(k,i)<=obj.
                theta_HWT_max];
238
239 %BESS
240 obj.Constraints = [obj.Constraints, 0<= obj.
                P_BESS_Charge(k,i) <= obj.P_BESS_Charge_max];
241 obj.Constraints = [obj.Constraints, 0<= obj.
                P_BESS_Discharge(k,i) <= obj.
                P_BESS_Discharge_max];
242 obj.Constraints = [obj.Constraints, obj.E_BESS_min
                <= obj.E_BESS(k,i) <= obj.E_BESS_max];
243
244 %Power flow
245 obj.Constraints = [obj.Constraints, obj.
                P_Appliance(k,i) + obj.P_Base(k) + obj.
                P_BESS_Charge(k,i) + obj.P_Ex(k,i)...

```

```

246         == obj.P_PV_Prediction(k,i) + obj.
           P_CHP(k,i)+ obj.
           P_BESS_Discharge(k,i) + obj.
           P_Im(k,i)];
247
248     %Interaction
249     obj.Constraints = [obj.Constraints, 0 <= obj.P_Ex(
           k,i) <= obj.P_PV_Prediction(k,i)+ obj.P_CHP(k,i
           )];
250     obj.Constraints = [obj.Constraints, 0 <= obj.P_Im(
           k,i) <= obj.P_Appliance(k,i)+ obj.P_Base(k)];
251     end
252 end
253
254 for i=1:obj.numberOfDisturbances
255     %Storage terminal constraints
256     obj.Constraints = [obj.Constraints, obj.theta_HWT_min
           <=obj.theta_HWT_end(i)<=obj.theta_HWT_max];
257     obj.Constraints = [obj.Constraints, obj.E_BESS_min <=
           obj.E_BESS_end(i) <= obj.E_BESS_max];
258
259     %Appliances
260     obj.Constraints = [obj.Constraints, sum(obj.
           u_Appliance(:,i),1) == obj.b_Appliance];
261     obj.Constraints = [obj.Constraints, obj.
           k_Appliance_min <= obj.k_vector * obj.u_Appliance
           (:,i) <= obj.k_Appliance_max];
262
263     %Objective function
264     obj.Objective = obj.Objective + (obj.Delta_k*obj.pi_Ex
           '*obj.P_Ex(:,i)...
265         + obj.Delta_k*obj.pi_Im '*obj.P_Im(:,i
           )...
266         + obj.Delta_k*obj.pi_Gas*sum(obj.
           G_CHP(:,i),1)...
267         + obj.pi_CHP_Start * sum(obj.s_CHP(:,
           i),1)) /obj.numberOfDisturbances;
268     end
269
270     for i=1:obj.numberOfDisturbances-1
271         obj.Constraints = [obj.Constraints, obj.u_CHP(1,i)
           ==obj.u_CHP(1,i+1)];

```

```
272         obj.Constraints = [obj.Constraints, obj.  
                u_Appliance(1,i)==obj.u_Appliance(1,i+1)];  
273     obj.Constraints = [obj.Constraints, obj.  
                P_BESS_Charge(1,i)==obj.P_BESS_Charge(1,i+1)];  
274     obj.Constraints = [obj.Constraints, obj.  
                P_BESS_Discharge(1,i)==obj.P_BESS_Discharge(1,i  
                +1)];  
275     end  
276  
277     ops = sdpsettings('solver','cplex', 'Cplex.timelimit',60);  
278     controller = optimizer(obj.Constraints,obj.Objective,ops,  
                obj.Parameters, obj.WantedVariables);  
279 end  
280 end  
281 end
```

B. Additional Results

B.1 Reference Control Scheme

Table B.1: Simulation results of the reference control scheme in the summer scenario with FT-1.

Δ_k in min	Δ_N in h	Electricity cost in cent	Gas cost in cent	$\tilde{E}_{\text{BESS},T+1}$ in Ws	$\tilde{\vartheta}_{\text{HWT},T+1}$ in °C	Total costs in cent
3	18	-1311	894	22	62	-518
3	24	-1328	918	28	64	-583
3	30	-1335	927	28	65	-600
3	36	-1346	951	26	67	-693
3	42	-1339	943	28	67	-667
3	48	-1343	951	41	67	-685
5	18	-1311	929	137	65	-606
5	24	-1306	902	11	63	-522
5	30	-1322	943	52	66	-633
5	36	-1330	957	0	68	-686
5	42	-1325	929	0	65	-617
5	48	-1332	957	0	67	-681
15	18	-1249	902	202	63	-466
15	24	-1292	943	248	65	-571
15	30	-1279	943	351	66	-585
15	36	-1301	943	214	66	-588
15	42	-1297	943	115	65	-568
15	48	-1295	943	114	66	-602

Table B.2: Simulation results of the reference control scheme in the summer scenario with FT-2.

Δ_k in min	Δ_N in h	Electricity cost in cent	Gas cost in cent	$\tilde{E}_{\text{BESS},T+1}$ in Ws	$\tilde{\vartheta}_{\text{HWT},T+1}$ in °C	Total costs in cent
3	18	-1408	902	317	63	-643
3	24	-1425	943	315	66	-739
3	30	-1435	910	334	63	-668
3	36	-1428	927	988	65	-711
3	42	-1438	935	312	66	-739
3	48	-1439	968	1058	68	-820
5	18	-1370	888	359	62	-564
5	24	-1408	916	577	64	-659
5	30	-1401	929	1031	65	-689
5	36	-1420	929	345	65	-707
5	42	-1410	943	1154	66	-729
5	48	-1435	943	353	67	-762
15	18	-1338	902	437	63	-552
15	24	-1357	943	437	66	-668
15	30	-1366	943	440	66	-669
15	36	-1385	943	436	66	-686
15	42	-1378	943	436	66	-688
15	48	-1383	943	293	66	-690

Table B.3: Simulation results of the reference control scheme in the summer scenario with FT-3.

Δ_k in min	Δ_N in h	Electricity cost in cent	Gas cost in cent	$\tilde{E}_{\text{BESS},T+1}$ in Ws	$\tilde{\vartheta}_{\text{HWT},T+1}$ in °C	Total costs in cent
3	18	-1599	910	1872	64	-846
3	24	-1614	927	728	65	-895
3	30	-1622	935	1306	66	-923
3	36	-1678	927	448	65	-952
3	42	-1670	951	1258	67	-1010
3	48	-1685	959	963	68	-1045
5	18	-1552	916	1179	64	-817
5	24	-1593	929	1447	65	-877
5	30	-1609	943	2268	66	-921
5	36	-1627	943	597	66	-944
5	42	-1642	957	1338	67	-992
5	48	-1633	957	1578	67	-984
15	18	-1466	902	338	63	-668
15	24	-1485	943	260	66	-774
15	30	-1499	943	325	65	-766
15	36	-1438	943	324	65	-720
15	42	-1439	943	534	65	-721
15	48	-1574	984	3118	69	-962

Table B.4: Simulation results of the reference control scheme in the spring scenario with FT-1.

Δ_k in min	Δ_N in h	Electricity cost in cent	Gas cost in cent	$\tilde{E}_{\text{BESS},T+1}$ in Ws	$\tilde{\vartheta}_{\text{HWT},T+1}$ in °C	Total costs in cent
3	18	-1296	3887	1	64	2419
3	24	-1305	3887	169	64	2416
3	30	-1301	3887	2	64	2416
3	36	-1294	3887	0	64	2414
3	42	-1318	3920	0	67	2305
3	48	-1325	3928	1	68	2272
5	18	-1283	3895	2	65	2409
5	24	-1298	3895	1	65	2408
5	30	-1291	3881	4	64	2427
5	36	-1286	3895	136	65	2400
5	42	-1294	3909	2	66	2368
5	48	-1298	3909	0	66	2360
15	18	-1240	3895	257	65	2466
15	24	-1262	3895	127	64	2449
15	30	-1267	3895	9	64	2446
15	36	-1249	3895	163	65	2452
15	42	-1279	3936	252	68	2328
15	48	-1267	3936	126	68	2327

Table B.5: Simulation results of the reference control scheme in the spring scenario with FT-2.

Δ_k in min	Δ_N in h	Electricity cost in cent	Gas cost in cent	$\tilde{E}_{\text{BESS},T+1}$ in Ws	$\tilde{\vartheta}_{\text{HWT},T+1}$ in °C	Total costs in cent
3	18	-1444	3887	619	63	2317
3	24	-1445	3895	640	64	2293
3	30	-1457	3903	640	65	2252
3	36	-1456	3936	1	67	2171
3	42	-1462	3944	24	68	2137
3	48	-1475	3928	27	67	2173
5	18	-1411	3895	964	64	2334
5	24	-1427	3895	960	64	2306
5	30	-1430	3909	959	65	2260
5	36	-1434	3936	226	68	2189
5	42	-1441	3922	1037	66	2220
5	48	-1449	3922	7	66	2210
15	18	-1376	3895	256	64	2371
15	24	-1398	3895	267	64	2340
15	30	-1404	3895	256	64	2336
15	36	-1405	3936	270	67	2226
15	42	-1419	3936	354	67	2215
15	48	-1422	3936	252	67	2212

Table B.6: Simulation results of the reference control scheme in the spring scenario with FT-3.

Δ_k in min	Δ_N in h	Electricity cost in cent	Gas cost in cent	$\tilde{E}_{\text{BESS},T+1}$ in Ws	$\tilde{\vartheta}_{\text{HWT},T+1}$ in °C	Total costs in cent
3	18	-2165	3903	171	64	1559
3	24	-2187	3903	168	64	1532
3	30	-2180	3903	168	64	1539
3	36	-2181	3903	185	64	1539
3	42	-2199	3944	190	68	1422
3	48	-2199	3944	190	68	1410
5	18	-2144	3909	227	65	1571
5	24	-2160	3909	230	65	1545
5	30	-2161	3909	90	65	1542
5	36	-2155	3909	170	65	1544
5	42	-2160	3909	107	65	1543
5	48	-2166	3922	38	66	1499
15	18	-2060	3895	346	63	1710
15	24	-2089	3895	346	64	1660
15	30	-2080	3895	345	63	1673
15	36	-2100	3936	346	67	1544
15	42	-2102	3936	346	67	1541
15	48	-2098	3936	154	67	1539

Table B.7: Simulation results of the reference control scheme in the winter scenario with FT-1.

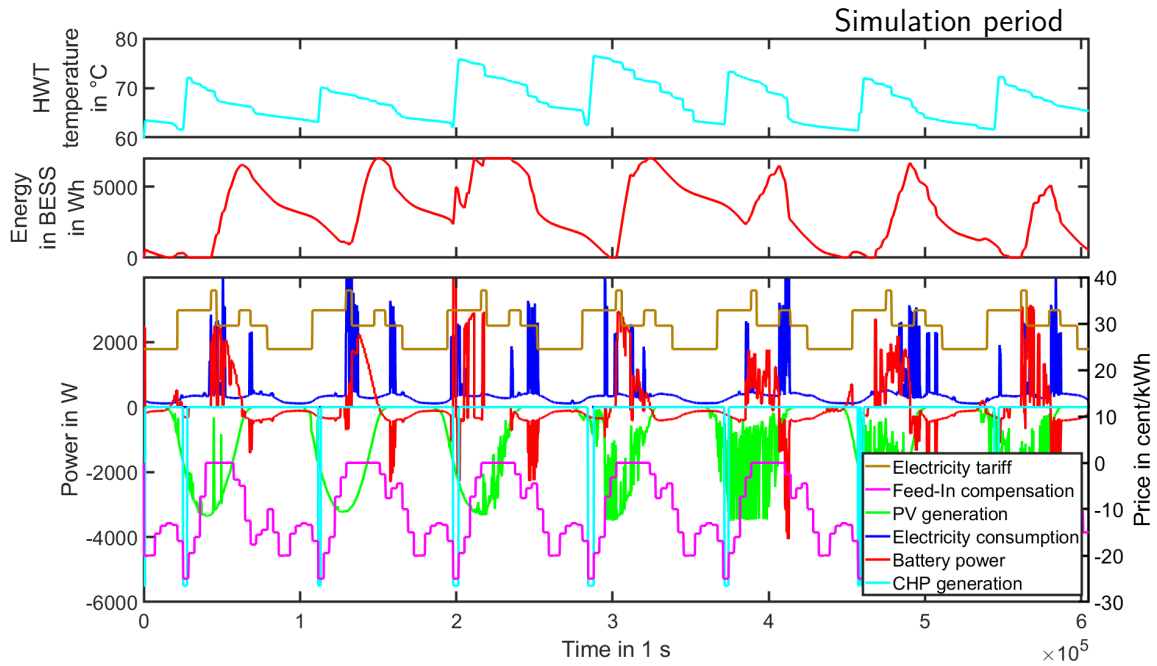
Δ_k in min	Δ_N in h	Electricity cost in cent	Gas cost in cent	$\tilde{E}_{\text{BESS},T+1}$ in Ws	$\tilde{\vartheta}_{\text{HWT},T+1}$ in °C	Total costs in cent
3	18	-890	5666	1	63	4649
3	24	-889	5674	1	64	4639
3	30	-904	5707	30	67	4531
3	36	-900	5699	0	66	4532
3	42	-901	5691	0	66	4552
3	48	-908	5699	0	66	4528
5	18	-871	5685	0	65	4621
5	24	-875	5685	0	65	4612
5	30	-878	5685	4	65	4605
5	36	-880	5699	0	66	4568
5	42	-879	5699	3	66	4572
5	48	-880	5713	3	67	4533
15	18	-815	5658	34	62	4759
15	24	-840	5699	33	66	4626
15	30	-826	5699	33	66	4640
15	36	-829	5699	33	66	4633
15	42	-820	5699	33	66	4646
15	48	-829	5699	33	66	4638

Table B.8: Simulation results of the reference control scheme in the winter scenario with FT-2.

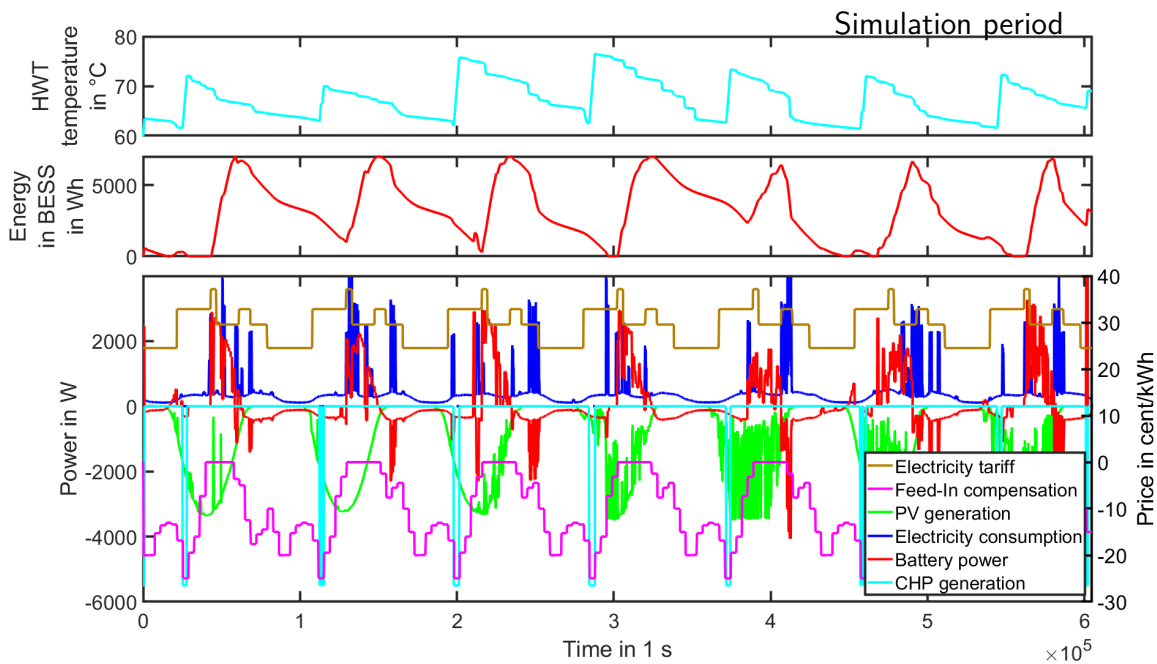
Δ_k in min	Δ_N in h	Electricity cost in cent	Gas cost in cent	$\tilde{E}_{\text{BESS},T+1}$ in Ws	$\tilde{\vartheta}_{\text{HWT},T+1}$ in °C	Total costs in cent
3	18	-982	5691	5	64	4550
3	24	-992	5691	4	64	4529
3	30	-983	5707	1	66	4466
3	36	-995	5691	6	65	4505
3	42	-1012	5732	4	68	4380
3	48	-1005	5740	2	69	4366
5	18	-966	5699	11	65	4544
5	24	-967	5685	21	64	4560
5	30	-962	5685	9	64	4552
5	36	-973	5685	7	64	4541
5	42	-986	5713	8	66	4467
5	48	-975	5740	2	69	4395
15	18	-911	5699	33	65	4594
15	24	-917	5699	33	65	4593
15	30	-917	5699	33	65	4577
15	36	-930	5699	33	65	4560
15	42	-931	5699	33	65	4556
15	48	-940	5740	33	69	4440

Table B.9: Simulation results of the reference control scheme in the winter scenario with FT-3.

Δ_k in min	Δ_N in h	Electricity cost in cent	Gas cost in cent	$\tilde{E}_{\text{BESS},T+1}$ in Ws	$\tilde{\vartheta}_{\text{HWT},T+1}$ in °C	Total costs in cent
3	18	-1584	5683	80	63	3974
3	24	-1586	5683	12	63	3959
3	30	-1581	5683	2	63	3960
3	36	-1590	5691	6	64	3923
3	42	-1596	5699	2	65	3899
3	48	-1602	5715	2	66	3856
5	18	-1558	5699	11	65	3950
5	24	-1554	5685	4	63	3998
5	30	-1546	5685	4	64	3989
5	36	-1550	5699	4	65	3936
5	42	-1557	5699	4	65	3941
5	48	-1568	5713	4	66	3896
15	18	-1492	5699	40	64	4027
15	24	-1480	5699	40	65	4027
15	30	-1477	5699	40	64	4040
15	36	-1471	5699	40	65	4023
15	42	-1519	5740	290	68	3896
15	48	-1517	5740	290	68	3897

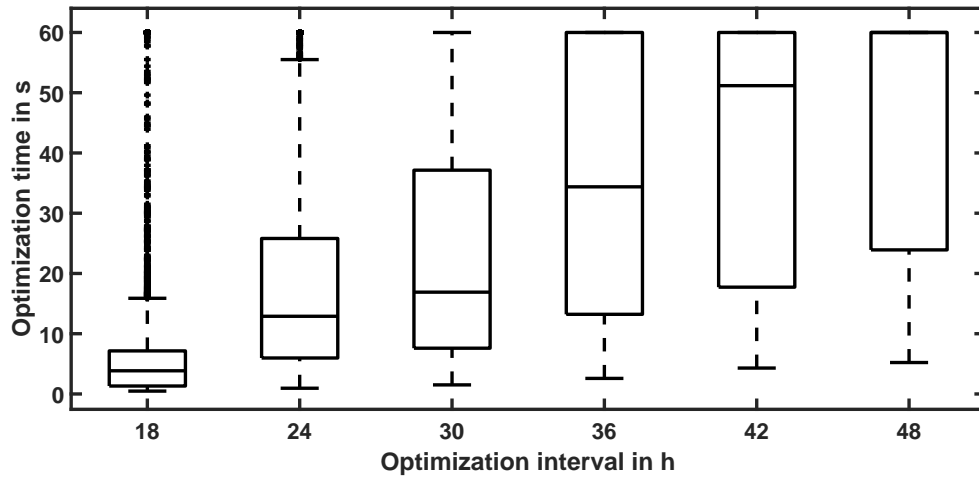


(a) Simulation results with $\Delta_N = 42$ h.

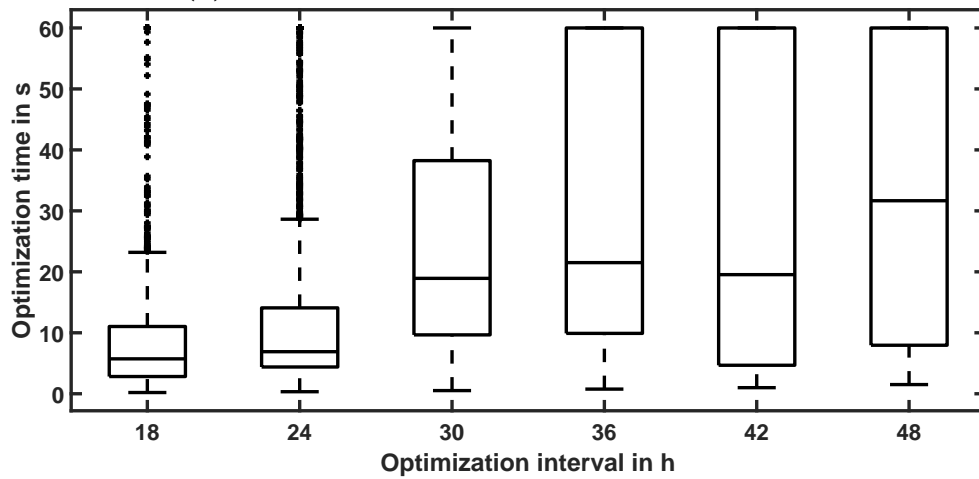


(b) Simulation results with $\Delta_N = 48$ h.

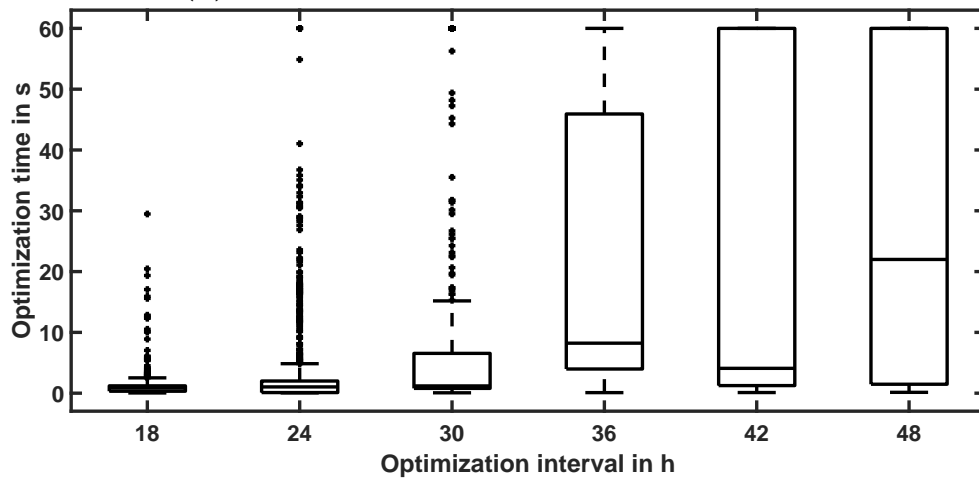
Figure B.1: Visualization of the electrical loads and ESS states in the building energy system using the reference control scheme. Simulation results on the summer scenario with FT-3 for a simulation with $\Delta_N = 42$ h (a) and a simulation with $\Delta_N = 48$ h (b).



(a) Summer scenario with FT-1 and $\Delta_k = 3$ min.

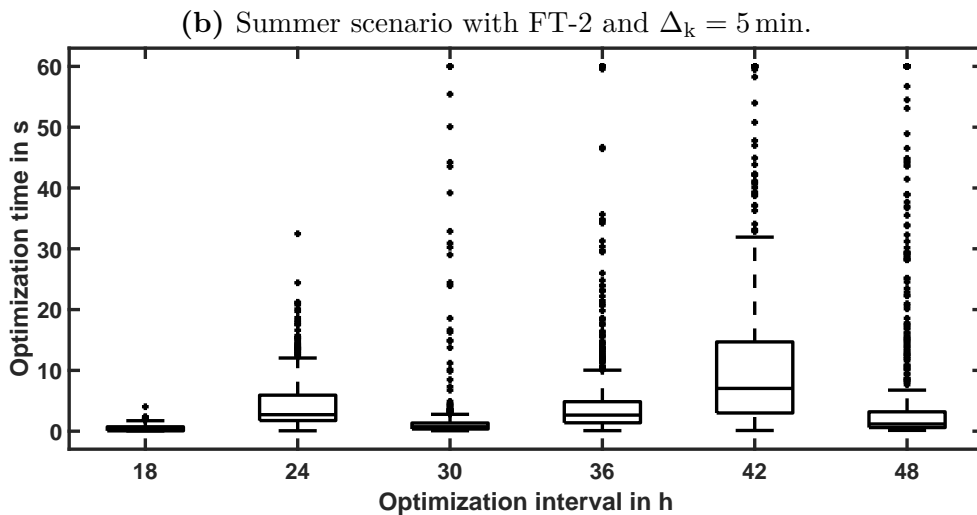
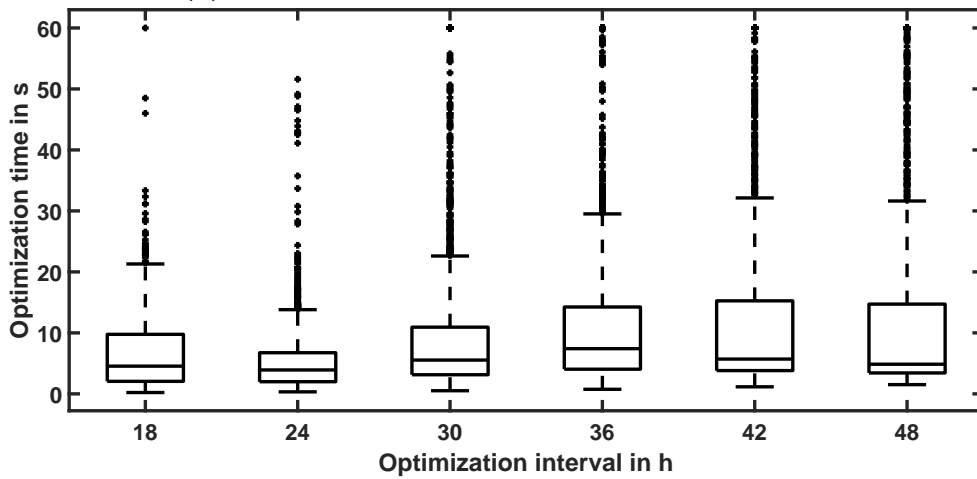
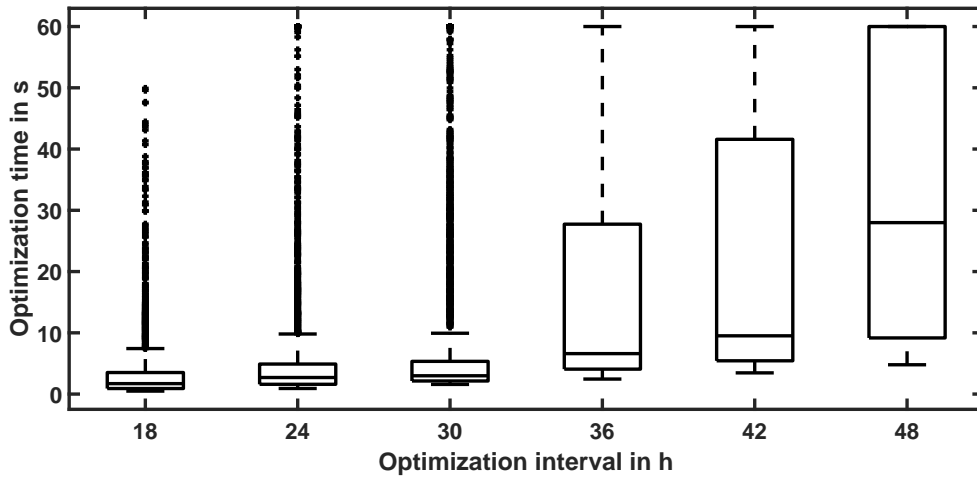


(b) Summer scenario with FT-1 and $\Delta_k = 5$ min.



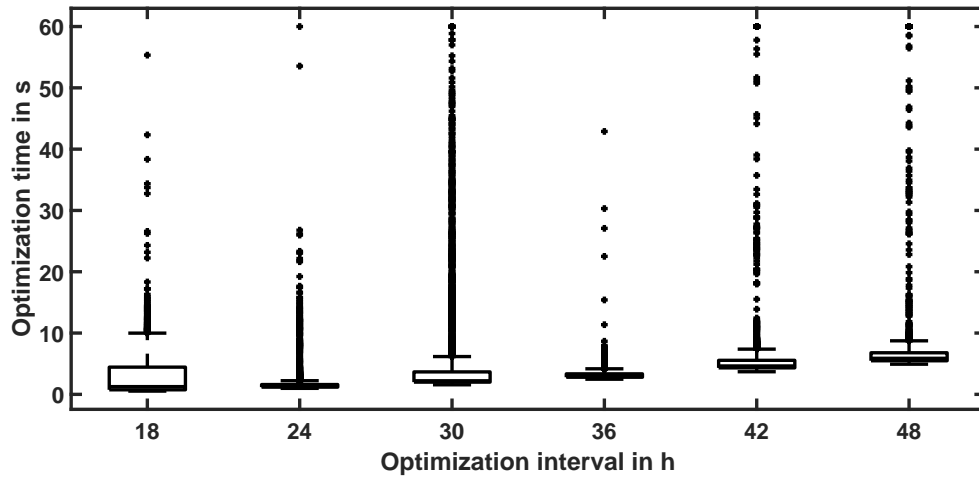
(c) Summer scenario with FT-1 and $\Delta_k = 15$ min.

Figure B.2: Visualization of the optimization times in dependence on the optimization interval and the time step duration in the reference control scheme in the summer scenario with FT-1



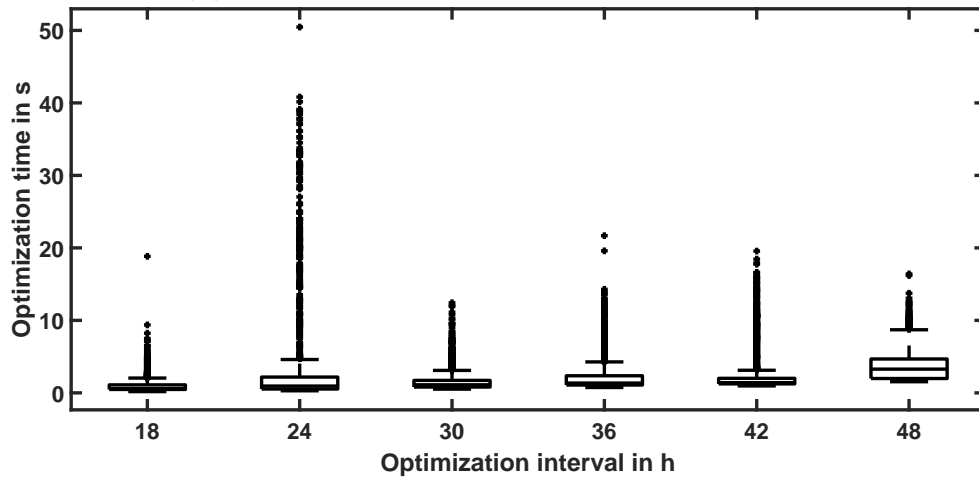
(d) Summer scenario with FT-2 and $\Delta_k = 15$ min.

Figure B.3: Visualization of the optimization times in dependence on the optimization interval and the time step duration in the reference control scheme in the summer scenario with FT-2

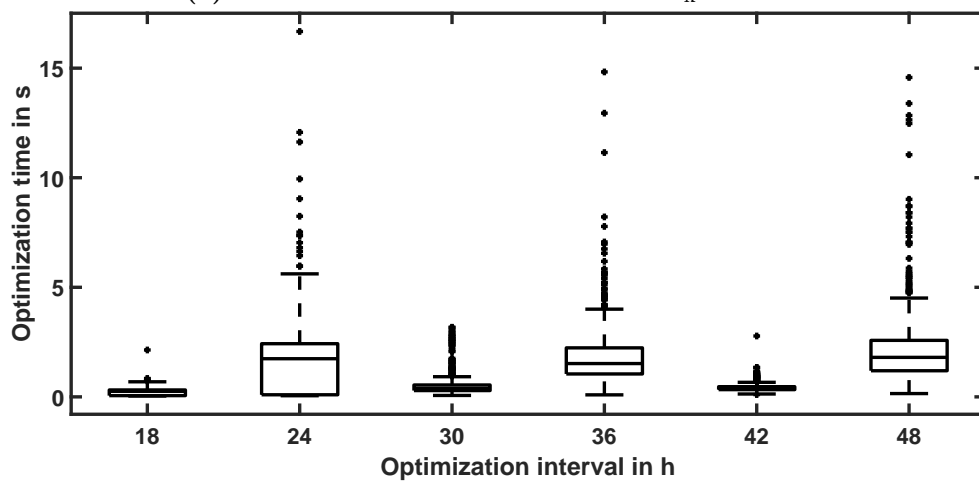


(a) FT3-DeltaK3

(b) Summer scenario with FT-3 and $\Delta_k = 3$ min.

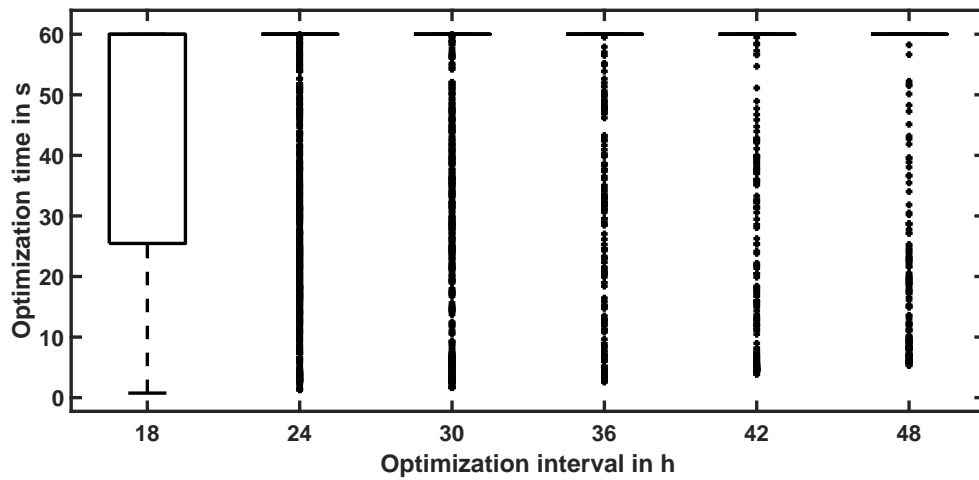


(c) Summer scenario with FT-3 and $\Delta_k = 5$ min.

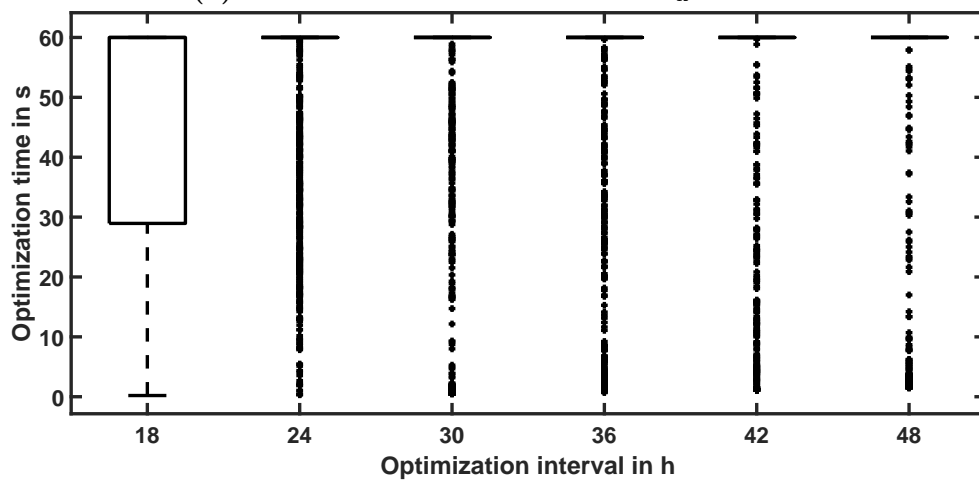


(d) Summer scenario with FT-3 and $\Delta_k = 15$ min.

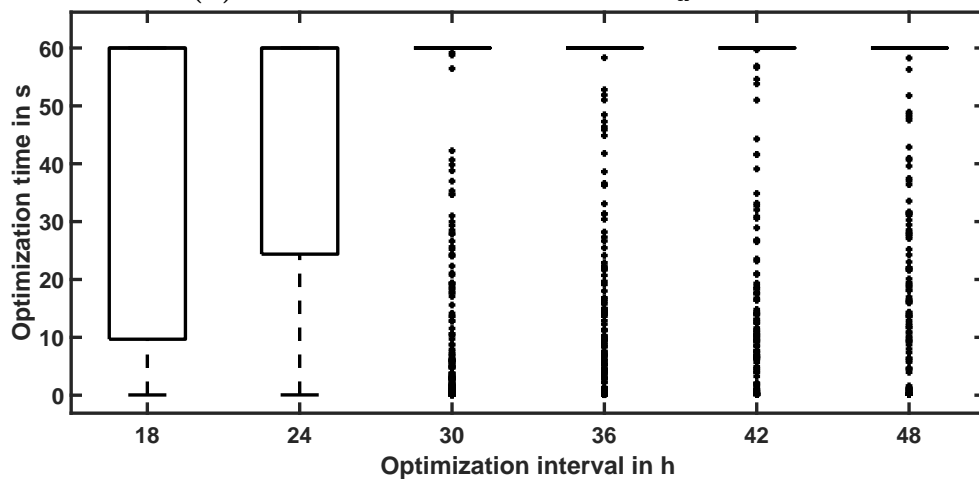
Figure B.4: Visualization of the optimization times in dependence on optimization interval and the time step duration in the reference control scheme in the summer scenario with FT-3



(a) Winter scenario with FT-1 and $\Delta_k = 3$ min.

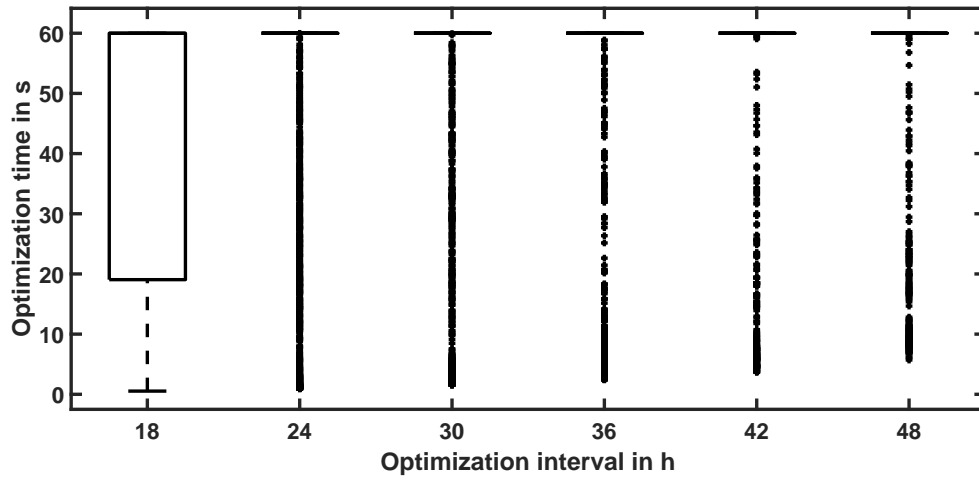


(b) Winter scenario with FT-1 and $\Delta_k = 5$ min.

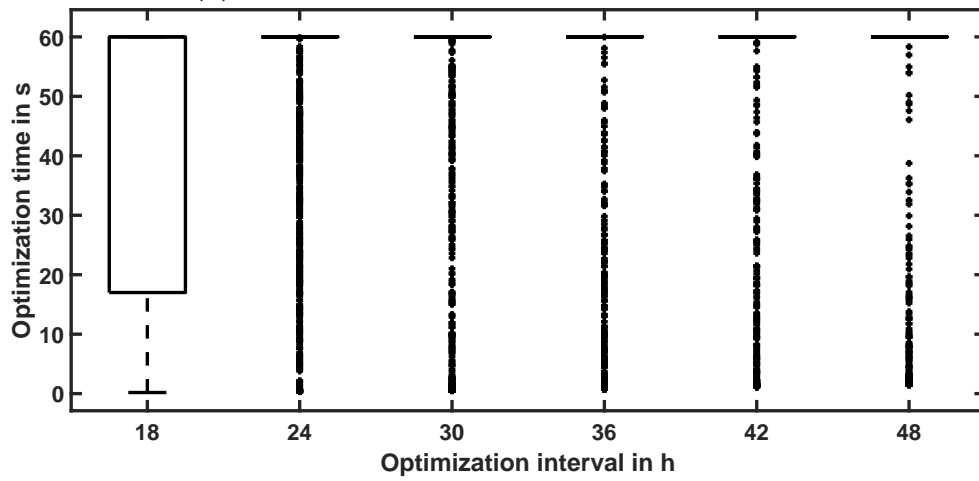


(c) Winter scenario with FT-1 and $\Delta_k = 15$ min.

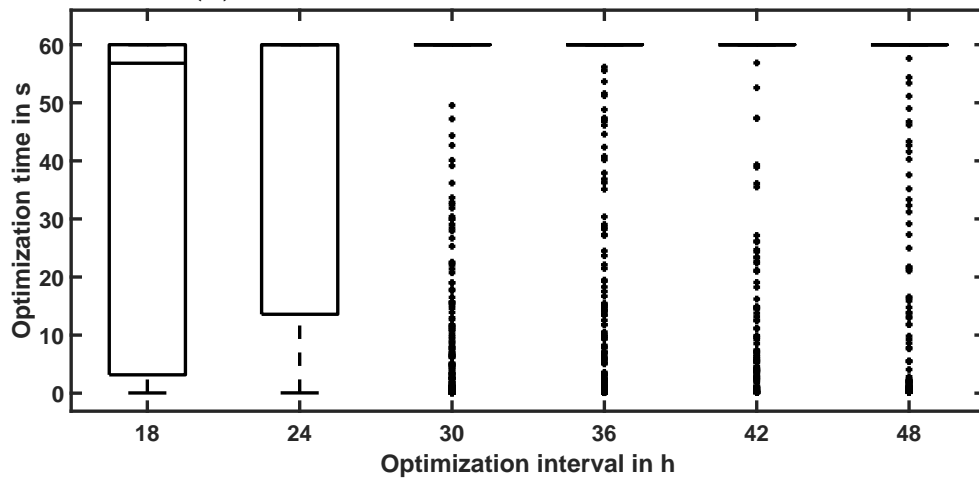
Figure B.5: Visualization of the optimization times in dependence on the optimization interval and the time step duration in the reference control scheme in the winter scenario with FT-1



(a) Winter scenario with FT-2 and $\Delta_k = 3$ min.

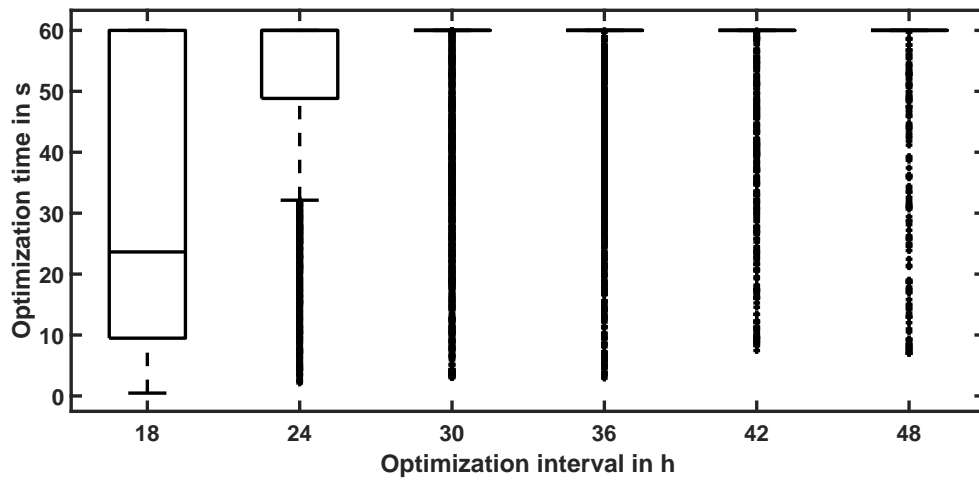


(b) Winter scenario with FT-2 and $\Delta_k = 5$ min.

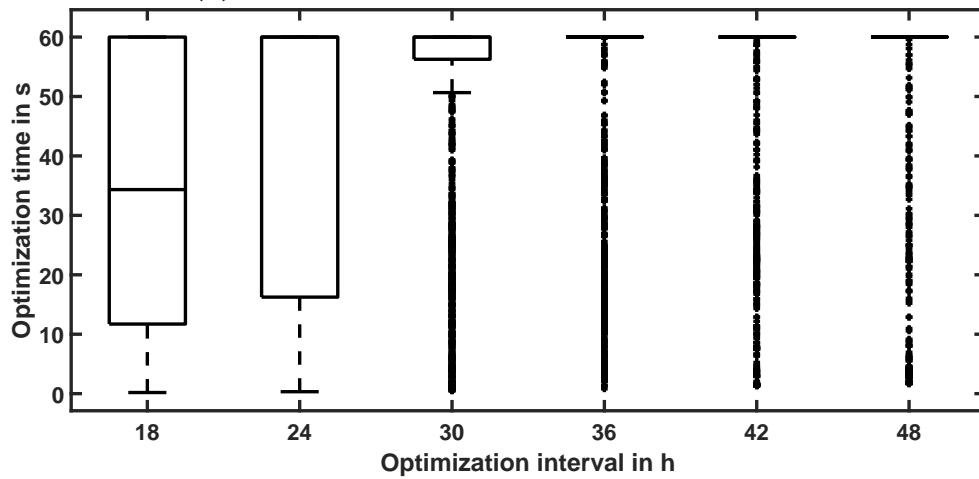


(c) Winter scenario with FT-2 and $\Delta_k = 15$ min.

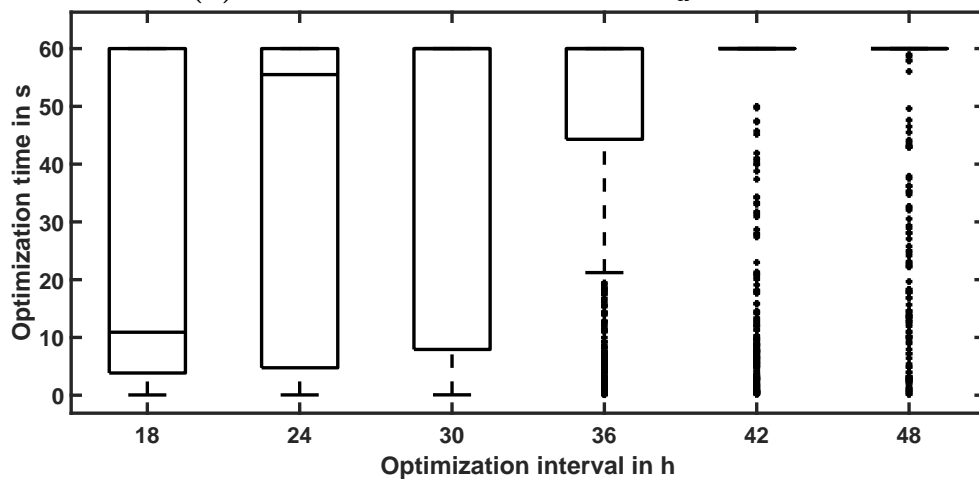
Figure B.6: Visualization of the optimization times in dependence on the tuning parameters optimization interval and the time step duration in the reference control scheme in the winter scenario with FT-2



(a) Winter scenario with FT-3 and $\Delta_k = 3$ min.

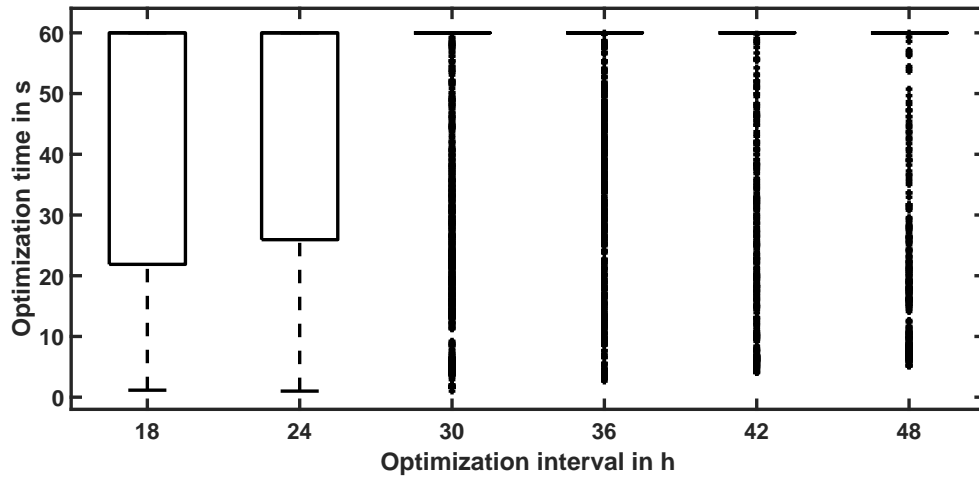


(b) Winter scenario with FT-3 and $\Delta_k = 5$ min.

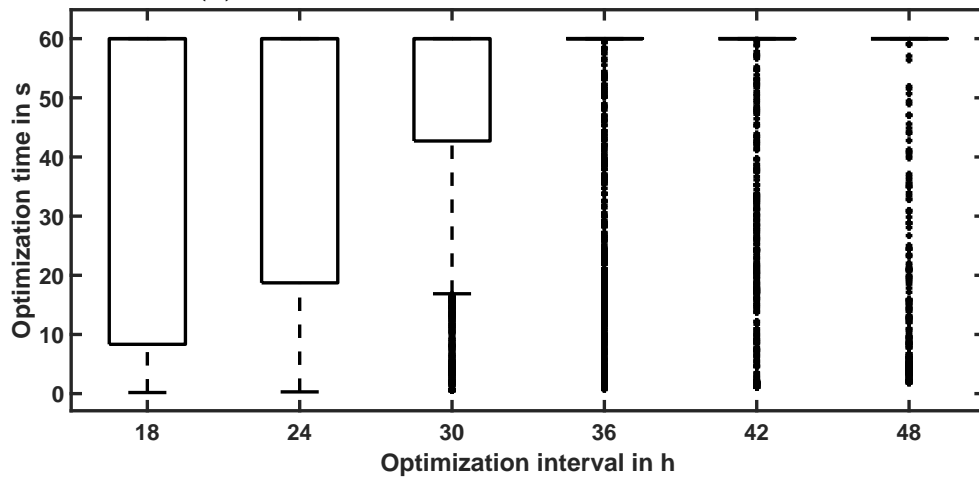


(c) Winter scenario with FT-3 and $\Delta_k = 15$ min.

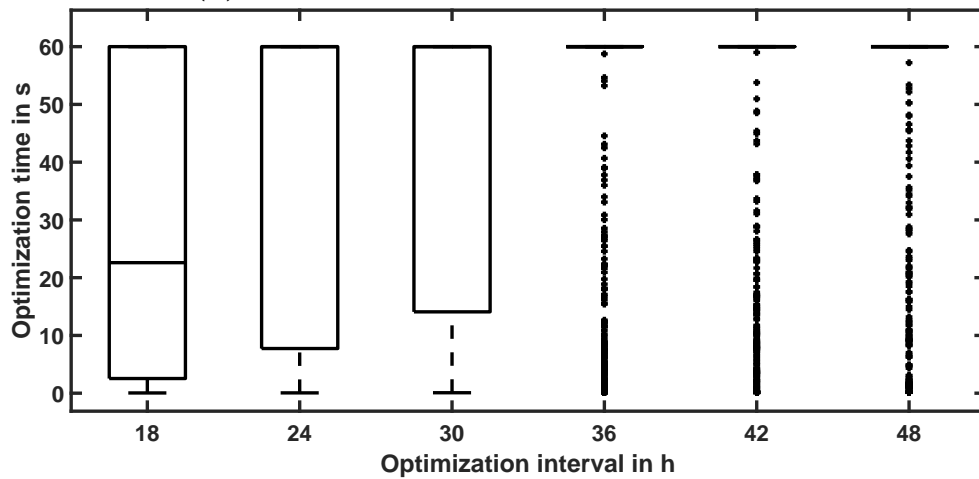
Figure B.7: Visualization of the optimization times in dependence on the optimization interval and the time step duration in the reference control scheme in the winter scenario with FT-3



(a) Spring scenario with FT-1 and $\Delta_k = 3$ min.

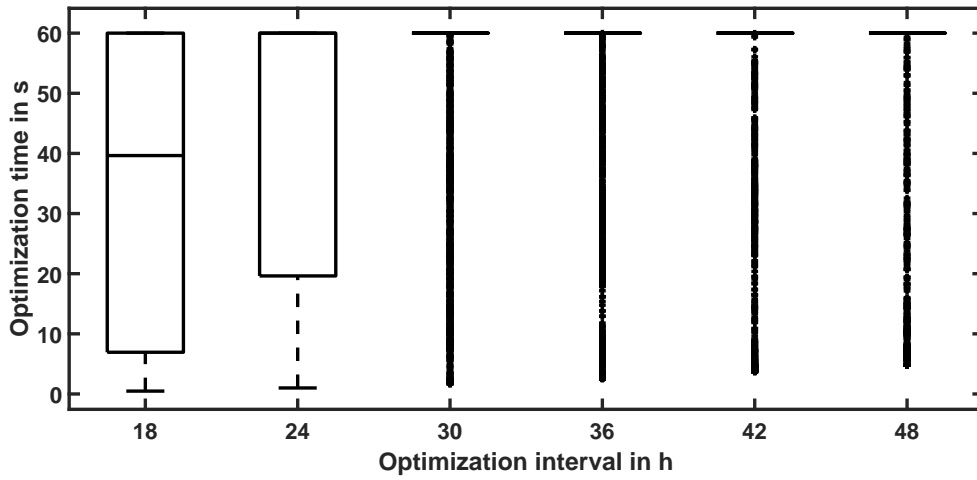


(b) Spring scenario with FT-1 and $\Delta_k = 5$ min.

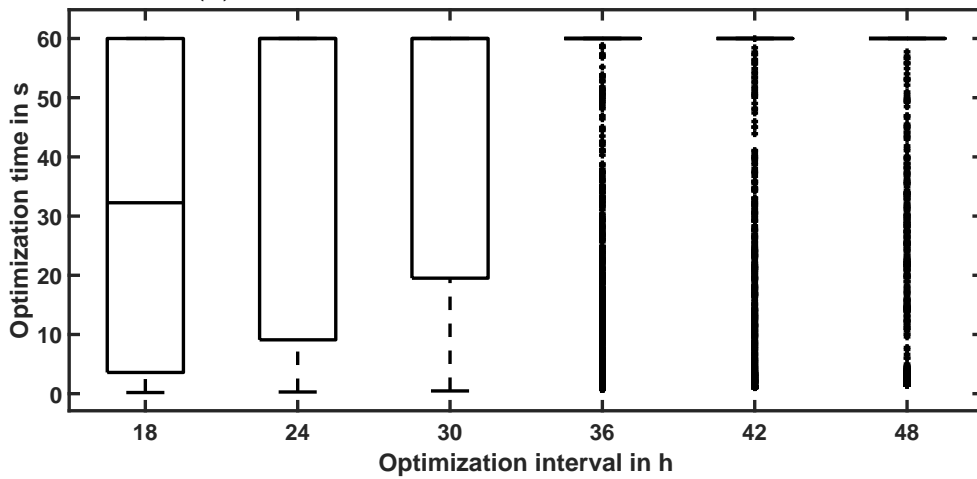


(c) Spring scenario with FT-1 and $\Delta_k = 15$ min.

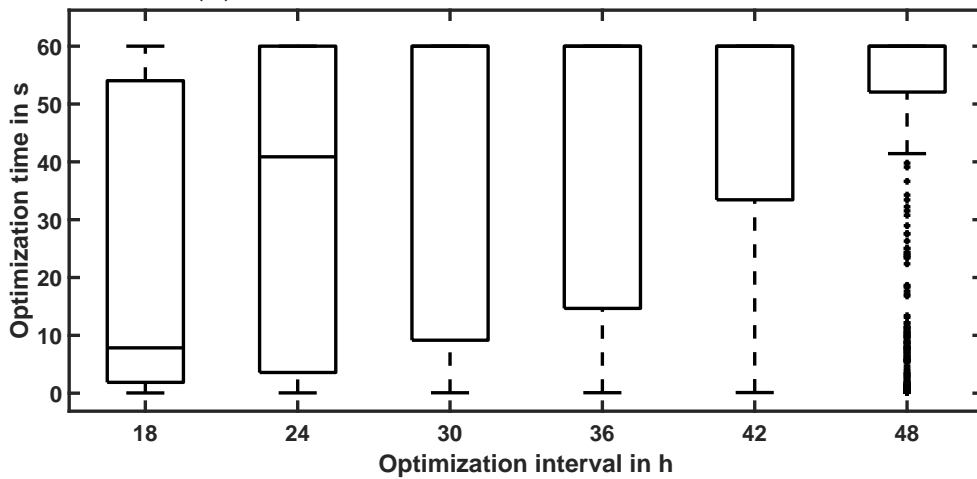
Figure B.8: Visualization of the optimization times in dependence on the optimization interval and the time step duration in the reference control scheme in the spring scenario with FT-1



(a) Spring scenario with FT-2 and $\Delta_k = 3$ min.

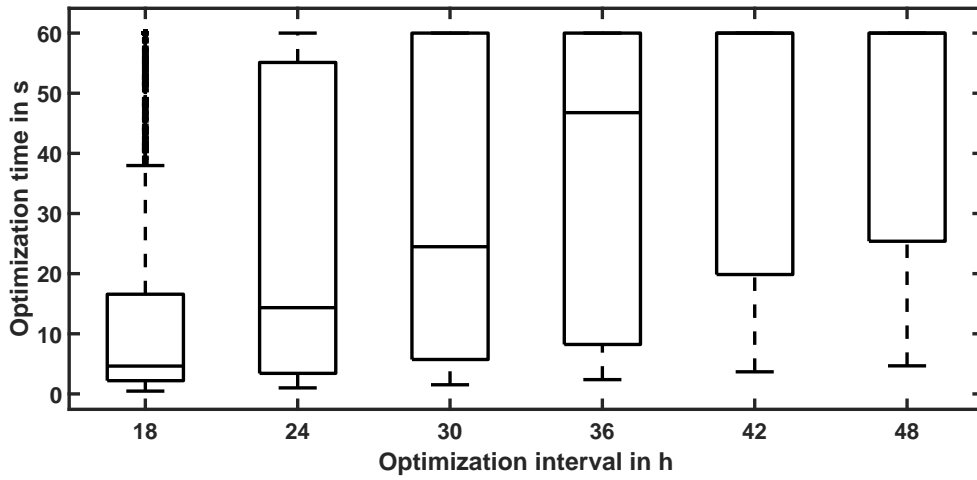


(b) Spring scenario with FT-2 and $\Delta_k = 5$ min.

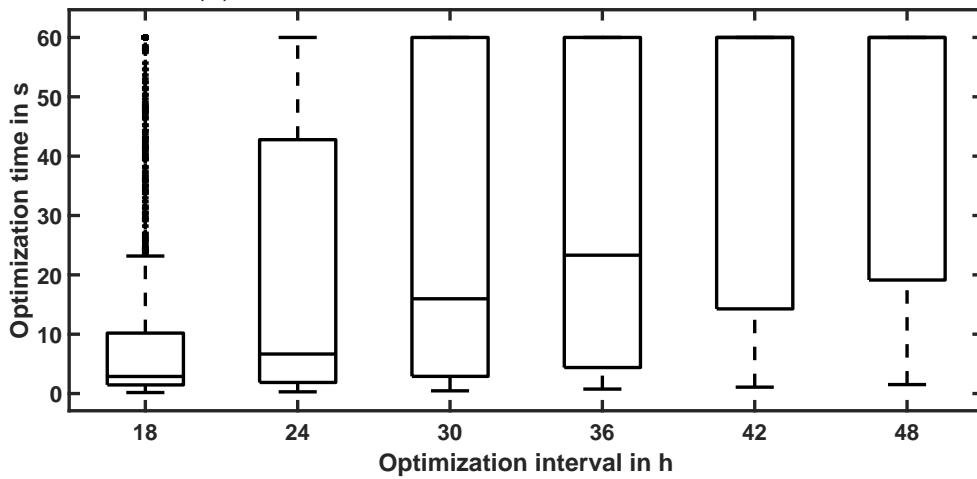


(c) Spring scenario with FT-2 and $\Delta_k = 15$ min.

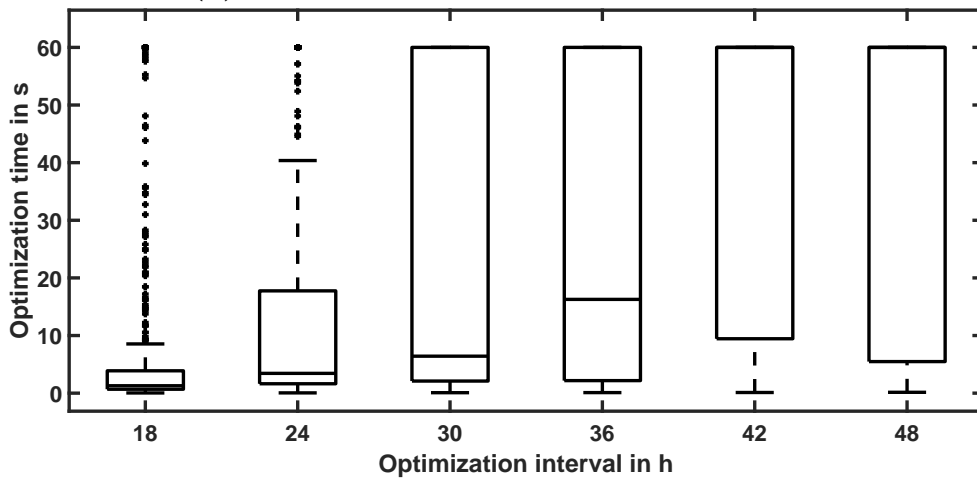
Figure B.9: Visualization of the optimization times in dependence on the optimization interval and the time step duration in the reference control scheme in the spring scenario with FT-2



(a) Spring scenario with FT-3 and $\Delta_k = 3$ min.



(b) Spring scenario with FT-3 and $\Delta_k = 5$ min.



(c) Spring scenario with FT-3 and $\Delta_k = 15$ min.

Figure B.10: Visualization of the optimization times in dependence on the optimization interval and the time step duration in the reference control scheme in the spring scenario with FT-3

B.2 State-of-the-art and Stochastic Control Scheme

Table B.10: Simulation results of the state-of-the-art and stochastic control scheme in the summer scenario with FT-1.

Δ_N in h	M	Electricity cost in cent	Gas cost in cent	$\tilde{E}_{\text{BESS},T+1}$ in W	$\tilde{\vartheta}_{\text{HWT},T+1}$ in °C	Total costs in cent
24	1	-1186	929	0	65	-447
24	3	-1198	916	0	64	-428
24	5	-1179	943	0	66	-490
24	7	-1175	929	0	65	-436
24	9	-1174	916	0	64	-406
24	11	-1092	943	0	64	-295
30	1	-1196	943	0	66	-497
30	3	-1208	943	0	66	-514
30	5	-1168	916	0	64	-411
30	7	-1158	916	0	64	-405
30	9	No valid solution found				
30	11	No valid solution found				

Table B.11: Simulation results of the state-of-the-art and stochastic control scheme in the summer scenario with FT-2.

Δ_N in h	M	Electricity cost in cent	Gas cost in cent	$\tilde{E}_{\text{BESS},T+1}$ in W	$\tilde{\vartheta}_{\text{HWT},T+1}$ in °C	Total costs in cent
24	1	-1213	916	0	64	-455
24	3	-1248	929	0	65	-525
24	5	-1234	943	0	66	-546
24	7	-1234	916	13	65	-505
24	9	-1226	929	67	64	-478
24	11	No valid solution found				
30	1	-1219	929	0	65	-493
30	3	-1249	929	0	65	-522
30	5	-1242	929	0	65	-532
30	7	-1243	916	0	64	-484
30	9	No valid solution found				
30	11	No valid solution found				

Table B.12: Simulation results of the state-of-the-art and stochastic control scheme the summer scenario and with FT-3.

Δ_N in h	M	Electricity cost in cent	Gas cost in cent	$\tilde{E}_{\text{BESS},T+1}$ in W	$\tilde{\vartheta}_{\text{HWT},T+1}$ in °C	Total costs in cent
24	1	-1394	929	276	65	-677
24	3	-1460	929	1113	65	-743
24	5	-1463	929	2181	65	-743
24	7	-1489	916	1884	64	-729
24	9	-1468	929	2210	65	-742
24	11	-683	957	2727	66	32
30	1	-1390	929	1442	65	-667
30	3	-1465	916	1716	64	-710
30	5	-1477	929	1875	65	-756
30	7	-1470	943	2333	66	-780
30	9		No valid solution found			
30	11		No valid solution found			

Table B.13: Simulation results of the state-of-the-art and stochastic control scheme in the winter scenario with FT-1.

Δ_N in h	M	Electricity cost in cent	Gas cost in cent	$\tilde{E}_{\text{BESS},T+1}$ in W	$\tilde{\vartheta}_{\text{HWT},T+1}$ in °C	Total costs in cent
24	1	-770	5672	1	64	4751
24	3	-765	5699	2	66	4681
24	5	-765	5699	7	66	4693
24	7	-728	5699	8	66	4740
24	9		No valid solution found			
24	11		No valid solution found			
30	1	-777	5699	0	66	4671
30	3	-762	5672	0	64	4760
30	5	-685	5672	0	64	4820
30	7	-550	5685	6	66	4883
30	9		No valid solution found			
30	11		No valid solution found			

Table B.14: Simulation results of the state-of-the-art and stochastic control scheme in the winter scenario with FT-2.

Δ_N in h	M	Electricity cost in cent	Gas cost in cent	$\tilde{E}_{\text{BESS},T+1}$ in W	$\tilde{\vartheta}_{\text{HWT},T+1}$ in °C	Total costs in cent
24	1	-867	5685	0	64	4667
24	3	-861	5685	9	64	4675
24	5	-844	5685	9	64	4686
24	7	-666	5685	11	64	4843
24	9	29	5672	11	64	5518
24	11	No valid solution found				
30	1	-140	6478	0	64	6178
30	3	-134	6492	0	65	6156
30	5	-138	6492	0	66	6125
30	7	No valid solution found				
30	9	No valid solution found				
30	11	No valid solution found				

Table B.15: Simulation results of the state-of-the-art and stochastic control scheme in the winter scenario with FT-3.

Δ_N in h	M	Electricity cost in cent	Gas cost in cent	$\tilde{E}_{\text{BESS}}(T)$ in W	$\tilde{\vartheta}_{\text{HWT}}$ in °C	Total costs in cent
24	1	-1440	5685	4	64	4101
24	3	-1443	5685	27	63	4114
24	5	-1366	5685	4	63	4191
24	7	-1084	5685	169	64	4453
24	9	No valid solution found				
24	11	No valid solution found				
30	1	-1438	5685	4	64	4102
30	3	-1403	5685	27	63	4138
30	5	-1202	5699	4	65	4278
30	7	-743	5672	26	65	4742
30	9	No valid solution found				
30	11	No valid solution found				

Table B.16: Simulation results of the state-of-the-art and stochastic control scheme in the spring scenario with FT-1.

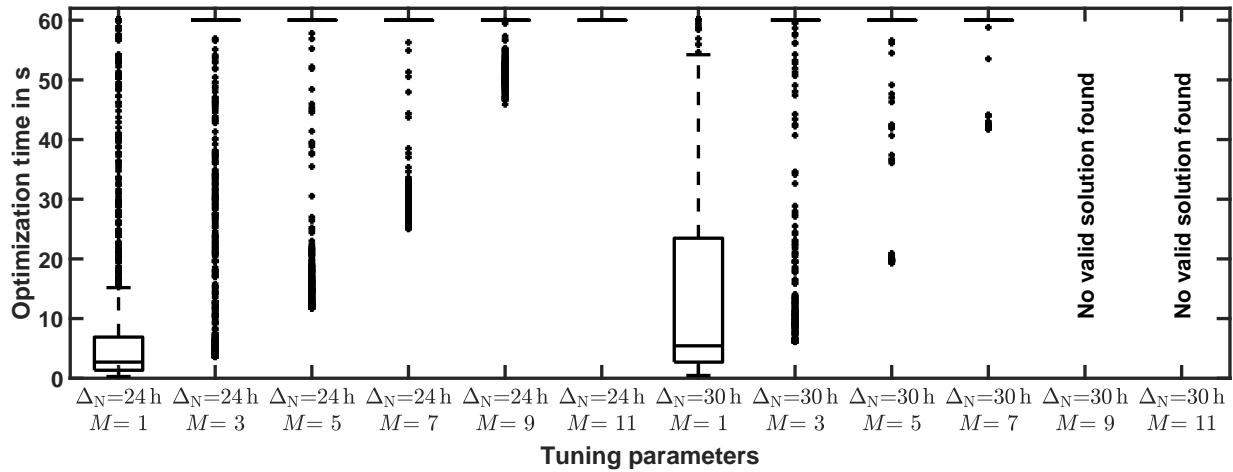
Δ_N in h	M	Electricity cost in cent	Gas cost in cent	$\tilde{E}_{\text{BESS},T+1}$ in W	$\tilde{\vartheta}_{\text{HWT},T+1}$ in °C	Total costs in cent
24	1	-939	3881	1	64	2784
24	3	-939	3868	5	63	2818
24	5	-945	3909	5	66	2723
24	7	-959	3909	5	65	2727
24	9	No valid solution found				
24	11	No valid solution found				
30	1	-942	3895	1	65	2739
30	3	-955	3909	2	66	2690
30	5	-952	3909	3	66	2703
30	7	-963	3881	5	64	2756
30	9	No valid solution found				
30	11	No valid solution found				

Table B.17: Simulation results of the state-of-the-art and stochastic control scheme in the spring scenario with FT-2.

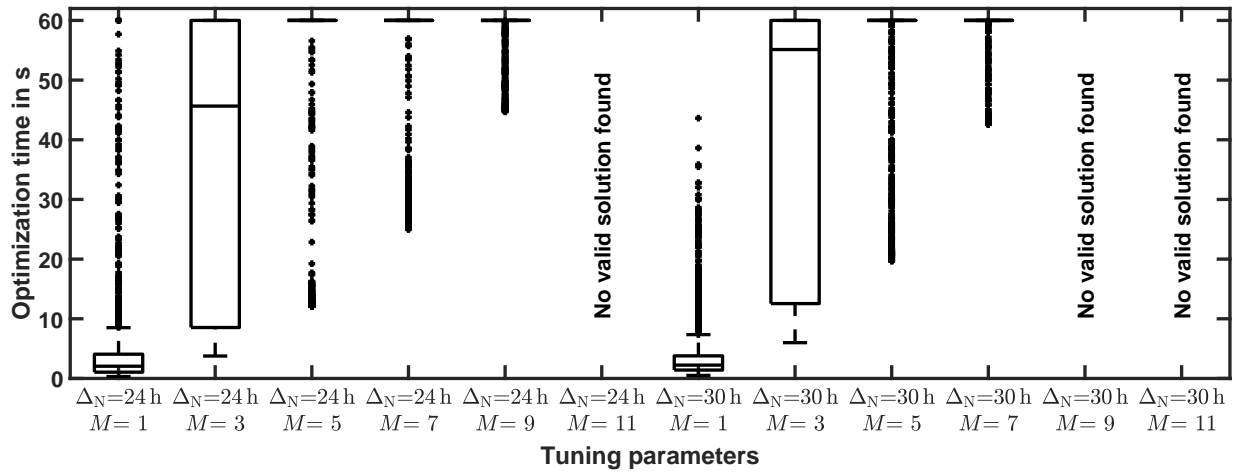
Δ_N in h	M	Electricity cost in cent	Gas cost in cent	$\tilde{E}_{\text{BESS},T+1}$ in W	$\tilde{\vartheta}_{\text{HWT},T+1}$ in °C	Total costs in cent
24	1	-1069	3909	1	65	2634
24	3	-1019	3881	5	63	2748
24	5	-1027	3895	2	64	2722
24	7	-1005	3895	5	63	2756
24	9	-617	3881	5	64	3118
24	11	No valid solution found				
30	1	-1047	3922	1	66	2612
30	3	-1023	3922	2	66	2632
30	5	-1061	3909	3	65	2648
30	7	-1019	3922	5	67	2619
30	9	No valid solution found				
30	11	No valid solution found				

Table B.18: Simulation results of the state-of-the-art and stochastic control scheme in the spring scenario with FT-3.

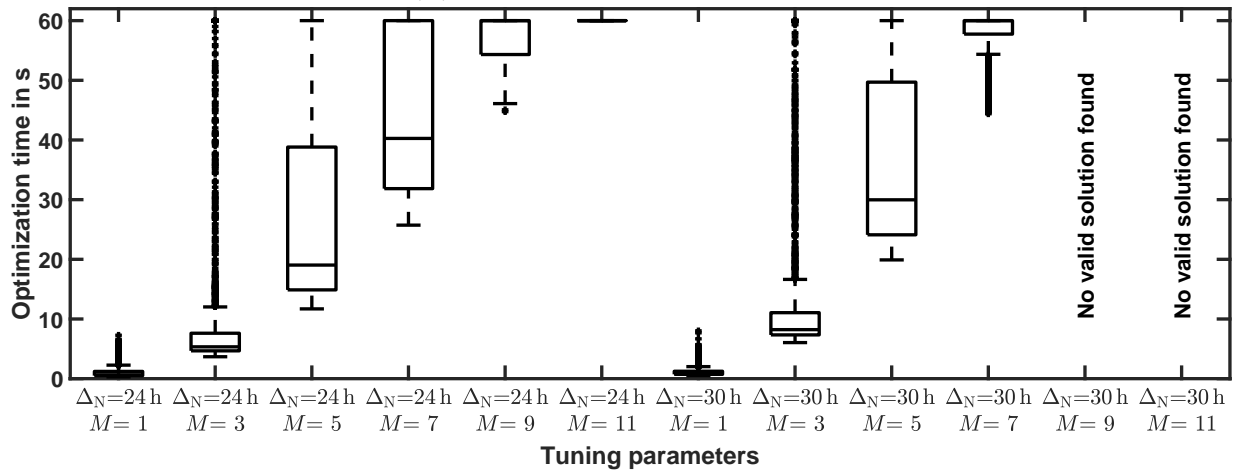
Δ_N in h	M	Electricity cost in cent	Gas cost in cent	$\tilde{E}_{\text{BESS},T+1}$ in W	$\tilde{\vartheta}_{\text{HWT},T+1}$ in °C	Total costs in cent
24	1	-1184	3909	1	65	2520
24	3	-1151	3881	5	63	2612
24	5	-1167	3895	2	64	2576
24	7	-1115	3922	2	66	2562
24	9	No valid solution found				
24	11	No valid solution found				
30	1	-1182	3909	1	65	2527
30	3	-1165	3895	5	64	2564
30	5	-1159	3909	3	65	2557
30	7	-878	3895	2	64	2855
30	9	No valid solution found				
30	11	No valid solution found				



(a) Summer scenario with FT-1.

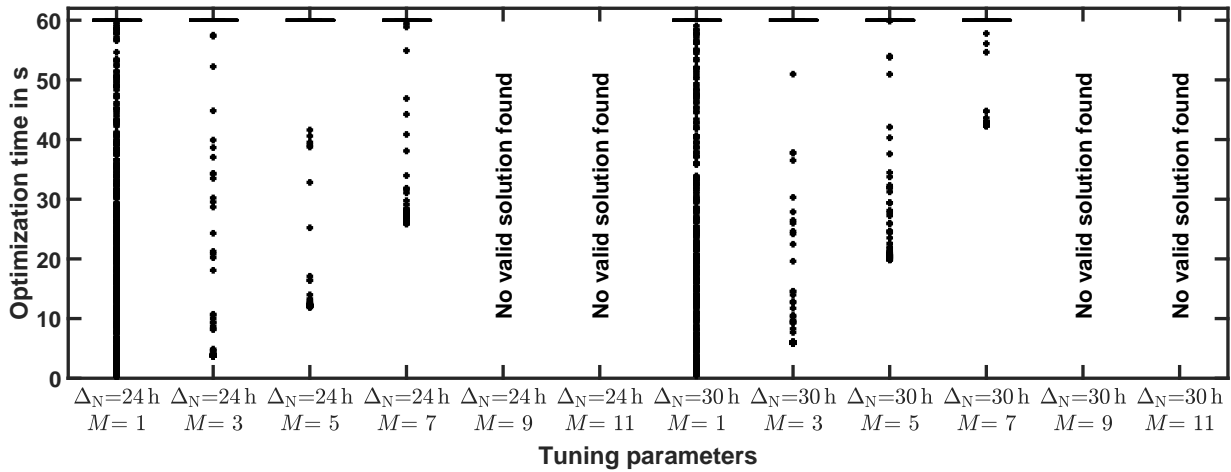


(b) Summer scenario with FT-2.

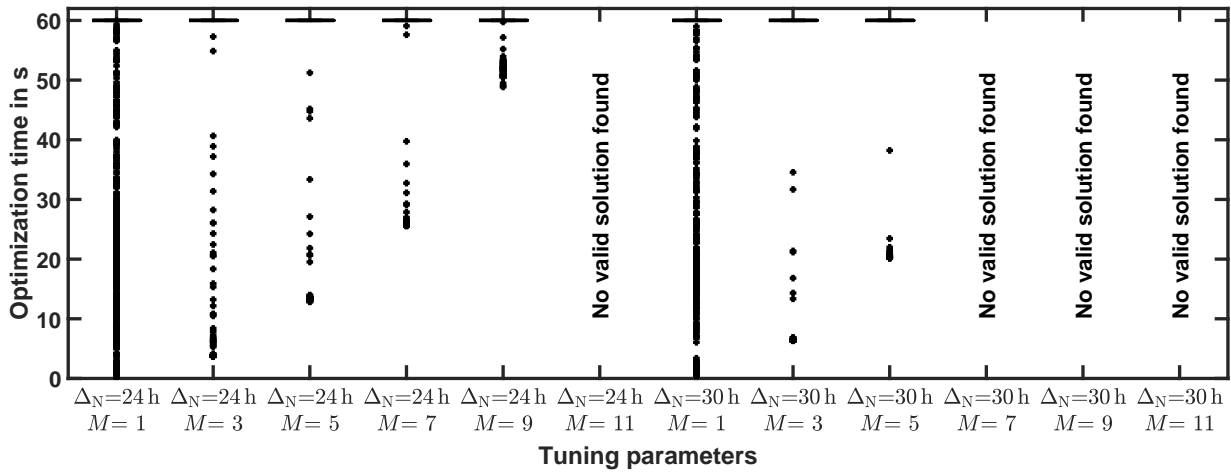


(c) Summer scenario with FT-3.

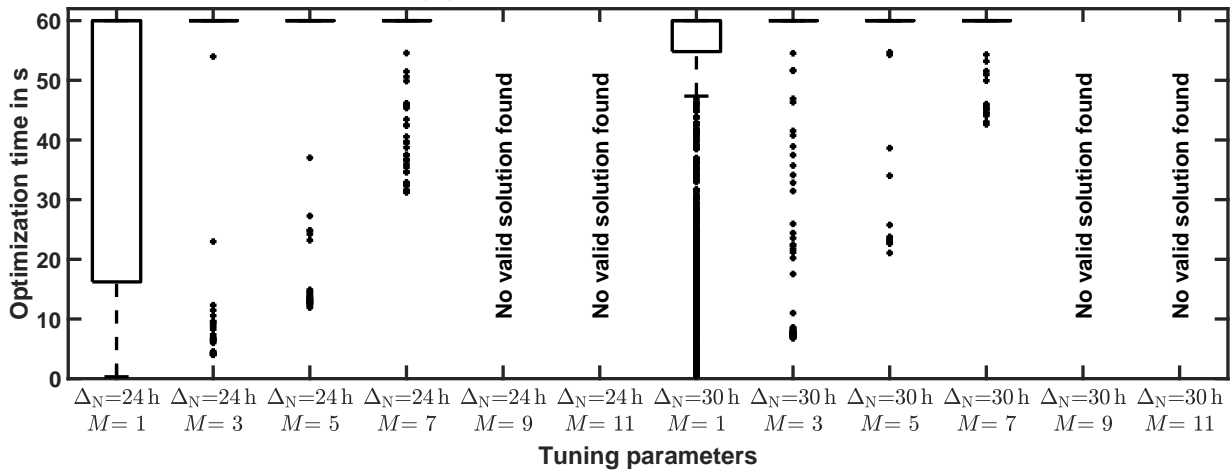
Figure B.11: Visualization of the optimization times in dependence on the optimization interval and the time step duration in the state-of-the-art and stochastic control scheme in the summer scenario for FT-1 (a), FT-2 (b) and FT-3 (c).



(a) Winter scenario with FT-1.

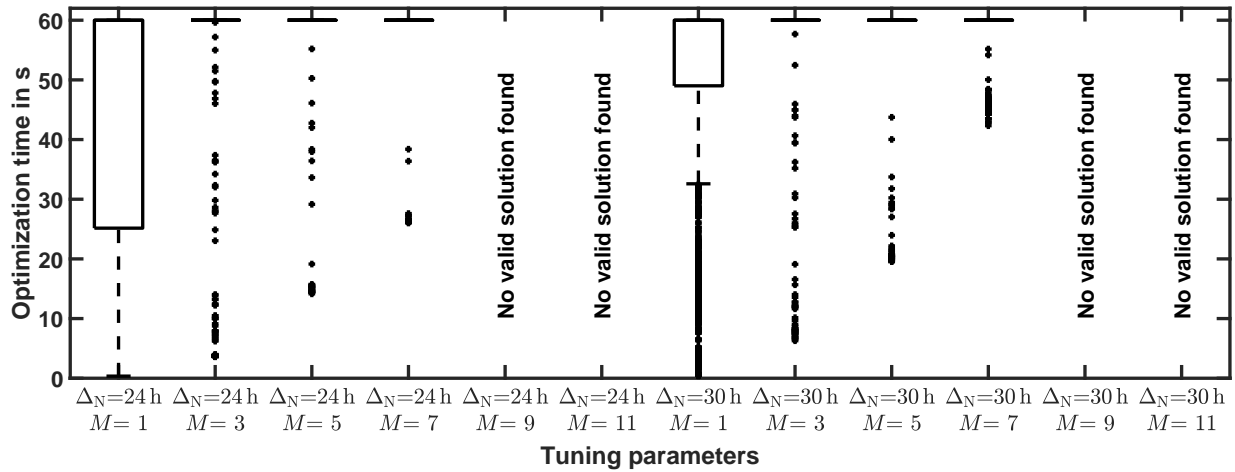


(b) Winter scenario with FT-2.

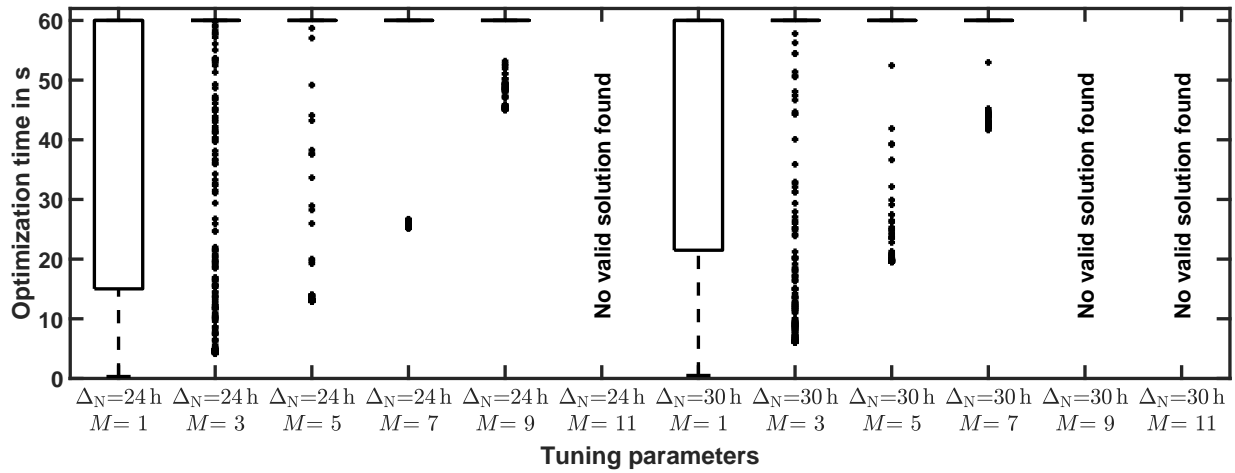


(c) Winter scenario with FT-3.

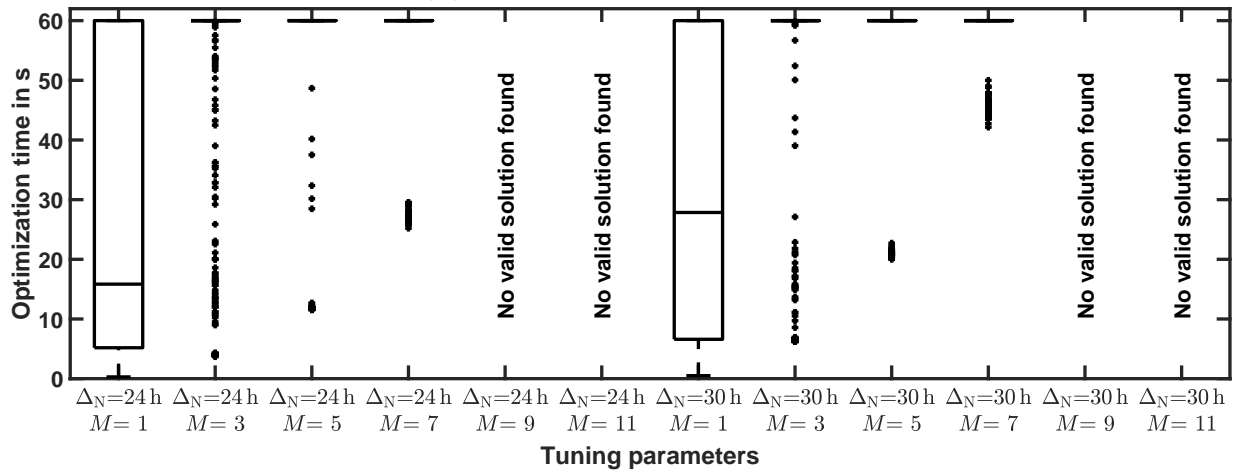
Figure B.12: Visualization of the optimization times in dependence on the optimization interval and the time step duration in the state-of-the-art and stochastic control scheme in the winter scenario for FT-1 (a), FT-2 (b) and FT-3 (c).



(a) Spring scenario with FT-1.



(b) Spring scenario with FT-2.



(c) Spring scenario with FT-3.

Figure B.13: Visualization of the optimization times in dependence on the optimization interval and the time step duration in the state-of-the-art and stochastic control scheme in the spring scenario for FT-1 (a), FT-2 (b) and FT-3 (c).

B.3 Rule-based Micro-CHP Scenario

Table B.19: Simulation results of the rule-based micro-CHP control scheme in the summer scenario with FT-1.

Δ_N in h	M	Electricity cost in cent	Gas cost in cent	$\tilde{E}_{\text{BESS},T+1}$ in Ws	$\tilde{\vartheta}_{\text{HWT},T+1}$ in °C	Total costs in cent
24	1	-1143	938	0	64	-370
24	3	-1156	938	0	64	-383
24	5	-1158	938	0	64	-385
24	7	-1158	938	0	64	-385
24	9	-1161	938	0	64	-389
24	11	-1155	938	0	64	-382
30	1	-1127	938	0	64	-354
30	3	-1161	938	0	64	-388
30	5	-1167	938	0	64	-395
30	7	-1164	938	0	64	-391
30	9	-1104	938	10	64	-332
30	11	No valid solution found				

Table B.20: Simulation results of the rule-based micro-CHP control scheme in the summer scenario with FT-2.

Δ_N in h	M	Electricity cost in cent	Gas cost in cent	$\tilde{E}_{\text{BESS},T+1}$ in Ws	$\tilde{\vartheta}_{\text{HWT},T+1}$ in °C	Total costs in cent
24	1	-1091	938	0	64	-318
24	3	-1159	938	0	64	-386
24	5	-1164	938	113	64	-392
24	7	-1158	938	113	64	-385
24	9	-1152	938	106	64	-379
24	11	-1144	938	155	64	-371
30	1	-1092	938	0	64	-320
30	3	-1167	938	0	64	-394
30	5	-1158	938	114	64	-385
30	7	-1166	938	116	64	-393
30	9	-1102	938	474	64	-329
30	11	No valid solution found				

Table B.21: Simulation results of the rule-based micro-CHP control scheme in the summer scenario with FT-3.

Δ_N in h	M	Electricity cost in cent	Gas cost in cent	$\tilde{E}_{\text{BESS},T+1}$ in Ws	$\tilde{\vartheta}_{\text{HWT},T+1}$ in °C	Total costs in cent
24	1	-653	938	1859	64	119
24	3	-1021	938	1671	64	-249
24	5	-1111	938	1884	64	-338
24	7	-1092	938	1884	64	-319
24	9	-1084	938	1884	64	-311
24	11	-1084	938	1884	64	-311
30	1	-714	938	1406	64	59
30	3	-1117	938	1593	64	-344
30	5	-1102	938	1875	64	-329
30	7	-1086	938	1884	64	-313
30	9	-963	938	3122	64	-191
30	11	No valid solution found				

Table B.22: Simulation results of the rule-based micro-CHP control scheme in the winter scenario with FT-1.

Δ_N in h	M	Electricity cost in cent	Gas cost in cent	$\tilde{E}_{\text{BESS},T+1}$ in Ws	$\tilde{\vartheta}_{\text{HWT},T+1}$ in °C	Total costs in cent
24	1	-686	5756	0	69	4696
24	3	-696	5756	6	69	4686
24	5	-690	5756	7	69	4693
24	7	-693	5756	7	69	4689
24	9	-693	5756	9	69	4689
24	11	-574	5756	73	69	4808
30	1	-684	5756	0	69	4698
30	3	-691	5756	9	69	4692
30	5	-692	5756	7	69	4690
30	7	-692	5756	6	69	4690
30	9	-577	5756	1574	69	4806
30	11	No valid solution found				

Table B.23: Simulation results of the rule-based micro-CHP control scheme in the winter scenario with FT-2.

Δ_N in h	M	Electricity cost in cent	Gas cost in cent	$\tilde{E}_{\text{BESS},T+1}$ in Ws	$\tilde{\vartheta}_{\text{HWT},T+1}$ in °C	Total costs in cent
24	1	-545	5756	7	69	4837
24	3	-560	5756	6	69	4822
24	5	-558	5756	7	69	4824
24	7	-559	5756	7	69	4824
24	9	-556	5756	9	69	4826
24	11	-557	5756	6	69	4826
30	1	-540	5756	5	69	4843
30	3	-559	5756	9	69	4824
30	5	-559	5756	7	69	4823
30	7	-558	5756	6	69	4824
30	9	-527	5756	8	69	4855
30	11	No valid solution found				

Table B.24: Simulation results of the rule-based micro-CHP control scheme in the winter scenario with FT-3.

Δ_N in h	M	Electricity cost in cent	Gas cost in cent	$\tilde{E}_{\text{BESS},T+1}$ in Ws	$\tilde{\vartheta}_{\text{HWT},T+1}$ in °C	Total costs in cent
24	1	-1003	5756	6	69	4380
24	3	-1008	5756	7	69	4374
24	5	-997	5756	8	69	4385
24	7	-992	5756	8	69	4390
24	9	-989	5756	9	69	4393
24	11	-986	5756	7	69	4396
30	1	-999	5756	4	69	4383
30	3	-1010	5756	9	69	4373
30	5	-985	5756	8	69	4398
30	7	-989	5756	5	69	4394
30	9	-612	5756	9	69	4770
30	11	No valid solution found				

Table B.25: Simulation results of the rule-based micro-CHP control scheme in the spring scenario with FT-1.

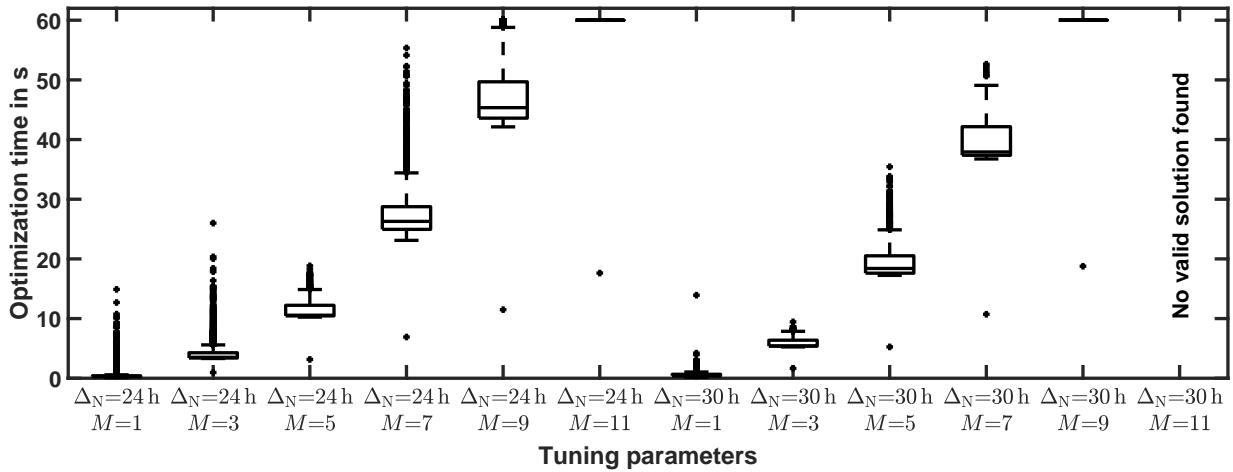
Δ_N in h	M	Electricity cost in cent	Gas cost in cent	$\tilde{E}_{\text{BESS},T+1}$ in Ws	$\tilde{\vartheta}_{\text{HWT},T+1}$ in °C	Total costs in cent
24	1	-930	4046	0	76	2447
24	3	-963	4046	2	76	2414
24	5	-967	4046	0	76	2410
24	7	-974	4046	0	76	2403
24	9	-973	4046	0	76	2404
24	11	-960	4046	2	76	2417
30	1	-917	4046	0	76	2460
30	3	-967	4046	2	76	2410
30	5	-970	4046	0	76	2407
30	7	-970	4046	2	76	2407
30	9	-970	4046	2	76	2407
30	11	No valid solution found				

Table B.26: Simulation results of the rule-based micro-CHP control scheme in the spring scenario with FT-2.

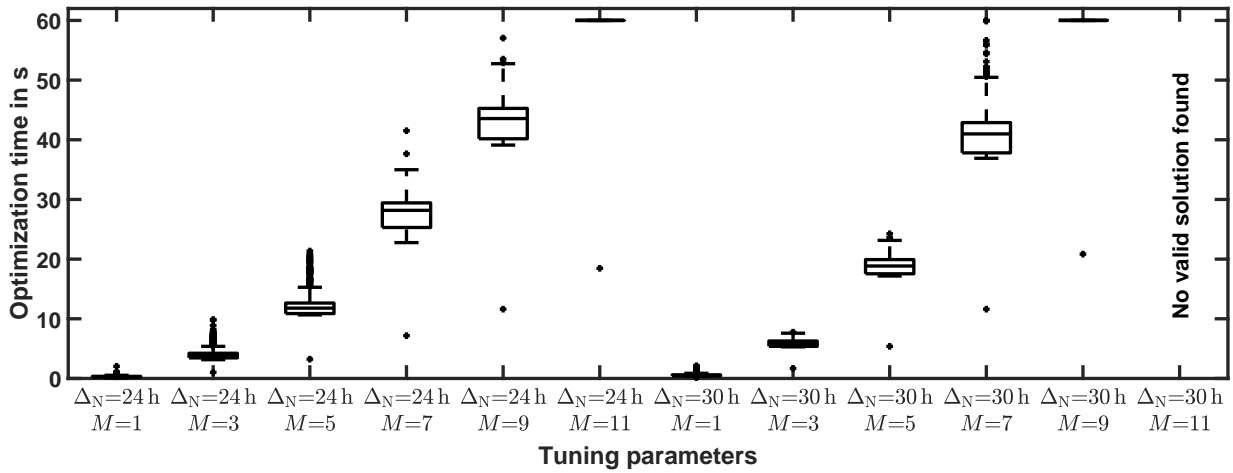
Δ_N in h	M	Electricity cost in cent	Gas cost in cent	$\tilde{E}_{\text{BESS},T+1}$ in Ws	$\tilde{\vartheta}_{\text{HWT},T+1}$ in °C	Total costs in cent
24	1	-873	4046	0	76	2504
24	3	-969	4046	0	76	2408
24	5	-958	4046	0	76	2419
24	7	-968	4046	0	76	2409
24	9	-972	4046	0	76	2405
24	11	-956	4046	0	76	2421
30	1	-876	4046	0	76	2501
30	3	-963	4046	0	76	2414
30	5	-964	4046	0	76	2413
30	7	-977	4046	0	76	2400
30	9	-982	4046	0	76	2395
30	11	No valid solution found				

Table B.27: Simulation results of the rule-based micro-CHP control scheme spring in the spring scenario with FT-3.

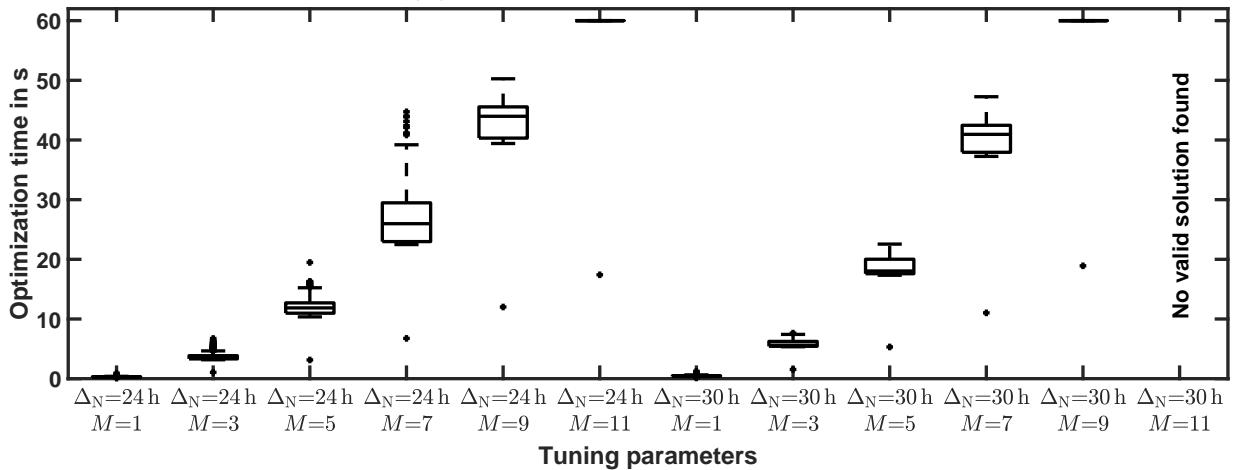
Δ_N in h	M	Electricity cost in cent	Gas cost in cent	$\tilde{E}_{\text{BESS},T+1}$ in Ws	$\tilde{\vartheta}_{\text{HWT},T+1}$ in °C	Total costs in cent	
24	1	-887	4046	2	76	2490	
24	3	-886	4046	32	76	2491	
24	5	-870	4046	77	76	2507	
24	7	-815	4046	3600	76	2562	
24	9	-856	4046	1129	76	2521	
24	11	-569	4046	275	76	2808	
30	1	-884	4046	2	76	2493	
30	3	-885	4046	45	76	2492	
30	5	-844	4046	1551	76	2533	
30	7	-869	4046	32	76	2508	
30	9	-789	4046	274	76	2588	
30	11	No valid solution found					



(a) Summer scenario with FT-1.

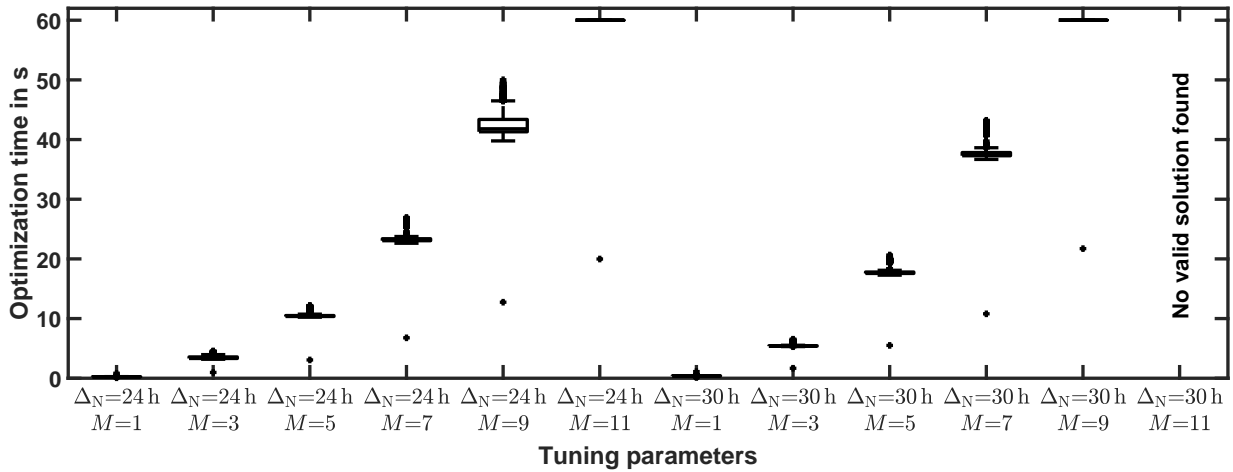


(b) Summer scenario with FT-2.

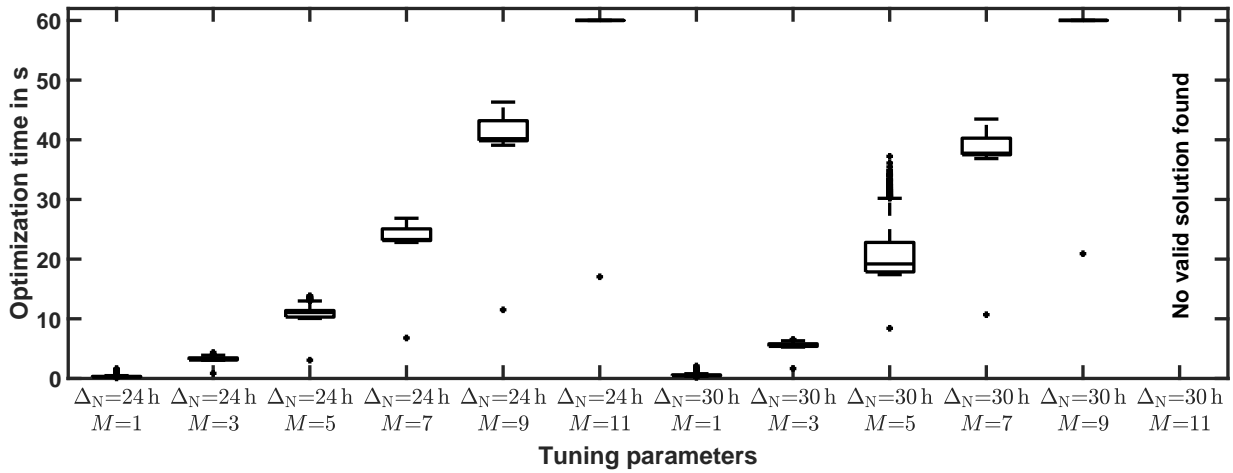


(c) Summer scenario with FT-3.

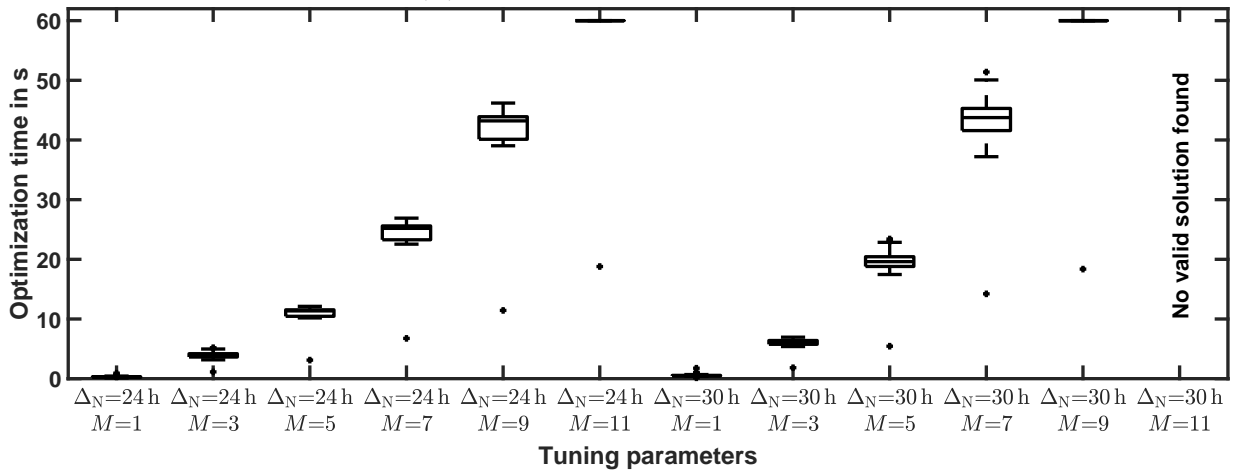
Figure B.14: Visualization of the optimization times in dependence on the optimization interval and the time step duration in the rule-based micro-CHP control scheme spring in the summer scenario for FT-1 (a), FT-2 (b) and FT-3 (c).



(a) Winter scenario with FT-1.

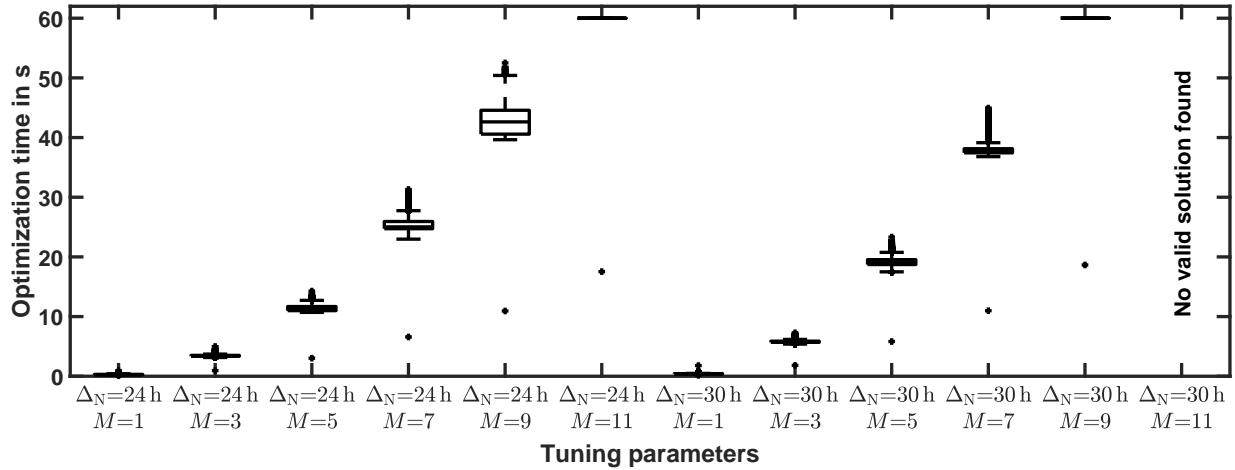


(b) Winter scenario with FT-2.

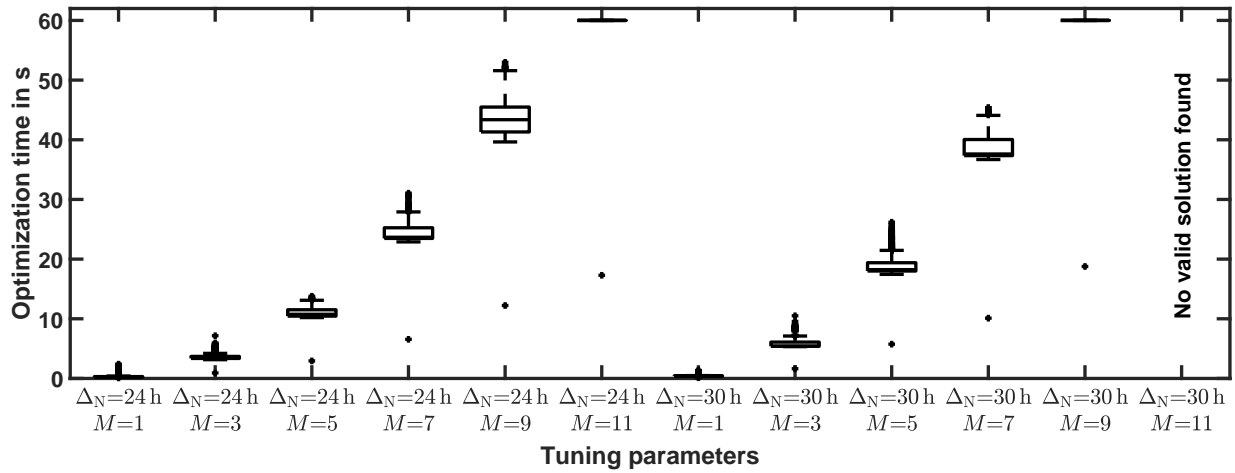


(c) Winter scenario with FT-3.

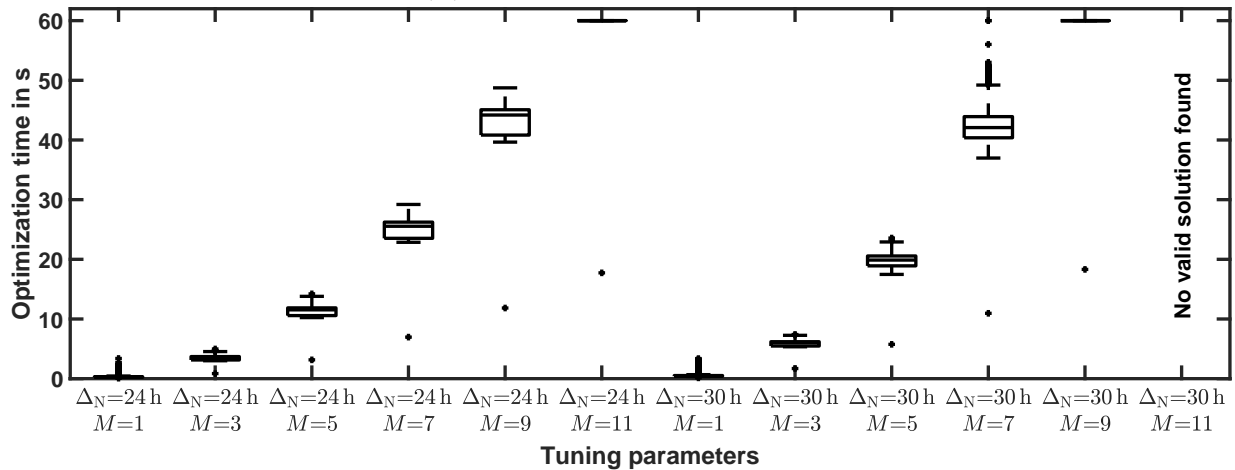
Figure B.15: Visualization of the optimization times in dependence on the optimization interval and the time step duration in the rule-based micro-CHP control scheme in the winter scenario for FT-1 (a), FT-2 (b) and FT-3 (c).



(a) Spring scenario with FT-1.



(b) Spring scenario with FT-2.



(c) Spring scenario with FT-3.

Figure B.16: Visualization of the optimization times in dependence on the optimization interval and the time step duration in the rule-based micro-CHP control scheme in the spring scenario for FT-1 (a), FT-2 (b) and FT-3 (c).

C. Related Publications by the Author

Table C.1: List of related publications by the author.

-
- | | | |
|------|--|-------|
| 2018 | J. Müller, M. Ahrens, I. Mauser, and H. Schmeck, “Achieving Optimized Decisions on Battery Operating Strategies in Smart Buildings,” in <i>Applications of Evolutionary Computation</i> . Springer International Publishing, 2018, pp. 205–221 | [174] |
|------|--|-------|

This publication extends the work presented in [179] by investigating the use of different BESS control strategies to achieve a high performance in the optimization of the operation of a building energy system. Even though, the approaches presented in this publication achieve a higher performance than the ones presented in [179], the uncertainty in the PV generation is not addressed directly.

The publication motivates the stochastic rolling horizon optimization approach that is presented in this thesis. In order to enable a suitable environment to investigate the influence of uncertainties and to provide a clear presentation of the building energy system model, the mixed-integer linear model presented in this thesis has been developed. The publication differs from this thesis in the model of the energy system and in the approach to the optimization. In contrast to this thesis, it uses the non-linear building energy system model presented in [165].

-
- 2017 J. Müller, “Evolutionary optimization under uncertainty in energy management systems,” *it - Information Technology*, vol. 59, no. 1, 2017 [173]

In this publication, a first concept of the stochastic rolling horizon optimization approach presented in this thesis has been developed.

The publication presents a first idea of the contribution of this thesis. The publication differs from this thesis in the choice of the model as well as in the choice of optimization algorithm. Furthermore, it presents no evaluation results.

-
- 2016 J. Müller, C. Gitte, M. Winter, and J. van der Geest, “Advanced configuration system for cost-effective integration of distributed energy systems,” in *2016 IEEE Innovative Smart Grid Technologies - Asia (ISGT-Asia)*. IEEE, 2016 [175]

In this publication, an approach to ease the configuration process of DERs, e.g., PV systems or whole building energy systems, is presented. The problems addressed in the publication are very important with respect to a possible application of the stochastic rolling horizon optimization approach in a product that can be sold and used in real buildings.

The content of the publication is not part of the contribution of this thesis. The publication is referenced in the related work chapter.

-
- 2016 J. Müller, M. März, I. Mauser, and H. Schmeck, “Optimization of Operation and Control Strategies for Battery Energy Storage Systems by Evolutionary Algorithms,” in *Applications of Evolutionary Computation*, A. M. Mora and G. Squillero, Eds. Springer International Publishing, 2016, vol. 9598, pp. 507–522 [179]

This publication presents an approach to the optimization of the parameters of a control strategy that is used by a BESS. It uses a rolling horizon optimization approach and a genetic algorithm to minimize the operation costs of a building energy system. The results indicate that the performance of the optimization approach is dependent on the uncertainty in the building energy system and in particular in the PV generation.

The publication inspired the work on incorporating the uncertainty in the PV generation into the optimization approach. The publication is referenced in the background in energy system and related work chapter. The underlying BESS controller from this publication is used in this thesis. Furthermore, the feed-in compensation tariffs presented in the publication are used in this thesis.

-
- 2017 I. Mauser, J. Müller, and H. Schmeck, “Utilizing Flexibility of Hybrid Appliances in Local Multi-modal Energy Management,” [166] in *Proceedings of the 9th International Conference EEDAL’2017 - Energy Efficiency in Domestic Appliances and Lighting*, ser. JRC Conference and Workshop Report. Publications Office of the European Union, 2017, Inproceedings, pp. 1282–1297

This publication investigates the optimization of a building energy system by a BEMS, in particular the optimization of hybrid energy systems in the form of hybrid appliances.

Such systems are a possible field of application of the stochastic rolling horizon optimization approach presented in this thesis. The content of the publication is not part of the contribution of this thesis. The publication is referenced in the related work chapter.

-
- 2017 I. Mauser, J. Müller, K. Förderer, and H. Schmeck, “Definition, Modeling, and Communication of Flexibility in Smart Buildings and Smart Grid,” [162] in *International ETG Congress 2017*, 2017, pp. 1–6

This publication presents a proposal of a general definition of the term flexibility and the categorization of different approaches to the representation and coordination of flexibility in smart grids, including important aspects concerning communication and coordination. This is not directly part of this thesis. However, the coordination of BEMSs in order to provide measures of demand side management is of high interests. Therefore, this paper discusses the background and environment of BEMSs in general and the presented BEMS.

The content of the publication is not part of the contribution of this thesis. The publication is referenced in the background on energy systems and the related work chapter.

-
- 2015 I. Mauser, J. Feder, J. Müller, and H. Schmeck, “Evolutionary Optimization of Smart Buildings with Interdependent Devices,” [164] in *Applications of Evolutionary Computation*, A. M. Mora and G. Squillero, Eds. Springer International Publishing, 2015, vol. 9028, pp. 239–251

This publication investigates the optimization of a building energy system by a BEMS. In particular, the optimization of a trigeneration system consisting of an adsorption chiller, a hot water tank and a micro-CHP. Such systems are a possible field of application of the stochastic rolling horizon optimization approach presented in this thesis.

The building energy system model used in this thesis is partially based on the one presented in the publication. In particular, the heating system and hot water tank models. Furthermore, the publication is referenced in the related work chapter.

-
- 2015 I. Mauser, J. Müller, F. Allerding, and H. Schmeck, “Adaptive Building Energy Management with Multiple Commodities and Flexible Evolutionary Optimization,” [165] *Renewable Energy*, vol. 87, Part 2, pp. 911–921, 2016

This publication investigates the optimization of a building energy system by a BEMS. It presents an approach to an adaptive building energy system model, optimization algorithm and BEMS. Therein, BESSs are not included in the optimization.

The building energy system model used in this thesis is partially based on the one presented in the publication. The choice of the building configuration used in this thesis is based on the publication. Furthermore, the publication is referenced in the background on energy systems, theory and the related work chapter.
